Emplacement processes of ignimbrites in the Ongatiti Valley, southeast Te Kuiti

A thesis submitted in partial fulfilment
of the requirements for the degree
of
Master of Science
in Earth and Ocean Sciences
at
The University of Waikato
By

Megan Brink

The University of Waikato
2012

THE UNIVERSITY OF
WAIKATO
Te Whare Wānanga o Waikato

Abstract

The Mangakino volcanic centre (MVC) is the oldest rhyolitic volcano of the Taupo Volcanic Zone (TVZ) located on the westernmost boundary. Ten eruptive deposits have been derived from the MVC and this study focuses on the 1.21 ± 0.04 Ma Ongatiti Ignimbrite and the 1.20 ± 0.04 Ma Unit D fall and overlying ignimbrite deposit. The Taupo volcanic centre (TVC), located at the southern boundary of the central TVZ is currently active and is considered to be the most active and productive rhyolitic centre on Earth. There have been multiple eruptions derived from the TVC over the past 350 – 320 ka, however the most recent Taupo eruption dated at 232 AD is the only deposit studied in this research. The study area is situated within the Ongatiti Valley, 15 km SE of Te Kuiti. It is 28 km west of the Mangakino caldera rim, and is located to the west of the upstanding Mesozoic basement block of the Rangitoto Range.

A 1:25 000 geological map of the volcanic geology exposed within the Ongatiti Valley is produced. Detailed stratigraphc logs, petrographic descriptions and quantitative analysis on the mineralogy are given for all of the exposed eruptive deposits. The geochemical composition of the Ongatiti Ignimbrite and Unit D are determined through XRF, Electron microprobe and ICPMS analyses.

Stratigraphic sections of the Ongatiti Ignimbrite in well exposed 25 m high outcrops in the Ongatiti Valley show variations in pumice, crystal, and lithic abundance, both vertically and laterally. Two units can be distinguished within the Ongatiti Ignimbrite overlying a poorly exposed lowermost fall deposit: a lower densely to partially welded, crystal-rich, pumice-poor flow sequence, and an upper densely to partially welded pumice and crystal-rich flow sequence. The boundary between the two units is wavy and gradational, and varies in altitude over relatively short distances. This undulating boundary is considered to result from interaction of pyroclastic density currents flowing both over and around the high-standing Rangitoto Range, and then covering a highly irregular pre-ignimbrite topography in the King Country.

In the Ongatiti Valley, Unit D consists of several phreatoplinian fall deposits, a fine-grained ignimbrite and an overlying coarser-grained ignimbrite with a combined thickness of 3 m. A stratigraphic log is presented and the characteristic textures, structure, petrography and geochemistry is described. A six stage process is suggested for the change in the conditions/styles and intensities between the different phases of the eruption.

A 15 m high valley-ponded section of the 232 AD Taupo Ignimbrite occurs in the Waipa River Valley, that contains fossilised tree trunks in position of growth. A possible origin involving variation in dynamic pressure and subsequent destructive power of pyroclastic density currents is developed.

Acknowledgements

Firstly I would like to acknowledge my research supervisors; Associate Professor Roger Briggs and Dr Adrian Pittari. Their support and encouragement has been influential in helping me to complete this project. Thank you both for editing my draft chapters and for the hours of discussions we have had regarding my topic. Your enthusiasm for geology and volcanology is infectious and makes undertaking a thesis like this an exciting and enjoyable experience.

Thank-you to the Templeton, Leinwebber and Mathieson families, the farmers in the study area, for allowing me to access their properties. In particular I would like to acknowledge the Holmes family for their hospitality and for allowing me to stay in their cottage while I undertook much of my field work.

It would not have been possible to undertake this research if it had not been for the financial assistance that I received over the last 18 months. I would like to thank the University of Waikato Masters Research Scholarship, the Broad Memorial Fund and the S.J. Hastie Scholarship Fund for the monetary support that they provided me with.

Many hours of field work was required for my thesis for which Kyle Wohlers, Holly Goddard and Kirsty Vincent provided some much needed assistance and companionship. I would also like to thank the University of Waikato technicians: Annette, Renat, Chris and Xu, for their invaluable help with the large amount of lab work that was involved in this project. Thank-you to Sydney, the department secretary, for her assistance and support over the last 18 months. The University of Auckland technician Ritchie Sims is to be thanked for his help and guidance with Electron Microprobe work. I am also very grateful to Massimo Raveggi from the School of Geosciences, Monash University in Melbourne for obtaining the ICP-MS analyses.

A special mention of my gratitude needs to be made to Tim Litton, thank-you for restoring and rebuilding my computer after it crashed mid-way through my research. Your urgent response and the hours of frustration you put in, is greatly appreciated.

My fellow students: Anna, Kirsty, Mike, Karl, Simon, Josh and Steph' thank-you for all your help and words of encouragement. It has been an honour to work with you all! To Simon and Josh especially, thank-you for taking the time to teach me the necessary skills on GIS required for the production of my geological map. Thank-you to all of my friends, and most importantly Matt for your constant support, being so understanding when I had to work so many long hours and providing me with 'time-out' when I needed it most.

Finally I need to thank my special family, particularly my mom and dad for their encouragement throughout this project. They helped me in every way possible and were instrumental in keeping me sane even at my lowest moments. Without you all I would not have been able to complete my thesis.

Table of contents

Chapter Two: Stratigraphy

Chapter Three: Ongatiti Ignimbrite

Chapter 6: Discussion

List of figures

List of tables

Chapter One

Introduction

1.1 Study objectives

The volcanic activity of the Mangakino Caldera marks the onset of volcanism in the Taupo Volcanic Zone with the oldest eruption recorded at 1.68 Ma. Large volume eruptions from the caldera are responsible for the formation of the Pakaumanu Group Ignimbrites exposed within the King Country. The location of the study area is approximately 30 km west of the Mangakino Caldera and contains deeply incised valleys which expose five of the 10 Mangakino Caldera derived eruptive deposits. These are the Ngaroma Ignimbrite, Ongatiti Ignimbrite, Unit D, Ahuroa Ignimbrite and the Rocky Hill Ignimbrite. The most recent volcanic deposit in the study area is the Taupo Ignimbrite (232 AD) which forms a valley pond in the Waipa River Valley.

The study area has been previously mapped by Blank (1965) and more recently by the Institute of Geological and Nuclear Sciences 1:250000 QMAP series (maps 4 and 5), although not in great detail. The Ngaroma Ignimbrite, Unit D and Taupo Ignimbrite are not presented on either of these maps, and the delineation between the different deposits is poorly defined. The aim of this research is to determine the geological evolution of the study area, focusing specifically on the eruption and emplacement processes of the Ongatiti, Unit D and Taupo ignimbrites. A key outcome of this research is the production of a 1:25 000 scale geological map.

The Ongatiti Ignimbrite has been described by several authors (Wilson 1986a,b, Moyle 1989, Briggs et al. 1993, Krippner et al. 1998, Cartwright 2003 and McGrath 2004) and the composition has been analysed in detail by Briggs et al (1993). The Ongatiti is classified as being one of the most voluminous eruptions produced from the TVZ where the ignimbrite deposit contains two distinct and broad units. The lower and upper units of the Ongatiti Ignimbrite are rarely exposed within the same area and as a result, there has been limited research undertaken on understanding the vertical and lateral variations within the deposit.

Briggs et al. (1993) has previously studied the vertical variations within the Hinuera Quarry but no research has been carried out to understand the lateral variations within the Ongatiti Ignimbrite.

Outcrops of Unit D are rare and it has only been described briefly by Wilson (1986a,b) and Moyle (1989) and limited geochemical analysis has been undertaken on the deposit by Moyle (1989).

There have been multiple studies on the Taupo Ignimbrite where the eruption mechanism, the transport and the emplacement processes of the violent pyroclastic flow sequence have been discussed (Walker 1980, Wilson and Walker 1985). The preservation of large amounts of charcoal fragments, carbonized and uncharred logs are characteristic of the Taupo Ignimbrite. Hudspith et al. (2010) and Hogg et al. (2011) have both examined these in detail however neither have documented the preservation of vegetation still in standing position of growth within the deposit.

The specific objectives of this research are:

- To discuss the vertical and lateral variations observed in the Ongatiti Ignimbrite southeast of Te Kuiti, and to discuss the eruption, transport and emplacement processes of the pyroclastic flow sequence.
- To characterise the deposits of Unit D based on exposures within the study area.
- To develop a theoretical explanation for the preservation of fossilised tree trunks still in standing position of growth in the Taupo Ignimbrite in the Waipa River Valley.

1.2 Study Area

1.2.1 Location of the study area

The study area is located within the King Country of New Zealand, approximately 15 km southeast of Te Kuiti Township, Southern Waikato (Fig 1.1). It intersects both geological maps 4 (Waikato area) and 5 (Rotorua area) of the 1:250000 QMAP series (Institute of Geological and Nuclear Sciences).

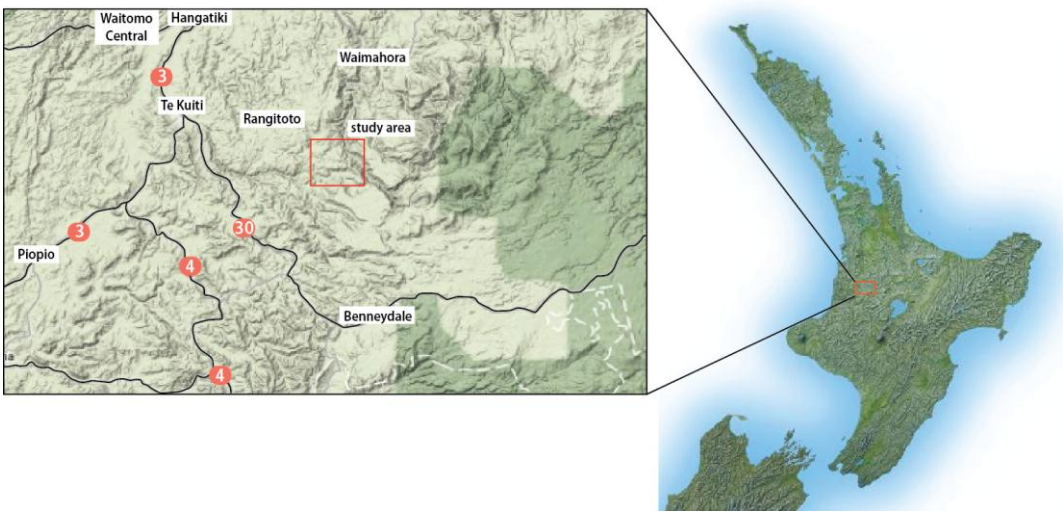

Figure 1.1: Map showing the location of the study area relative to the national and the regional (South Waikato) scales of New Zealand. Maps sourced from Google maps (August, 2011).

The study area stretches across three separate farms covering an area of approximately 34 km^2. It is best accessed along Ahoroa Rd (Fig 1.2). The grid references for the study area are displayed on the geological map (Enclosure 1).

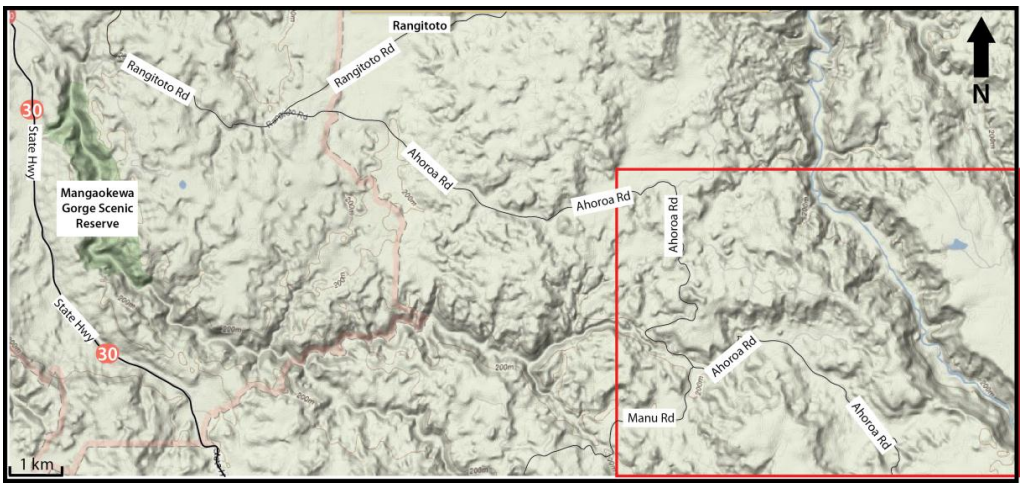

Figure 1.2: A localised map (sourced from Google maps, August, 2011) showing the main access into the study area (red box).

1.2.2 Landuse of the study area

The steep and rough terrain of the study area is predominantly utilised for the grazing of sheep and beef livestock. However, the farmers occasionally use the shallow dipping ignimbrite plateaux for the cultivation of supplementary feed. There is also an airstrip (used mainly by top dressers) located along the ridge

within the most south eastern segment of the study area. The Waipa River Valley is the only section of the study area which is not privately owned. It is protected by the Waikato Regional Council and is used mainly for recreational hunting and fishing by local residents

1.3 Methods

1.3.1 Field Mapping

Geological mapping of the study area was carried out by identifying and differentiating each of the geological units' diagnostic characteristics in the field, based on outcrop appearance, stratigraphic bounding units, vertical and lateral extent, degree of welding, texture and componentry. The geometric coordinate system used was New Zealand Map Grid (NZMG) and a geological map is presented in Enclosure One.

Detailed stratigraphic logs were constructed in each of the main geological units exposed in the study area; their locations are presented on the geological map (Enclosure 1) and their GPS coordinates are given in Appendix One. The locations were selected based on the maximum amount of exposure and access available. The variation in the overall grainsize and the appearance of the profiles were described in detail and samples and measurements were collected from specific stratigraphic elevations (approximately every 1– 3 m). The measurements obtained included bulk visual field estimates of the abundance (percentages) of pumice and lithics. The average length (measured along their long axes) of the five maximum lithic and pumice clasts observed in the outcrop, and the corresponding aspect ratios of these pumice clasts were measured and calculated. The recorded measurements are given in Appendix One. Samples were also collected from other specific outcrop exposures around the study area, mainly for the purpose of confirming the distribution of the different geological units. The descriptions of the samples and their locations are shown in Appendix One and in some cases on the geological map.

1.3.2 Petrography

At least one petrographic thin section was made for each sample collected. The mineralogy, glass shard matrix and pumice textures were described, and lithic clasts were identified. The phenocrysts within pumice clasts and crystals within the matrix were point counted in thin section to express accurate quantitative data on their abundance. This data was obtained for selected samples and is presented within Appendix Two.

1.3.3 X-Ray Fluorescence

33 samples were selected for major and trace element geochemical analysis where their abundances were measured using the XRF SPECTRO X-LAB 2000 in the Department of Earth and Ocean Sciences at the University of Waikato. The results obtained are presented in Appendix Three for the Ongatiti Ignimbrite samples and in Chapter Four for the Unit D samples. Samples were prepared initially as a crushed powder using a tungsten-carbide ring-mill. Glass fused discs were prepared for major element analysis and pressed powder pellets were prepared for trace element analysis.

Preparation of glass fused discs: Approximately 0.3 g of rock powder was fused with 2.5 g of LM100 flux (PURE 100% Li-metaborate) and with a pinch of NH_4I by a progressive step heating process. The step heating process lasted for approximately 1.5 h where the samples were heated within Pt/Au crucibles at set temperatures of 650, 720, 780, 825 °C for approximately 15 minutes each and finally at 1000 °C for approximately 30 minutes. The molten rock samples were then pressed and cooled using a press and graphite disc on a hot plate heated up to 230 °C. The discs were left to anneal on a second hot plate with an aluminium sheet at 160-180 °C overnight. The Loss of Ignition (LOI) was calculated after heating to 1000 °C .

Preparation of pressed powder pellets: Approximately 5 g of rock powder was bound using 10-15 drops of PVA binder which was then pressed into an aluminium cup using a hydraulic press. The pressed pellets were then heated for approximately 2 hours at 70 °C to evaporate off the binder.

1.3.4 Electron Microprobe

The geochemistry of individual crystals, glass shards and glass within pumice was also investigated in eleven polished thin-sections using the JEOL JXA-840A electron probe micro-analyser at the School of Environment, The University of Auckland, with the assistance of Ritchie Sims. Each polished thin-section was coated with a 25 ηm carbon film in an Edwards vacuum evaporator. The analysis conditions included an electron gun accelerating voltage of 15 kV, a 1000 pA beam current, and an electron spot diameter of approximately 2μm. The X-Ray analysis system used included a eumeX Si(Li) Be-window detector and Moran Scientific pulse-processor and software. Each spectrum was collected for 100 seconds of live time. Standardisation used a set of Astimex mineral standards. The measurements for the samples from the Ongatiti Ignimbrite are presented in Appendix Three and the measurements obtained from Unit D are given within Chapter Four.

1.3.5 Inductively Coupled Plasma Mass Spectrometry (ICPMS)

Rare earth and selected trace elements analyses of 9 of the crushed powder samples were selected to be analysed using a Thermo Finnigan X series II, quadrupole ICP-MS. at the Monash University's School of Geosciences, Melbourne. The results obtained for the samples from the Ongatiti Ignimbrite are presented within Appendix Five and in Chapter Four for the samples analysed from Unit D.

Sample solutions were produced from approximately 50 mg of sample powder using high-pressure digestion methods. ICP-MS count rates were externally standardised by means of calibration curves based on the in house standard BNB basalt. Drift corrections were applied by the combined use of In, Bi as internal standards and the repeated analysis of dummy standards throughout the analytical session. Reproducibility on replicate analyses and accuracy is in the order of 5% for all elements.

1.4 Tectonic evolution of the Taupo Volcanic Zone

The ongoing westward subduction of the Pacific plate beneath the Australian plate has produced the continuous NNE trending 2,550 km long and highly active Tonga-Kermadec island arc, southwestern Pacific (Fig 1.3). It can be traced from Tafahi Island, northern Tonga into the Tongariro National Park of the Central North Island, New Zealand (Ewart et al. 1977, Smith and Price 2006). The rates of convergence, subduction and back-arc extension along the Pacific-Australian plate boundary are controlled by the distance from the Pacific-Australian pole of rotation. As a result, these rates tend to significantly increase northwards from New Zealand (southern extent) into Tonga (northern extent) subduction system (Smith and Price 2006). The back-arc extension is represented by the Lau Basin in the north and the Havre Trough in the south. The Taupo Volcanic Zone (TVZ) represents the southern wedged shaped continuation and termination of the Kermadec Ridge-Havre Trough system (Ewart et al. 1977, Smith and Price 2006).

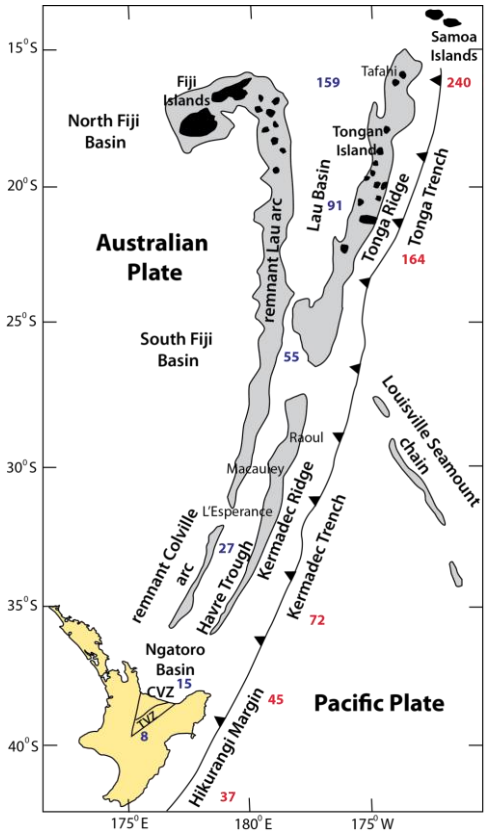

Figure 1.3: The southwest Pacific Region illustrating the key features of the Tonga-Kermadec arc system. Note the numbers shown in red represent the measured subduction rates along the arc and the numbers in blue represent the measured rates of extension. (modified from Stern et al. 2006, Smith and Price 2006, Davey 2010).

The subduction system within the New Zealand setting is proven to be dynamic. The continuous translation and rotation of volcanism through the North Island of New Zealand during the last 23 Myr has been controlled and influenced by the ongoing increase in the rate of subduction and crustal extension throughout this period (Briggs et al. 2010).

Rowland et al. (2010) state that approximately 23 My of subduction and andesite arc volcanism began in the New Zealand region in Northland along the NW- SE Colville arc. Volcanism eventually ceased along the Colville arc at approximately 16 Ma as the position of the active volcanic arc migrated and developed into the NNE-SSW Coromandel Volcanic Zone (CVZ). Volcanism evolved continuously into southern CVZ up until 3-4 Ma. It is inferred that during this period, extension within the Central North Island began as the Havre Trough back arc basin started to open and progressively widen, inducing further clockwise rotation of the Hikurangi Margin and active volcanic arc (Briggs et al. 2010). Volcanism intensified and continued as it migrated southeast into the Central Volcanic Region (CVR). This region encompasses the transition in volcanism that took place from the extinction of the Miocene-Pliocene CVZ into the Pleistocene – Recent TVZ. It is represented by the Pliocene-Pleistocene Tauranga and Kaimai volcanic region as well as the TVZ which is the current setting of the active volcanic arc (Briggs et al. 2010).

1.4.1 Current tectonic setting of the Taupo Volcanic Zone

The subduction system within the New Zealand setting (Fig. 1.4) is characterised by the Hikurangi Margin/ Trench which is positioned just off the east coast of the North Island. Onshore and parallel to the east coast, the steep section of the subducting Pacific Plate (fore-arc basin) is revealed along the surface as the 5 km deep east coast basin (Stern et al. 1995). The northeast-southwest trending TVZ is 60 km wide, 200 km long, and extends from the Bay of Plenty coastline to the central North Island of New Zealand (Briggs et al. 2010). The TVZ is a volcano-tectonic rift zone with very thin crust (15 km), high frequency volcanism and rapid rates of rifting by arc standards. The active volcanic front is located along the southern boundary of the TVZ by the currently active Okataina, Taupo, White Island, Ruapehu and Tongariro volcanic centres. The entire TVZ is currently

rifting at 8 mm/yr at the south end to 15 mm/yr at the Bay of Plenty coastline in the northern end (Davey 2010, Rowland et al. 2010). Stern et al. (1995) explain that the TVZ transitions into a mildly compressive regime in the southwest of the North Island where subduction continues for another 300 km. The obliquity of the subducting Pacific plate progressively increases southwards to form a geophysically defined crustal downwarp zone at the leading edge of the subducting plate. The downwarp zone is responsible for the formation of the Waitemata, Te Kuiti, and Taranaki sedimentary basin depocentres (along the west coast of the North Island) as the subduction zone migrated southwards during the Oligocene – Pliocene. The Pleistocene-Recent Wanganui Basin and drowning topography of the Marlborough Sounds marks the current position of the leading edge of the subducting Pacific plate whilst the previously formed basins are currently being exhumed and/or eroded (Stern et al. 2006).

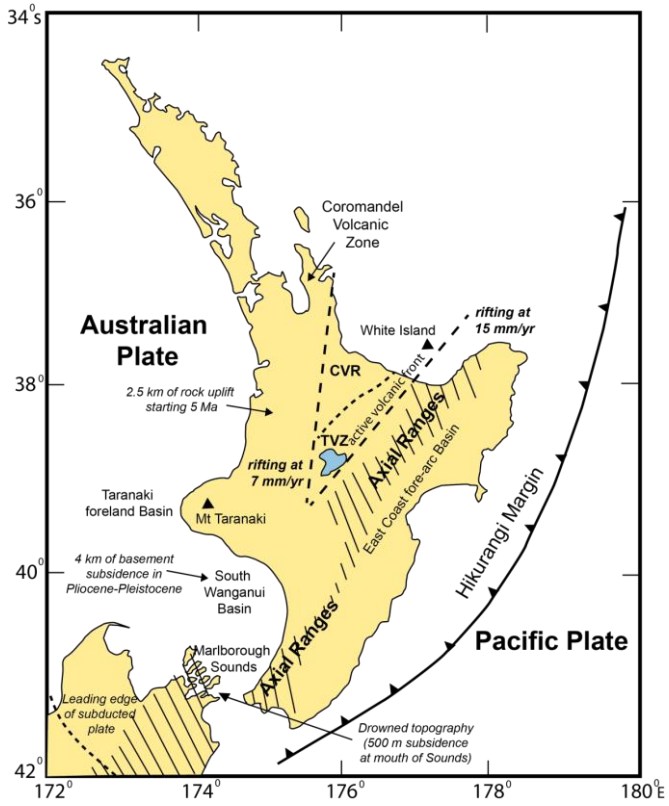

Figure 1.4: A summary of the current tectonic setting and the associated key features of the subduction system beneath the North Island of New Zealand (modified from Stern et al. 1995).

1.5 The volcanic evolution of the Taupo Volcanic Zone

1.5.1 Introduction

The TVZ is delineated by the structural NNE-SSW trending arrangement of vent positions and caldera margins of calc-alkaline volcanoes that have been active within the last 2 Ma (Wilson et al. 1995, Houghton et al. 1995, Spinks et al. 2005, Allan et al. 2008). The central 6,000 km^2 of the TVZ is renowned for having some of the highest arc-related heat flows (700 mW/ m^2) on earth, where 80% (4.5 GW) of it is transmitted as geothermal fluids from 23 fields (Wilson et al. 1994, Price et al. 2004, Davey 2010, Rowland et al. 2010). The remaining 20% is transmitted as prolific volcanism which is controlled by upper crustal tectonic extension enhancing the rapid rise of magma (Wilson et al. 1995, Spinks et al. 2005). Subsequently, the TVZ is considered the most productive and active silicic volcanic system on Earth, having erupted approximately 15,000 km^3 of predominantly rhyolite magma during the Quaternary (Briggs et al. 1993, Price et al. 2004, Allan et al. 2008). This equates to more than 90% of the total eruptives produced in New Zealand during the late Pliocene to Quaternary and is further demonstrated by the significant distribution of rhyolitic pyroclastic deposits and lavas over most of the central North Island (Ewart et al. 1977, Wilson et al. 1994, Leonard et al. 2010).

The TVZ is a unique case when compared to other examples of silicic systems around the world because of its unusually high frequency and production of rhyolite volcanism derived from small overlapping volcanic centres and calderas (Wilson et al. 1995, Houghton et al. 1995). Wilson (2008) mentions that rhyolite magma bodies at Taupo have grown at rates as high as 10-40 km^3/ky during several periods over the past 60 ky.

1.5.2 Volcanic setting

Houghton et al. (1995) suggests that the thickness of volcanic deposits is at least 2.5-3 km in the TVZ. Based on geophysical data, tunnel borings, drill cores, and xenoliths and xenocrysts within the erupted material, it is currently inferred that Mesozoic metasediments which have been intruded by granitoids, meta-igneous granulites and intermediate mafic to andesitic intrusive rocks make up the crust

beneath the TVZ (Ewart et al. 1977, Wilson et al. 1995, Price et al. 2004, Rowland et al. 2010). The TVZ is bounded to the east and west by uplifted (up to 2 km high) Mesozoic basement mountain ranges which are surrounded by Quaternary rhyolitic pyroclastic deposits derived from the TVZ (Ewart et al. 1977, Stern et al. 2006).

The TVZ (Fig 1.5) is divided into 3 segments (central, northeast and southwest TVZ) based on the distinct geographic distribution of the type, style, volume and rate of volcanism (Sutton et al. 1994, Houghton et al. 1995, Rowland et al. 2010).

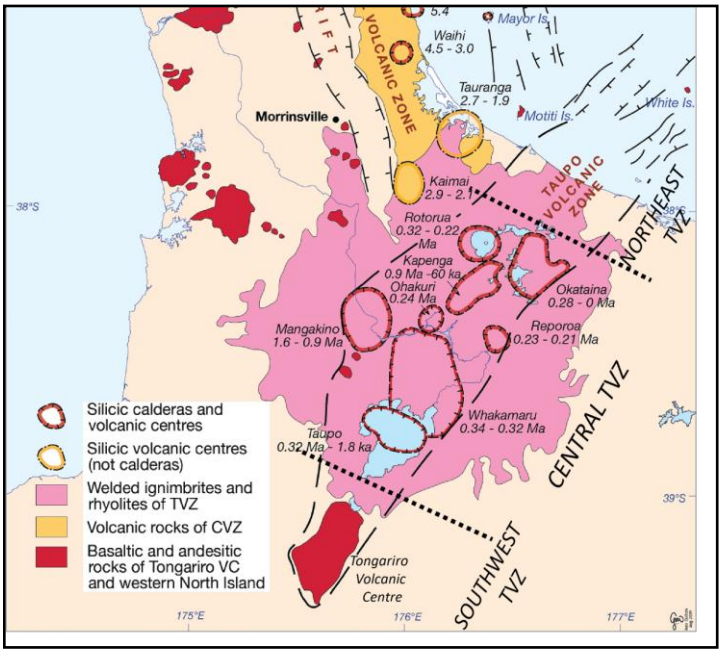

Figure 1.5: The volcanic setting of the Taupo Volcanic Zone. Note the distinct variation in the type of volcanic centres exposed between the southwest, central and northeast segments. (Figure adapted from Briggs 2004 and Rowland et al. 2010).

Rhyolitic volcanism is restricted to the 125 km long central TVZ segment which is characterised by a broad structural depression consisting of tectonic basins and 8 caldera centres. The heat flow is an order of magnitude higher than in the northeast and southwest segments, and the explosiveness, volume and rate of the rhyolite dominant volcanism is therefore much more significant (Sutton et al. 1994, Houghton et al. 1995, Rowland et al. 2010). Basaltic, andesitic and dacitic volcanism exists both irregularly in time and space throughout the TVZ although with a minimal erupted volume in comparison to the rhyolitic volcanism (Briggs et al. 1993, Wilson et al. 1995, Rowland et al. 2010). The northeast and southwest

segments of the TVZ consist of andesitic to dacitic composite volcanoes where the currently active White Island (northeast segment) and Ruapehu (southeast segment) mark the maximum extent of the TVZ (Ewart et al. 1977, Houghton et al. 1995, Stern et al. 2006).

There is no adequate explanation to account for this complex and multipart nature of the TVZ but Rowland et al. (2010) suggest it could be the result of variation in the plumbing networks within the crust. Wilson et al. (1995) infer that mafic magmatism fuels almost all the other volcanism in the TVZ, but through density filtering, assimilation and fractional crystallisation processes, rhyolite is produced and is therefore the dominant magma erupted at the surface. Only in rare situations does the more mafic material reach the surface unaffected by these magmatic processes.

There is furthermore discrepancy within these segments, for example there are different caldera structures and features in the central TVZ in relation to the distance from the active rifting axial zone. This is demonstrated by the Taupo and Okataina calderas which are intra-rift calderas where the degree of extension is the highest. Subsequently they have formed from multiple collapsing episodes and have the largest eruptive volumes. Rotorua in comparison is further from the axial zone and is characterised as a monogenetic collapse caldera with lesser eruptive volumes (Spinks et al. 2005).

1.5.3 Eruption history

Older eruptives and smaller composite cones/ non-rhyolite volcanism are poorly documented in the geological record. Therefore the current knowledge of the eruptive history of the TVZ (Table 1.1) is strongly influenced and limited to what is preserved in the geological record (Wilson et al. 1995). Wilson et al. (1995) have distinguished the evolution of the TVZ into two distinct periods: the old TVZ includes eruptions that took place between 2 to 0.34 Ma, although these deposits are poorly preserved as a result of erosion, downfaulting, and destruction and burial by younger volcanic deposits. The young TVZ represents the eruption record from 0.34 Ma to present where only the most recent eruptions of the modern TVZ (< 65 ka) are preserved well enough to be studied in great detail (Briggs et al. 1993, Allan et al. 2008, Briggs et al. 2010, Rowland et al. 2010).

During the earliest evolutionary stages of the TVZ (pre 1.6 Ma) andesitic volcanism was most dominant, but this rapidly transitioned over a few hundred thousand years into a more intense and voluminous silicic volcanism system (Wilson et al. 1994, Price et al. 2004, Rowland et al. 2010). As Wilson et al. (1995) state, the progressive increase in the heat flow enabled significant amounts of crustal melting which then led to the increase and vast production of rhyolitic magma.

Table 1.1: A summary of the eruption history of the TVZ (Ewart et al. 1977, Froggatt 1982,Wilson et al. 1995, Houghton et al. 1995, Stern et al. 1995, Price et al. 2004, Allan et al. 2008, Briggs et al. 2010, Rowland et al. 2010).

	Basaltic	***Andesitic***	***Dacitic***	***Rhyolitic***
Volcano types	- basaltic - andesitic monogenetic vents - eruption at Mt Tarawera composite cone is an exception	- andesitic - dacitic composite cones - earliest volcanism in TVZ (Titiraupenga & Pureora) - large polygenetic composite cones at northern & southern extremities of TVZ - smaller composite cone edifices buried in central TVZ	- 5 isolated domes	- 8 prominent rhyolitic caldera centres - Intra caldera lava domes - extra caldera lava domes (south east and west of Taupo caldera)
Eruption style and deposits	- basaltic - andesitic lavas producing cinder cones and sporadic flows - violent scoria eruption of Mt Tarawera 1886	- strombolian to plinian style eruptions - andesitic - dacitic fall deposits - locally to regionally dispersed pyroclastic fall deposits - lava flows - minor pyroclastic flows on flanks of composite cones	- lavas	***3 main forms:*** - large pyroclastic eruptions generating widespread ignimbrites, fall deposits & caldera formation - (dacitic to dominantly rhyolitic mixed pumices in ignimbrites) - small pyroclastic eruptions within calderas, no collapse, small fall deposits & occasional ignimbrites - Dome building eruptions, either dependent on or independent of caldera eruptions generating locally to widely dispersed pyroclastic deposits and lavas
Eruption volumes	- last 0.34 Ma, erupted volume estimated at 5 km^3 - Tarawera is the largest eruption at 1 km^3 and is 1 order of magnitude smaller than the largest andesite/dacite eruptions & 2-3 times smaller than the largest rhyolite eruption	- last 0.34 Ma, erupted volume estimated at 300 km^3 - order of magnitude less abundant than rhyolite - cone size ranges from 10 to 200 km^3 - smaller buried cones <10 km^3 - eruptions range from <1 to 10 km^3	- last 0.34 Ma, erupted volume estimated at 20 km^3 - few eruptions exceeding 1 km^3	- last 0.34 Ma, erupted volumes estimated at 3000 km^3 - Central TVZ alone in last 61 ka, approximately 780 km^3 released in 3 moderate to large caldera forming events - eruption volumes range from 0.01 to 500 km^3 - pyroclastic eruptions range from 30 - >300 km^3 - dome building eruptions rarely exceed 10 km^3
Eruption frequency	- only documented eruptions are post 0.34 Ma so the frequency of eruptions is poorly understood	- composite cones have extended life times >300 ka - White Island, Ruapehu & Tongariro massif (northern & southern extremities of TVZ) have been active within the last 10 ka - Ruapehu and White Island have erupted in the last decade	- limited documentation of erupted history	- 34 caldera forming eruptions since the initiation of rhyolitic volcanism in TVZ (1.65 Ma) - Last 65 ka, 3 caldera forming eruptions (61, 26.5 & 1.8 ka) and 52 smaller eruptions - eruptive frequency of explosive caldera forming eruptions depict a pattern/ cluster of intense volcanism (20 -50 ka), followed by a period of quiescence (100-130 ka) & a change in vent position - 3 periods of explosive caldera forming eruptions 1 - 1.68 to 1.53 Ma 2 - 1.21 to 0.68 Ma 3 - 0.34 Ma to present - During the infancy of the TVZ, these large caldera forming eruptions had a frequency of 1 every 7 ka

1.6 Mangakino Volcanic Centre

1.6.1 Introduction

The Mangakino Volcanic Centre (MVC) is located on the westernmost boundary of the TVZ (Fig 1.5). It is the oldest caldera and was active from the commencement of rhyolitic volcanism in the TVZ 1.6 Ma through to the last eruption that took place 0.91 Ma (Wilson 1986a, Briggs et al. 1993, Wilson et al. 1995)

1.6.2 Volcanic evolution and eruption history

The extra-caldera ignimbrites and included cognate lithic clasts provide the best insight to the volcanic evolution of the MVC (Table 1.2). This is because the infilling of the caldera post 0.91 Ma has buried most evidence (outcrop exposure) for the intracaldera deposits, and less extensive, effusive magmatism (Briggs et al. 1993, Wilson et al. 1995, Krippner et al. 2010).

1.6.3 Geological setting

The Mangakino caldera is currently expressed as a low lying oval shaped basin 200-400 m below the surrounding ignimbrite plateaux which is about 30 km long and 15 km wide. It is further characterised by a major gravity anomaly where thick volcanic and epiclastic deposits have partly infilled the basin to a maximum depth of 4 km, below which Mesozoic basement underlies (Briggs et al. 1993, Krippner et al. 2010). Both MVC-derived and younger volcanic deposits (from nearby centres), in particular the 0.34 Ma Whakamaru Ignimbrites (> 200 m thick), infilled the depocentre and produced a thick volcanic pile over time. In addition, prior to 0.34 Ma, the MVC is inferred to have been occupied by a lake where up to 280 m of lacustrine sediments were deposited and this is further confirmed with the presence of phreatomagmatic deposits erupted from the centre (Wilson 1986a, Briggs et al. 1993, Wilson et al. 1995).

Table 1.2: A summary of the volcanic evolution and eruption history of the MVC, the highlighted eruptions are the focus of this research (Wilson et al. 1986b, Briggs et al. 1993, Wilson et al. 1995, Houghton et al. 1995, Stratford and Stern 2008).

Timeline (Ma)	Name of eruption and deposit	Exposure	Nature of eruption	Volume DRE (km^3)	
				Briggs et al (1993)	Houghton et al (1995)
pre 1.68 — **pre-caldera activity**	rhyolite lava domes	lithic clasts	effusive activity	? buried and/ or destroyed	?
	andesitic lavas	abundant lithic clasts	andesitic activity generated at MVC/ buried andesite volcano beneath MVC	? buried and/ or destroyed	?
1.68 — **Period 1** earliest ignimbrite volcanism	Ignimbrite C	very poorly exposed outcrop	explosive andesitic eruption producing pyroclastic flow	> 10	30 - 100
1.55	Ngaroma Ignimbrite	poorly exposed outcrop	explosive pyroclastic flow forming eruption	> 50	100 - 300
1.53 — **Intracaldera effusive volcanism**, (although a single dome is mapped, multiple are inferred to have existed)	Ignimbrite B	very poorly exposed outcrop	explosive pyroclastic flow forming eruption	?	30 - 100
1.27	Tumai lava dome	mapped	effusive activity	< 0.1	?
1.21 — **Period 2** intense volcanism with 2 caldera forming eruptions	Ongatiti Ignimbrite	exposed outcrop	most voluminous eruption causing caldera collapse and formation	> 300	300 - 1000
1.20	Unit D fall deposit	exposed outcrop	phreatomagmatic eruption producing widespread fall deposit	> 10	100 - 300
1.18	Ahuroa Ignimbrite	exposed outcrop	explosive & energetic pyroclastic flow forming eruption	> 50	100 - 300
1.01	Kidnappers/ Unit E fall deposit and overlying ignimbrite	poorly exposed outcrop	phreatoplinian eruption producing the most widespread deposit derived from the MVC	> 300	100 - 300
0.97	Rocky Hill Ignimbrite	exposed outcrop	most voluminous eruption causing caldera collapse and formation	> 300	300 - 1000
0.92 ?	Kaahu Ignimbrite/ Unit H	poorly exposed outcrop	explosive pyroclastic flow forming eruption	< 0.5	?
0.95 — **Intracaldera effusive volcanism,** (amount is unknown)	Marshall Ignimbrites	exposed outcrop	explosive pyroclastic flow forming eruption	> 50	?
0.87	Whakaahu lava dome	mapped	effusive activity	< 1	?

The exact distribution of the explosive, more commonly exposed deposits derived from the MVC is poorly understood and underestimated. The distal, poorly to non-welded portions of the ignimbrites and associated fall deposits are extensively eroded and weathered. Therefore the current preservation is restricted to the proximal to medial more resistant and welded to partially welded portions (Briggs et al. 1993).

The distribution of the individual ignimbrite deposits is documented in more detail in chapter 2. However as Briggs et al. (1993) describe, on a broader scale, the deposits derived from the MVC were constrained to the north, west and south of the caldera where they transformed the landscape into thick ignimbrite plateaux leaving only the highest Mesozoic ranges and older volcanoes exposed. Traces of the most voluminous MVC ignimbrite deposits (Ongatiti, Rocky Hill and Marshall Ignimbrites) are present in deep drill holes to the east of the MVC. Therefore these ignimbrites were deposited to the east but have been partly buried by younger (mainly the Whakamaru Group) ignimbrites and/or partly eroded during the uplift of the axial ranges (Briggs et al.1993).

1.7 Taupo Volcanic Centre

1.7.1 Introduction

The Taupo Volcanic Centre (TVC) is one of the two currently active calderas within the TVZ. Okataina is the other and they are both situated at the southern and northern boundaries respectively of the central TVZ. The TVC is a very young and highly active centre which has been active for the past 350 – 320 ka and is considered to be the most active and productive rhyolitic centre on Earth. Over the last 65 ka it has had an eruption rate estimated at 6.5 km^3/ky where the repose periods between eruptions are short lived (Sutton et al. 1994, Spinks et al. 2005).

1.7.2 Volcanic evolution and eruption history

Sutton et al. (1994) explain that the Taupo Volcanic Centre has developed as a composite magmatic system with considerable diversity in the style and type of relatively small scale volcanism. 95 % of the erupted volume has been generated

during separate eruptions as compositionally distinct rhyolite magma. However, basalt, andesite and dacite compositions have also been produced. Rather than tapping a single gradually evolving magma chamber, eruptions are controlled by multiple and relatively small volumes of separate magma bodies entering into the upper crust briefly before being erupted at the surface. This is the most plausible explanation for the high production rate and diversification in magma produced in the TVZ (Sutton et al. 1994).

Through the earliest record of the TVC and through to 65 ka, eruptions were confined to comparatively small scale (> 1 km^3) dome building eruptions with minor production of pyroclastic deposits (Sutton et al. 1994). Wilson et al. (1994) infer that this period included at least one caldera forming eruption. Both the frequency and explosiveness of the eruptions progressively increased from approximately 60 ka through to 26.5 ka where the most significant eruption (Oruanui) in terms of the history of the TVC took place where > 400 km^3 of material was ejected (Sutton et al. 1994). The Oruanui eruption as Sutton et al. (1994) explain, marked the major turning point in the development of the TVC. There was a significant change in the centre both structurally, as the eruption resulted in the formation of the current caldera and the modern Lake Taupo, and magmatically, where the volcano has been frequently more active since then. There have been 28 eruptions since, and 25 of these took place in the last 12,000 years. Only one eruption did not result in the production of pyroclastic deposits (Sutton et al. 1994, Wilson et al. 1995). The Taupo eruption (1.7 ka) was the next most significant event since 26.5 ka where further caldera collapse took place in the northeast (Sutton et al. 1994). There has been a period of quiescence for the last 1.7 kyr, although Rowland et al. (2010) mention that in the last 100 years, there have been 3 separate periods of earthquake swarm activity and surface deformation/ faulting recorded in the TVC.

1.8 The geological evolution of the Central Te Kuiti Basin (King Country Region)

1.8.1 The current geological setting

The mean topography over the King Country is approximately 200 – 300 m above sea level (Kamp et al. 2004), but it reaches up to 1100 m above sea level along the eastern volcanic uplands (Wilson et al. 1986b, Edbrooke 2005). These are the major landscape and principal structural elements (Fig 1.6) forming the eastern boundary of the Te Kuiti Basin (Blank 1965). The eastern volcanic uplands consist of uplifted blocks of Mesozoic greywacke basement (Hauhungaroa and Rangitoto Ranges) and a thick succession of Quaternary ignimbrites (Pakaumanu and Whakamaru Group) (Wilson et al. 1986b, Edbrooke 2005).

The north-west tilted ranges are composed of Waipapa terrane rocks or more specifically the Manaia Hill unit and are extensively covered by these Quaternary ignimbrites (Blank 1965, Edbrooke 2005). To the east of the ranges, the Oruanui Formation and the Whakamaru and Pakaumanu Group ignimbrites are the most dominant units outcropping in and around the Mangakino and Taupo basins. To the west of the ranges, the Manaia Hill unit rocks disappear beneath the thick ignimbrite plateaux, (Pakaumanu and Whakamaru Group ignimbrites) and beneath the Tertiary Sedimentary rocks further to the west (Blank 1965, Edbrooke 2005). There are however several smaller (down to < 1 km^2 in area) isolated hills and ridge caps of the Manaia Hill rocks found to the west above the Tertiary sedimentary rocks (Wilson et al. 1986b, Edbrooke 2005). The Tertiary sedimentary rocks within the central Te Kuiti Basin are found outcropping to the west of the eastern volcanic uplands. They consist of the shallow dipping to subhorizontal late Eocene – Oligocene Te Kuiti Sequence and early Miocene (Otaian) Mahoenui Group/ sequence (Kamp et al. 2004).

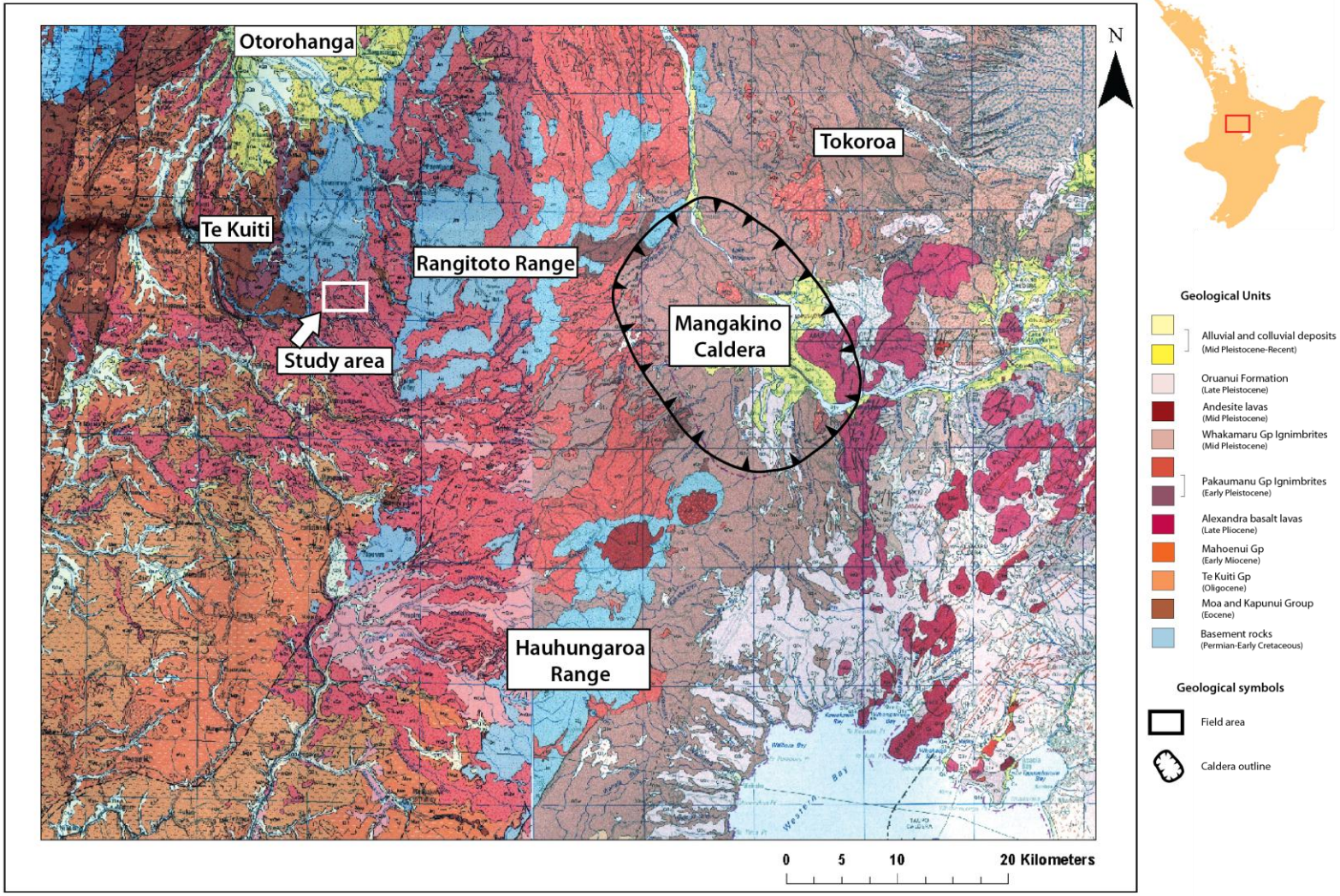

Figure: 1.6: A map of the current geological setting of the central Te Kuiti Basin to the east and part of the central North Island to the west of the Mangakino Caldera. Note the location and geology of the study area (highlighted) with respect to the surrounding geology, townships and the source area (Mangakino Caldera). This map is adapted from the Waikato QMAP 1:250000, Map 4 (Edbrooke 2005).

It is poorly understood how far east these Tertiary sedimentary rocks extend. However based on the Waikato QMAP (Institute of Geological and Nuclear Sciences 1:250000 Geological Map 4) they have been mapped within a valley underlying the Pakaumanu Group Ignimbrites alongside the Rangitoto Range which is the maximum observed extent. Additionally, Wilson et al. (1986b) indicate that due to very few Tertiary sedimentary lithic clasts present within the Mangakino derived (Pleistocene aged) ignimbrites, no Tertiary sediments underlie the source area which is further to the east.

1.8.2 Geological Evolution

Edbrooke (2005) infers that during the late Jurassic and through into the Early Cretaceous before the break up of Gondwana, the Manaia Hill Group accumulated in a forearc basin as slope and basin floor fan deposits. The deposits consist of a massive to poorly bedded volcaniclastic sandstone with thin beds of siltstone and conglomerate interspersed. These sediments have been partially metamorphosed to form well indurated and fractured basement rocks below the Te Kuiti Basin (Edbrooke 2005). Wilson et al. (1986b) suggests that prior to deposition of the Tertiary marine sediments, some block faulting of the Manaia Hill unit in the King Country Basin must have taken place, and this is made evident by the localisation of Tertiary shallow marine – terrestrial facies onlapping them.

Kamp et al. (2004) infer that during the earliest Miocene (Otaian), the leading edge of the subducting Pacific Plate continued to migrate towards the southwest through the west coast of the North Island. Its position is marked by broad crustal downwarping which we see happening today in the South Wanganui Basin and Marlborough Sounds areas further to the southwest. The leading edge was located beneath the Te Kuiti region during the earliest Miocene which subsequently resulted in a dramatic pull down of the crust. The Te Kuiti area formed as a piggyback basin where the area subsided rapidly into bathyal depths within the depocentre. The basement terrane was over-thrust along the Taranaki fault and erosion of this material fed sediments eastwards into the basin, this deposit is recognised as the Mahoenui Group. A basal glauconitic mudstone deposit is conformable on the underlying Te Kuiti Group which represents a prominent

flooding surface of the basin. This basal unit is overlain by 1000 m or more of redeposited flysch or massive to weakly bedded calcareous to fine sandy mudstone which formed in outer shelf to mid bathyal settings (Kamp et al. 2004, Edbrooke 2005).

Once the leading edge of the subducted plate migrated further to the southwest, crustal shortening and associated reverse movement on the major fault systems resulted in the inversion and erosion of the Te Kuiti depocentre during the end of the Otaian to earliest Altonian (Late early Miocene) (Kamp et al. 2004, Edbrooke 2005).

Significant uplift and erosion intensified over the King Country Basin as the volcanic arc migrated from the NNE-SSW into the NE-SW orientation during the Pliocene-Pleistocene. The 2,500 m of uplift was created by tectonically driven long wavelength up-doming of the crust over the entire central North Island and was accompanied by a significant erosion episode which began prior to TVZ volcanism (Late Pliocene) through to present. Up to 2,000 m of Miocene strata from the King country has been removed and the magnitude of erosion reduces southward into the Wanganui Basin and westward into the eastern Taranaki region (Kamp et al. 2004, Edbrooke 2005, Stern et al. 2006).

A succession of Mangakino derived ignimbrite deposits (Pakaumanu Group) separated by minor erosion constructed ignimbrite plateaux within the King Country throughout the Pleistocene (1.68-0.95 Ma). The Rangitoto and Hauhungaroa Ranges have played a significant role as physical barriers in the distribution of these ignimbrites. The pyroclastic flows were mostly directed westwards through a fault-angle depression (Bennydale gap) in between the two ranges before they poured into the King Country, wrapping around the ranges and inundating the low lying areas. Poorly preserved ignimbrite deposits however, have spread across the ranges where few of the highly energetic flows managed to traverse across these and into the King Country. The Pakaumanu Group have in part been significantly eroded prior to 0.34 Ma to form local valleys > 300 m in depth. The Whakamaru Group Ignimbrites and the most recent Taupo Ignimbrite deposits have partly infilled these essentially modern day valley systems (Blank 1965, Wilson 1986a, Wilson et al. 1986b).

Chapter Two

Stratigraphy

2.1 Introduction

This chapter presents an overall description of the stratigraphy exposed in the Ongatiti Valley. Detailed stratigraphic descriptions are made on each geological unit exposed focusing on the Ngaroma, Ahuroa and Rocky Hill Ignimbrites. The Ongatiti, Unit D and Taupo Ignimbrites will be discussed in more detail in later chapters. The descriptions of each of the geological units are in stratigraphic order from the oldest to the youngest and are based on both previous literature and observations made within the study area.

2.2 Physiography and overall stratigraphy

2.2.1 Physiography

As shown on the geological map (Enclosure 1), the field area consists of deep valleys dissecting the thick ignimbrite plateau revealing significant exposure of 5 of the Mangakino Caldera derived eruptive deposits. The ridges are typically capped with flat tops or rolling hills depending on what ignimbrite is outcropping. The surface of the plateau has a shallow dip towards the west where the amount of preserved ignimbrite decreases and eventually disappears giving way to units of the Te Kuiti Basin.

Prominent and continuous bluffs of the welded to partially welded sections of the ignimbrites are best exposed in the Ongatiti Valley where the Ongatiti Stream has carved its way through the ignimbrite deposits (Fig. 2.1).

Figure 2.1: View across the Ongatiti Valley looking to the northwest through the study area, where the outcrops of the geological units are best exposed.

The steep sides of the valleys are scarred with multiple slump scarps and hummocky deposits fanning out at the base. As shown in Fig. 2.2, the areas less exposed to the dissection of the Waipa River and major stream systems consist of a combination of low angle slopes and soft depressions where the bluffs rarely outcrop.

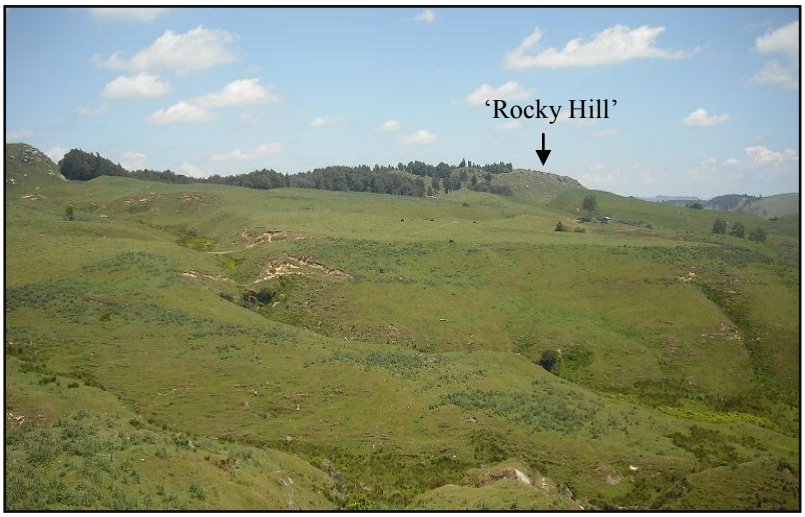

Figure 2.2: Slopes descending from the ridge capped by the Rocky Hill Ignimbrite. View to the southwest with the type locality 'Rocky Hill' (location 1, geological map) in the background.

2.2.2 Overall stratigraphy within the study area

It is difficult to determine the geology prior to the Quaternary volcanism of the MVC and the eruptions of the Pakaumanu Group flooding this area especially

because there is no exposure of it. However, as outlined within the previous chapter, this is inferred to be the Mahoenui and Te Kuiti Group overlying the Mesozoic Basement or more specifically, the Waipapa Terrane Rocks.

Four of the six formations within the Pakaumanu Group are found outcropping within this field area (Fig 2.3): Ngaroma Formation (Ngaroma Ignimbrite), Ongatiti Formation (Ongatiti Ignimbrite), Mangaoweka Formation (Unit D and Ahuroa Ignimbrite) and part of the Raepahu Formation (Rocky Hill Ignimbrite and the Kidnappers fall deposit and Ignimbrite), (Edbrooke 2005).

A description of the overall stratigraphy is within a location (location 2, geological map) where there is maximum exposure of the geological units. The Ongatiti Valley has a typical geomorphic pattern to it where there is a repetitive sequence of grass covered slopes receding back and into prominent bluffs. The pattern is strongly controlled by the variation in welding within and between the different geological units (Fig. 2.3).

The Ongatiti Ignimbrite is at the base with an alluvial terrace lapping up against it. The whole geological unit is recognised by transitioning from a weakly to a densely then back into a weakly welded deposit. The weakly welded Unit D fall deposit and associated ignimbrite overlies the Ongatiti Ignimbrite but is poorly exposed. Directly overlying this is the non-welded to densely welded Ahuroa Ignimbrite. The thin densely welded zone outcrops as a pronounced and continuous bluff. The grass covered gently receding slope above is inferred to be the poorly - partially welded basal to mid section of the Rocky Hill Ignimbrite, based on observed outcrop evidence within other locations of the field area (refer to geological map, location SL.4). At the top of the ridge, the prominent upper densely welded bluff of the Rocky Hill Ignimbrite outcrops. The widespread Kidnappers fall and overlying non-welded ignimbrite deposits may lie between the welded component of the Ahuroa and the Rocky Hill Ignimbrites but is not exposed, hence the Kidnappers fall deposit and ignimbrite have not been mapped.

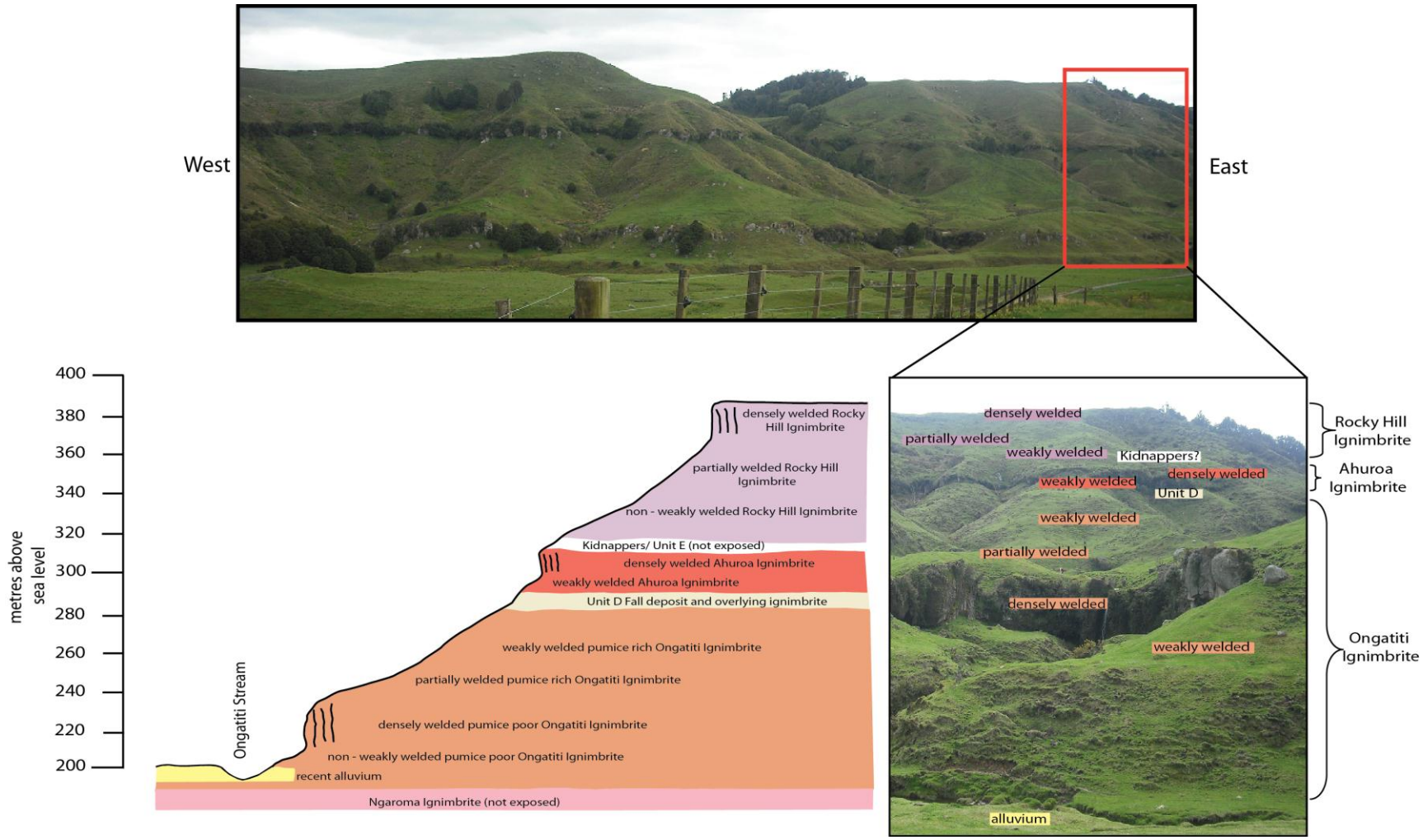

Figure 2.3: Geomorphic profile of the Ongatiti Valley showing prominent vertical bluffs of densely welded units, and approximately 25° slopes of partially to weakly welded units.

There has been a deeper incision and therefore additional geological units are exposed within the Waipa River Valley. However it is densely vegetated and less accessible to distinguish the boundaries between the units and was less favourable than the Ongatiti Valley to produce a profile of the overall stratigraphy. The partially welded zone of the Ngaroma Ignimbrite outcrops beneath the weakly welded base of the Ongatiti Ignimbrite in the Waipa River Valley. The non-welded Taupo Ignimbrite forms a thick terrace above recent alluvial gravels on the valley floor and onlaps the Ngaroma Ignimbrite.

2.3 Ngaroma Ignimbrite

2.3.1 Introduction

The Ngaroma Ignimbrite was sourced from the Mangakino volcanic centre during the earliest period of ignimbrite volcanism of the TVZ. It has an age of 1.55 ± 0.05 m.y. (Houghton et al. 1995). The Ngaroma Ignimbrite is poorly exposed and rarely exceeds 20-30m thick. Its distribution is relatively widespread (Fig 2.4) which suggests it was emplaced energetically (Wilson 1986a). The Ngaroma Ignimbrite typically overlies Mesozoic Basement greywacke of the Rangitoto Range and less commonly Tertiary sedimentary rocks (Wilson et al. 1986b, Edbrooke 2005 and Leonard et al. 2010).

Most previous descriptions of the Ngaroma Ignimbrite are of the partially-welded proportion of the ignimbrite. However it is exposed along Mangaokewa Road with having a 2 metre non-welded base and an 8 metre thick welded upper unit (Wilson et al. 1986b). The Ngaroma Ignimbrite has been described as a pastel pink, purple or brown, pumice-rich ignimbrite with obvious eutaxitic textures. It has suffered intensive weathering, devitrification and vapour phase alteration and therefore has abundance of recrystallised secondary minerals which give it a distinctive chalky texture (Blank 1965, Wilson 1986a and Wilson et al. 1986b, Dyah Hastuti 1992 and Edbrooke 2005).

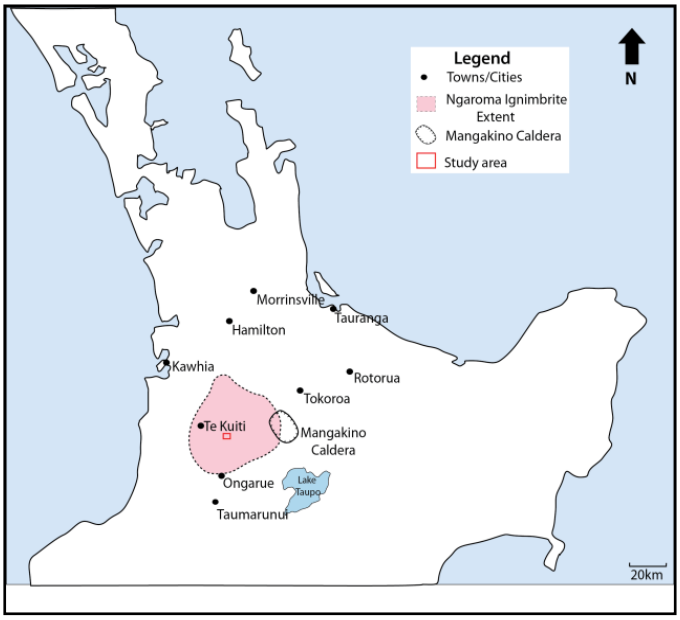

Figure 2.4: The maximum extent of the Ngaroma Ignimbrite based on observations by Briggs et al. (1993), Edbrooke (2005) and Leonard et al. (2010) of the welded proportion of the Ngaroma Ignimbrite.

2.3.2 Distribution within the study area

There is only one location where the Ngaroma Ignimbrite is exposed and this is within the Waipa River Valley along the western boundary of the field area at an elevation of 180 metres above sea level. At this locality the basal contact is not exposed and the ignimbrite is estimated to be about 30 metres thick. It is overlain by the non to weakly welded base of the Ongatiti Ignimbrite.

2.3.3 Lithology

Due to very poor exposure of a complete profile through the Ngaroma Ignimbrite, no stratigraphic log was produced and samples were collected from only one stratigraphic elevation within the deposit. The ignimbrite has a distinct pale pink to purple matrix, with cream to yellow pumice clasts and dark purple lithics (Fig 2.5). It is densely welded but strongly weathered to an unusual clay and chalky texture. Pumice abundance is about 20% and the average clast size ranges between 10-20mm.

In thin section, the pumice clasts are mostly elliptical, but some are lenticular and fiamme like. The pumice crystal content is low (<5%) and the glass is extremely

devitrified (Fig 2.6). The internal structures of the clasts have been completely destroyed and re-crystallisation has produced spherulitic textures.

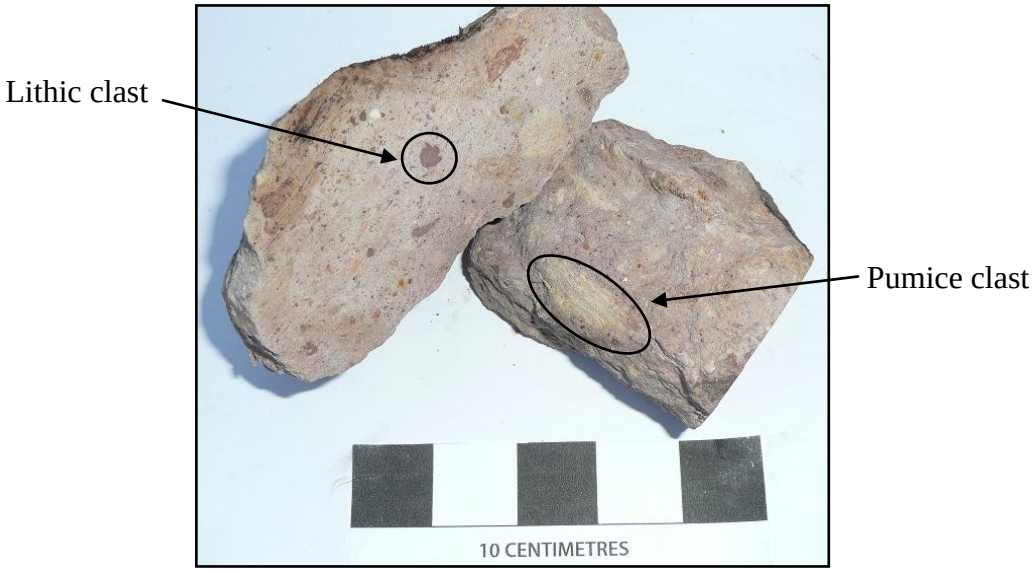

Figure 2.5: Ngaroma Ignimbrite at location 3, geological map. Note the scale bar represents a width of 10 centimetres.

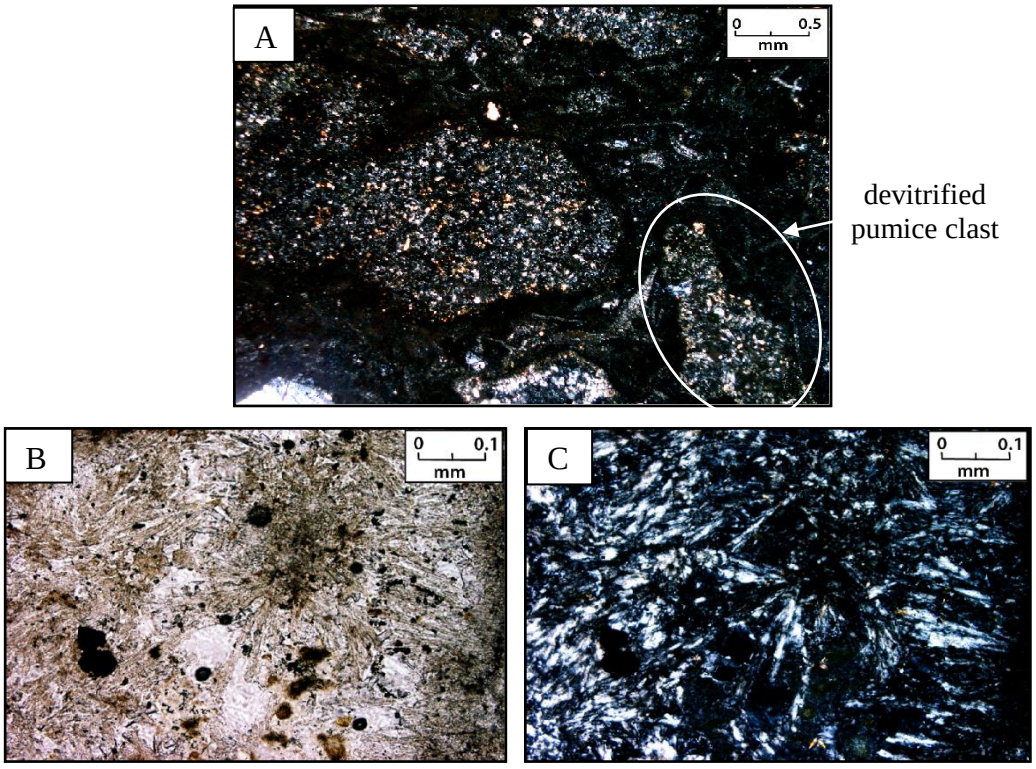

Figure 2.6: (A) Pumice clasts showing a high degree of devitrification (cross polarized light). (B) Devitrified pumice showing spherulitic textures and absence of vesicles (plane polarized light). (C) Same view as B under cross polarized light.

The lithic abundance is 3-4% which is relatively high in comparison to the other Mangakino derived ignimbrites. They predominantly consist of greywacke and argillite with a few andesite clasts. The bulk crystal abundance constitutes 8% within this sample where the dominant crystals present are plagioclase (> 85%) with minor quartz and opaque crystals and traces of orthopyroxene and zircon.

The glass shard matrix shows obvious signs of alteration. It is poorly vitriclastic and has minimal preserved evidence of devitrification. The textures of the glass shards are poorly outlined and the groundmass is homogenous with few specks of limonite throughout.

2.4 Ongatiti Ignimbrite

2.4.1 Introduction

The Ongatiti is one of the most voluminous ignimbrites within the TVZ and was formed during a major caldera forming eruption from the Mangakino Volcanic centre 1.21 ± 0.04 m.y. ago (Wilson 1986a, Houghton et al. 1995 and Leonard et al. 2010). The partially–welded proportion of the ignimbrite is very extensive (Fig 2.7). Outcrops of the welded component have been located at the west coast near Kawhia, to the Bay of Plenty coast within the Tauranga Basin west of Wairoa River, and as far north as Ngaruawahia and just south of Ongarue. All older ignimbrites were covered by this deposit, with only the upland greywacke terrain escaping burial (Blank 1965). The Ongatiti Ignimbrite is a very thick deposit, reaching up to a 100 metres within the Ongatiti Valley. It is found overlying the Ngaroma Ignimbrite, Mesozoic Basement, and Tertiary sedimentary rocks (McGrath 2004 and Edbrooke 2005).

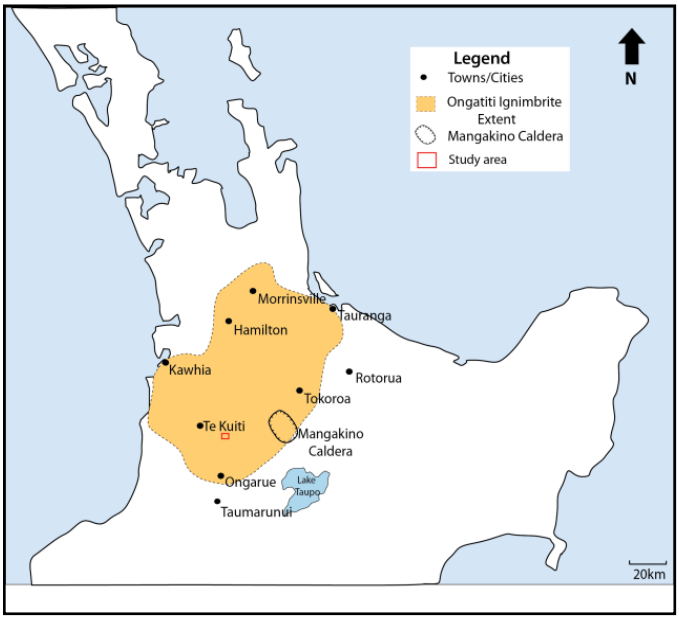

Figure 2.7: Distribution of the welded proportion of the Ongatiti Ignimbrite (Briggs et al. 1993, Edbrooke 2005, Leonard et al. 2010).

2.4.2 Distribution within the study area

The Ongatiti Ignimbrite is distributed throughout the field area underlying the poorly welded base of the Ahuroa Ignimbrite or less commonly Unit D. In the Waipa River Valley it stratigraphically overlies the Ngaroma Ignimbrite but throughout the rest of the field area, there is no evidence for the underlying geological unit. Along the south-eastern boundary of the field area where the topographic elevation reduces, the Ongatiti Ignimbrite is the only geological unit found outcropping. The thickness of the ignimbrite ranges from 40 to 60 m but reaches up to 100 m in the Ongatiti Valley. The lithology of the Ongatiti Ignimbrite is complex and is described in detail in chapter 3.

2.5 Unit D

2.5.1 Introduction

Unit D was sourced from the Mangakino Caldera as a large scale phreatoplinian style eruption 1.20 ± 0.04 m.y. ago (Wilson 1986a, Houghton et al. 1995 and Edbrooke 2005). The deposit is very rarely exposed due to its thin and non-welded nature and therefore its distribution is poorly defined. The few exposures

of Unit D are found stratigraphically overlying the weakly welded Ongatiti Ignimbrite (Wilson 1986a, Moyle 1989).

2.5.2 Distribution within the study area

Unit D has only been observed at three localities in the study area overlying the Ongatiti Ignimbrite. It ranges between 1.5 - 3 m in thickness and is described in detail in chapter 4.

2.6 Ahuroa Ignimbrite

2.6.1 Introduction

Houghton et al. (1995) has dated the Ahuroa Ignimbrite at 1.18 ± 0.02 m.y. The ignimbrite is not as voluminous as the Ongatiti or Rocky Hill Ignimbrites and is described as a thin (up to 20m) non-welded to densely welded veneer deposit. It has a widespread distribution as shown in Fig. 2.8 and typically overlies the Ongatiti Formation as a horizontal cap but is also found onlapping uplifted Mesozoic Basement rocks (Leonard et al. 2010).

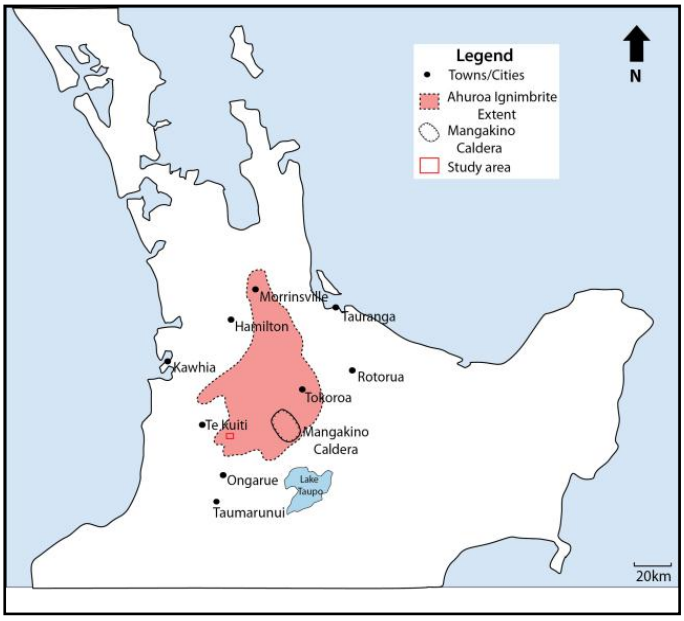

Figure 2.8: The maximum extent of the welded proportion of the Ahuroa Ignimbrite based on observations by Briggs et al. (1993), Edbrooke (2005) and Leonard et al. (2010).

The Ahuroa Ignimbrite is inversely thermally zoned, consisting of a lower non-welded base grading to partially-welded and a densely welded lenticulite top

(Wilson 1986a, Briggs et al. 1993, McGrath 2004 and Edbrooke 2005). One of the distinguishing features of the Ahuroa Ignimbrite is its non-welded base which is often referred to as the 'sandy black' due to its dark grey to black vitric appearance and this gradually fades into a pale grey to buff colour within the microfractured upper unit. The Ahuroa Ignimbrite is very distinctive with the presence of numerous types of juvenile pumice clasts. McGrath (2004) segregated these into 5 different types which have very high aspect ratios within the upper unit. In terms of its petrography, it tends to be dominated by feldspars and lacks the presence of quartz which is unique to the Mangakino derived eruptives (Wilson 1986a, Briggs et al. 1993, McGrath 2004 and Leonard et al. 2010).

2.6.2 Distribution within the study area

The distribution of the Ahuroa Ignimbrite within the mapping area is constrained to elevations greater than 260 metres above sea level. It is laterally extensive; the outcrops are present throughout the study area directly overlying either the Unit D or the upper Ongatiti Ignimbrite. It is however absent in the southwest - west of the study area where the Ongatiti Ignimbrite is only found outcropping. The thickness of this geological unit varies between locations from 4-5 m to a maximum of 20 m.

2.6.3 Outcrop appearance

The appearance of the Ahuroa Ignimbrite is fairly uniform throughout the field area. The lower non to poorly welded base forms a gentle slope which transitions into densely welded and very pronounced bluffs forming flat mesas (Fig. 2.9).

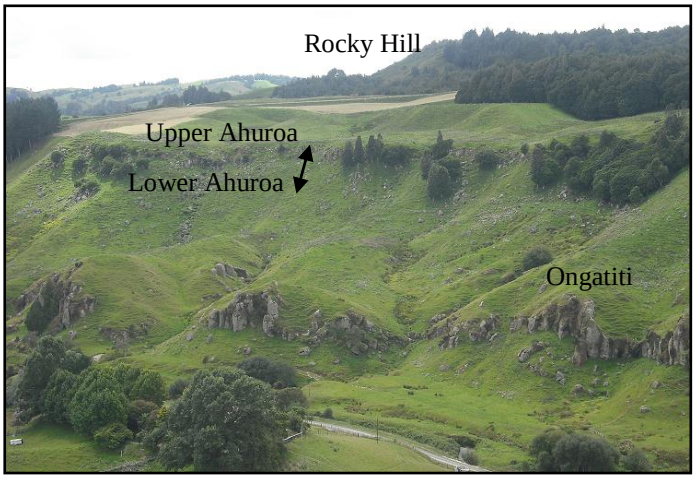

Figure 2.9: The typical outcrop appearance of the Ahuroa Ignimbrite when the Rocky Hill Ignimbrite is not completely overlying it.

The upper densely welded zone has a hackly fracture pattern with abundant horizontal and vertical joints (Fig. 2.10A and B). It is therefore often affected by limonite staining and weathering, and forms small (1-2 m) angular boulders which tend to litter the base of the outcrops (Fig. 2.10C).

2.6.4 Lithology and petrographic description of the Ahuroa Ignimbrite

The best exposure within the study area of the most complete and accessible profile through the Ahuroa Ignimbrite is located at SL.10 (refer to geological map). Here the Ahuroa Ignimbrite (Fig 2.11) is 10 m thick and increases in welding up through the profile. The appearance of the matrix grades from very dark brown at the base (Fig.2.12A), to a beige at the top (Fig 2.12B). The deposit is massive with no clast concentration zones. The abundance and size of the lithic and pumice clasts tend to increase vertically upwards through the ignimbrite.

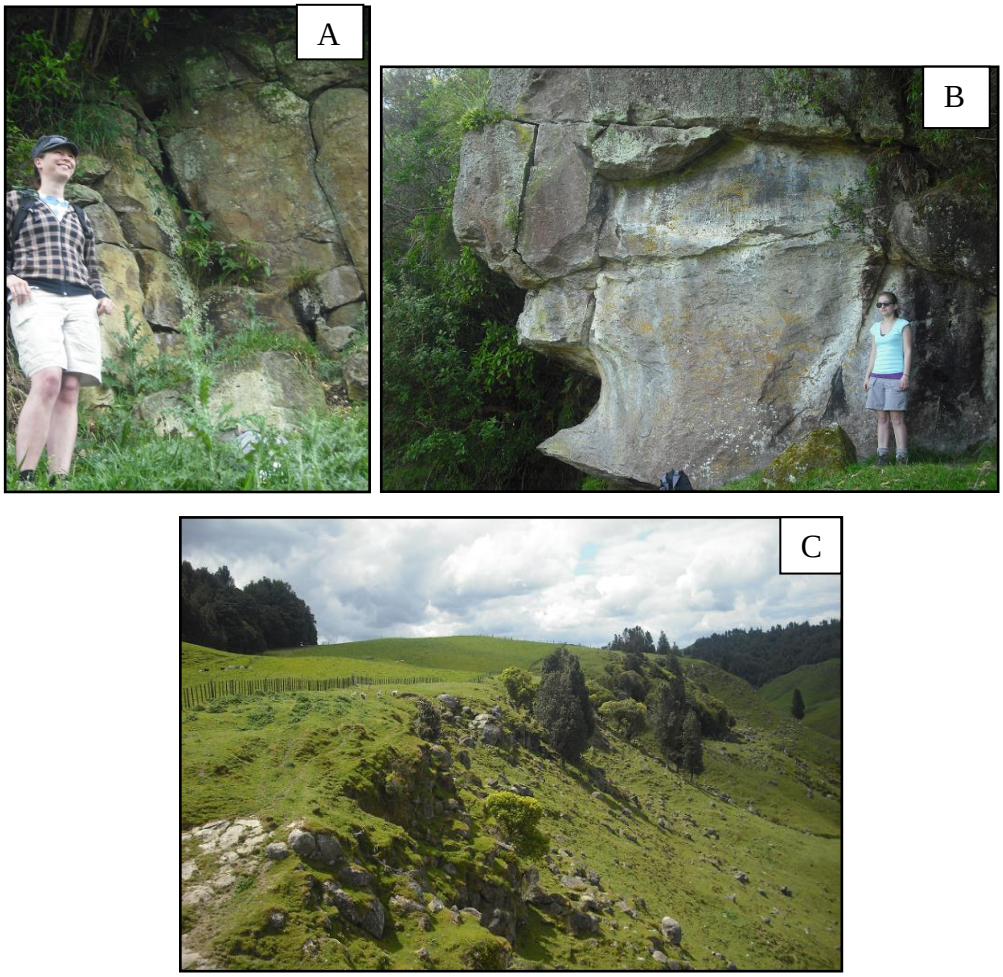

Figure 2.10: Closely spaced vertical and horizontal jointing in the upper welded Ahuroa Ignimbrite (A) and (B), and the typical weathering pattern of the outcrops (C).

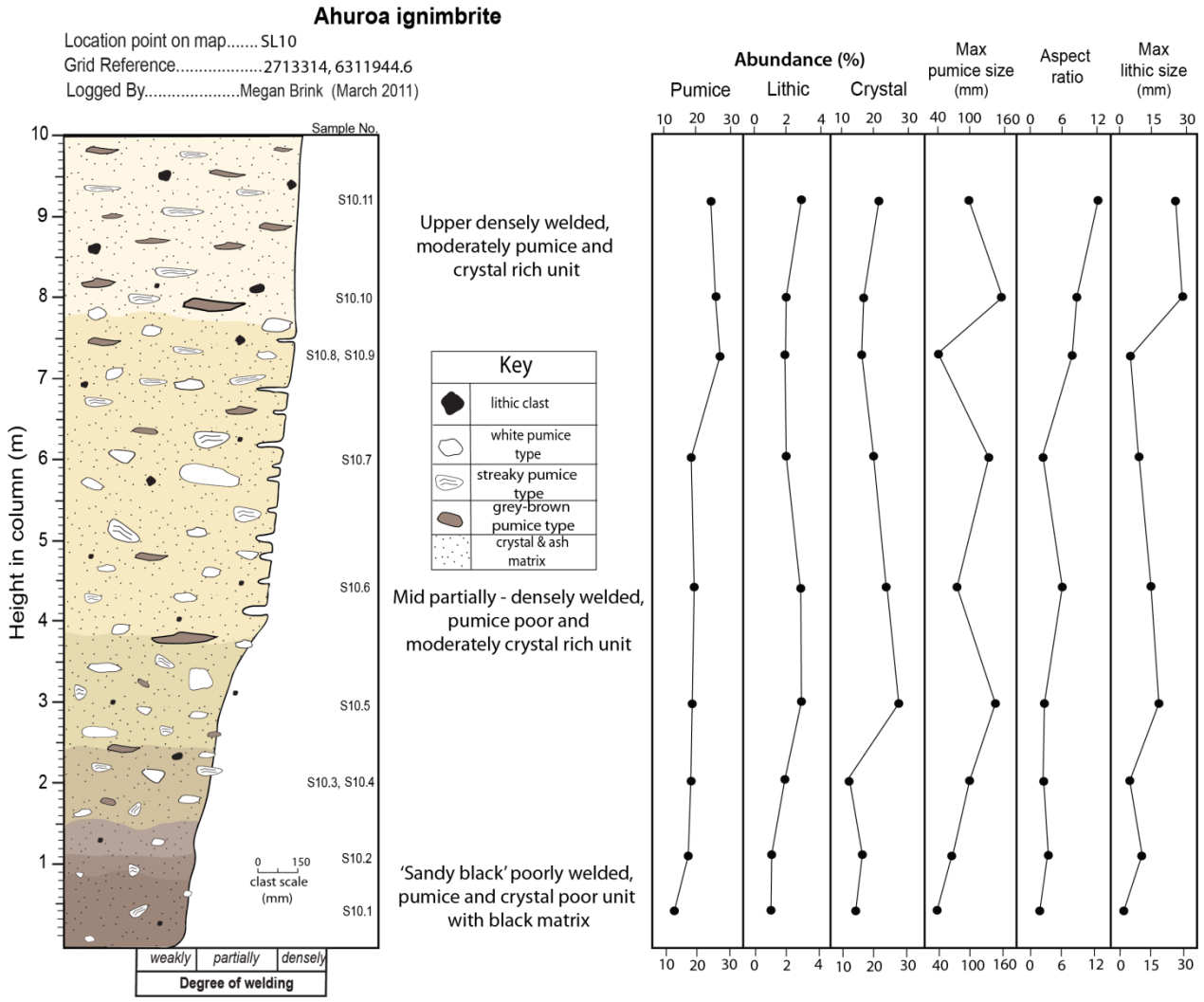

Figure 2.11: Stratigraphic log through the Ahuroa Ignimbrite within the study area, highlighting the degree of welding (horizontal scale) and variation in colour. The abundance of pumice, lithics and crystals, maximum pumice size, average aspect ratio of pumice clasts, and maximum lithic size are plotted against the log. Note the pumice and lithic abundances are bulk rock visual field estimates, whereas crystal abundances are of the matrix based on point counting.

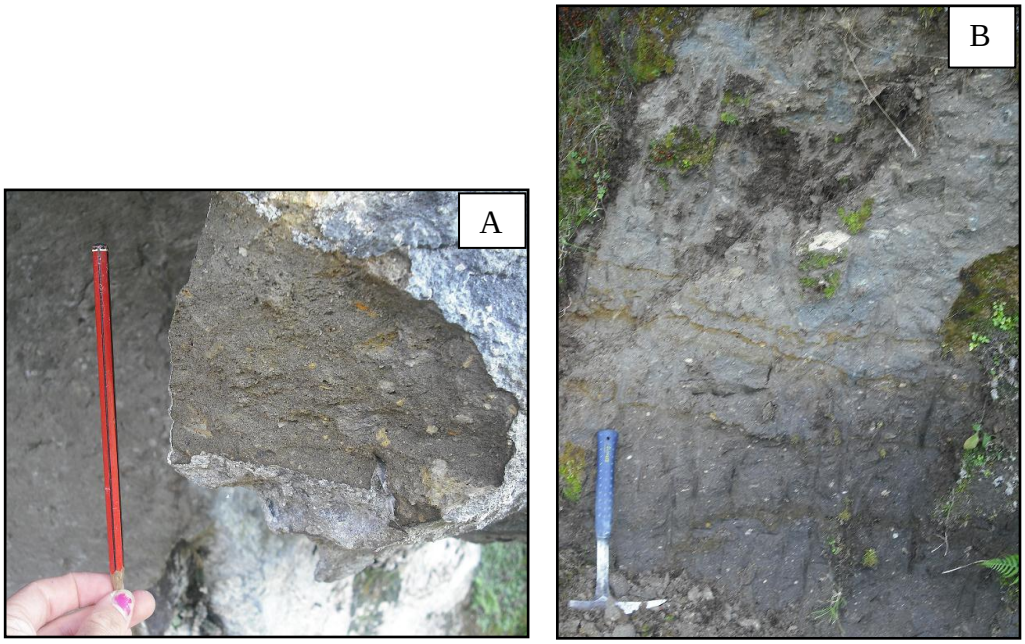

Figure 2.12: The base of the Ahuroa Ignimbrite has a distinct black appearance (A) which grades into a light grey in the upper section of the basal zone (B).

There is a general increase in the quantity and aspect ratios of the pumice clasts up the stratigraphic log, with a more divergent increase from the mid to upper proportion of the profile. The largest pumice clast sizes (Fig. 2.13) are within the mid – upper section where they are > 160 mm in diameter, and the overall average size is 30-50 mm. The aspect ratio of the pumice clasts reaches up to 12 within the uppermost section (Fig. 2.13).

Figure 2.13: Ahuroa Ignimbrite 3-4 m from the base. The clast sizes of both type 1 and 2 pumice can be some of the largest within the deposit.

At this type section of the Ahuroa Ignimbrite, there are three types of pumice (Fig 2.14): (1) a common white, dense and moderately crystal rich type , (2) a common grey to brown, dense pumice with a high aspect ratio and (3) a less abundant streaky, fibrous and vesicular type.

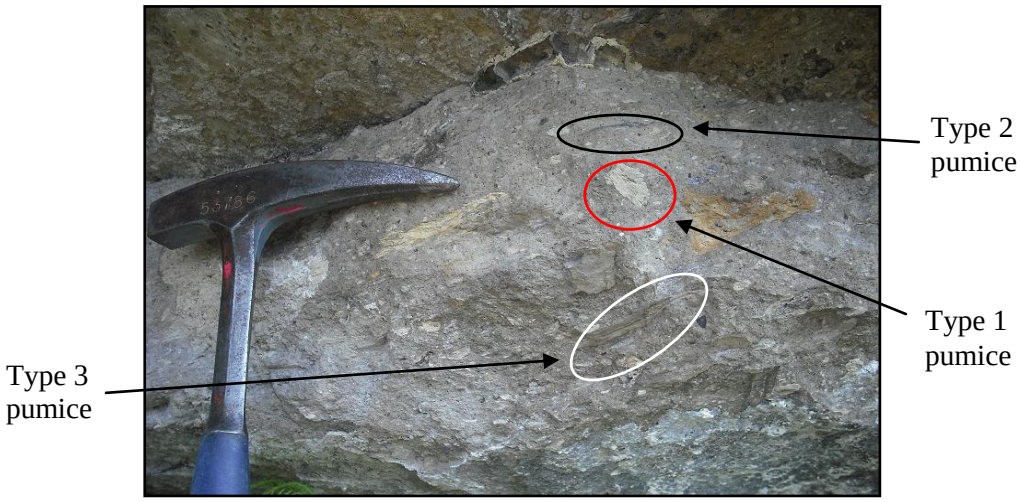

Figure 2.14: Ahuroa Ignimbrite 8-9 m from the base. The aspect ratios of types 2 and 3 pumice are very high, the abundance of type 1 pumice is minimal and the clasts have significantly lower aspect ratios in comparison.

All pumice clasts are crystal poor (< 5%) but there is an upward increase in crystal abundance in the type 1 pumice (10-12%) between 3 - 5 m. The abundance of the type 3 pumice tends to increase whilst type 1 tends to decrease up the profile and is absent from the uppermost proportion. Type 2 is absent from the base of the outcrop and is most common within the mid - upper section. There are three typical textural differences made evident under the microscope. The most common is wispy, fibrous and highly vesicular (Fig 2.15A). The vesicles are very elongated and increase in aspect ratio in the upper densely welded zone of the deposit. In the upper zone, the pumice clasts often tend to deform around the phenocrysts (Fig 2.15B), or have in some cases completely shattered or fractured them. The other two types are less common, both being smaller, fairly spherical in shape and less vesicular. One is very dense and highly devitrified (Fig 2.15C) and the other is moderately vesicular with spherical vesicles (Fig 2.15D).

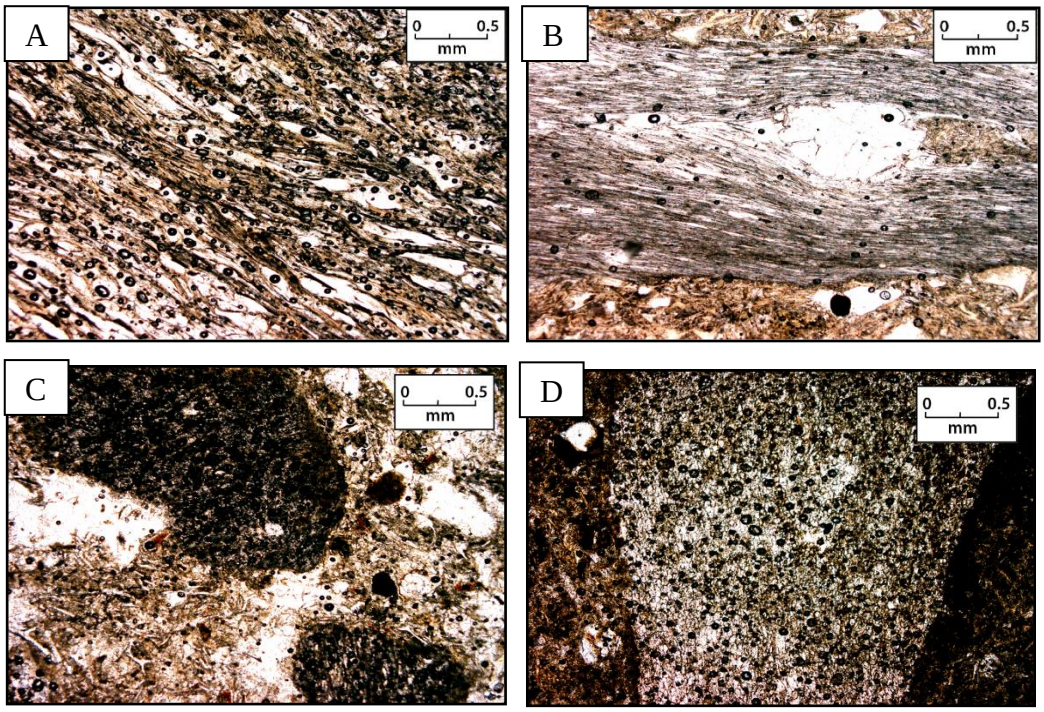

Figure 2.15: The typical structural features of the pumice clasts in the Ahuroa Ignimbrite: (A) wispy and fibrous vesicles; (B) wispy and vesicular texture deformed around phenocryst; (C) spherical clast shape and poorly vesicular; (D) spherical clast shape and moderately vesicular.

Both the abundance and maximum size of the lithic clasts increase up the stratigraphic profile of the Ahuroa Ignimbrite. The largest lithic clasts and the highest abundance are found within the upper 2 metres where the maximum-sized lithics were measured up to 70 mm in diameter. The most common type of lithic present is glassy and porphyritic rhyolite. Welded ignimbrite (Ongatiti Ignimbrite), greywacke, argillite and fine-grained and highly devitrified cream-beige rhyolite clasts are also present.

The crystal content within the matrix is poor at the base of the outcrop (< 15%) and this significantly increases within the mid section and tends to remain fairly consistent around 25% through to the top of the profile. Plagioclase is the most dominant (85-90%) mineral present within all of the samples collected throughout the stratigraphic log. Fe – Ti oxides, orthopyroxene and hornblende are also present.

The glass shard matrix is compact throughout the section typically with elongated platy and the occasional Y-shaped and lunate shards. The level of devitrification

and welding within the matrix tends to decrease then increase respectively up the profile. Therefore within the uppermost part of the deposit, the shards become deformed and have developed a eutaxitic texture.

2.7 Rocky Hill Ignimbrite

2.7.1 Introduction

The Rocky Hill Ignimbrite eruption took place 1.00 ± 0.05 m.y ago (Houghton et al. 1995). The welded sections of the Rocky Hill Ignimbrite have a widespread distribution (Fig 2.16) however it is severely eroded in comparison to the Ongatiti and Ahuroa Ignimbrites. Blank (1965), Briggs et al. (1993) and Edbrooke (2005) describe its distribution as isolated and scattered eroded caprock hills resting on either the Ongatiti or Mangoweka formations, on Mesozoic basement, or on Tertiary sedimentary rocks.

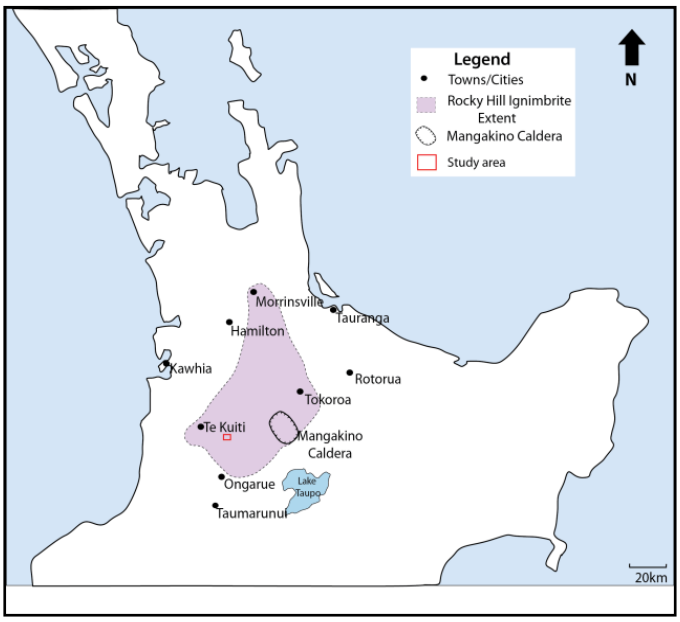

Figure 2.16: The maximum extent of the welded proportion of the Rocky Hill Ignimbrite based on observations by Briggs et al. (1993), Edbrooke (2005) and Leonard et al. (2010).

The most distinct characteristic of the Rocky Hill Ignimbrite, which is similar to the Ahuroa Ignimbrite is the inverse thermal zonation where the degree of welding increases up the profile. The Ignimbrite has been previously described (Moyle 1989) as consisting of two units, each with a distinct lithology where no flow boundaries are present or at least obvious. The basal vitriclastic layer grades

into a partially welded base where the pumice protrudes out of the outcrop and this is capped by a densely welded and hackly fractured top which can be up to 25 m thick. The ignimbrite is pumice and crystal rich and is further characterised by having streaky pumices with glomeroporphyritic clots of crystals with conspicuous hornblende (Blank 1965, Wilson 1986a, Moyle 1989, Edbrooke 2005).

2.7.2 Distribution within the study area

The Rocky Hill Ignimbrite is always found overlying the Mangoweka Formation in the study area and forms the major ridge tops where the elevation is greater than 300 metres above sea level, and its maximum thickness reaches up to 80 m. Towards the north west of the area, the outcrops become slightly more sporadic and less continuous, and the thickness significantly reduces to approximately 40 m.

2.7.3 Outcrop appearance

The outcrop appearance of the Rocky Hill Ignimbrite is similar to the Ahuroa Ignimbrite in the fact that it shows reverse welding but it is over a greater thickness. The lower weakly to partially welded zone of the deposit is mostly not exposed and appears as a grass covered receding slope. However where it is exposed the jointing is widely spaced and the Ignimbrite suffers differential erosion (Fig 2.17).

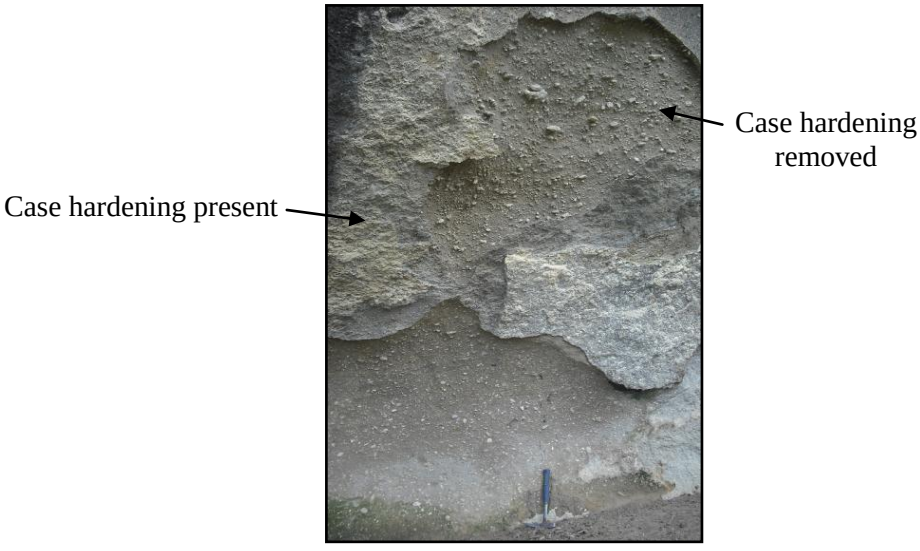

Figure 2.17: The lower weakly welded base of the Rocky Hill Ignimbrite showing variation in case hardening and erosion (location SL.4, geological map).

There are several different outcrop patterns within the upper partially to densely welded zone exposed around the field area which made it very challenging at first to identify and track the Rocky Hill Ignimbrite. The geomorphology along the main ridge tops capped with the Rocky Hill Ignimbrite form very extensive and gently dipping plateaux to the west (Fig 2.18A,B) which are sometimes eroded and reduced to rounded hill tops (Fig 2.18C).

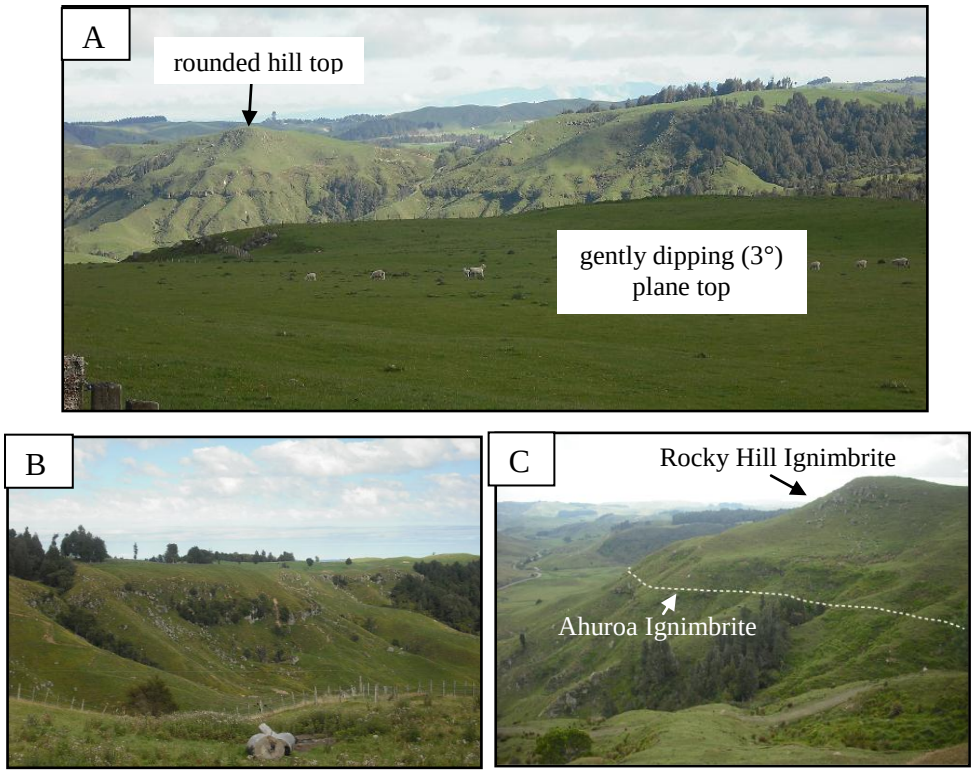

Figure 2.18: View to the northwest across the Ongatiti Valley; (A and B) the gently dipping plateaux of the Rocky Hill Ignimbrite, (C) the rounded hill remnants of the Rocky Hill Ignimbrite.

The upper densely welded zone of the Rocky Hill Ignimbrite forms a bench geomorphology similar to the Ahuroa Ignimbrite. The appearance of the outcrop varies between locations where the upper Rocky Hill Ignimbrite is either exposed with columnar jointing (Fig 2.19A) or with irregular and small (< 1 m) spaced jointing (Fig. 2.19B).

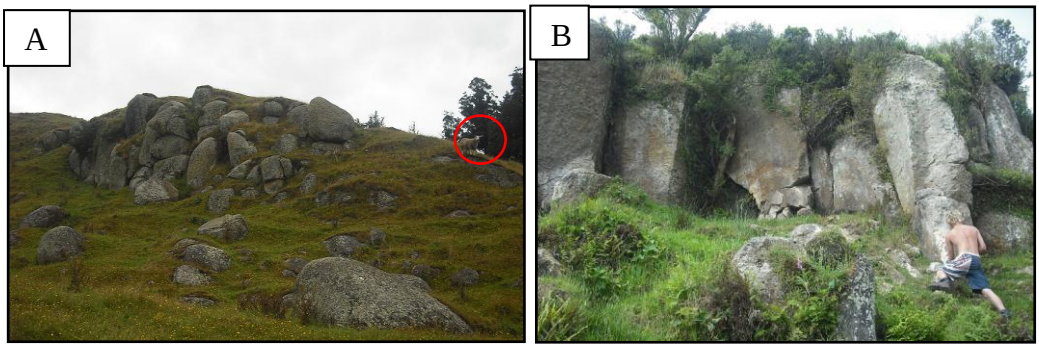

Figure 2.19: (A) Irregular jointing in densely welded Rocky Hill Ignimbrite as small bluffs with small fractures and joints, note the sheep for scale. (B) Bluffs of columnar jointing (location 4, geological map).

Remnants of the middle partially-welded proportion of the ignimbrite are found as scattered large disjointed angular boulders throughout the hill top (Fig. 2.20).

Figure 2.20: Large 2-3 metre wide angular boulders of the middle partially-welded zone of the Rocky Hill Ignimbrite, forming rounded hills along the ridge tops. This is the type locality of "Rocky Hill' along Aharoa Road (location 1, geological map).

2.7.4 Lithology and petrographic description of the Rocky Hill Ignimbrite

The best exposure within the study area of the most complete and accessible profile through the Rocky Hill Ignimbrite is at the location SL.4 (geological map), (Fig 2.21). Samples and measurements were collected from 1 - 3 m intervals over a fairly wide area (20 m) due to discontinuous outcrop. Between 10-16 m up the profile, the outcrop was not exposed and therefore no data or descriptions could be retrieved. The outcrop is 23 m high and shows an upwards increase in welding. The matrix grades from very dark brown to beige with an increase in height. The deposit is massive and shows an overall gradational increasing trend in abundance and modal size of pumice, lithics and crystals (Fig. 2.22).

The pumice abundance at the base of the outcrop is low and the clasts are mostly small (10-15mm) and rounded. Both the abundance and modal size of the clasts increase towards the middle zone where it becomes moderately pumice rich with few coarse (100 mm) clasts present. Within the upper zone, the deposit becomes progressively pumice rich and the clast aspect ratios show a steady increase up the profile. The maximum clast sizes and highest aspect ratios are within the upper 2 m of the outcrop, here the clasts are difficult to distinguish due to their extreme flattening (Fig. 2.21).

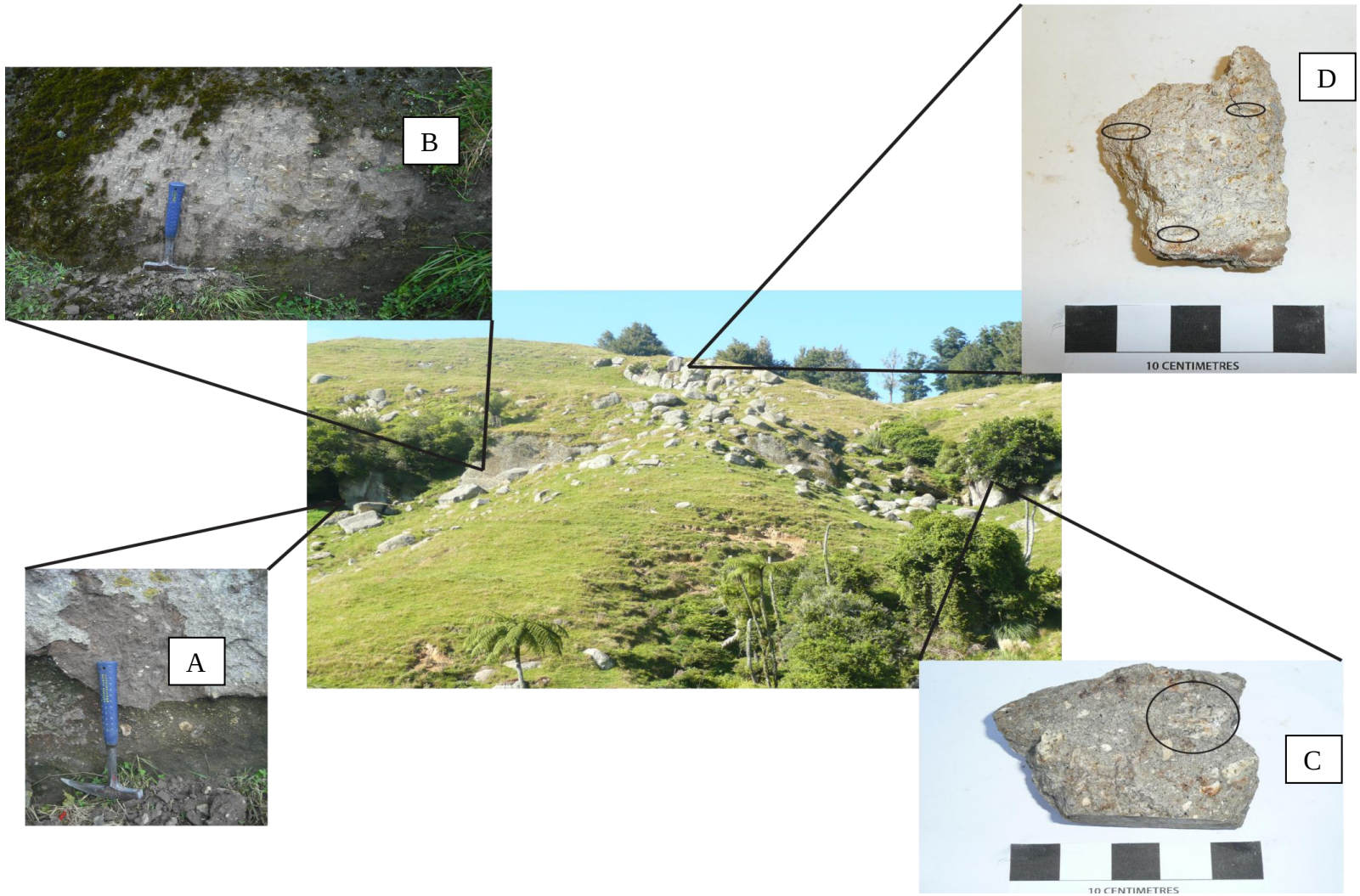

Figure 2.21: Site of stratigraphic description within the Rocky Hill Ignimbrite with examples of outcrops and hand specimens: (A and B) the lower zone is soft and non-welded. (C) the middle zone is partially welded with rounded pumice clasts (outlined). (D) the upper zone is densely welded with highly lenticular clasts (outlined). Note the scale bar used in the photos of the hand specimen represents 10 cm.

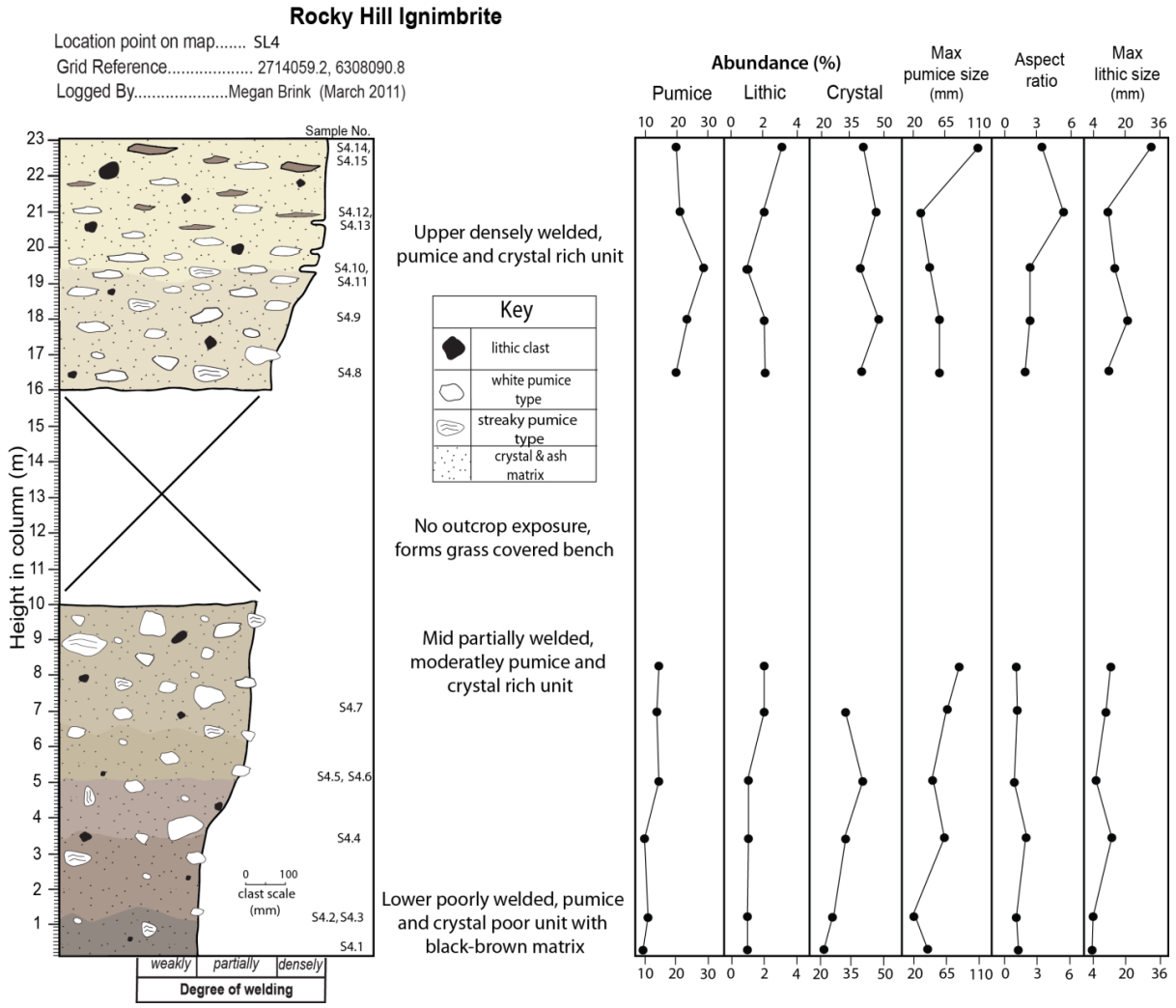

Figure 2.22: Stratigraphic log through the Rocky Hill Ignimbrite within the study area, highlighting the degree of welding (horizontal scale) and variation in colour. The abundance of pumice, lithics and crystals, maximum pumice size, average aspect ratio of pumice clasts, and maximum lithic size are plotted against the log. Note the pumice and lithic abundances are bulk rock visual field estimates, whereas crystal abundances are of the matrix based on point counting.

There are 2 types of pumice present: (1) a common (85%) white, dense, non to poorly vesicular and fibrous type, and (2) a moderate to highly vesicular, wispy and fibrous type, in which the larger clasts show alternating dark, poorly vesicular and light, highly vesicular streaky bands. Both clast types have a glomeroporphyritic texture (Fig. 2.23A,B). The crystal abundance within the pumice clasts increases from <5% in the lower 4 m where it reaches up to and remains at approximately 20% from 10 m up into the upper section. It is important to note that in the upper section, only the large and less flattened/ deformed pumice clasts contain crystals. The pumice clasts however are crystal poor in comparison to the crystal enrichment within the matrix.

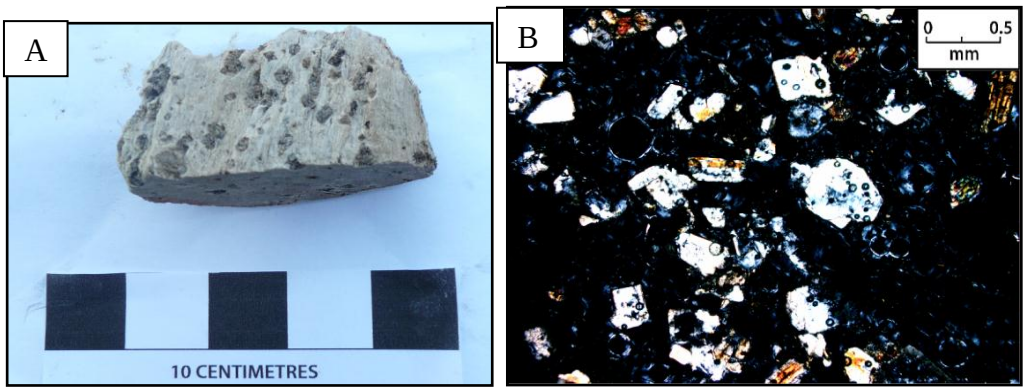

Figure 2.23: (A) crystal clots and glomeroporphyritic texture of type 1 pumice in the Rocky Hill Ignimbrite, note the scale bar represents 10 cm. (B) cross polarized light photomicrograph of the crystal clots; note the high concentration of small (mostly plagioclase) crystals.

The vesicularity of the pumice clasts tends to decrease upwards and the deformation around the larger phenocrysts also increases upwards. The clasts are mostly spherical in shape at the base and become more elongate to distinctly fiamme-like in the mid to upper zones respectively. The fiamme-like clasts are dense, fibrous, grey and contain spherulitic textures.

Lithics within the Rocky Hill Ignimbrite are not common but there is a slight increase in lithic clast size in the upper 2 m. The most common type of lithics are vitrophyric rhyolites and welded ignimbrite (Ongatiti Ignimbrite). However greywacke, argillite, porphyritic rhyolite, fine grained microdiorites, and fine grained amphibole and plagioclase-rich clasts are also present throughout.

The Rocky Hill Ignimbrite is crystal rich and the abundance of crystals tends to increase upwards through the deposit where it becomes very crystal rich (35-40%) within the upper welded zone. In order of most dominance: plagioclase (70%) >> quartz (15%) > pyroxenes (5%) > hornblende (3%) ≥ opaques (3%) > biotite (trace). The abundance of hornblende increases through the profile and is most common within the upper densely welded zone (Fig. 2.24).

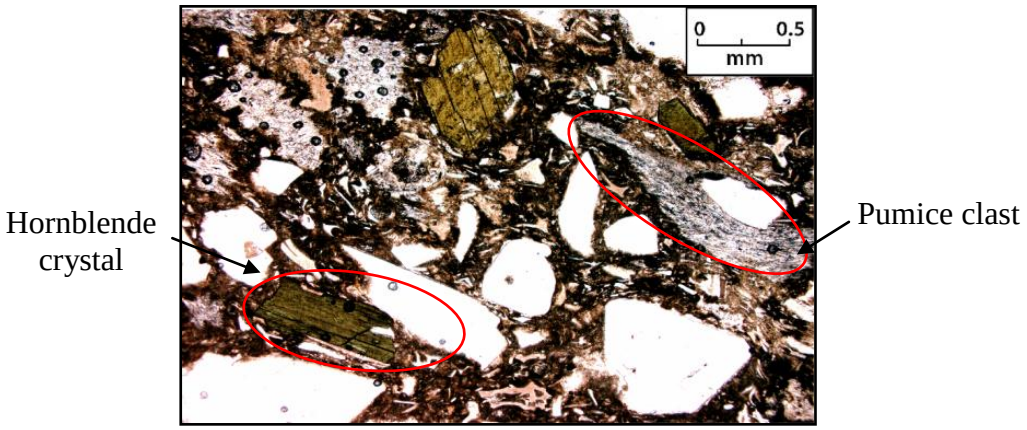

Figure 2.24: Photomicrograph (PPL) of upper densely welded, pumice and crystal-rich unit of the Rocky Hill Ignimbrite.

The glass shard matrix is vitriclastic where distinct shard shapes can be identified, which are mostly large cuspate types with fewer platy and Y-shaped shards. Compaction of the shards increases upwards to form eutaxitic textures within the upper welded zone where the shards start to become aligned with the orientation of the flattened pumice clasts.

2.8 Taupo Ignimbrite

2.8.1 Introduction

The most recent TVZ explosive caldera forming eruption occurred in the surrounding area of the Horomatangi Reefs within Lake Taupo (Leonard et al. 2010, Hogg et al. 2011). The current most accurate and precise date of the eruption has been dated at 232 AD or 1718 ky by ^{14}C wiggle – matching using a New Zealand kauri ^{14}C calibration data set method (Hogg et al. 2011). As Walker et al. (1980) and Hogg et al. (2011) state, the deposits from the eruption are remarkably well preserved and easily accessible due to both its youthfulness and because the vegetation which flourishes within the New Zealand climate rapidly

stabilizes any loose pyroclastic deposits. As a result, the current knowledge and understandings of physical volcanology, volcanic hazards and volcanic petrology has in part derived from the multiple studies undertaken on the Taupo Ignimbrite. The Ignimbrite is referred to in text books as case studies and numerous articles have been published in a wide range of international journals (Hogg et al. 2011).

The Taupo eruption is referred as a global chronostratigraphic marker because it generated a number of ultraplinian fall deposits with an eruption column extending 50 km up into the stratosphere, distributing ash worldwide. Associated with the eruption phase was the ejection and violent emplacement of a low aspect ratio ignimbrite which has a volume of 30 km^3. It is suggested that the emplacement of the ignimbrite generated a global volcano-meterological tsunami (Hogg et al. 2011). The ignimbrite deposit is distributed over an area of 20000 km^2 where it travelled over 60 km to the northeast and southwest of Lake Taupo and formed a radial deposit 165 km across centred on its vent (Walker et al. 1980, Manville et al. 2009, Hogg et al. 2011) (Fig. 2.25).

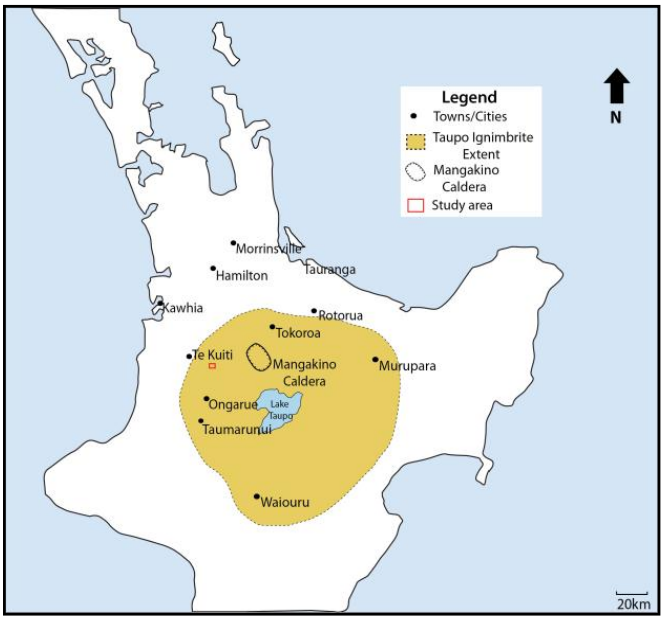

Figure 2.25: The maximum extent of the Taupo Ignimbrite based on observations by Walker et al. (1980), Wilson et al. (1986b) and Manville et al. (2009).

2.8.2 Distribution within the study area

The Taupo Ignimbrite has partly in filled the Waipa Valley floor to a thickness of up to 25 m forming a terrace which is currently being cut into and eroded by the Waipa River system. The terrace has been deposited up against the valley wall at

the same topographic elevation as the Ngaroma Ignimbrite (Fig. 2.26) and stratigraphically overlies the small alluvial terraces built up along the river bed. This is the only sighting of the Taupo Ignimbrite within the field area and it will be described further in more detail in chapter 5.

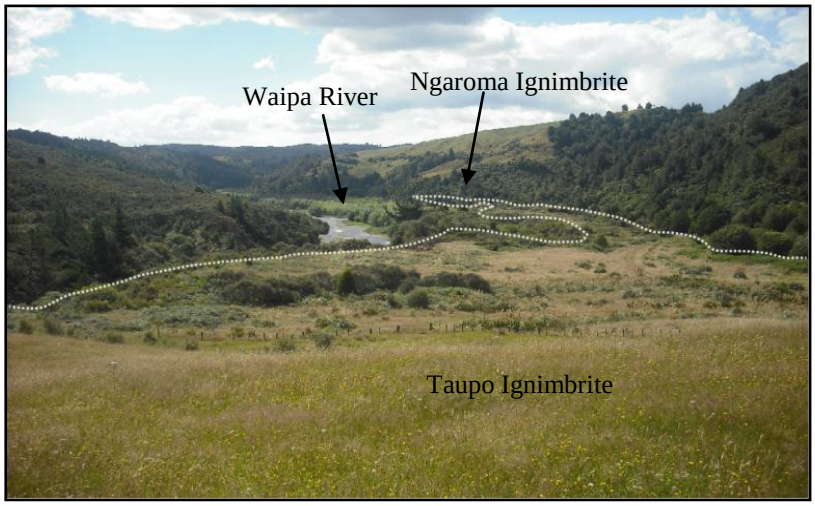

Figure 2.26: View to the north, looking downstream the Waipa River where the discontinuous Taupo Ignimbrite terrace is outcropping.

2.9 Alluvium

2.9.1 Distribution within the study area

Recent alluvium has been deposited along the river and stream beds where the aggradations of weathered and reworked material from the surrounding geology have built up small and flat terraces throughout the study area (Fig. 2.27).

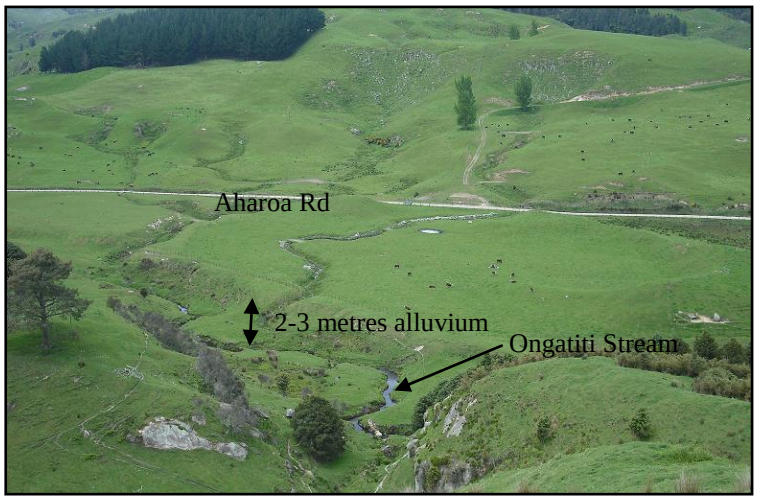

Figure 2.27: A 3-4m thick flat terrace of recent alluvium has been deposited across the entire Ongatiti Valley floor onlapping the valley walls.

Significant deposition has taken place within the Waipa and Ongatiti Valleys where the alluvial systems are typically active throughout the year. The low lying terraces onlap the lowermost ignimbrites exposed alongside the river and stream systems. These are the Ngaroma/ Taupo and the Ongatiti Ignimbrites within the Waipa and Ongatiti Valleys respectively (Fig. 2.28).

Figure 2.28: Alluvium onlapping against the base of the Ongatiti Ignimbrite, Ongatiti Valley, SL.2 (geological map). Note the back pack for scale.

2.9.2 The lithological description within the study area

The alluvium within the Waipa Valley consists predominantly of loosely packed rounded pebbles, cobbles and boulders of greywacke and argillite, and occasional rounded boulders of densely welded Ahuroa and Rocky Hill Ignimbrites (Fig. 2.29).

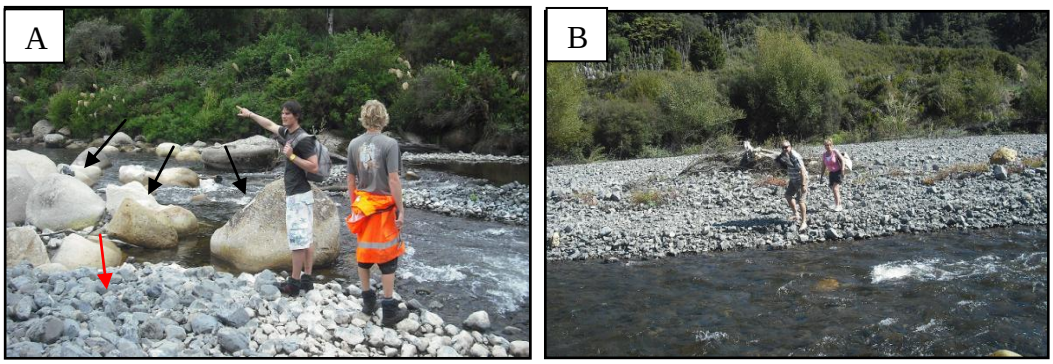

Figure 2.29: Alluvial deposits in the Waipa River Valley. (A) large boulders of welded ignimbrite (black arrows) and cobble sized greywacke and argillite (red arrow); (B) small alluvial terraces built up along the Waipa river.

Within the Ongatiti Valley and the remainder of the study area the alluvium is poorly consolidated, massive to finely bedded with a pale cream to grey appearance. It tends to be moderately well sorted, with coarse sand-sized grains of siliclastic materials dominating (Fig. 2.30). Some coarse, rounded boulders of densely welded Ahuroa and Rocky Hill Ignimbrites also occur, probably resulting from slumping and erosion of bluffs.

Figure 2.30: Alluvium within the Ongatiti Valley, SL.2 (geological map) consisting of fine, well-sorted buff coloured massive silts and sands.

2.10 Slump scarps and deposits

2.10.1 Distribution within the study area

Slumping scarps and deposits are a common feature among the physiography of the study area and this is especially noticeable within the Ongatiti Valley where the slopes are steep and the vegetation has been removed. The slumps and their deposits are characterised by either rounded bowl-like head scarps with a small talus pile (Fig 2.31A), or by steep ragged cliff faces with coarse talus piling up at the base of the slope (Fig. 2.31B). In a few areas where large slumps have occurred there is a large arcuate head scarp (10's of metres wide) with an extensive hummocky deposit consisting of both coarse angular boulders and finer material.

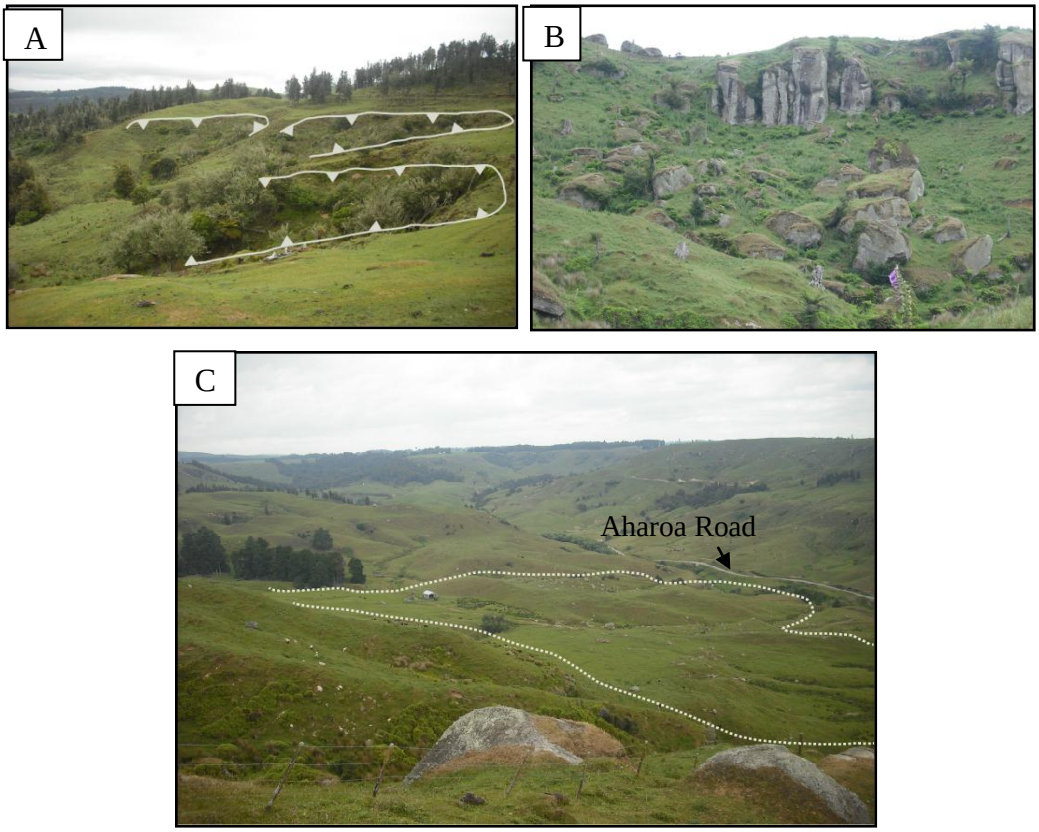

Figure 2.31: Erosion patterns within the study area. (A) multiple bowl-like scarps (few m's wide) in partially to non-welded zones of the ignimbrites with a small talus pile at the base (not shown in the image). (B) welded zones of the ignimbrites showing steep and jagged cliff faces and coarse angular boulders at the base. (C) the large scale events include a large circular scarp (few 10's of metres) at the head of the slope (not shown in the image) with a widespread fan like deposit including large boulders of predominantly the Rocky Hill Ignimbrite. This slump is a significant feature within the study area and has been outlined on the geological map on the northern side of Aharoa Road.

Chapter 3

Ongatiti Ignimbrite

3.1 Introduction

This chapter documents the outcrop appearance, lithology, petrography, mineralogy, geochemistry and the vertical and lateral variations within the Ongatiti Ignimbrite.

Two broad units have been identified within the Ongatiti Ignimbrite. The flow boundary between the two is gradational and the abrupt change in the lithological appearance is enough to determine the deviation of two main units (Wilson 1986a). Most descriptions consist of the upper unit of the Ongatiti Ignimbrite which is more confined to lower lying areas and to the north of the vent. There are few descriptions of the lower unit which are more widespread to the west of the vent (Wilson 1986a). As a result it is very rare to find a complete profile through both units, and consequently there has been a lot of confusion in understanding the overall geology of the Ongatiti Ignimbrite.

The lower unit of the Ongatiti Ignimbrite can be characterised by having a partially to densely welded, crystal rich, lithic poor and pumice-poor (Wilson 1986a, Cartwright 2003). As Cartwright (2003) describes, it often forms the caps of the tops of hills due to its densely welded nature with tall columnar jointing. Due to the lack of pumice, Cartwright (2003) named this unit the 'Ongarue Ignimbrite' which he recognised as being significantly different from the typical Ongatiti Ignimbrite descriptions. However, it was suggested by Wilson (1986a) that this unit was an unusual facies of the Ongatiti Ignimbrite which has been confirmed in this chapter.

The more commonly exposed upper unit of the Ongatiti Ignimbrite is densely to partially to weakly welded, vitriclastic, pumice, crystal, and lithic rich (Briggs et al. 1993, McGrath 2004, Edbrooke 2005). A diagnostic feature of this unit is the

high abundance of coarse pumice clasts with glomeroporphyritic clots of crystals. The pumice clasts can reach up to 100 cm in diameter and some have a streaky and fibrous texture (Wilson 1986a, Moyle 1989). Wilson (1986a), Briggs et al (1993) and Krippner et al. (1998) describe a wide range of lithic types in the Ongatiti Ignimbrite which include andesite, rhyolite, greywacke, densely welded ignimbrite (some of which are 'Ongatiti-like'), amphibolites and hornblende microdiorite.

3.2 Underlying fall deposit

A 1 m thick white – grey fall deposit is exposed underlying the densely welded base of the Ongatiti Ignimbrite at location SL2 (refer to map, Enclosure 1). No direct contact with the overlying Ongatiti Ignimbrite was observed in the field area. The deposit is weathered and has a highly fractured appearance (Fig 3.1) where it responds with a brittle failure during removal from the outcrop.

Figure 3.1: Fall deposit underlying the densely welded base of the Ongatiti Ignimbrite at the location SL2 (Enclosure 1).

It consists of a very fine ash grainsize, is very well sorted, is non-welded and contains no sign of bedding structures or any variation in grainsize (Fig 3.2). It lacks any pumice and it is therefore inferred to be a phreatoplinian fall deposit.

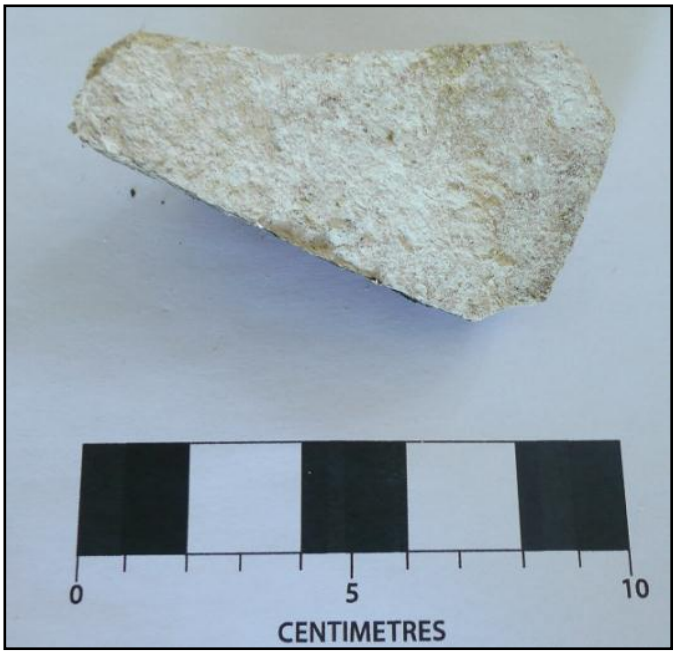

Figure 3.2: The deposit is composed of very well sorted fine ash grains.

In thin section, it is difficult to make out the texture and composition of the matrix due to the highly weathered nature of the deposit. No pumice clasts and only 1 very small (< 2 mm) lithic was observed. The crystal abundance is poor (< 8 %) and the crystals are small (< 0.2 mm) and appear to be highly fragmented. Quartz and plagioclase are most abundant with traces of iron oxides and biotite. The absence of orthopyroxene and hornblende, suggests this phreatoplinian fall deposit is not related to the Ongatiti eruption.

3.3 Outcrop appearance of the Ongatiti Ignimbrite in the study area

The Ongatiti Ignimbrite is a major component of the ignimbrite plateaux exposed in the study area and is found outcropping throughout. It has a common thickness of approximately 60 m but reaches up to 100 m thick within the Ongatiti Valley (Fig 3.3). No direct contact is observed with the underlying Ngaroma Ignimbrite or the overlying Unit D and Ahuroa Ignimbrite.

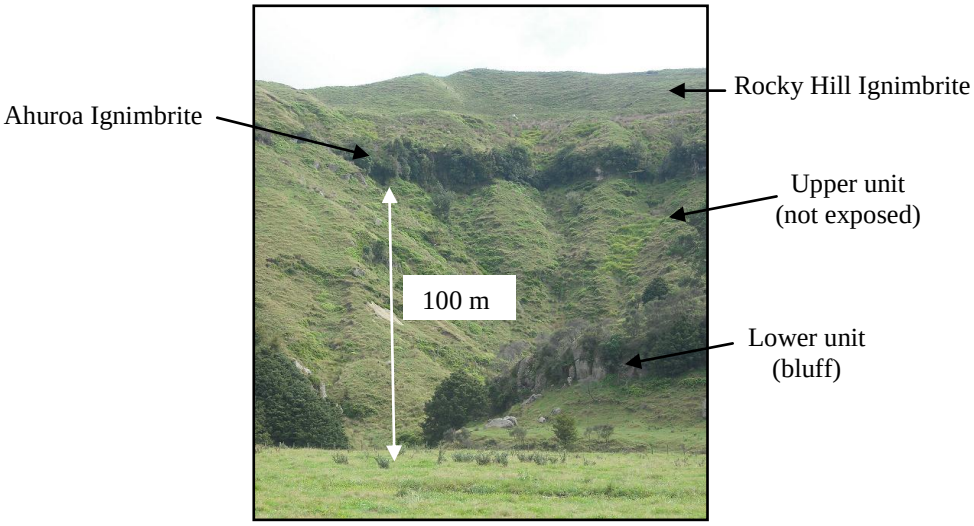

Figure 3.3: View of the lower and upper units of the Ongatiti Ignimbrite exposed within the Ongatiti Valley, note the substantial thickness of the ignimbrite in this particular location (SL2, Enclosure 1). The underlying contact with the Ngaroma Ignimbrite is not exposed.

Outcrops of both the distinctive lower and the upper units of the Ongatiti Ignimbrite are exposed within the study area. The lower unit is very crystal rich and is almost completely depleted in pumice. It contrasts with the upper unit which has a crystal and very pumice-rich composition.

Parts of the Ongatiti Ignimbrite are exposed as prominent bluffs almost continuously through the Ongatiti Valley (Fig 3.4). In specific sections, the entire vertical extent of the bluff consists of the lower pumice-poor unit which transitions laterally over a few hundred metres into bluffs consisting of the upper pumice-rich unit. In other areas of the valley, the bluff reveals a vertical transition from the lower pumice-poor unit into a moderately, pumice-rich lithology, (transitional unit). The topographic elevation between these locations remains fairly consistent where there is no dramatic change in slope observed.

Figure 3.4: Bluffs of the lower zone of the Ongatiti Ignimbrite, Ongatiti Valley.

The lower pumice-poor facies is densely – partially welded and is therefore less susceptible to erosion in comparison to its upper less welded counterpart. As a result, it tends to form a pronounced bluff (Fig 3.4).

The exposed bluffs range in height from less than 5 m to more than 15 m and are characterised by distinct tall columnar jointing where the vertical joints extend for the whole length of the bluff. The weathering pattern of the lower unit is strongly influenced and controlled by the wide spaced vertical and horizontal columnar joints where large (2 – 6 m) rotated angular boulders accumulate at the base of the bluff (Fig 3.5).

Figure 3.5: Toppled large angular boulders accumulating at the foot of the tall columnar jointed bluff of the lower, pumice poor unit within the Ongatiti Valley.

The outcrop appearance of the upper pumice-rich unit significantly varies between locations. It is very rarely exposed above the exposed bluff of the lower, pumice-poor unit. It is more commonly observed as a receding grass covered slope (Fig 3.3) with occasional exposures of poorly-welded ignimbrite with no joints or fractures present.

In other localities of the study area (especially in the southwest zone) where the lower unit is presumably buried, tall (> 20 m) bluffs of the upper pumice-rich unit are exposed (Fig 3.6). These consist of very irregular and widely spaced (2 - 15 m) vertical joints and fractures.

Figure 3.6: Bluff exposure of the upper, partially welded, pumice-rich unit of the Ongatiti Ignimbrite showing a lack of distinct jointing along Manu Road (Enclosure 1).

The outcrop suffers from differential erosion which is more pronounced in the areas of the outcrop where the case hardening has been removed (Fig 3.7).

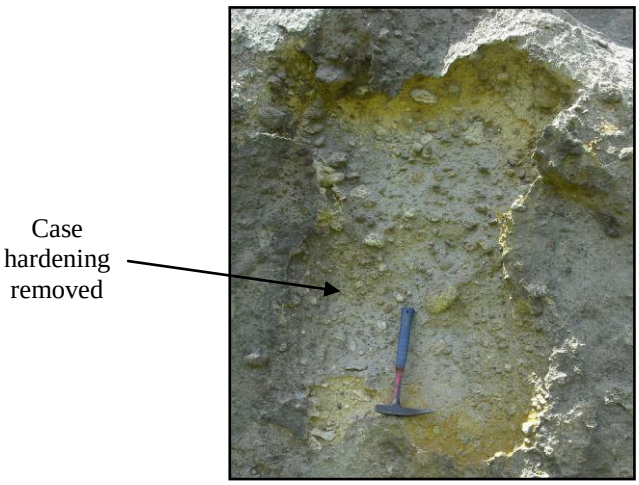

Figure 3.7: The upper, pumice-rich unit of the Ongatiti Ignimbrite (location SL7, Enclosure 1).

The outcrop appearance of the sections of the bluff which consist of a combination of the pumice poor – pumice rich units effectively show a transition in appearance approximately half way up the profile. The base is densely welded and contains columnar jointed structures. These however become less defined with an increase in stratigraphic height where the bluff tends to recede back into the outcrop (Fig 3.8). This is probably a result of being less welded and therefore more susceptible to erosion.

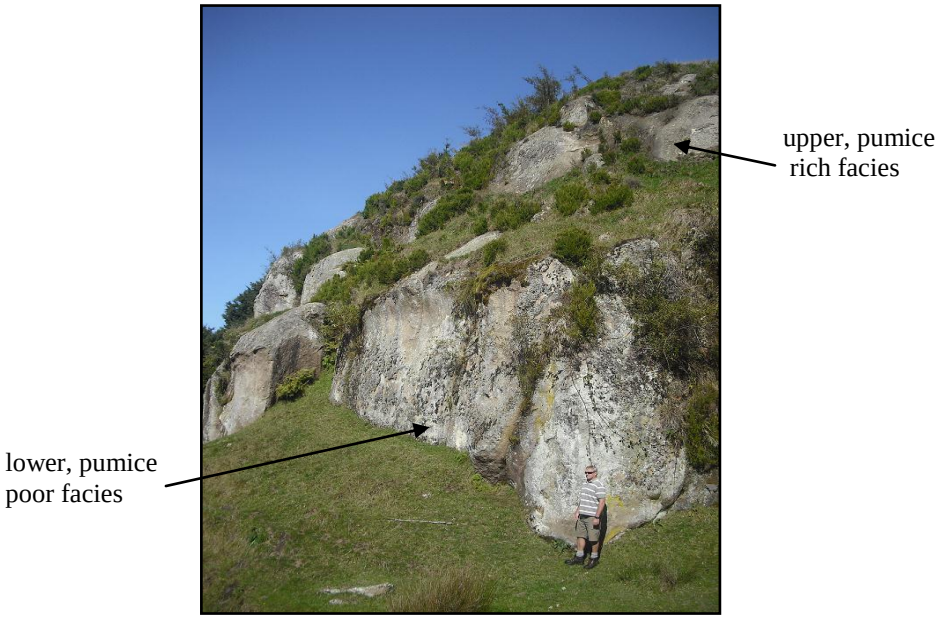

Figure 3.8: The outcrop appearance of the sections of the bluff which consist of both the pumice poor and pumice rich units (location SL2, Enclosure 1).

3.4 Lithology and petrographic description of the lower pumice-poor Unit

3.4.1 Introduction

Three separate (> 300 m apart) areas consisting of the lower pumice-poor unit along the exposed and continuous bluff of the Ongatiti Ignimbrite were selected for the production of detailed stratigraphic logs 1, 6 and 8 (SL1, SL6 and SL8). The selection was based on the maximum amount of exposure and access available. Their locations are shown on the map (Enclosure 1).

3.4.2 Stratigraphic variation

The three stratigraphic profiles appear fairly uniform with little variation (Fig 3.9). The matrix is light beige to cream. The degree of welding gradually reduces with an increase in stratigraphic height, from densely-welded within the lower half to partially-welded within the upper zone. The ignimbrite is massive, poorly sorted and shows no bedding structures, concentration zones, or variation in grainsize. Log holes were observed in two of the three stratigraphic column locations (SL1 and SL6), which vary in size, shape and stratigraphic position (Figs 3.10). The different components (pumice, lithics, crystals and glass shards) of the lower facies will be described in detail.

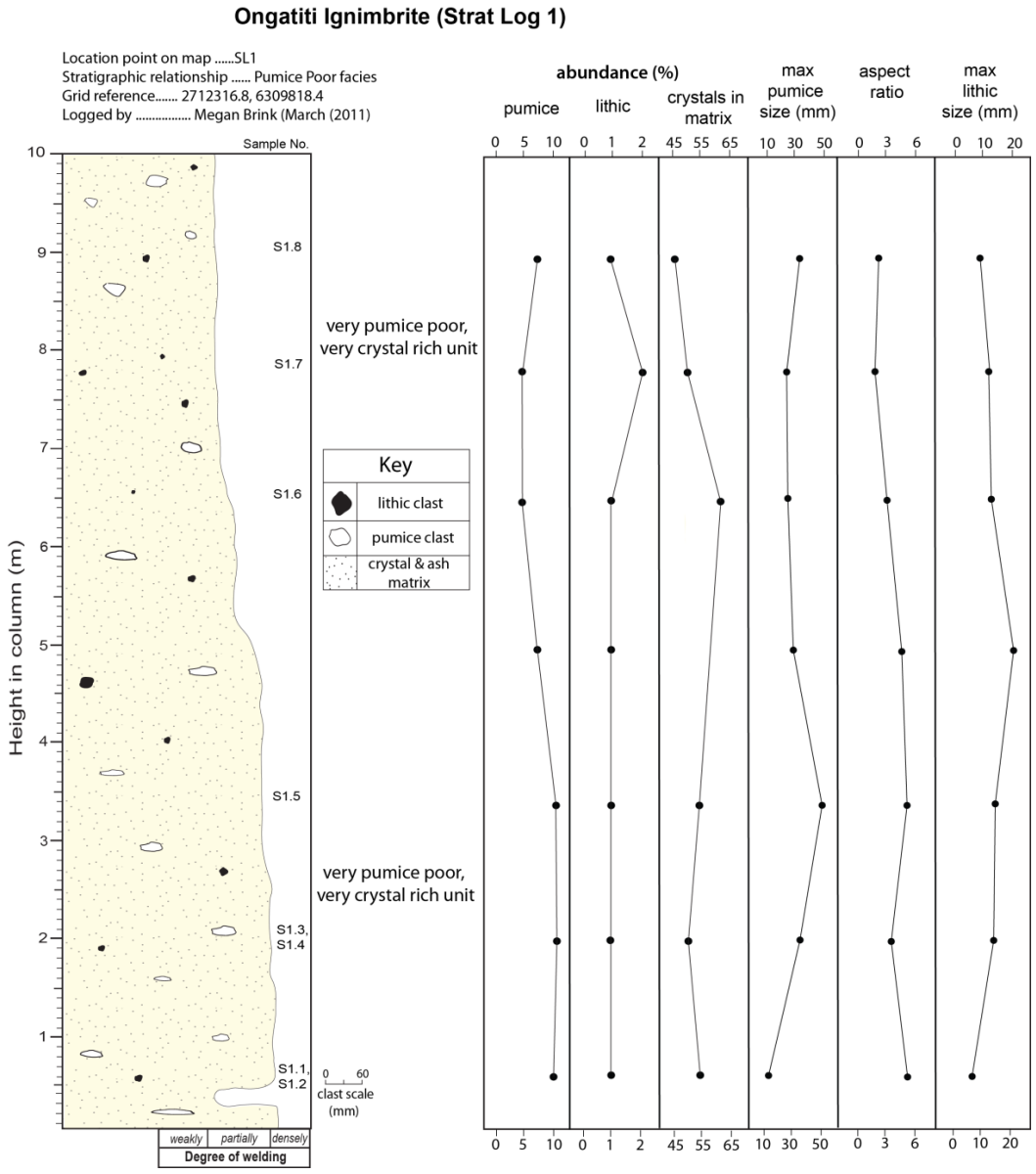

(A)

Figure 3.9: A, B, C, stratigraphic logs through the lower facies of the Ongatiti Ignimbrite at localities (A) SL1, (B) SL6, and (C) SL8 (see Enclosure 1), highlighting the variation in the overall grainsize and appearance of the profile. The abundance of pumice, lithics and crystals, the maximum clast size of the pumice and their average aspect ratio, the maximum clast size of the lithics and the individual proportions of the main mineral phases (figures B and C) are plotted against the log. Note the pumice and lithic abundances, their maximum clast size and the average aspect ratio of the pumice are all bulk rock visual field estimates, and the crystal abundances have been determined in thin section by point counting.

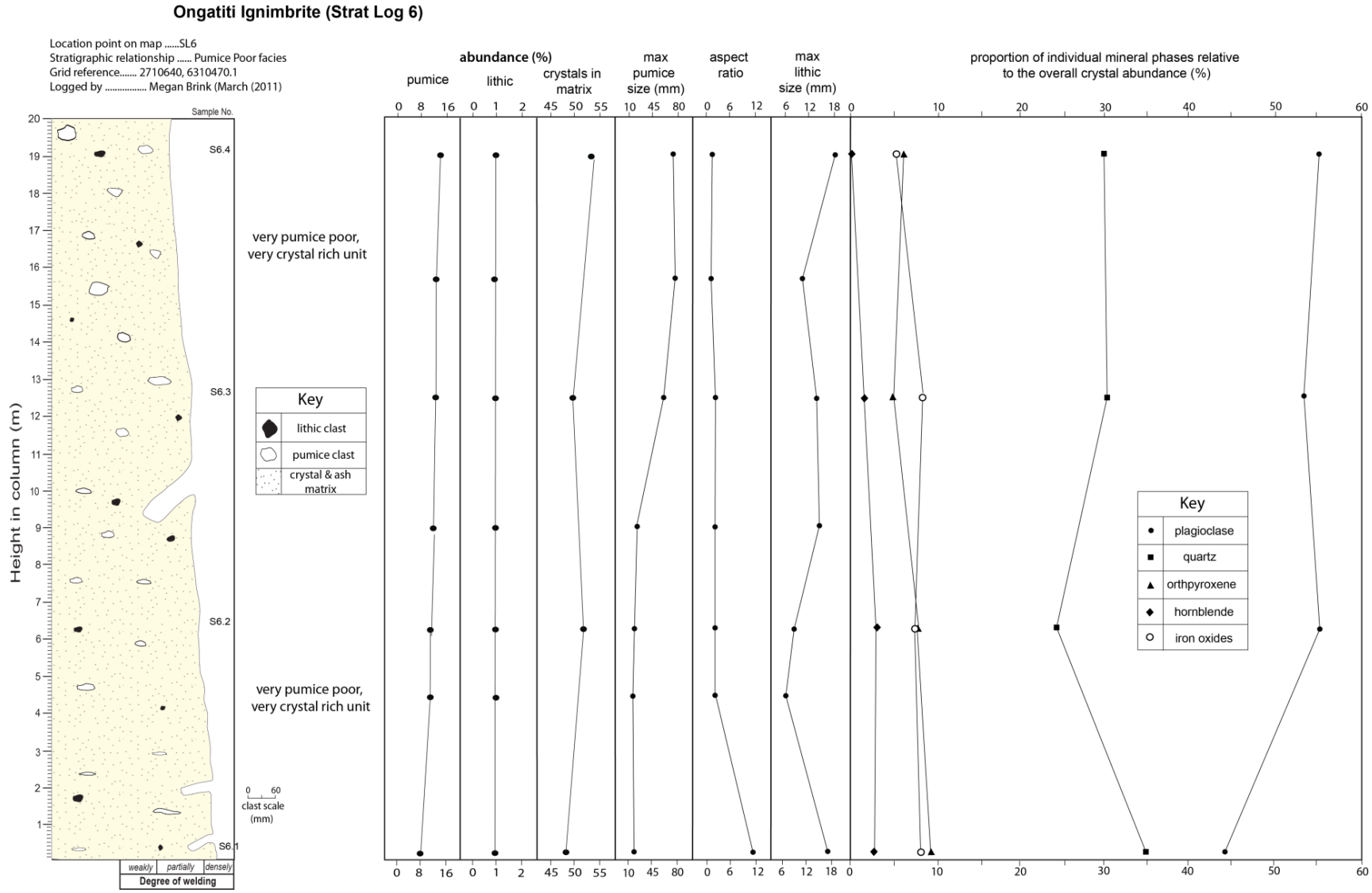
Ongatiti Ignimbrite (Strat Log 6)
Location point on map SL6
Stratigraphic relationship ..... Pumice Poor facies
Grid reference..... 2710640, 6310470.1
Logged by ..... Megan Brink (March (2011)
Sample No.
S6.4
S6.3
S6.2
S6.1
Height in column (m)
very pumice poor, very crystal rich unit
very pumice poor, very crystal rich unit
Key
lithic clast
pumice clast
crystal & ash matrix
0 60
clast scale (mm)
weakly
partially
densely
Degree of welding
abundance (%)
pumice
lithic
crystals in matrix
max pumice size (mm)
aspect ratio
max lithic size (mm)
proportion of individual mineral phases relative to the overall crystal abundance (%)
Key
plagioclase
quartz
orthpyroxene
hornblende
iron oxides

(B)

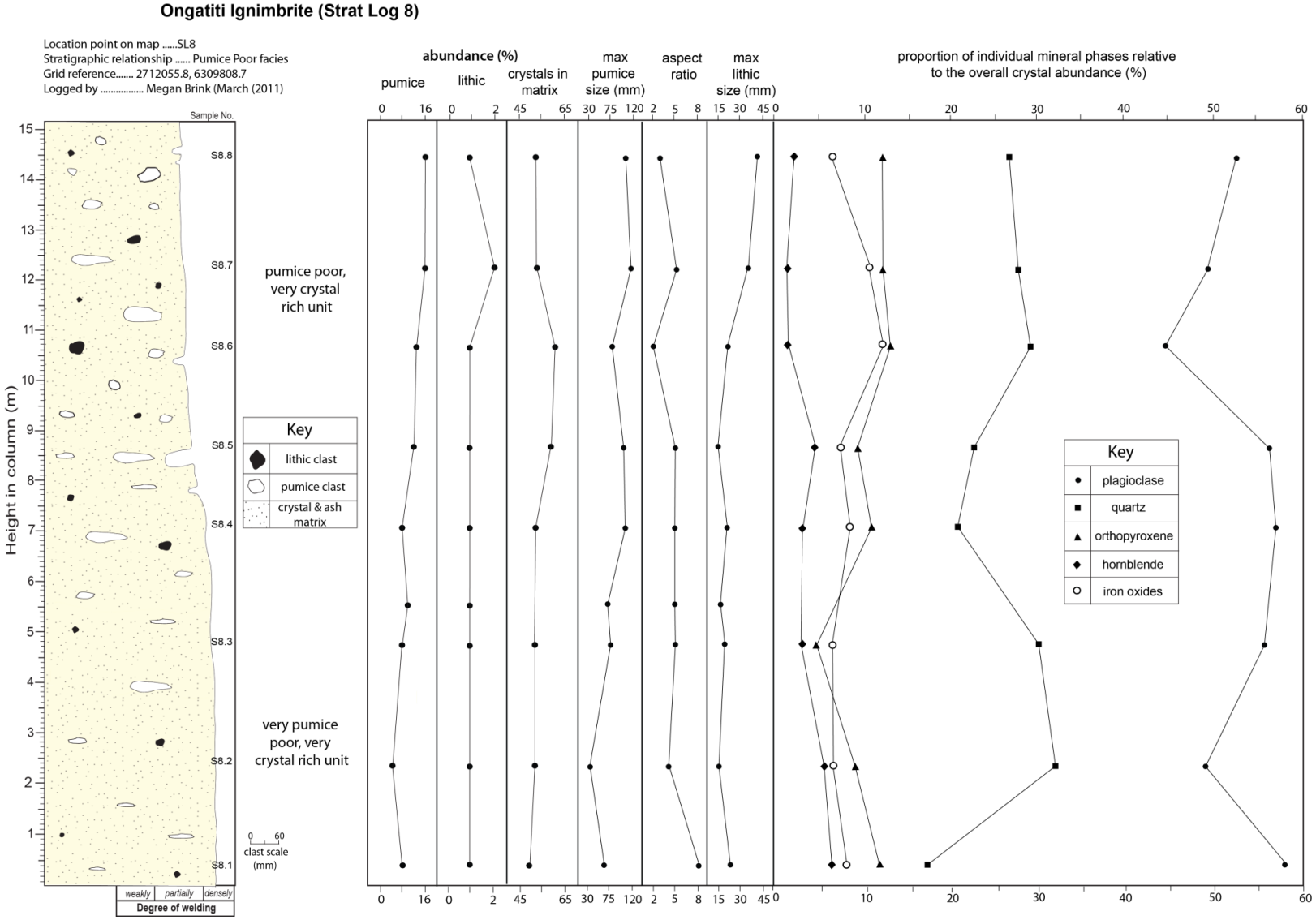
Ongatiti Ignimbrite (Strat Log 8)
Location point on map SL8
Stratigraphic relationship ..... Pumice Poor facies
Grid reference..... 2712055.8, 6309808.7
Logged by ..... Megan Brink (March (2011)
Sample No.
S8.8
S8.7
S8.6
S8.5
S8.4
S8.3
S8.2
S8.1
Height in column (m)
pumice poor, very crystal rich unit
very pumice poor, very crystal rich unit
Key
lithic clast
pumice clast
crystal & ash matrix
0 60
clast scale (mm)
weakly
partially
densely
Degree of welding
abundance (%)
pumice
lithic
crystals in matrix
max pumice size (mm)
aspect ratio
max lithic size (mm)
proportion of individual mineral phases relative to the overall crystal abundance (%)
Key
plagioclase
quartz
orthopyroxene
hornblende
iron oxides

(C)

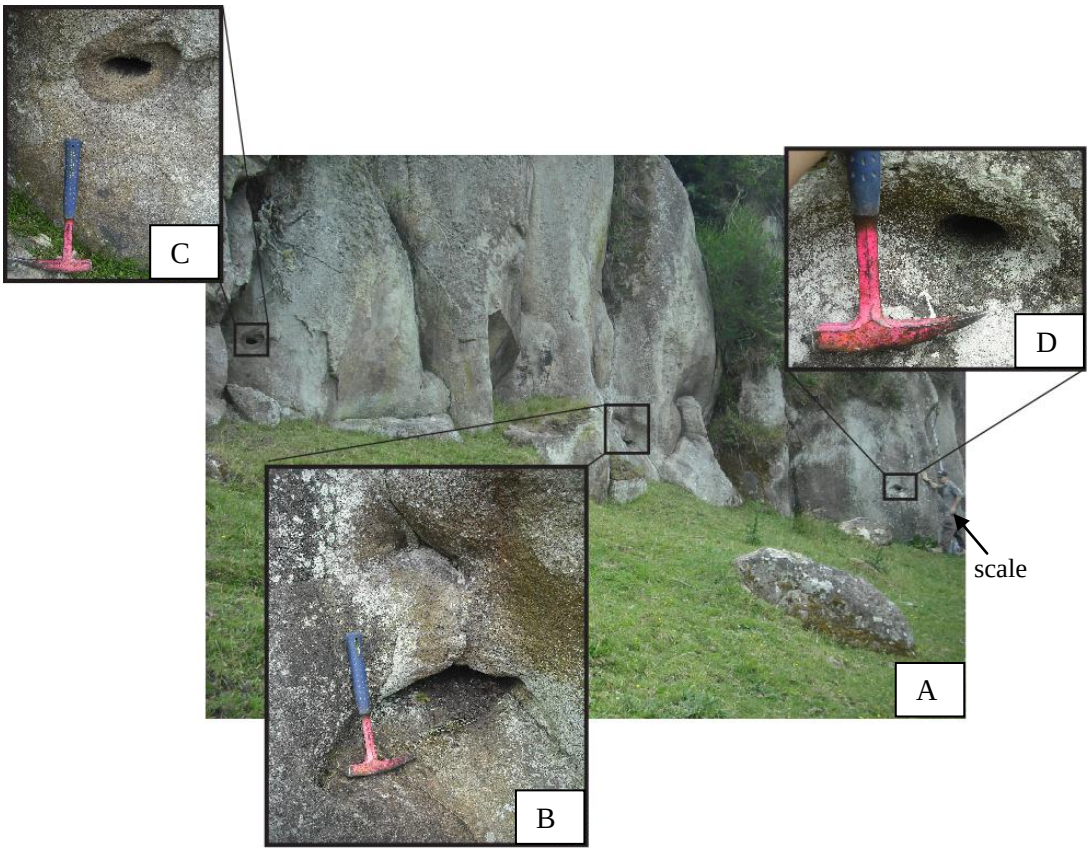

Figure 3.10: Tree log moulds in the lower pumice-poor unit of the Ongatiti Ignimbrite at location SL1 (Enclosure 1). (A) three log hole moulds are present within the lower 3 m of the profile. (B) a slightly flattened mould which is approximately 25 cm wide, 10 cm tall and > 1 m deep. (C) a more spherical mould (10 cm wide, 10 cm high and > 1 m deep) with a distinct brown-orange discolouration around the outer perimeter. (D) a small spherical (< 10 cm wide,< 10 cm tall and > 2 m deep) mould.

3.4.3 Pumice abundance and petrography

The abundance of pumice clasts (> 2 mm) in the lower unit of the Ongatiti Ignimbrite is low. In SL1 (Fig 3.9 A), it is less than 10 % throughout and shows a slight decline from the base towards the upper zone of the profile. In SL6 and SL8, the abundance of pumice is slightly higher than in SL1 where both profiles show a general increase from 8 % at the base to 16 % at the top (Fig 3.9 B,C).

The maximum size of the pumice clasts tends to increase with an increase in the height of the column. This is more noticeable within SL6 and SL8 in comparison to SL1 where the sizes of the pumice clasts show little variation up the profile.

The aspect ratio of the pumice clasts is high ranging from 6 to 12 (Fig 3.11) within the lower 5 m of all three profiles, but significantly reduces and remains constant up through the remainder of the column (Fig 3.9).

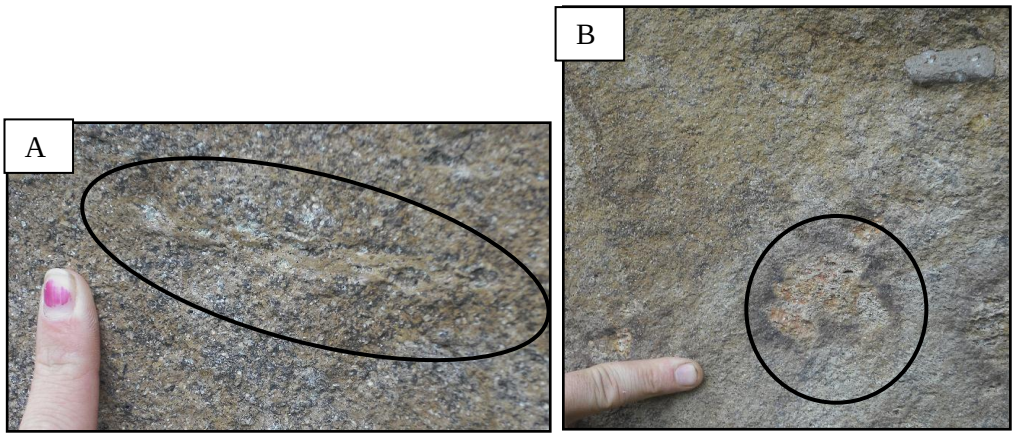

Figure 3.11: Pumice in densely welded zone approximately 2 m from the base of the outcrop at location SL9 (Enclosure 1). (A) view of a high aspect ratio, fiamme-like pumice clast and (B) low aspect ratio pumice clast; these are rarely observed within the lower 5 m of the outcrop.

One type of pumice was observed in the lower unit of the Ongatiti Ignimbrite, and is characterised as yellow – cream in colour, poorly vesicular and very crystal rich (Fig 3.12).

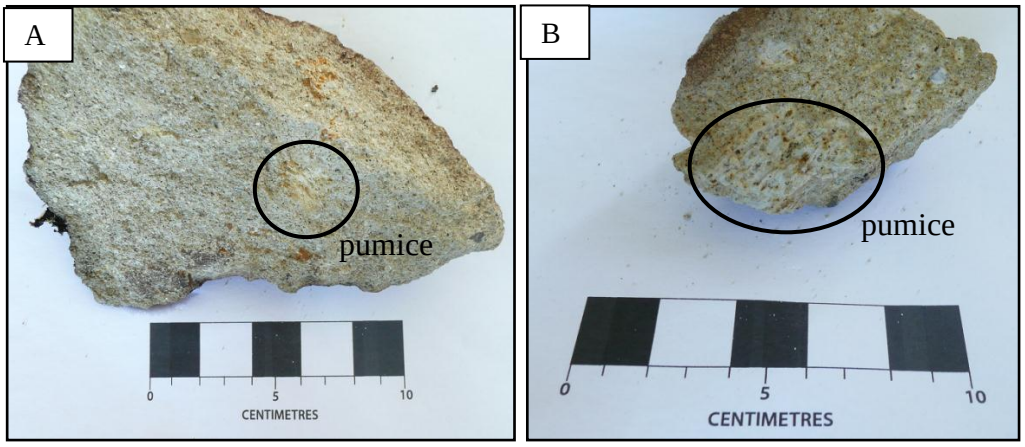

Figure 3.12: (A) The pumice clasts at the base are generally small and rare within the very crystal rich matrix. (B) Towards the top of the profile, the clasts are larger and more common. The specks shown throughout the clast represent coarse crystals.

The crystal abundance of the pumice varies between clasts and increases with an increase in stratigraphic elevation. Some clasts have no phenocrysts and others are

phenocryst rich. The phenocrysts appear to be more rounded and less fragmented in the pumice clasts in comparison with the crystals in the surrounding matrix.
In thin section (Fig 3.13), and where the matrix is homogenous, the outline of the pumice clasts are poorly pronounced and this is because the clasts are glassy, dense and have no structure or vesicles present. The clasts become less glassy, less dense and more devitrified with an increase in stratigraphic height.

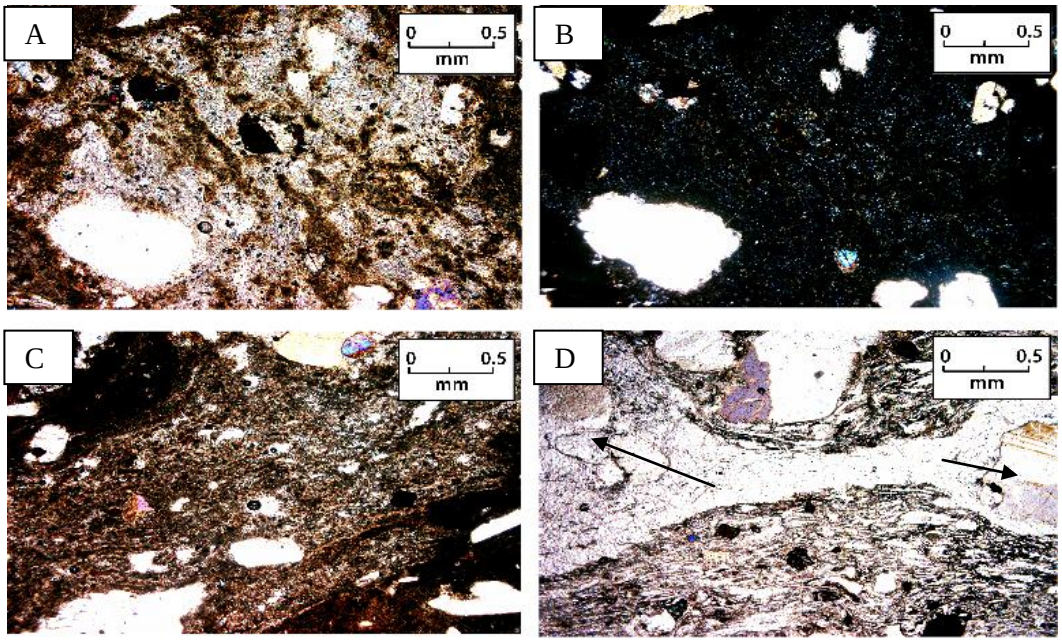

Figure 3.13: (A) Photomicrograph of a pumice clast under plane polarised light within sample S8.8 (14 m up from the base of SL8, Fig 3.7 A), note the absence of vesicles. (B) The same clast under cross polarised light showing slight devitrification. (C) A pumice clast within sample S8.1 (0.4 m up from the base of SL8, Fig 3.7 B), note how the clast is more dense than the one shown in image A and B. (D) A very condensed, glassy and fiamme like pumice clast showing strong deformation around the phenocrysts (arrows) in sample O.28 (base of the lower unit, section 7, Enclosure 1).

3.4.4 Lithic abundance and types

The abundance of lithics within each of the three profiles is approximately 1 % and shows little variation throughout (Figs 3.9). The maximum size of the lithics follows no distinct trend, although some of the larger clasts (> 20 mm) are found within the uppermost zone of SL6 and SL8.

The predominant lithic type found within the lower facies of the Ongatiti Ignimbrite is porphyritic rhyolite with lesser amounts of vitrophyric rhyolite (Fig 3.14 A), greywacke (Fig 3.14 B) and glassy rhyolite. Highly vesicular and fine grained hornblende rhyolite clasts are rare.

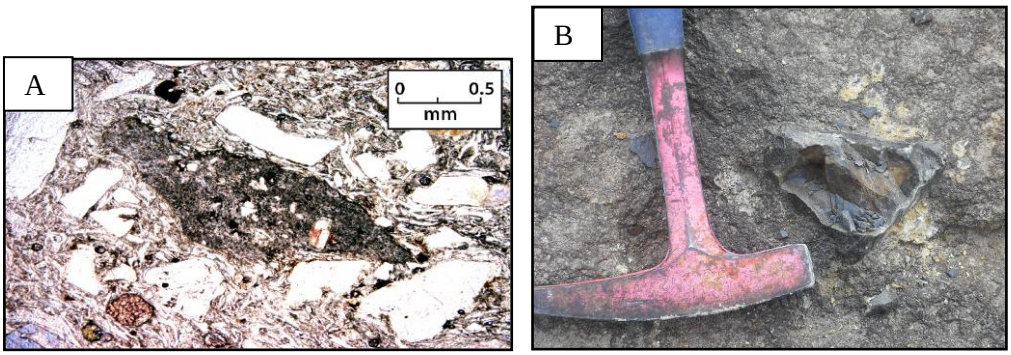

Figure 3.14: (A) Photomicrograph of vitrophyric rhyolite lithic in sample O.28 (location 7, Enclosure 1). (B) Greywacke lithic clast within the mid zone of stratigraphic log 1.

3.4.5 Crystals

The crystal abundance within the matrix of the lower facies of the Ongatiti Ignimbrite is very high (Fig 3.13) and shows crystal enrichment when compared to the crystal content of the pumice clasts. The crystals constitute 45 – 65 % of the matrix, where mostly welded glass shards and few small fragments (< 2 mm) of pumice and lithics make up the remainder. There is no distinct variation in the abundance of crystals with an increase in stratigraphic height in SL6 and SL8 (Figs 3.9 B, C), although there is a slight reduction observed within SL1 (Fig 3.9 A).

The crystals (Fig 3.15) are large and generally anhedral. The plagioclase and quartz crystals (dominant crystal type) reach up to 2.5 mm but are predominantly 1 – 1.5 mm in diameter. It appears that the crystals however become more fragmented and therefore are slightly smaller with an increase in stratigraphic height.

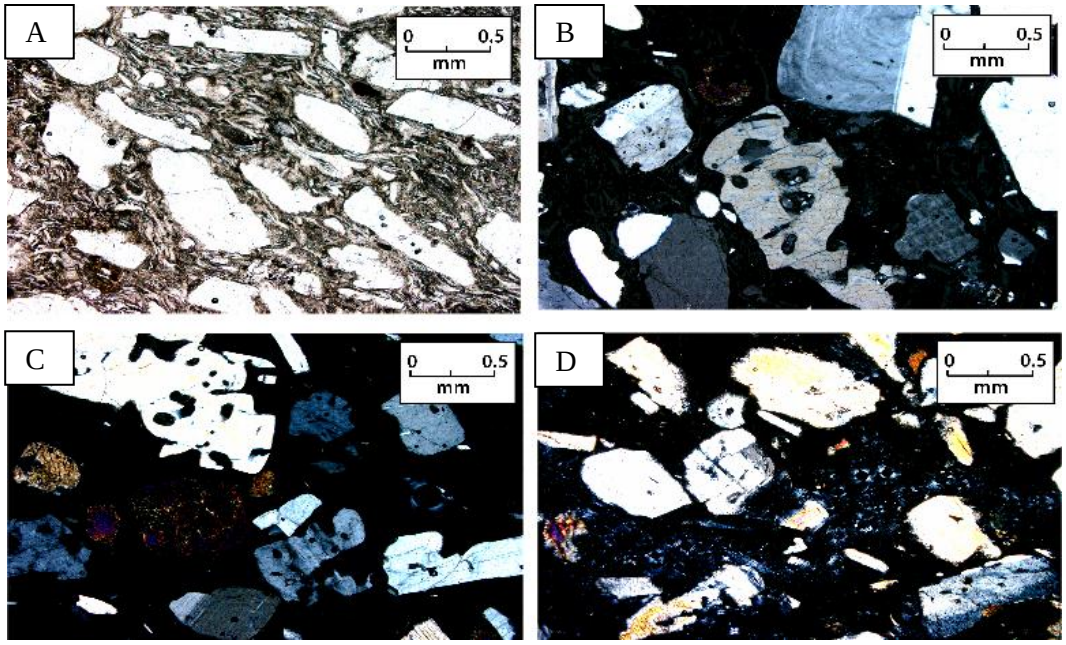

Figure 3.15 Photomicrographs of the crystal-rich lower unit of the Ongatiti Ignimbrite. (A) Sample O.28 (location 7, Enclosure 1) showing alignment of crystals. (B and C) Under cross polarised light, 7 m up from the base of SL8 (Fig 3.7 C) showing the large size of the crystals and the crystal rich nature of the facies. Note how the crystals are almost in contact with one another. (D) Crystals within the top of the profile of SL8 (14.5 m up from the base) where the crystal size is smaller and the crystals are more fragmented in comparison to the samples from further down the profile.

Plagioclase, quartz, orthopyroxene, iron oxides and hornblende, in decreasing order of abundance, is the mineral assemblage in the lower unit of the Ongatiti Ignimbrite (Fig 3.9 B, C). The proportions of orthopyroxene, iron oxides and hornblende relative to the overall crystal abundance show minimal variation with an increase in the stratigraphic height of the SL6 and SL8 profiles. The proportions of plagioclase and quartz however are more significant and show complementary abundances. There appears to be two areas within the SL8 profile (between 1 – 5 m and between 10 – 11 m) where there is a sudden increase in quartz/ an abrupt decrease in plagioclase (Fig 3.9 C).

3.4.6 Glass shard texture

Most samples have a homogenous, welded and glassy matrix with few having a vitriclastic matrix. The base of the profiles are generally vitriclastic and become homogeneous with an increase in stratigraphic height, probably as a result of increasing weathering and alteration. Where the glass shards are visible, they appear to consist of mostly platy with lesser amounts of Y-shaped and cuspate

textures. They have a eutaxitic nature where the shards are aligned in the same orientation and show deformation around large crystals and pumice clasts (Fig 3.16).

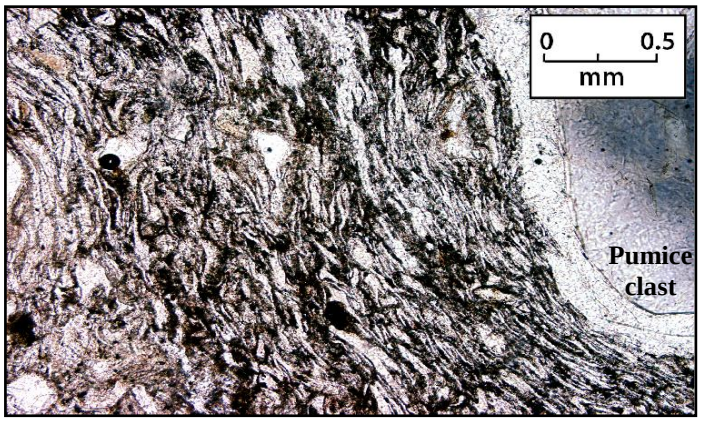

Figure 3.16: Photomicrograph of vitriclastic matrix of sample O.28 (location 7, Enclosure 1) under plane polarized light showing the clear eutaxitic nature of the glass shards and how they deform around the pumice clast.

3.5 Lithology and petrographic description of the upper Pumice-Rich Unit

3.5.1 Introduction

The best and most accessible exposed sections of the upper pumice-rich unit are at locations SL5 and SL7 (3.17 A, B) (see map, Enclosure 1). Stratigraphic log 5 (SL5) is located within the Ongatiti Valley and the base of the profile is at a similar topographic elevation to the other five stratigraphic logs produced in the Ongatiti Ignimbrite. Stratigraphic log 7 (SL7) however is 1500 m further north of the Ongatiti Valley. The base of the profile is at a higher topographic elevation (approximately 35 m) than the rest of the stratigraphic profiles produced within the Ongatiti Ignimbrite.

3.5.2 Stratigraphic variation

Both profiles contain similar characteristics typical of the upper unit of the Ongatiti Ignimbrite, and are massive, poorly sorted, and contain no bedding structures, concentration zones or variation in grainsize. They do however differ

slightly in terms of their degree of welding. The lower half of the upper unit at SL5 is partially-welded and this gradually reduces with height to become weakly-welded within the upper half of the profile (Fig 3.17 A). SL7 is weakly welded at the base and the degree of welding continues to show a slight decrease with an increase in stratigraphic height (Fig 3.17 B). The abundance and size of the different components (pumice, lithics, crystals and glass shard matrix), and the variation of these relative to an increase in stratigraphic height varies slightly between the two profiles and these will be described in detail.

3.5.3 Pumice abundance and petrography

The pumice abundance within the upper unit of the Ongatiti Ignimbrite is considerably higher (20 - 30%) than the lower unit (3.18). The only significant change in the abundance of pumice observed at SL5 and SL7 is within the base of both profiles (3.17) which shows a sudden increase and then remains constant throughout the extent of both columns.

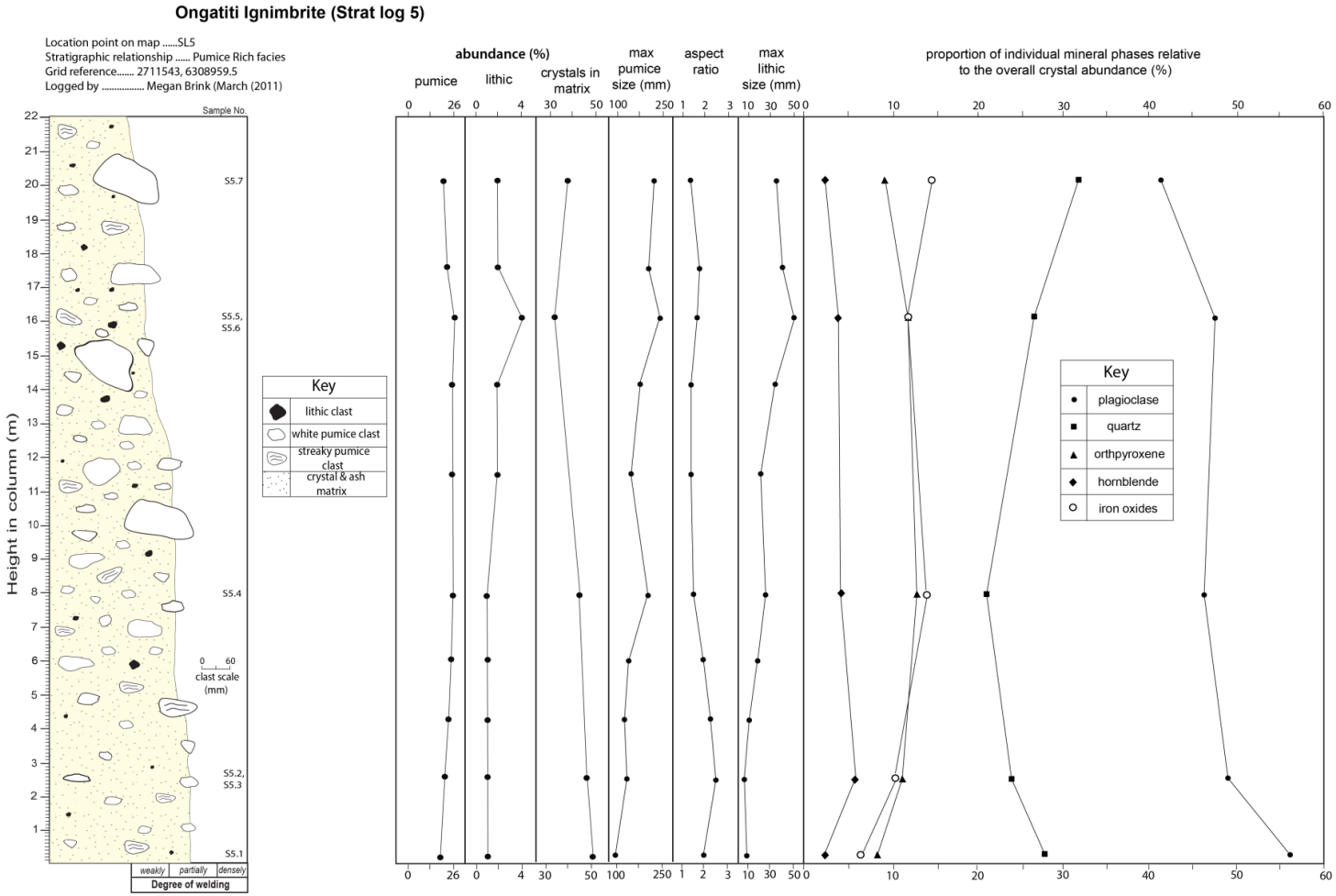

(A)

Figure 3.17: (A, B) Stratigraphic logs through the upper facies of the Ongatiti Ignimbrite within the study area, highlighting the variation in the overall grainsize and appearance of the profile. The abundance of pumice, lithics and crystals, the maximum clast size of the pumice and their average aspect ratio, the maximum clast size of the lithics and the individual proportions of the main mineral phases are plotted against the log.

Note the pumice and lithic abundances, their maximum clast size and the average aspect ratio of the pumice are all bulk rock visual field estimates, and the crystal abundances have been determined in thin section by point counting.

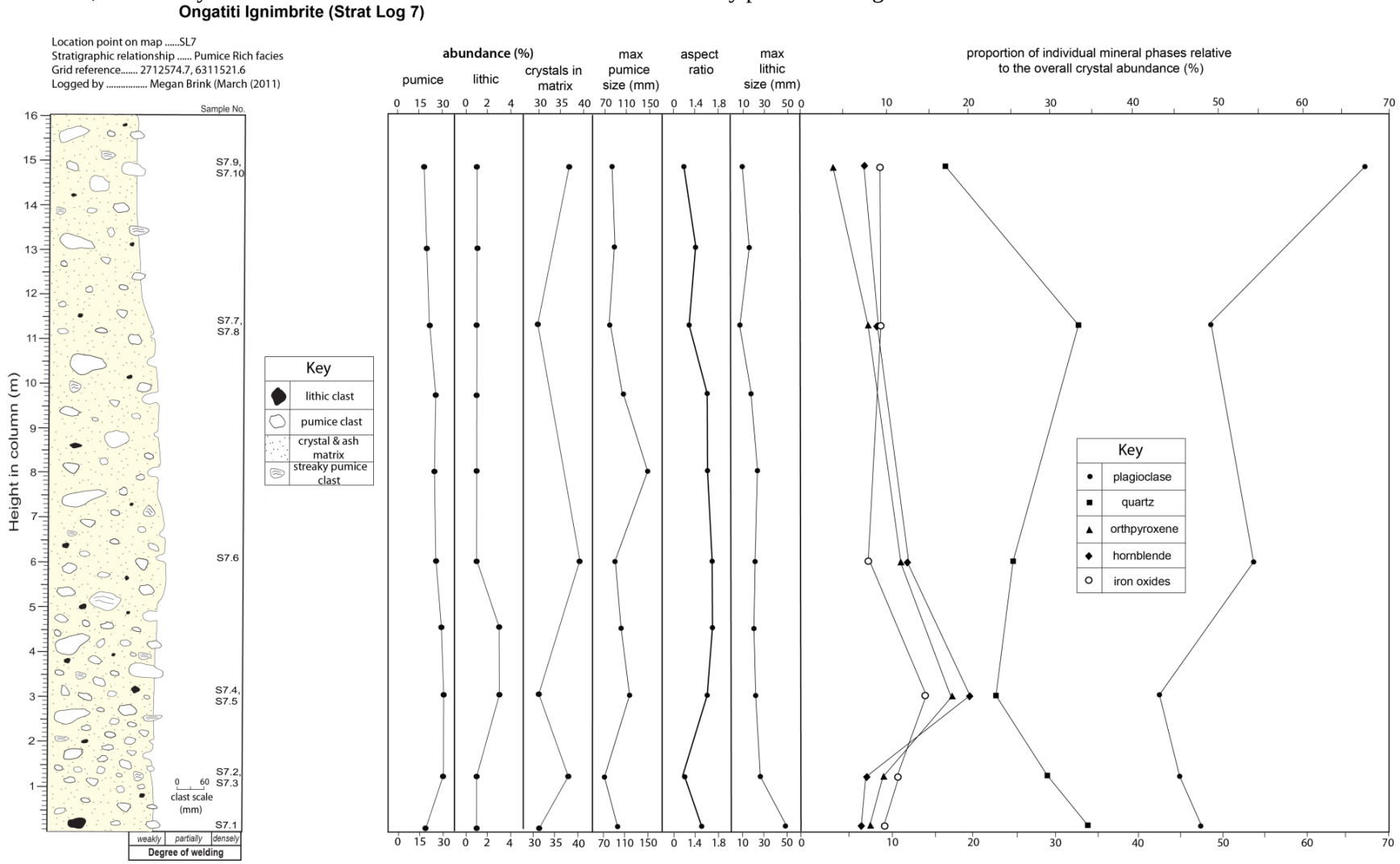

(B)

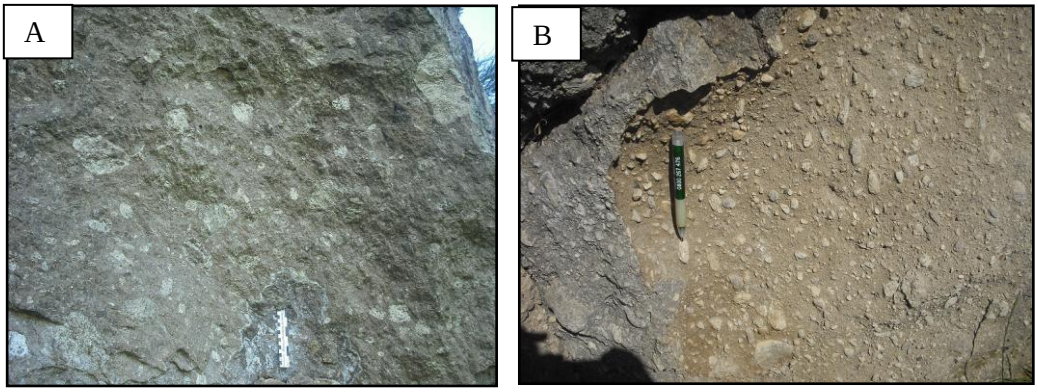

Figure 3.18: (A) Outcrop photo 10 m up from the base of the outcrop at location SL5 (Enclosure 1), note the high concentration and size of some of the pumice clasts with respect to the scale (10 cm). (B) pumice-rich outcrop at SL7 (Enclosure 1) approximately 3 m up from the base.

There is an increasing trend in the maximum size of the pumice clasts observed within SL5 (Fig 3.17 A). The average of the 5 maximum clasts measured reaches up to 250 mm between 16 – 17 m up the profile. Most clasts however measure < 60 mm along the long axis. There is no variation or trend observed in the maximum size of the pumice clasts for SL7 (Fig 3.17 B). The clast sizes are smaller (average of 60 mm) than they are in SL5 and appear to be of a similar size throughout the stratigraphic column. The aspect ratios of the pumice clasts in both profiles are low (< 2) and these tend to decrease very slightly with an increase in stratigraphic height.

There are 2 types of pumice (Fig 3.19) within the upper unit: type 1 clasts are predominant and are white – cream, highly vesicular and crystal rich; type 2 is minor and is grey/brown, streaky, moderately vesicular, and crystal rich. Both types have a glomeroporphyritc texture. In thin section, some clasts are highly vesicular (Fig 3.20 A) where the vesicles range in size and shape (elliptical – spherical) and the larger vesicles are often lined with numerous small crystals as a result of vapour phase crystallization (Fig 3.20 B). Most of the clasts are wispy, non-devitrified and poorly-moderately vesicular where the vesicles are sub-parallel and tubular and the clasts show deformation around the large phenocrysts (Fig 3.20 C, D).

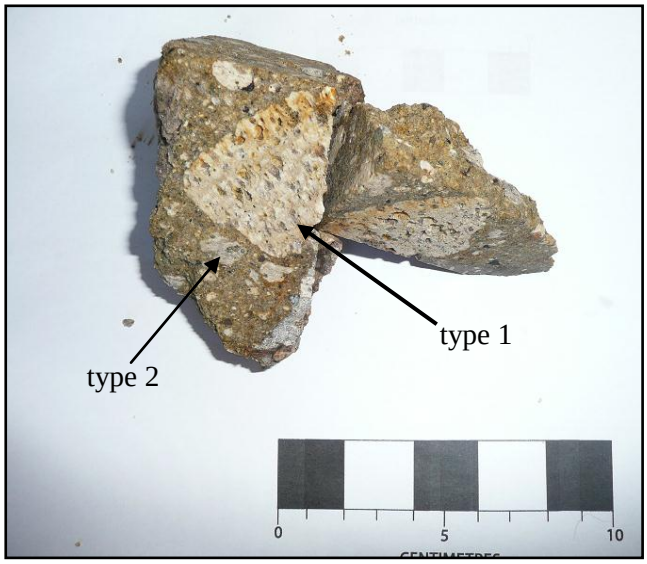

Figure 3.19: Two pumice types in the upper unit of the Ongatiti Ignimbrite. Sample retrieved 8 m from the base of SL5.

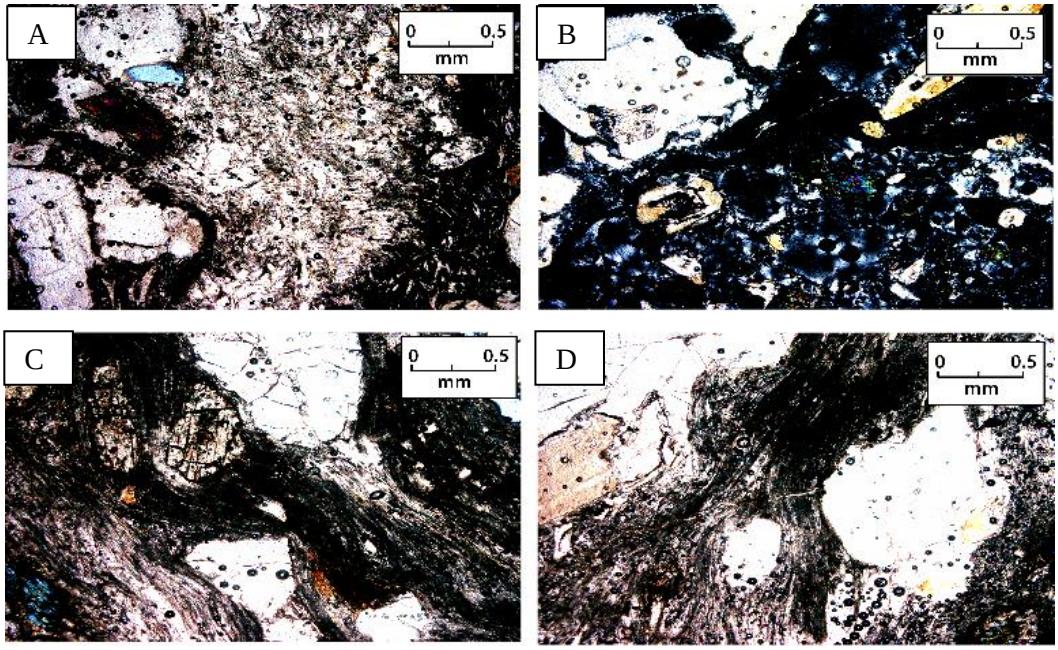

Figure 3.20: Photomicrographs of pumices in the upper pumice-rich unit of the Ongatiti Ignimbrite: (A) the highly vesicular type and (B) vapour-phase crystallisation in a large vesicle of the highly vesicular type. (C) and (D) the wispy, moderately vesicular type showing the deformation of the clasts around the large phenocrysts. Note how crystal rich both clasts are.

The proportion of crystals was point counted within thin sections of whole pumice clasts in the upper unit of the Ongatiti Ignimbrite. This method however was not carried out in the lower unit because of the lack of pumice and it is therefore not accurate to make a comparison between the two. It appears that the pumice clasts within SL5 have a higher proportion of crystals in comparison to those in SL7.

Two clasts were analysed in SL5 (3 and 16 m up from the base) where both contain 33 % of crystals. Three clasts were analysed in SL7 (1.2, 3 and 15 m up from the base) and the clasts tend to show an increase in the crystal proportion relative to an increase in the stratigraphic height. The proportion of crystals measured was 11 % (1.2 m), 13 % (3 m) and 19 % (15 m).

3.5.4 Lithic abundance and types

In contrast to the lower unit, the upper unit of the Ongatiti Ignimbrite is slightly richer in lithics. The abundance of lithics increases from 1 % to a maximum of 4 % and the maximum size of the lithics increases from 10 mm to a maximum of 50 mm from the base to the top of the profile of SL5 (Fig 3.17 A). The abundance of lithics remains fairly constant (< 2 %) and the maximum sizes tend to decrease slightly from 50 mm to 10 mm with stratigraphic height of SL7 (Fig 3.17 B).

A wide range of lithic types were identified in the upper facies of the Ongatiti Ignimbrite (Fig 3.21). The most dominant type observed was porphyritic and vitrophyric rhyolite clasts with lesser amounts of partially flow banded and partially spherulitic rhyolite lava, greywacke, argillite and welded ignimbrite (strong similarities with the lower facies of Ongatiti Ignimbrite) clasts. There were rare observations of highly vesicular hornblende rhyolite clasts, fine grained (aphanitic), grey microdiorite clasts and felsophyric rhyolite clasts.

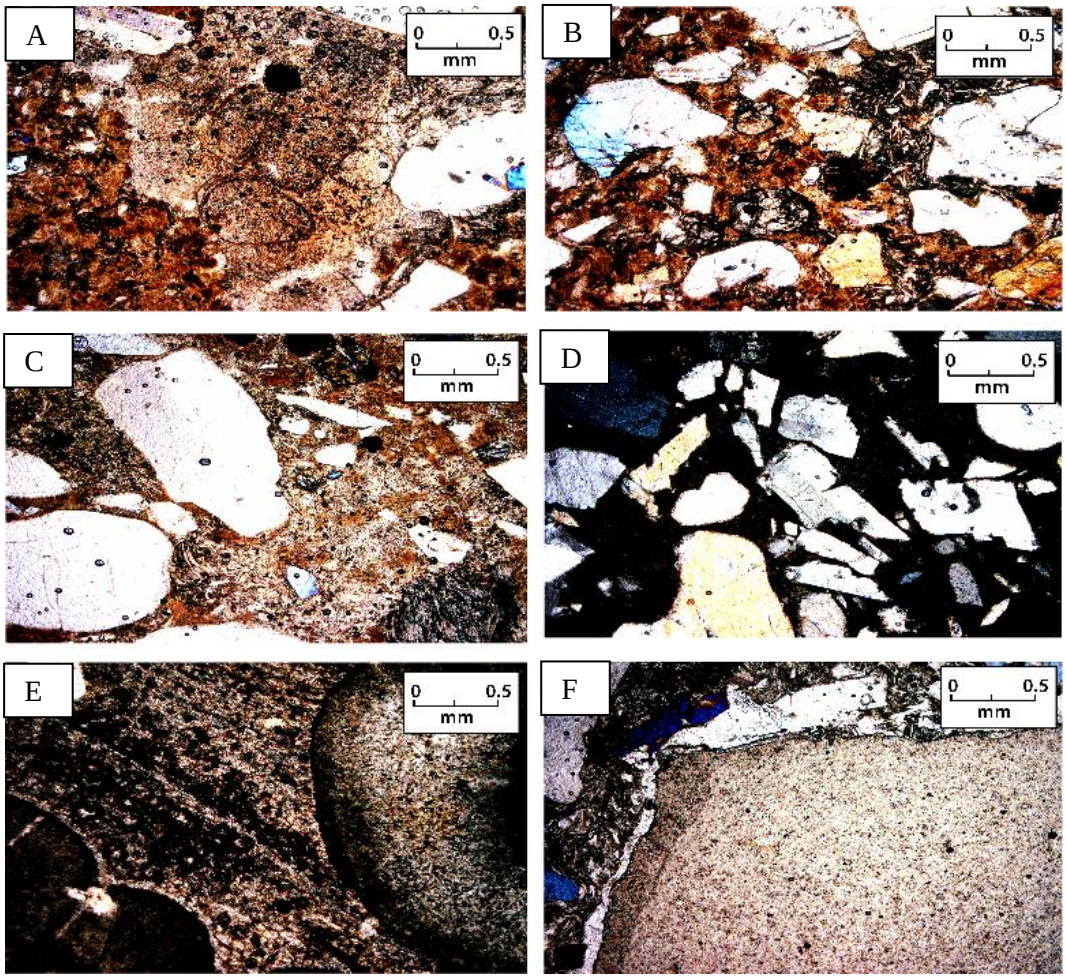

Figure 3.21: Photomicrographs of lithic clasts in the upper pumice-rich unit of the Ongatiti Ignimbrite: (A) partially devitrified, welded ignimbrite clast with perlitic cracks; (B) crystal rich matrix in the same lithic clast as shown in A; (C) welded, crystal rich ignimbrite clast showing the presence of pumice and large crystals in the matrix; (D) crystal rich nature of the matrix of the same ignimbrite clast as shown in C; (E) partially flow banded, partially spherulitic rhyolite clast; and (F) fine grained/ aphanitic microdiorite clast.

3.5.5 Crystals

The crystal abundance within the matrix of the upper facies of the Ongatiti Ignimbrite is high (30 – 50%) and crystal enrichment of the matrix is still apparent, although not as high as it is within the lower facies. A large proportion of small (< 2 mm) pumiceous fragments (Fig 3.22), along with small (< 2 mm) lithics and glass shards make up the remainder (50 -70 %) of the matrix.

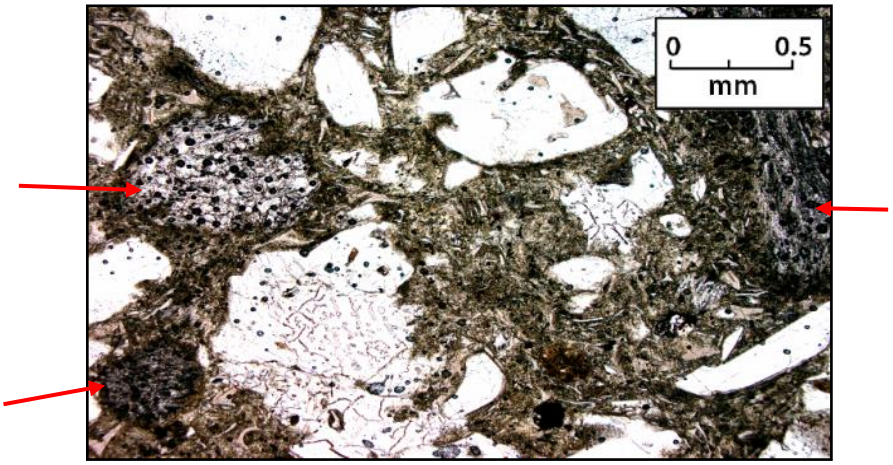

Figure 3.22: Photomicrograph of the matrix of the upper unit of the Ongatiti Ignimbrite under plane polarised light (sample from between 2 – 3 m of SL5). Note how the matrix contains a high abundance of both crystals and pumice (red arrows).

The abundance of crystals within the matrix of stratigraphic log 5 (Fig 3.17 A) shows an overall decreasing trend with an increase in stratigraphic height, but there is no trend in SL7.

The upper unit of the Ongatiti Ignimbrite contains the same mineral assemblage as the lower unit where plagioclase and quartz are the major components with lesser amounts of iron oxides, orthopyroxene and hornblende. The proportions of hornblende, orthopyroxene and iron oxides relative to the overall crystal abundance are lesser at the base but remain constant throughout the remainder of SL5 (Fig 3.17 A). The proportion of quartz and plagioclase are both higher at the base of the profile but then show little variation through most of the column. Within the upper zone of the profile, there is a slight increase in the proportion of quartz and a subsequent reduction in the proportion of plagioclase.

SL7 contains a higher proportion of hornblende and there appears to be an increase in the proportion of hornblende, orthopyroxene, and iron oxides around 3 m from the base, and therefore a slight reduction in plagioclase and quartz. The upper zone of the profile shows a sudden enrichment in plagioclase and as a result a sudden reduction in quartz.

The crystals are generally smaller (average of 0.5 mm) and anhedral (Fig 3.23). The crystals appear to be more fragmented and this is especially noticeable in

quartz. The size decreases and the shapes of the crystals become more irregular with an increase in stratigraphic height. The average size of the crystals within the upper zone of stratigraphic log 7 is less than 0.3 mm.

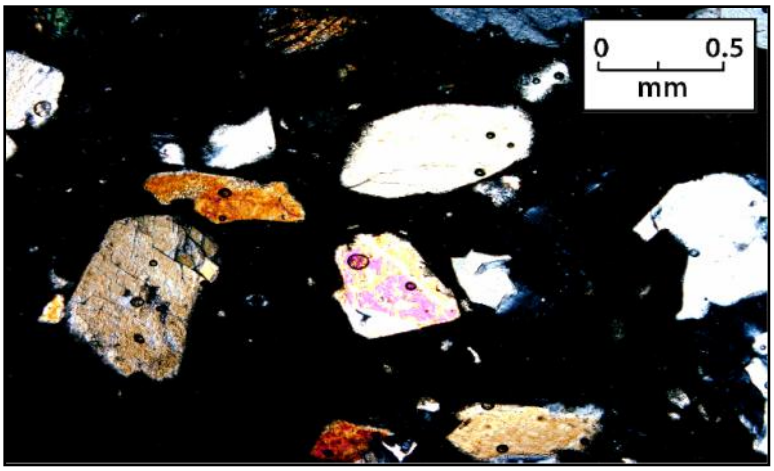

Figure 3.23: Photomicrograph (XPL) of crystals observed in the upper unit of the Ongatiti Ignimbrite, sample retrieved 3 m up from the base of SL5.

3.5.6 Glass shard texture

The matrix of the upper facies constitutes a larger volume percentage in comparison to the lower unit of the Ongatiti Ignimbrite (mainly due to the lower concentration of crystals and higher concentration of small (< 2 mm) pumiceous fragments). It consists of a vitriclastic matrix which becomes less well defined and more homogenous with an increase in stratigraphic height. The vitriclastic matrix consists of mainly large platy, lunate and cuspate shards with lesser amounts of Y- shaped and whole intact vesicle textures. The shards are more compact within the lower zone of stratigraphic log 5. They appear to have been exposed to vapour phase alteration (shards discoloured to a peach colour) in the upper zone and through the entire profile of stratigraphic logs 5 and 7 respectively.

3.6 Lithology and petrographic description of the transitional unit

3.6.1 Introduction

There are two main sections (approximately 1 km apart) along the continuous exposed bluff of the Ongatiti Ignimbrite within the Ongatiti Valley which are transitional between the lower pumice-poor and upper pumice-rich unit. These

sections of the bluff show a combination of characteristics from both, SL2 (Fig and SL3 (Fig 3.24) and their locations are shown on the map (Enclosure 1).

3.6.2 Stratigraphic variation

The deposited SL2 and SL3 have the most rapid vertical variation observed in comparison to the rest of the stratigraphic logs produced within the Ongatiti Ignimbrite. The most diagnostic feature was the sudden increase in the abundance of pumice with an increase in stratigraphic height.

There is no change in the colour of the matrix as it remains cream – light beige throughout. Both profiles are massive, poorly sorted and have no bedding structures or show any variation in grainsize. The welding in both however reduces with an increase in stratigraphic height. Welding is dense at the base of the SL2 and becomes partially to weakly-welded approximately 6 m up from the base. SL3 is partially – densely welded within the lower 3 m of the exposed profile and this slightly reduces with height. Both profiles show a pocky appearance from erosion of vapour-phase altered pumice from approximately half way up the exposed bluff (Fig 2.25). There are no contacts or distinct boundaries marking the transition from the pumice poor into the pumice rich composition in both SL2 and SL3.

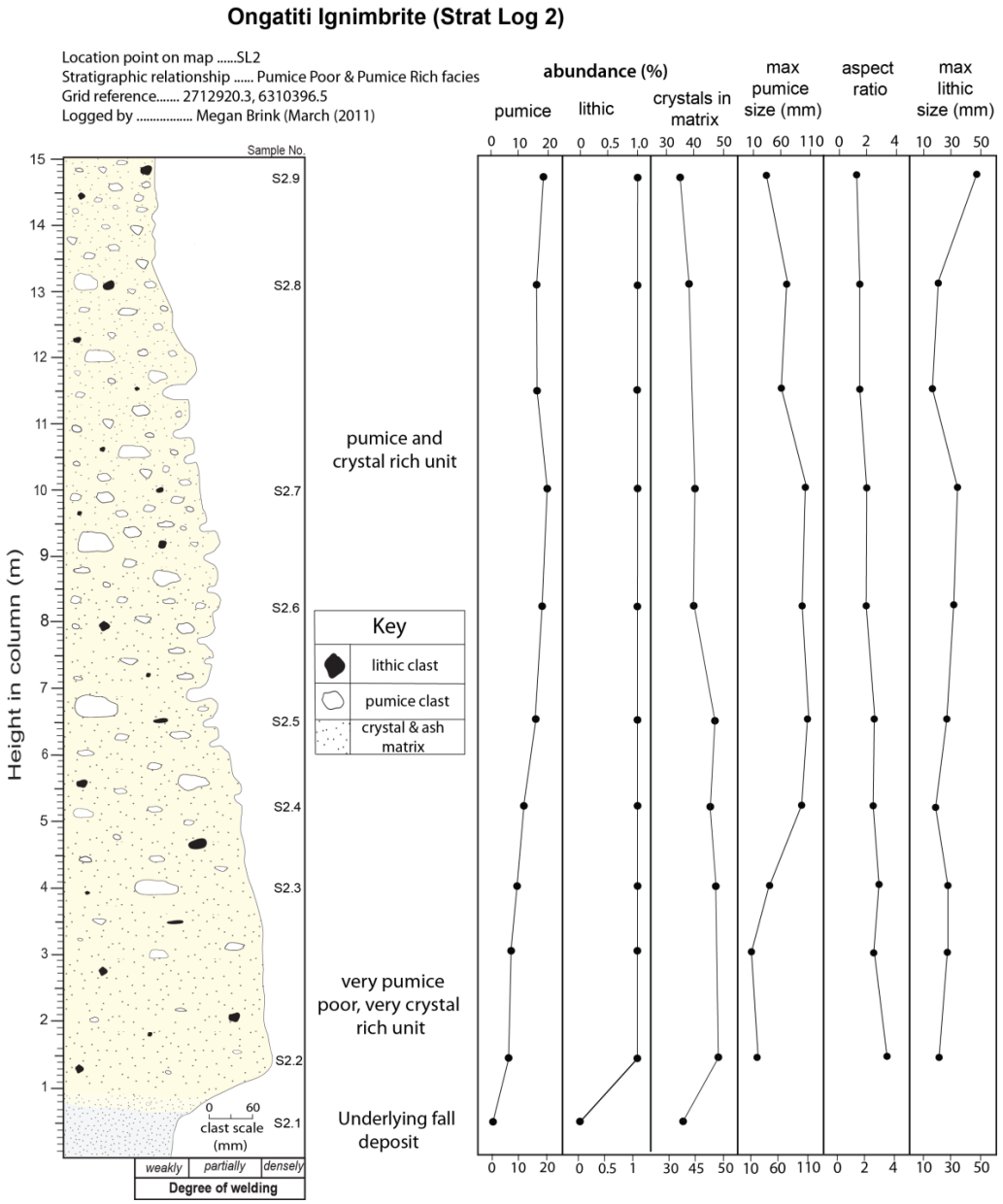

(A)

Figure 3.24: (A, B) Stratigraphic logs through the transitional unit of the Ongatiti Ignimbrite within the study area, highlighting the variation in the overall grainsize and appearance of the profile. The abundance of pumice, lithics and crystals, the maximum clast size of the pumice and their average aspect ratio, the maximum clast size of the lithics and the individual proportions of the main mineral phases (B) are plotted against the log. Note the pumice and lithic abundances, their maximum clast size and the average aspect ratio of the pumice are all bulk rock visual field estimates, and the crystal abundances have been determined in thin section by point counting.

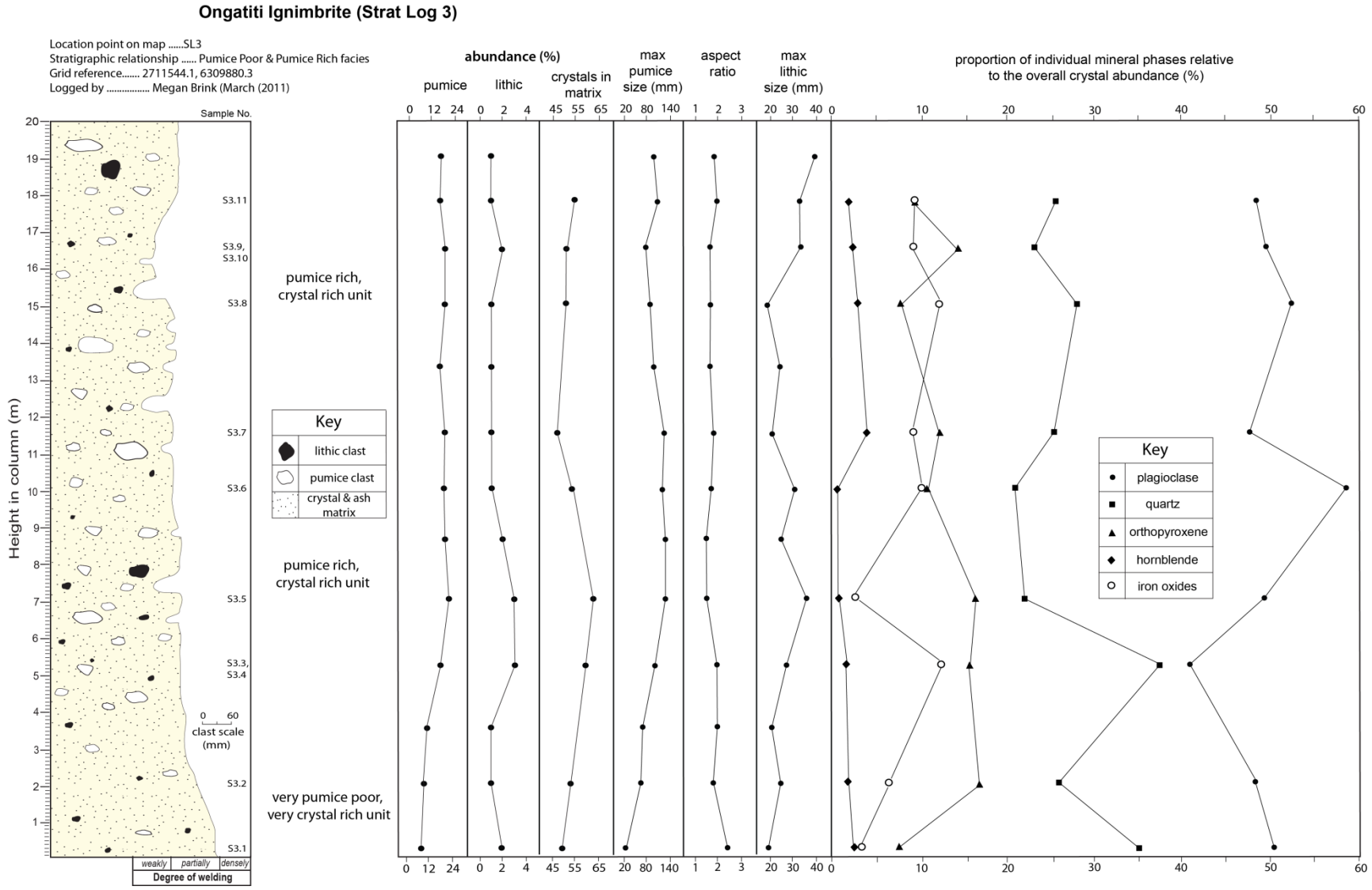
Ongatiti Ignimbrite (Strat Log 3)
Location point on map SL3
Stratigraphic relationship ..... Pumice Poor & Pumice Rich facies
Grid reference..... 2711544.1, 6309880.3
Logged by ..... Megan Brink (March (2011)
Sample No.
Height in column (m)
S3.11
S3.9, S3.10
S3.8
S3.7
S3.6
S3.5
S3.3, S3.4
S3.2
S3.1
pumice rich, crystal rich unit
pumice rich, crystal rich unit
very pumice poor, very crystal rich unit
Key
lithic clast
pumice clast
crystal & ash matrix
0 60
clast scale (mm)
weakly
partially
densely
Degree of welding
abundance (%)
pumice
lithic
crystals in matrix
max pumice size (mm)
aspect ratio
max lithic size (mm)
proportion of individual mineral phases relative to the overall crystal abundance (%)
Key
plagioclase
quartz
orthopyroxene
hornblende
iron oxides

(B)

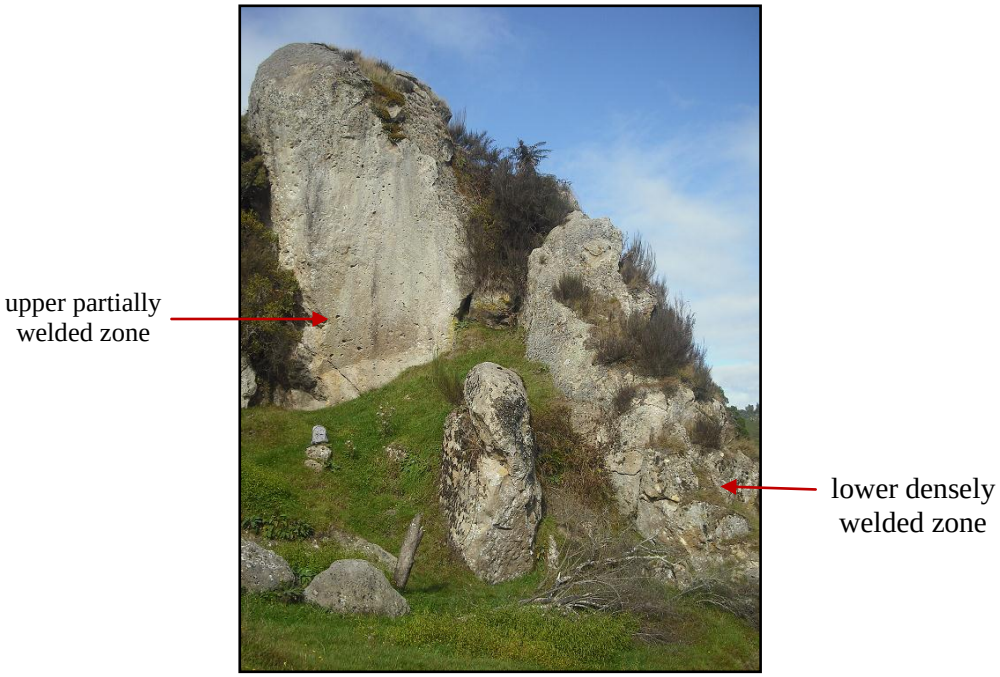

Figure 3.25: Ongatiti Ignimbrite at location SL3 (Enclosure 1) showing the pocky appearance of the outcrop within the partially welded zone which is absent in the lower, densely welded zone.

3.6.3 Pumice abundance and petrography

Both SL2 and SL3 show an increasing trend in the abundance of pumice with an increase in stratigraphic height. In SL2 (Fig 3.24 A) the abundance is moderate (< 10 %) within the lower 3.5 m and this gradually increases and reaches up to 20 %. SL3 (Fig 3.24 B) consists of a moderate abundance of pumice (< 12 %) within the lower 3 m of the deposit and a more sudden increase to approximately 20 % 5 m up from the base, and remains fairly consistent throughout the remainder of the profile.

The largest pumice clasts are located within the middle zone of both profiles where they reach up to 110 mm in SL2 and 140 mm in SL3. The aspect ratio of the pumice tends to gradually reduce with an increase in stratigraphic height where the base of both profiles contain pumice clasts with the highest aspect ratios measured.

There is no variation in the texture of the pumice clasts throughout the stratigraphic height of both SL2 and SL3. The pumice is similar to that in the lower unit of the Ongatiti Ignimbrite. The pumice is yellow – cream, crystal rich,

dense and poorly vesicular. However where the outcrop has been affected by vapour phase alteration (pocky zones of both outcrops) and weathering, the clasts have a more distinct darker yellow – orange appearance and tend to crumble with contact (Fig 3.26).

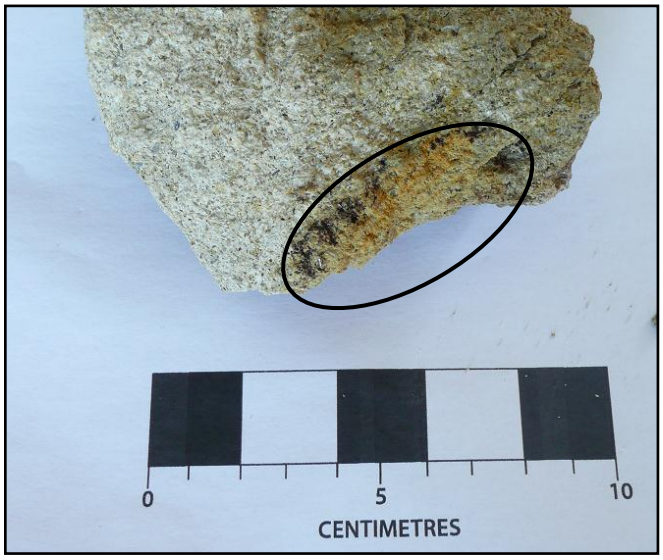

Figure 3.26: Altered pumice at location SL2.

The crystal content in the pumice varies from < 5 % to 40 %. Pumice clasts are compact with no fabric observed, instead they appear dense, poorly vesicular and glassy (refer to Fig 3.13). The clasts become less compact and are slightly more devitrified with an increase in stratigraphic height. Within the upper zone of SL3, type 2 streaky pumice occurs. The clasts are crystal poor, wispy and have a slight alignment of thin, tubular and small vesicles.

3.6.4 Lithic abundance and types

The distribution and abundance of lithic clasts is low (1 %) and constant throughout the stratigraphic height of SL2 (Fig 3.24 A). The abundance is slightly higher in SL3 (2 %) and is especially high (3 - 4 %) between 5 – 8 m from the base (Fig 3.24 B). There is a general increasing trend in the maximum lithic clast sizes for both SL2 and SL3. The range in lithic types show no significant difference from the types observed within both the upper and lower facies of the Ongatiti Ignimbrite. Greywacke and argillite clasts are most abundant, with

common glassy spherulitic, porphyritic, and vitrophyric rhyolite lavas and fine grained (aphanitic) grey microdiorite clasts.

3.6.5 Crystals

Both profiles have a high concentration of crystals within the matrix and show crystal enrichment when compared to the average crystal abundance within the pumice clasts. The abundance of crystals ranges between 30 – 50 % in SL2 (Fig 3.24 A) and between 45 – 65 % in SL3 (Fig 3.24 B), with the remainder of the matrix comprised of glass shards and small (< 2 mm) lithics and pumice. The decreasing trend observed in the crystal abundance for SL2 is relative to the increasing trend in the abundance of pumice. However in SL3, the abundance of crystals is more consistent throughout the height of the profile. The mineral assemblage in both SL2 and SL3 (Fig. 3.24) shows no variation from both the lower and upper units of the Ongatiti Ignimbrite.

3.7 Distribution of the different facies

A fence diagram is used to illustrate and put the vertical and lateral variations observed along the continuous exposed bluffs of the Ongatiti Ignimbrite through the Ongatiti Valley into perspective (Fig 3.27). This was created by aligning the 6 stratigraphic profiles produced within the valley (Figs 3.9, 3.17, 3.24) relative to the topographic elevation of their base (vertical scale) and the distance between each profile is clearly labelled. SL7 was not used in the illustration because this study is focusing on the lateral and vertical variations within the Ongatiti Valley. Also, the topographic elevation of the base of SL7 is not consistent with the rest of the stratigraphic logs (30 – 40 m higher in topographic elevation).

The Ongatiti Ignimbrite tends to show an uneven or non-uniform vertical transition between the different units (pumice-poor, pumice-rich and transitional) from the base to the top of the exposed bluffs. As a consequence, moving laterally from the east and through to the west of the Ongatiti Valley, and relatively at the same topographic elevation, the different units of the Ongatiti Ignimbrite are observed.

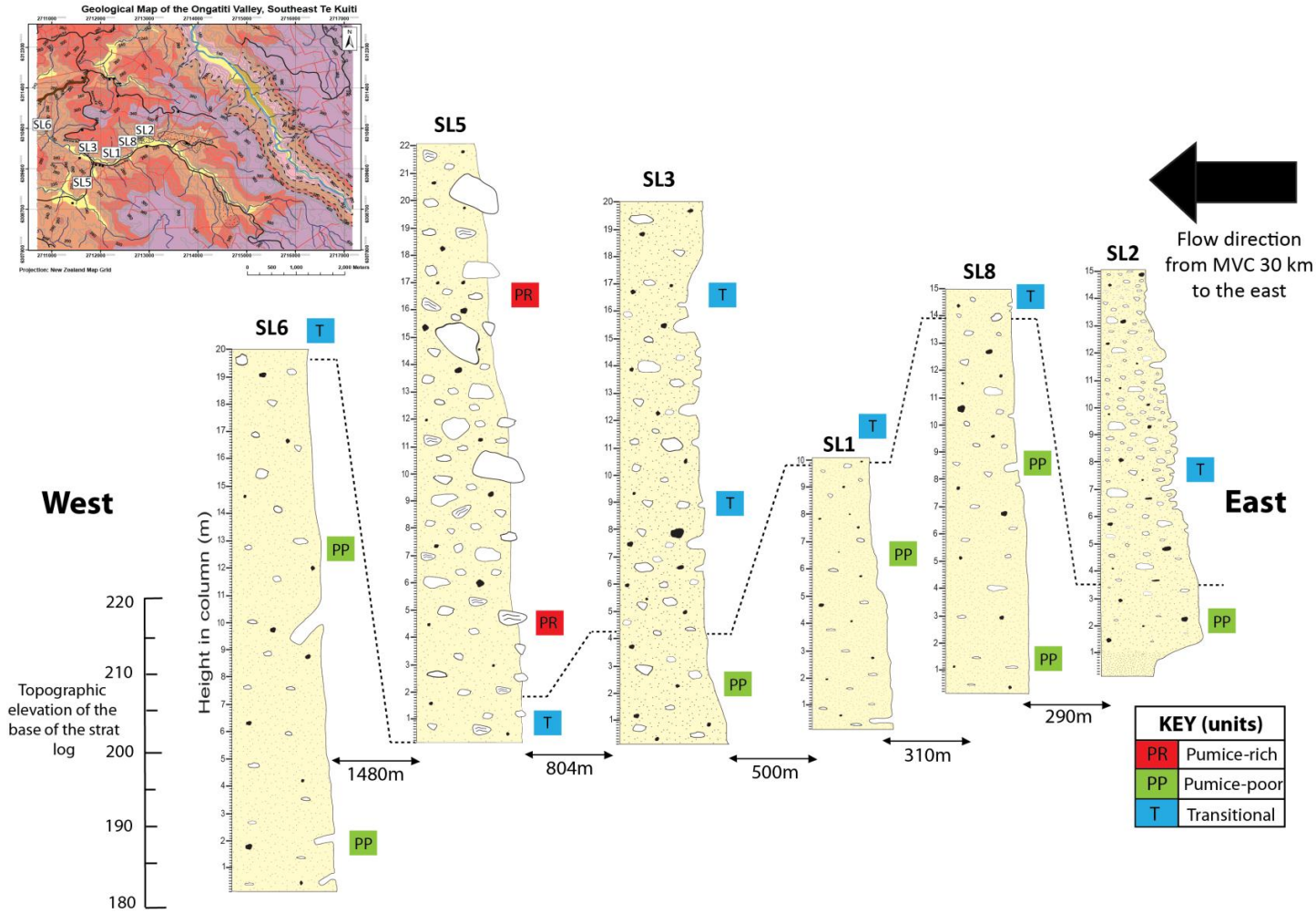

Figure 3.27: Vertical and lateral variation observed between the different stratigraphic profiles of the Ongatiti Ignimbrite in the Ongatiti Valley. The dashed line represents the inferred boundary between the lower pumice-poor (PP in the green label), the upper pumice-rich (PR in the red label) and the transitional (T in the blue label) units. The topographic elevation is shown on the vertical scale (left side of image) and the distance between each profile is labelled. Note the position of each profile with respect to each other is further explained in the geological map (top left corner).

3.8 Mineralogy

3.8.1 Introduction

The mineral assemblage of the Ongatiti Ignimbrite is quartz, plagioclase, orthopyroxene, hornblende, Fe-Ti oxides, zircon, and an unknown accessory mineral.

3.8.2 Quartz

The quartz crystals show a wide range in size but on average are 1.5 mm – 2 mm in diameter. The small broken crystals which are common are usually < 0.25 mm but larger crystals can reach diameters of > 2.5 mm (Fig 3.28). They are typically subhedral – anhedral and are often resorbed with large embayments present throughout.

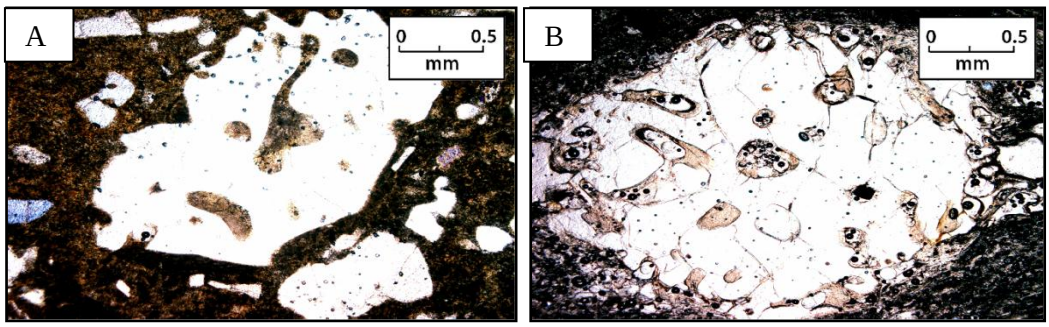

Figure 3.28: (A) Large anhedral quartz in the matrix of the Ongatiti Ignimbrite showing a resorbed texture with large embayments. (B) A large, anhedral quartz phenocryst (in pumice clast) with large embayments.

3.8.3 Plagioclase

The plagioclase crystals are mostly about 1.5 mm in diameter within the Ongatiti Ignimbrite but range from < 0.25 - > 2.5 mm. They are mostly tabular and anhedral (Fig 3.29 A-D). Some crystals show zoning (Fig 3.29 D) and may also contain resorbed sieve like textures.

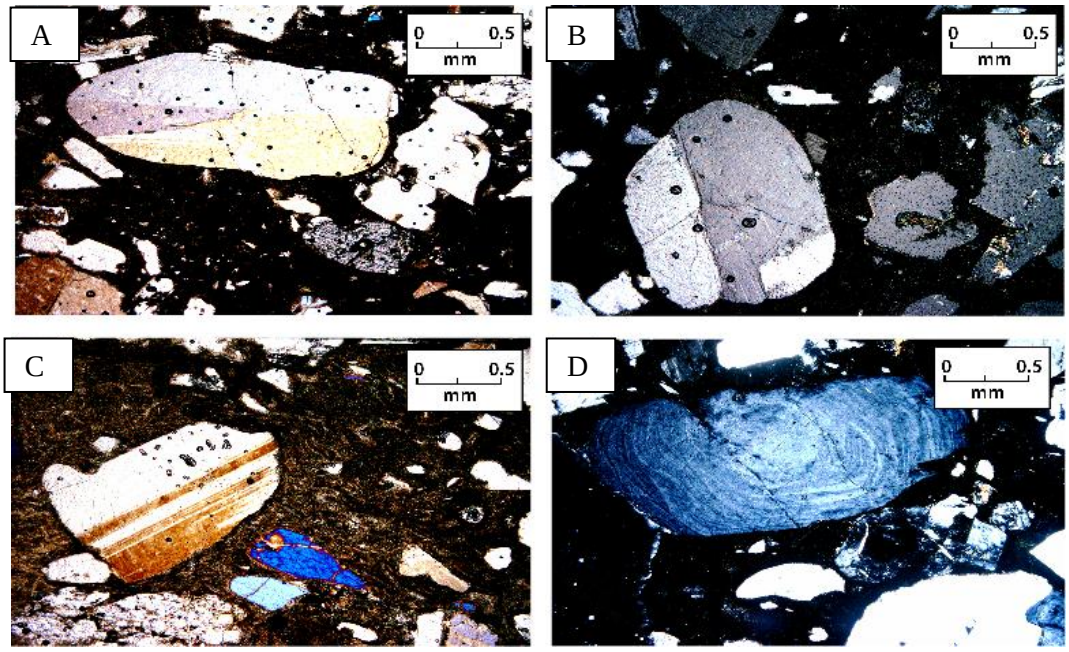

Figure 3.29: (A) and (B) anhedral and tabular plagioclase in the Ongatiti Ignimbrite, note the rounded edges of the prismatic shaped crystals. Plagioclase showing polysynthetic twinning (C) and zoning (D).

Plagioclase within the Ongatiti Ignimbrite ranges from oligoclase to andesine in composition ($An_{20.2 - 36.4}$) as shown in Figure 3.30. The cores, middle and rims of zoned crystals also vary within this compositional range.

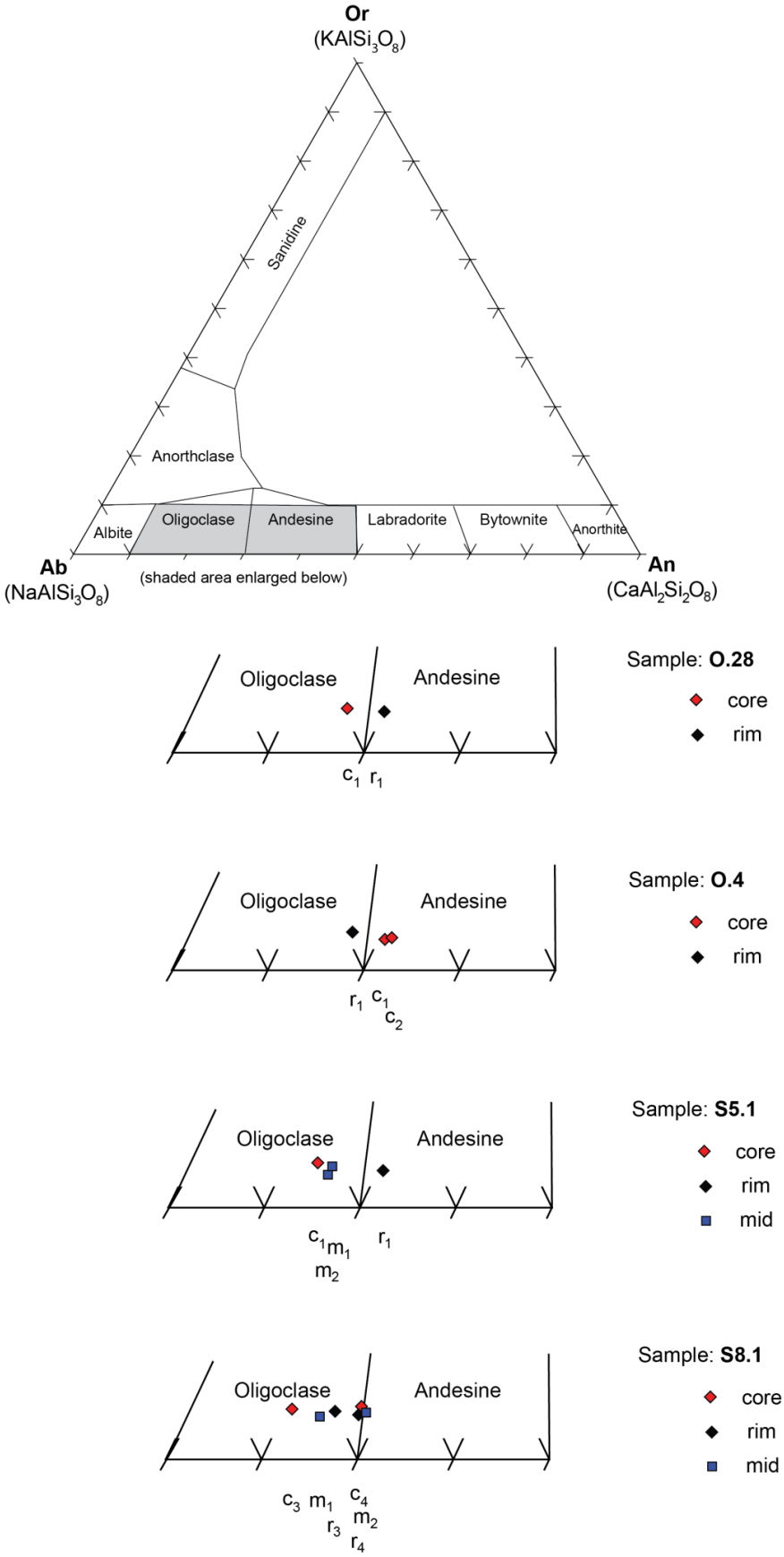

Figure 3.30: Classification of plagioclase within the Ongatiti Ignimbrite showing the difference in composition between the probed rims, middle sections and cores of the zoned crystals.

3.8.4 Hornblende

The hornblende crystals within the Ongatiti Ignimbrite are mostly small (0.5 mm in diameter) but few reach up to 1.5 mm. The hornblende is prismatic, green-brown, and subhedral (Fig 3.31).

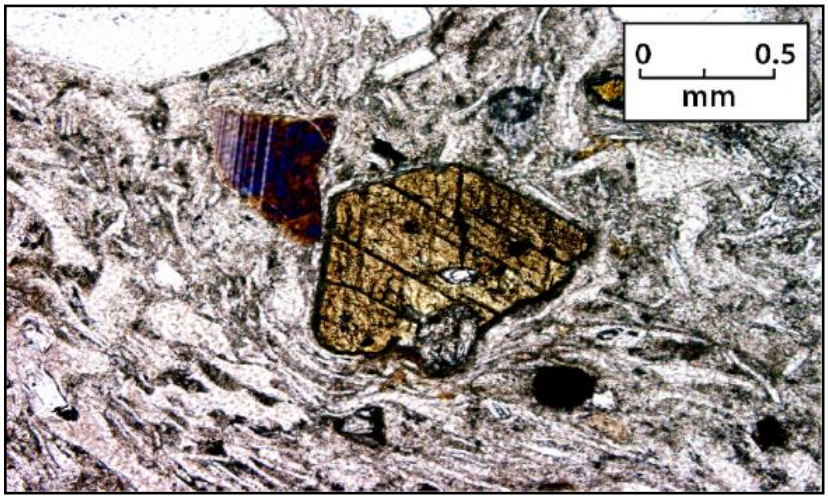

Figure 3.31: Photomicrograph of a hornblende crystal within the matrix of the Ongatiti Ignimbrite.

3.8.5 Orthopyroxene

Orthopyroxene crystals are often found in association with Fe-Ti oxides and are generally small (0.5 mm) and can reach up to 1.5 mm in diameter. The crystals are often observed as prismatic shapes with torn or ragged edges (Fig 3.32).

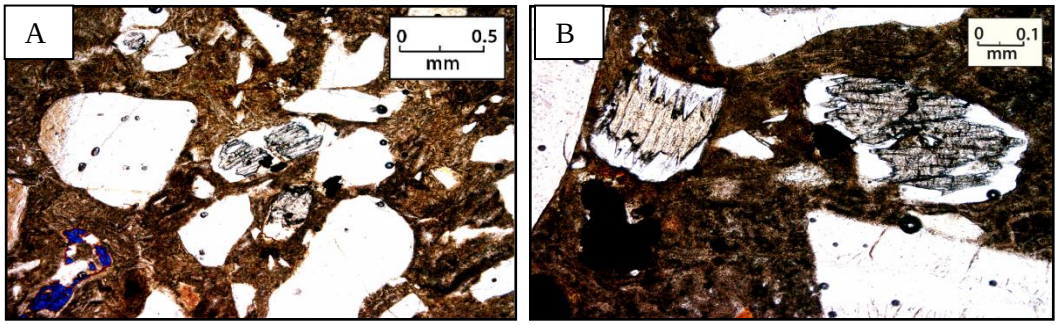

Figure 3.32: (A) 2 small orthopyroxene crystals surrounded by Fe-Ti oxides. (B) View under 10 x magnification of 2 crystals, note their ragged and torn edges.

The orthopyroxene crystals within the Ongatiti Ignimbrite are ferrosilite ($En_{42.9-45.6}$) in composition (Fig 3.33).

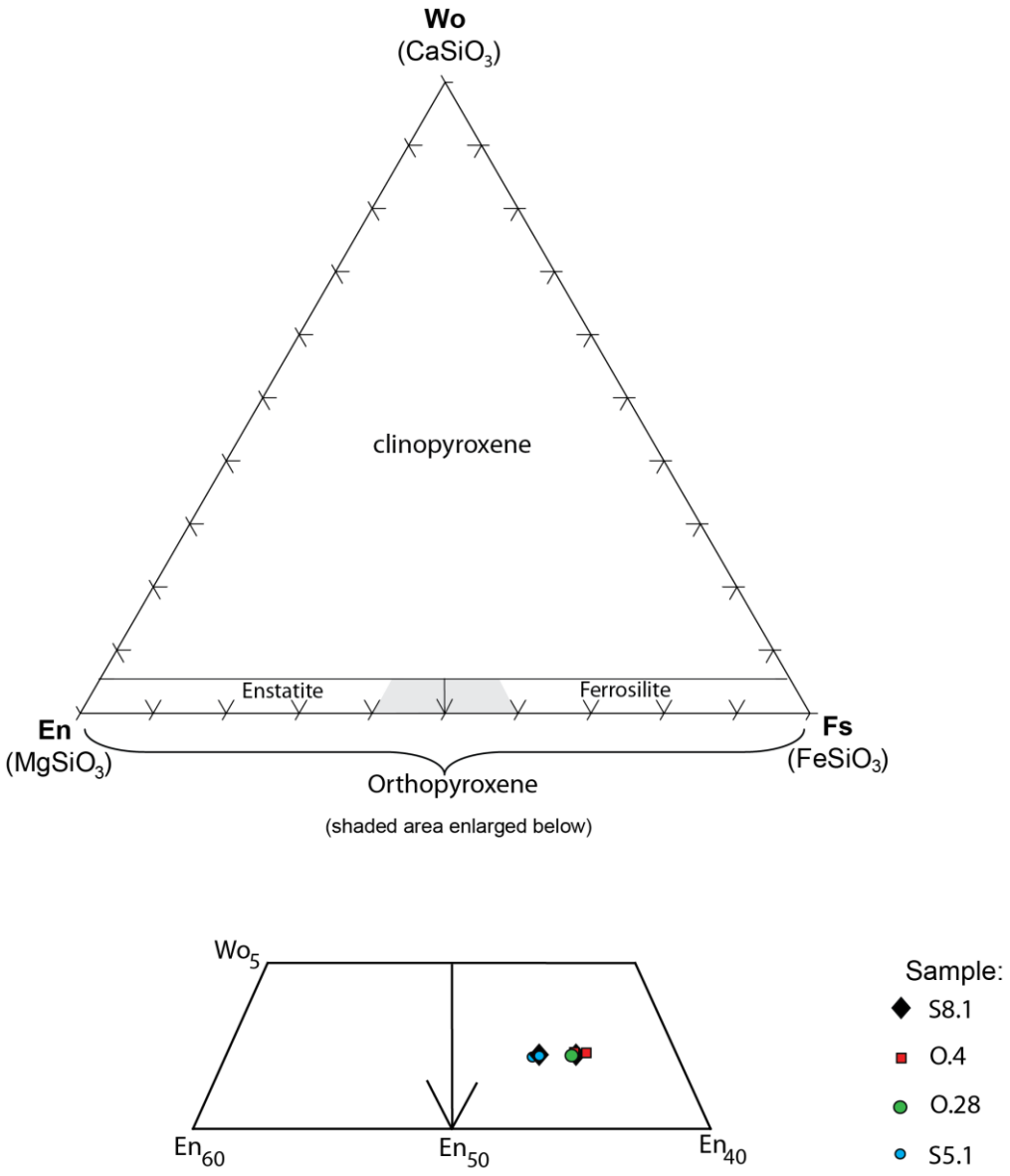

Figure 3.33: Classification of orthopyroxene crystals from 4 different samples within the Ongatiti Ignimbrite.

3.8.6 Unknown mineral

Within the sample O.4 (location 7, Enclosure 1) which is within the lower pumice poor facies of the Ongatiti Ignimbrite, a rare unidentified orange – red mineral which ranged in size and shape is observed. Its identification is unknown. Approximately 10 crystals were observed within a single thin section and these were generally < 0.25 mm (Fig 3.34 A-F). One crystal however is slightly larger than the rest (Fig 3.34 A) and appears to be a cluster of the smaller crystals. The optical and geochemical properties are summarised in Tables 3.1 and 3.2 respectively.

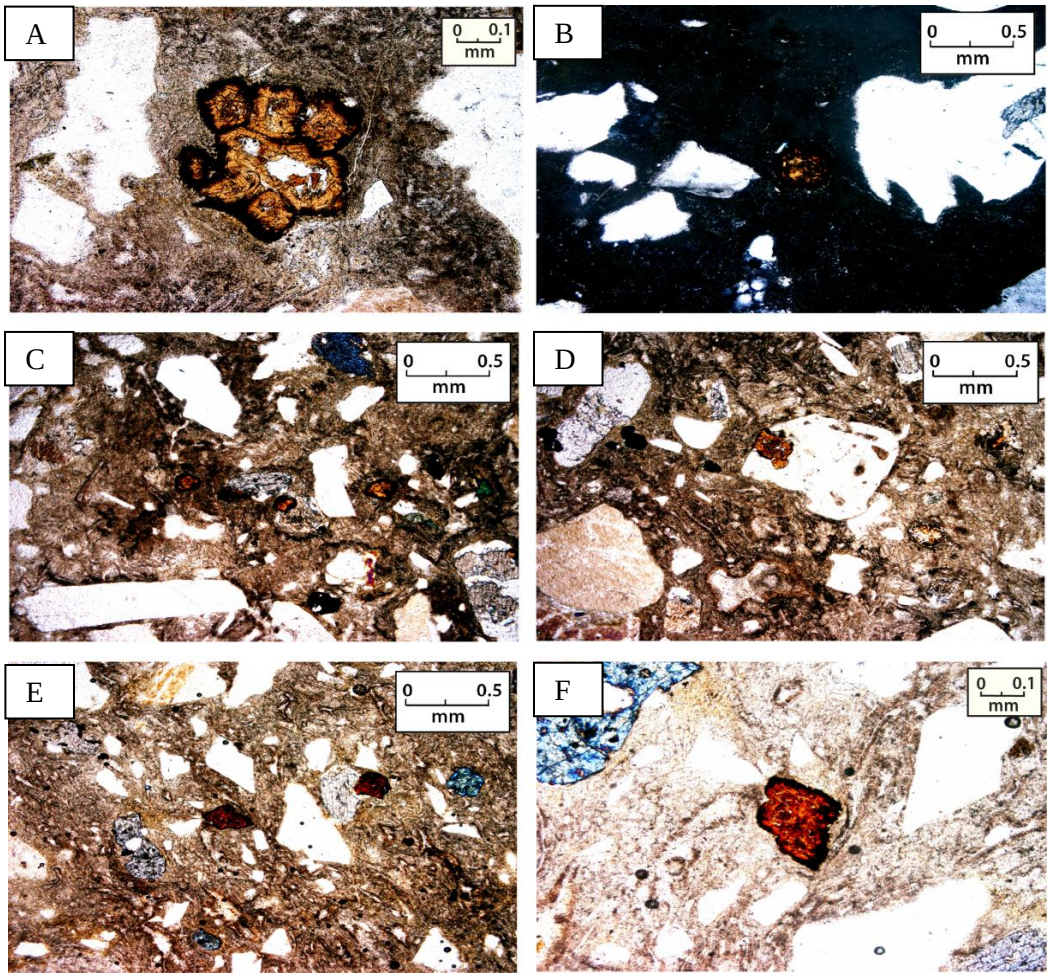

Figure 3.34: Photomicrographs of unknown mineral in the Ongatiti Ignimbrite: **(**A) Cluster of crystals with a distinct orange appearance. (B) XPL, note the colour darkens and does not show interference colours. (C) The typical size of the crystals , note their distinct high relief. (D) The crystal is occasionally found within the embayments of quartz crystals. (E) Darker shade where the crystals appear darker red. (F) Dark red crystal, note the lack of cleavage and high relief.

Table 3.1: A summary of the optical properties of the unknown mineral.

Habit	subhedral -anhedral
Cleavage	absent
Relief	Very high
Twinning	absent
Colour	orange - red
Extinction	non-defined (does not go into complete extinction)
Pleochroism	a slight change from lighter to darker orange or red

Table 3.2: The electron microprobe partial analyses of major elements from the unknown mineral in the Ongatiti Ignimbrite.

UoW (petlab no.	2011 0903					
Sample no.	O.4					
Crystal:	**1**	**2**	**3**	**4**	**5**	**6**
(wt. %)						
SiO2	28.19	26.98	2.89	4.4	5.01	3.3
TiO2	38.54	35.39	27.64	48.44	53.16	32.66
Al2O3	2.24	1.87	3.77	6.93	8.34	3.9
FeO	7.96	7.12	0.94	1.69	0.96	0.83
MnO	-0.02	0.27	0.04	0.07	-0.04	0.07
MgO	0.94	1.14	0.07	0.24	0.27	0.12
CaO	0.66	0.69	0.28	0.59	0.77	0.36
Na2O	2.44	3.21	0	-0.01	–	0.08
K2O	2.03	2.12	0.09	0.15	0.16	0.1
P2O5	0.2	0.05	3.9	7.08	8.18	3.88
SO3	0.05	-0.02	0.11	-0.01	0.21	0.01
Cl	0.26	0.2	0.28	0.08	0.09	0.25
Cr2O3	-0.07	-0.07	0.05	0.04	0.09	0.11
NiO	0.15	-0.06	0.04	-0.07	-0.03	0.1
TOTAL	83.57	78.88	40.07	69.63	77.16	45.77

3.9 Geochemistry

3.9.1 Introduction

Selected samples from both the lower and the upper facies of the Ongatiti Ignimbrite were analysed by XRF, ICPMS and electron microprobe analyses (EPMA) ttermine their geochemical composition. The results are used to firstly classify the samples and then to confirm that both the lower and upper units of the Ongatiti Ignimbrite are the same ignimbrite. The major and trace element geochemistry will be used to examine the variation in composition with an increase in stratigraphic height. The analyses are given in appendix 3 (XRF analyses),appendix 4 (Electron microprobe analyses) and appendix 5 (ICPMS analyses).

Due to the low abundance and small size of the pumice clasts within the lower facies of the Ongatiti Ignimbrite, whole rock rather than whole pumice samples were used in this investigation. These included two key samples collected from around the study area (O.28 and O.4, locations 6 and 7, Enclosure 1) and samples

through the entire vertical extent of SL8 (7 samples) and SL6 (4 samples). Whole pumice samples were used in the analysis of the upper facies of the Ongatiti Ignimbrite from both SL5 (4 samples) and SL7 (7 samples). All 22 samples were analysed through XRF analysis but specific samples were selected for ICPMS and electron microprobe analysis.

3.9.2 Rock Classification

The silica composition and rock classification for all 22 samples of the Ongatiti Ignimbrite are displayed on the total alkalis (Na_2O + K_2O wt %) versus silica (SiO_2 wt %) diagram of Le Maitre et al. (1989) (Fig 3.35). The SiO_2 composition of the samples (normalised to 100 %, volatile-free) show a small range from 69 through to 73 %. Based on both these silica measurements and on this rock classification scheme, the Ongatiti Ignimbrite consists of both dacite and rhyolite compositions. There is a slight variation in composition but no systematic distinction between the lower and the upper units.

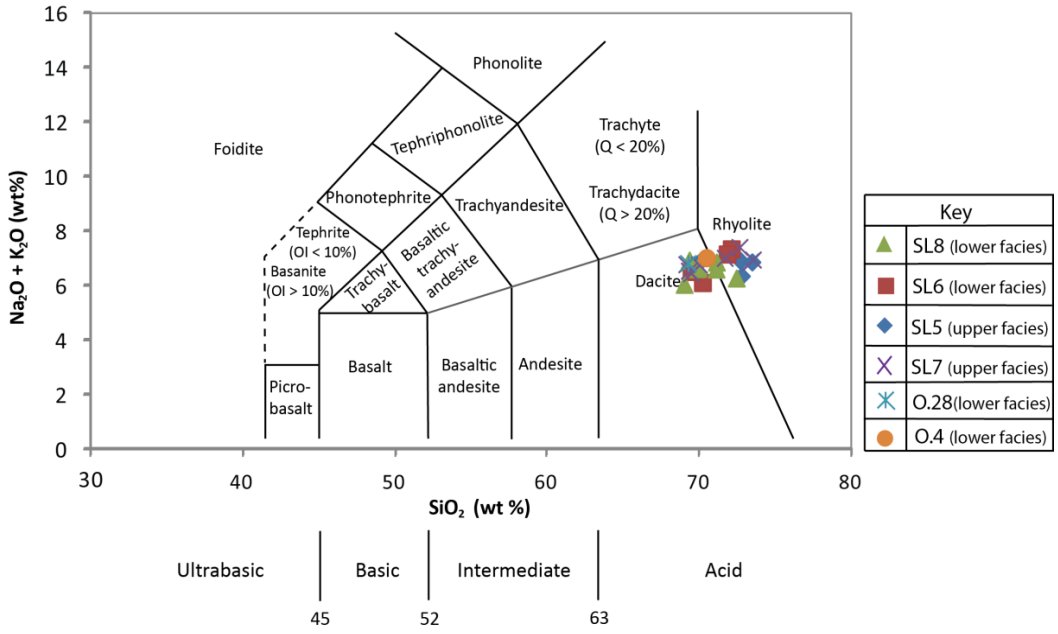

Figure 3.35: The chemical composition of whole rock and whole pumice samples from the Ongatiti Ignimbrite displayed and classified using the total alkalis versus silica diagram of Le Maitre et al. (1989).

The 22 samples are further classified by using the subdivision of subalkalic rocks based on the K_2O vs silica wt % diagram of Rollinson (1993). Most of the samples (Fig 3.36) belong to the medium K or the calc-alkaline rock series

however five of the samples from the upper facies of the Ongatiti Ignimbrite fall within the boundary division between the medium K / calc-alkaline and high K calc-alkaline series.

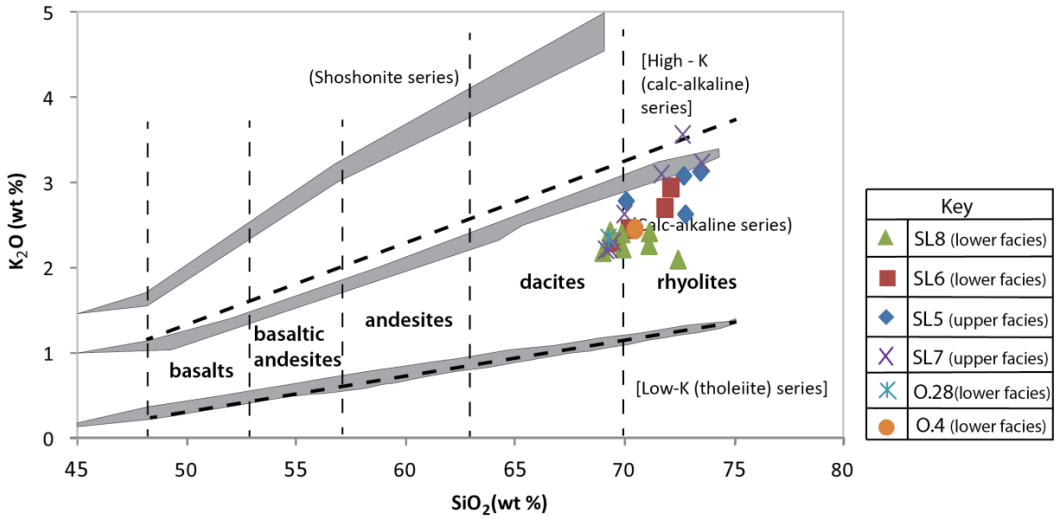

Figure 3.36: K_2O vs SiO_2 diagram (based on Fig 3.5 in Rollinson 1993) displaying and classifying the whole rock and whole pumice samples of the Ongatiti Ignimbrite relative to the subdivision of subalkalic rocks.

3.9.3 Major Element Chemistry

Major element compositions of pumice, whole-rock and glass shards and glass in pumice are shown in Fig. 3.37. The major element concentrations determined through electron microprobe analysis on glass shards within the lower facies (green circles) and within the glass of pumice from both the lower (blue diamonds) and the upper facies (green triangles) are displayed on the same plot. The major element compositions of the whole pumice samples (red squares) are much more variable than the compositions of the glass shards and glass within the pumice. They also tend to have a much lower SiO_2 wt % content due to being a representation of the composition of glass plus phenocrysts rather than just the glass as it is with microprobe analyses of glass shards and glass in pumice. In comparison, glass compositions tend to cluster and have a high SiO_2 wt % composition.

Microprobe analyses confirm that the lower and upper facies are both components of the Ongatiti Ignimbrite. There is no clear distinction between the major element

composition of the glass within the lower pumice poor and the upper pumice rich units.

The trends observed in the major element composition of the whole pumice clasts indicate that the Ongatiti magma chamber was zoned as a result of fractional crystallisation. The concentration of Al_2O_3, CaO, Fe_2O_3 and Na_2O decrease with increasing SiO_2. These negative trends are indicative of the fractionation of plagioclase (Al_2O_3, CaO), and iron oxides, orthopyroxene and hornblende (Fe_2O_3). K_2O shows a strong positive correlation with an increase in the SiO_2 content indicating that it is behaving as an incompatible element and was not involved in crystal fractionation.

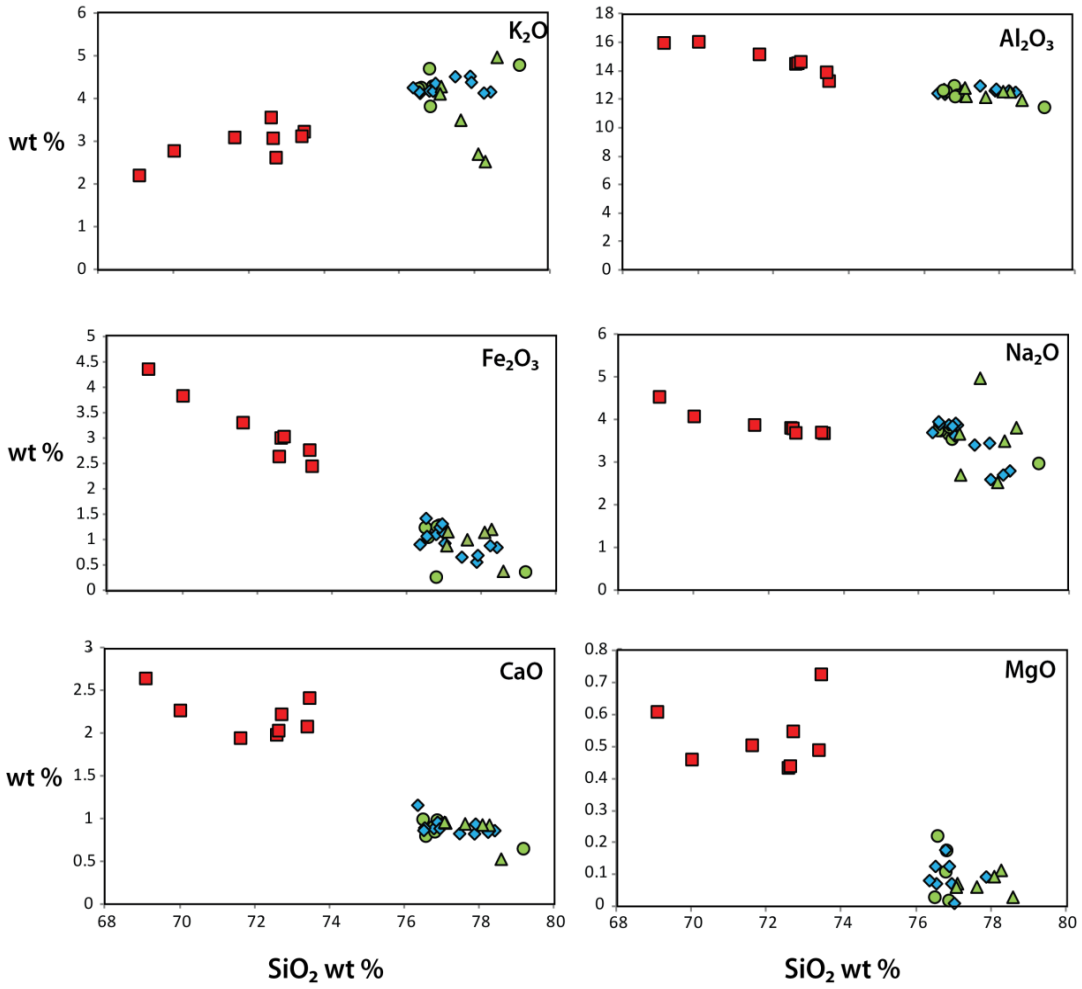

Figure 3.37: Major element Harker variation diagrams for whole pumice samples (XRF, red square symbols), individual glass shards from the lower facies (EPMA, green circles), and the glass within pumice clasts from both the lower facies (EPMA, green triangles) and the upper facies (EPMA, blue diamonds).

3.9.4 Trace Element Chemistry

Trace element compositions were determined by XRF analysis for all 22 samples of the Ongatiti Ignimbrite (whole rock and pumice). The concentrations (ppm) of these 8 trace elements (Ba, Rb, Th, La, Ce, Sr, Zr, Y) relative to the SiO_2 (wt %) content are presented in Fig 3.38. Ba and Rb show slight positive trends with an increase in the silica content and were therefore incompatible elements in the melt during crystal fractionation. Sr and Zr show a slight decrease, indicating that plagioclase and zircon respectively, could have been involved in crystal fractionation.

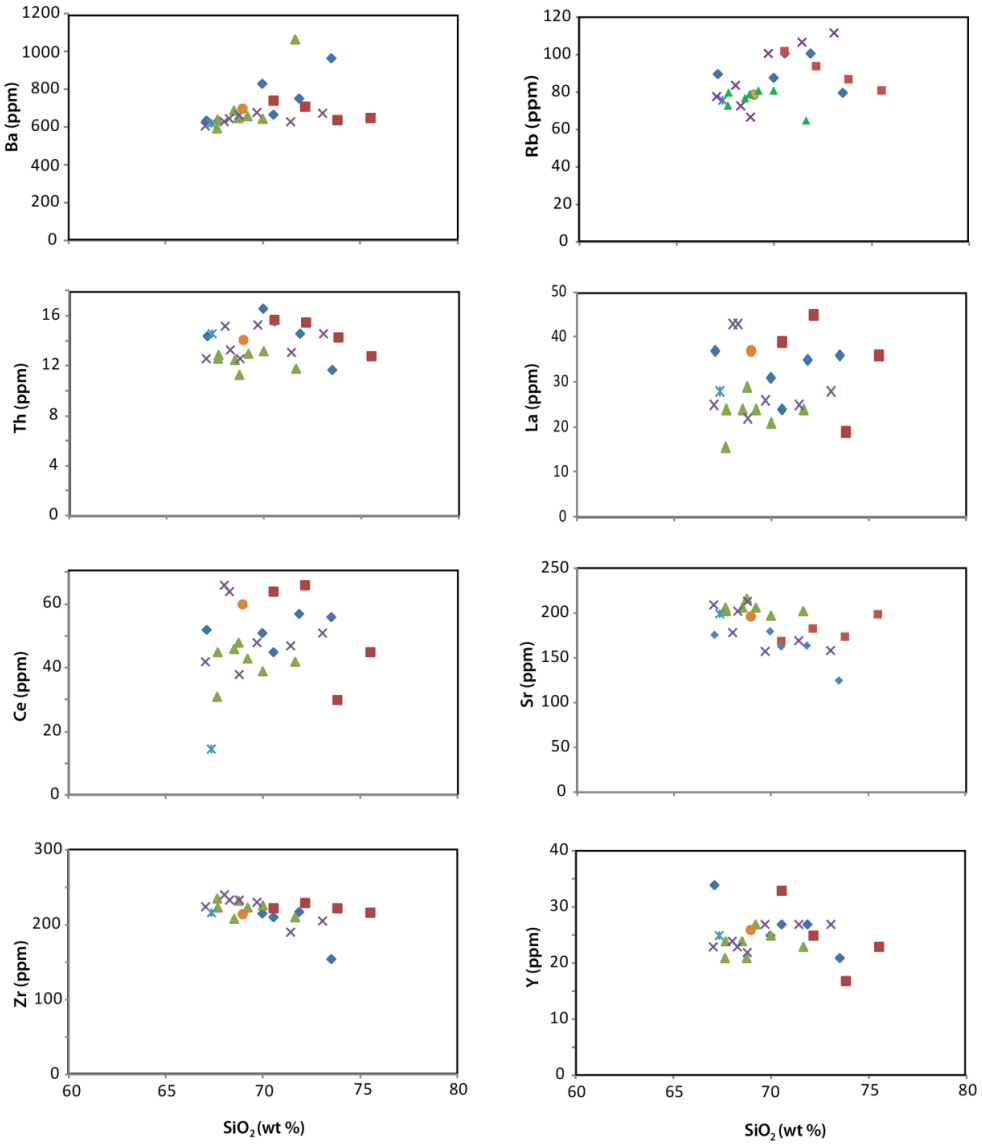

Figure 3.38: Harker variation diagrams for specific trace element compositions in the whole rock and whole pumice samples of the Ongatiti Ignimbrite. The data includes samples from both the lower unit; SL6 (red squares), SL8 (green triangles), O.4 (orange circle), O.28 (blue cross) and the upper facies; SL5 (blue diamonds), SL7 (purple crosses).

The trace element concentrations of six selected whole rock samples from the lower unit of the Ongatiti Ignimbrite (O.4 and 5 samples from SL8) were further measured using ICPMS analysis at Monash University, Melbourne. Their measurements have been normalized to the primitive mantle reference standards of Sun and McDonough (1989) and the results are displayed as a multi-element diagram (Fig 3.39).

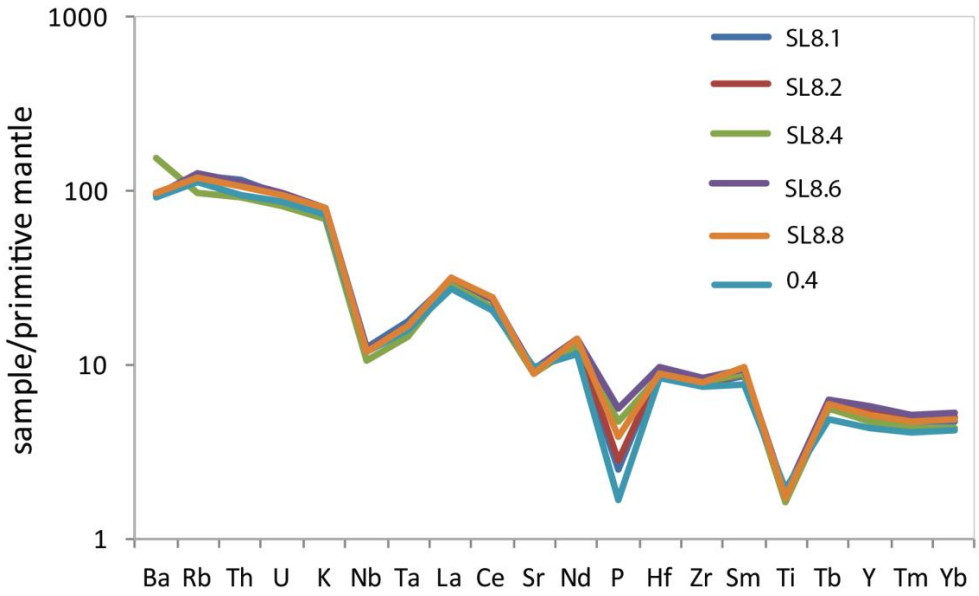

Figure 3.39: Multi-element abundance diagram (spider diagram) for specific whole rock samples of the Ongatiti Ignimbrite normalized to the primitive mantle values of Sun and McDonough (1989).

All six samples have an identical trend where there is a distinct depletion in Nb, P and Ti (compatible elements) and an enrichment observed in Ba, Rb, Th and U (incompatible elements). This pattern could represent the fractional crystallisation of ilmenite and titanomagnetite (Ti), apatite (P) and titanomagnetite (Nb) (Bowyer 1997). Sample O.4 shows a depletion in P relative to SL8 and could also represent the fractional crystallisation of the unknown mineral described in section 7, which contains high amounts of P_2O_5 (Table 3.2). Or alternatively, these patterns shown could be a source effect which is typical of TVZ rhyolites and shows strong similarities with the pattern observed in Unit D (Chapter 4, Fig 4.27).

The rare earth element concentrations for the whole rock samples of the lower unit of the Ongatiti Ignimbrite (O.4 and 5 samples from SL8) were also analysed using

ICPMS analysis. Their measurements have been normalised to a common chondritic reference standard of Sun and McDonough (1989) and are displayed in Figure 3.40.

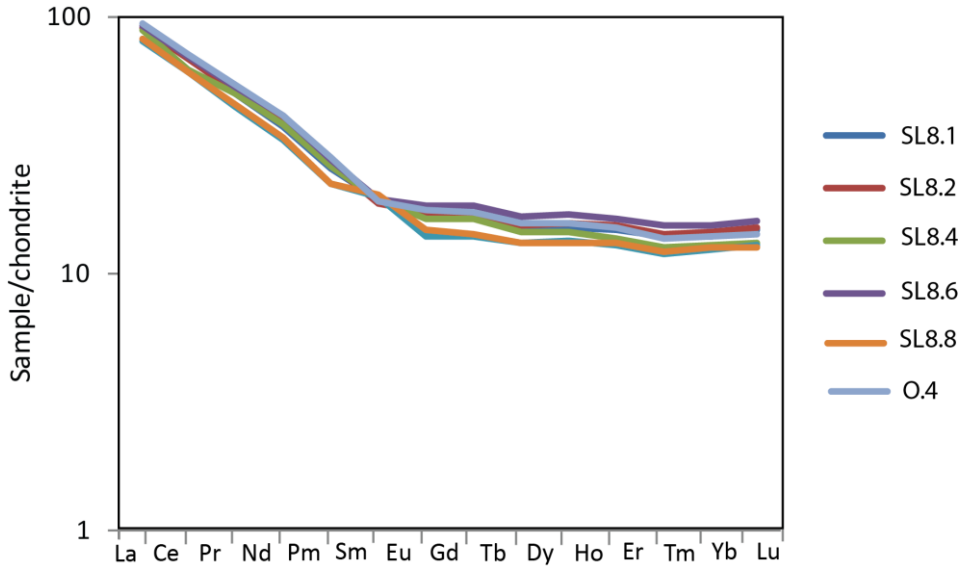

Figure 3.40: Rare earth abundances of whole rock samples of the Ongatiti Ignimbrite normalized to chondritic values of Sun and McDonough (1989).

The fractionation of the accessory phases within the lower unit of the Ongatiti Ignimbrite are characterised by having a strongly enriched light REE pattern with steep slopes. They contain no pronounced negative Eu anomaly and show depletion in the heavy REE which is revealed by the flat pattern and lower concentration in comparison to the light REE. The pattern is very similar for all samples but S8.8 (from the upper zone of the lower unit of the Ongatiti Ignimbrite) is slightly more enriched in Eu. These patterns differ slightly from those revealed in Unit D (chapter 4, Fig 4.28) by the absence of a negative Eu anomaly.

3.9.5 Major and trace element variation with height

The variation in the composition of the major (Fig 3.41) and trace elements (Fig 3.42, 3.43) with respect to an increase in stratigraphic height through both the lower and upper units of the Ongatiti Ignimbrite were examined. Both SL8 and SL5 show a general decrease in the wt % of SiO_2 with an increase in stratigraphic height however the highest concentrations are mid way up both profiles (Fig 3.41). There are no systematic trends in major elements composition with stratigraphic height, consistent with the data from Briggs et al (1993).

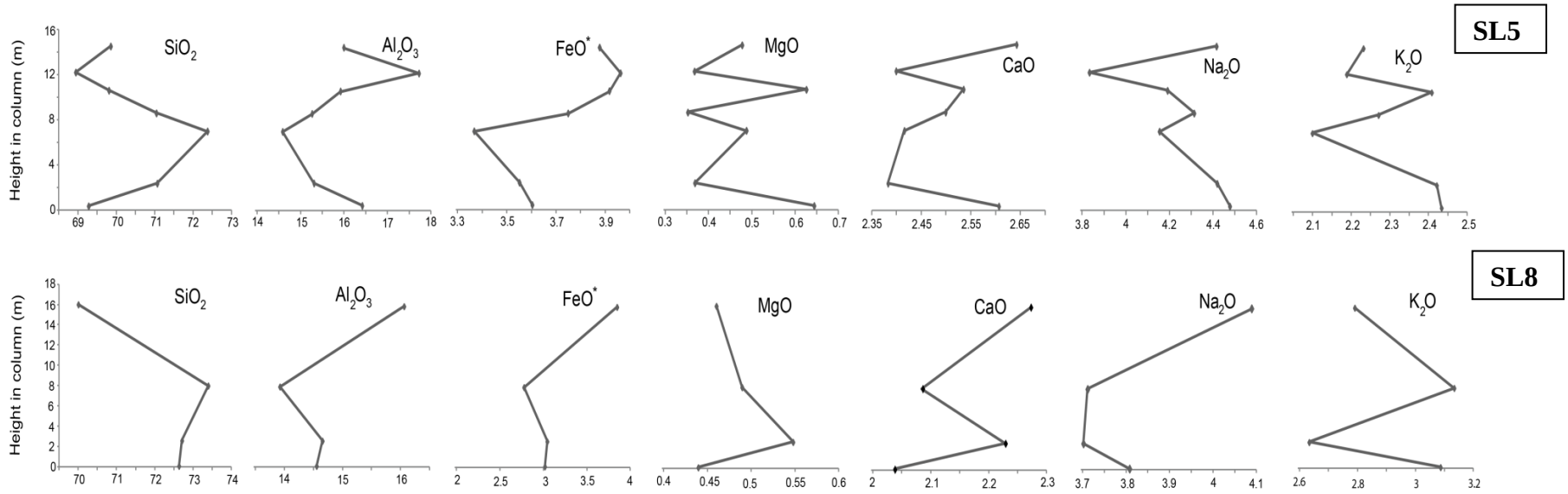

Figure 3.41: Variation in the major element composition in whole pumice samples from the upper unit/SL5 (top) and in whole rock samples from the lower unit/SL8 (bottom) of the Ongatiti Ignimbrite relative to the height of the column. The concentration of the major elements is in wt %.

Similarly, there are no trends in trace element composition with stratigraphic height (Figs 3.42, 3.43). These data are consistent with those of Briggs et al (1993) who showed that the Ongatiti magma chamber was zoned, as seen in Figure 3.39 of major elements, but this zonation was destroyed by syn-eruptive mixing. Syn-eruptive mixing prior to emplacement then explains the non-systematic trends in composition with stratigraphic height.

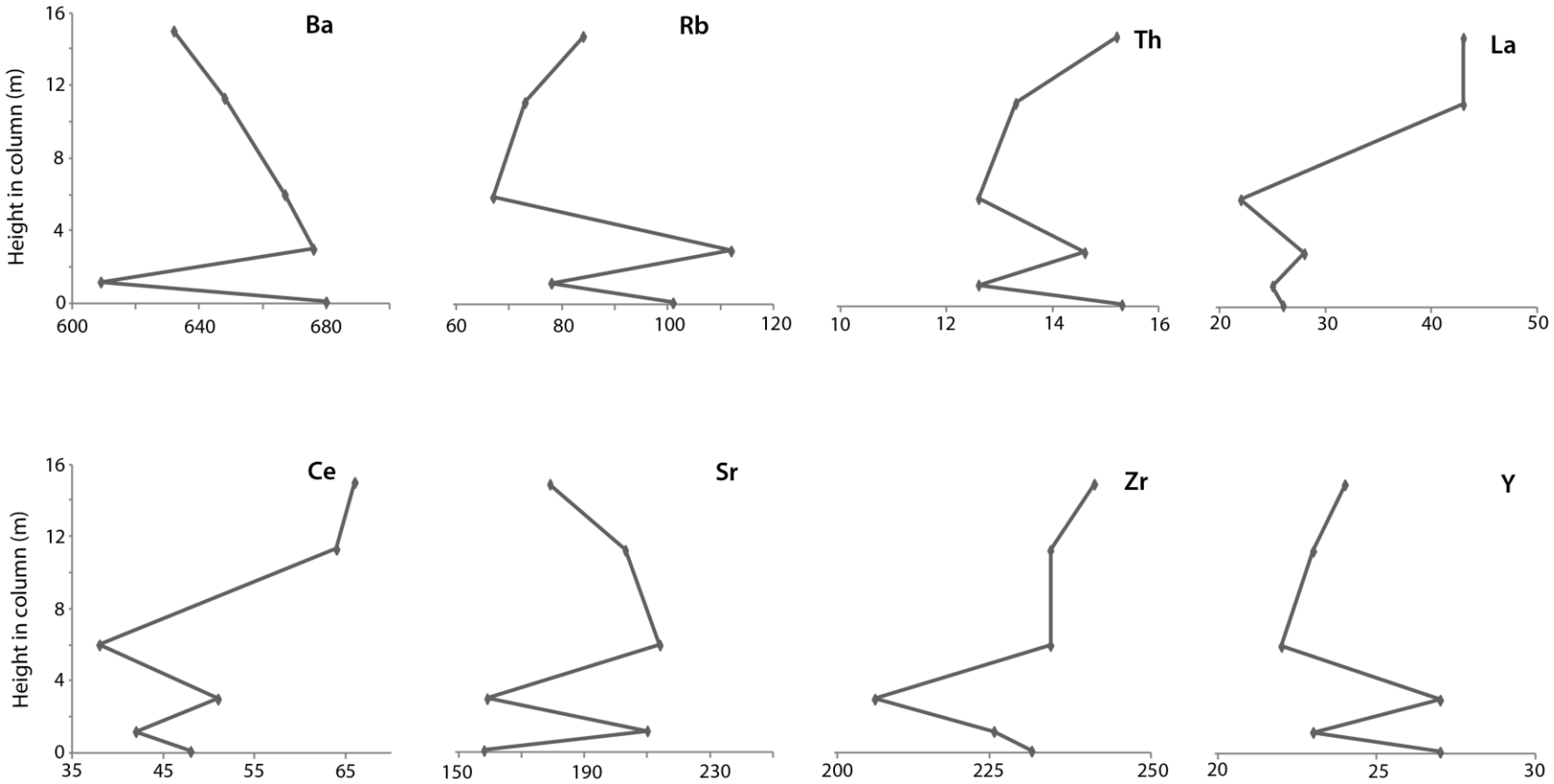

Figure 3.42: Variation in the trace element composition in whole pumice samples from the upper unit/ SL7 of the Ongatiti Ignimbrite relative to the height of the column. The concentration of the trace elements is in ppm.

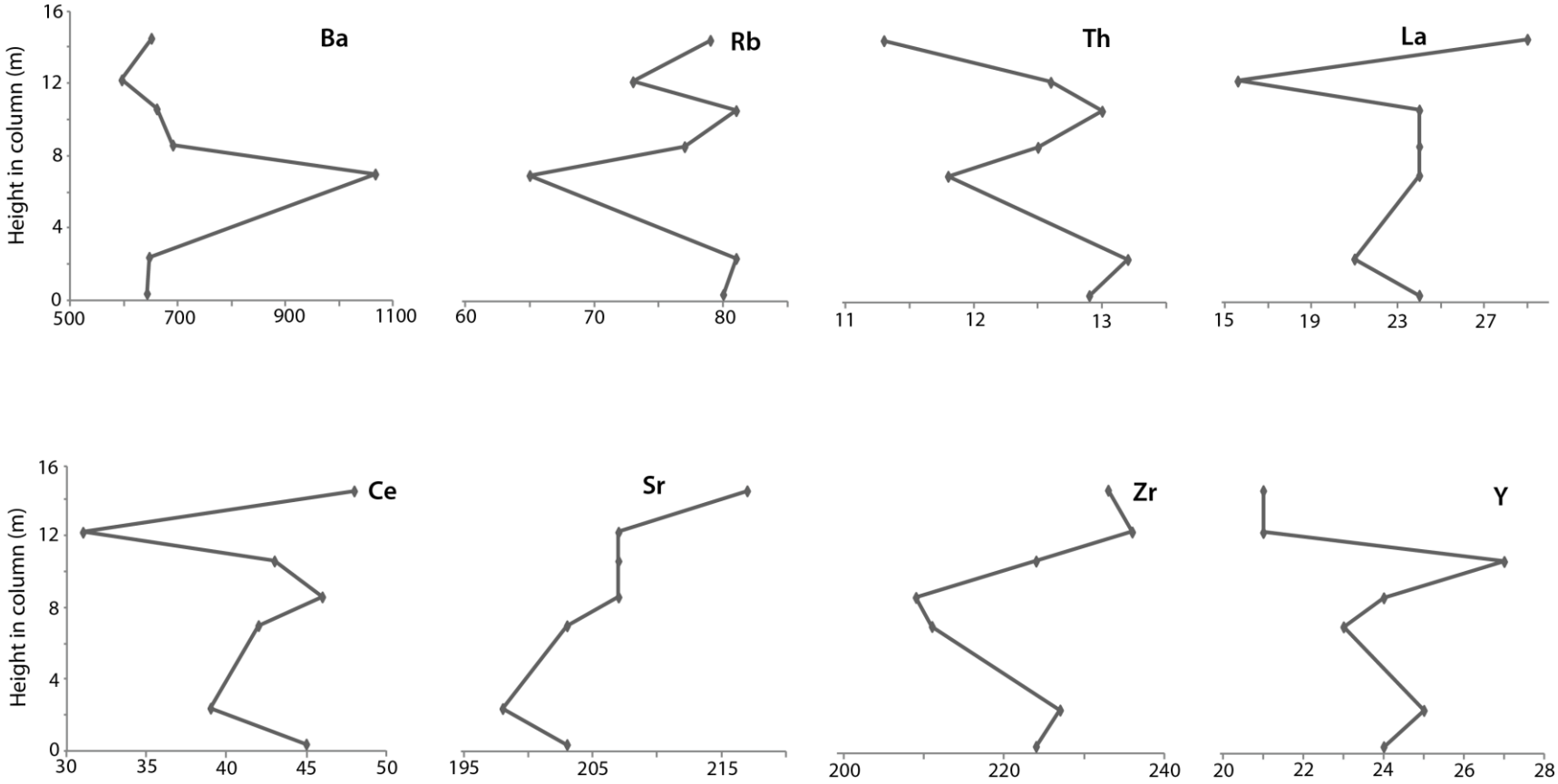

Figure 3.43: Variation in the trace element composition in whole rock samples from the lower unit/ SL8 of the Ongatiti Ignimbrite relative to the height of the column. The concentration of the trace elements is in ppm.

Chapter Four

Unit D

4.1 Introduction

This chapter comprises a brief background description of Unit D derived from previous published literature, descriptions of outcrops in the study area, lithology and petrography relative to the stratigraphic height of the deposit and whole-rock geochemical data.

Unit D has previously been described by Wilson (1986a,b) and Moyle (1989) as consisting of a lower 0.5 - 1.5 m thick bedded phreatoplinian fall deposit overlain by a 2 - 6m thick non-welded ignimbrite. There is a sharp and wavy contact between the lower fall deposit and the upper ignimbrite. The lower fall deposit displays a multiple-bedded nature with an overall fine grainsize (maximum pumice clasts rarely exceed 3 cm), however individual beds vary slightly in grainsize, sorting and the presence or absence of accretionary lapilli (often reaching 2 cm in diameter). The upper non-welded ignimbrite is crystal- and pumice-rich with few small lithics and accretionary lapilli. Overall, it is a fine grained ignimbrite deposit where the maximum pumice clast size does not exceed 2 - 3 cm.

4.2 Outcrop appearance of Unit D in the study area

The Unit D fall deposit and overlying ignimbrite are poorly exposed in the study area. However, where it is found outcropping, the thickness of the deposit does not exceed 3 m and it is never exposed laterally for more than 10 m at a time (Fig 4.1).

Figure 4.1: Unit D observed in the study area (SL9, Enclosure 1) where the dashed line represents the upper contact of the deposit beneath the Ahuroa Ignimbrite.

The contact of Unit D with the overlying Ahuroa Ignimbrite (Figs 4.1, 4.2) is sharp, highly irregular and has significant relief on it (> 2 m). The contact tends to disappear abruptly and is mostly hidden beneath the grass covered slopes underlying the bluffs of the Ahuroa Ignimbrite. This indicates that Unit D has either been extensively eroded before the emplacement and deposition of the Ahuroa Ignimbrite or that the underlying topography of Unit D was highly variable.

Figure 4.2: The upper contact between Unit D and Ahuroa Ignimbrite (dashed line). Note how the exposed thickness of the deposit rapidly reduces from 3 m and disappears beneath the grass covered slope over a distance of < 4 m.

Both Unit D fall deposit and ignimbrite are poorly-welded throughout. There is significant and rapid variation in the texture, componentry and bedding nature of the deposit. As a result, certain zones more resistant to erosion of the deposit tend to protrude out of the outcrop (Fig 4.3).

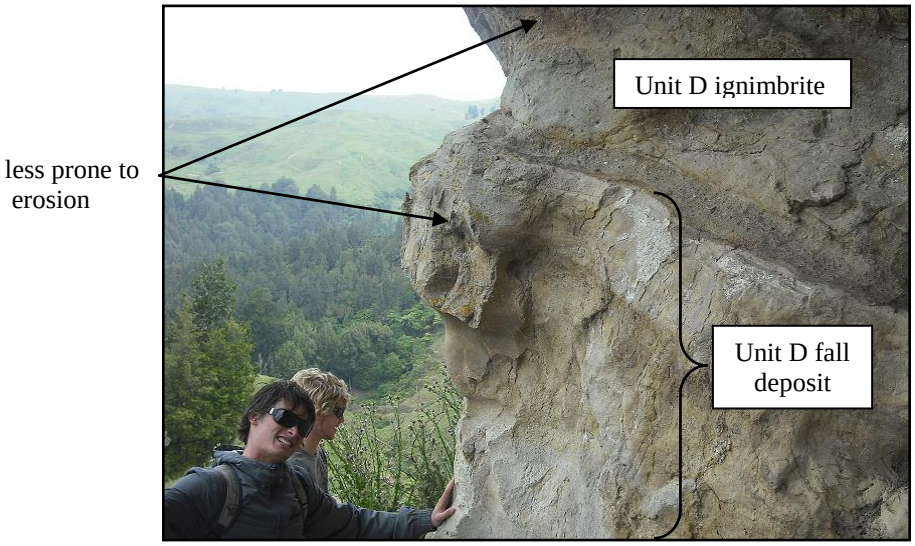

Figure 4.3: The coarser and more resistant beds of Unit D are less prone to erosion than the softer and finer zones and therefore protrude from the outcrop.

Unit D as a whole also tends to show differential degrees of erosion with respect to the inconsistent removal of case hardening. The outcrop reveals no apparent jointing structures throughout because it is poorly or non-welded, but, small and irregular spaced horizontal and vertical fractures are present, possibly as a result of compaction (Fig 4.4).

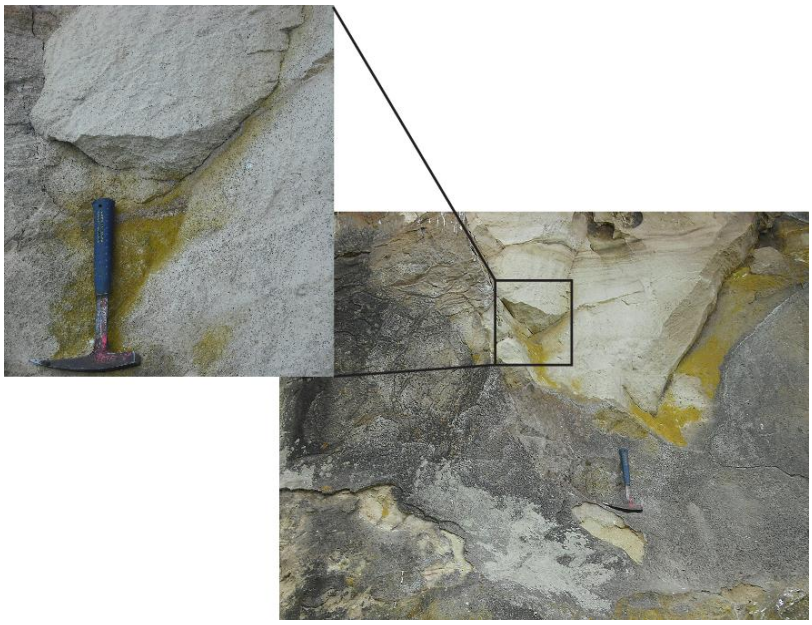

Figure 4.4: Unit D outcropping at location 6 (Enclosure 1) showing variation in case hardening and erosion. Inset shows how the outcrop contains small and irregular spaced fracturing.

4.2 Lithology and Petrographic description

4.2.1 Variation in the deposit as a whole

The most complete sequence of Unit D is best exposed in the study area at location SL.9 (Enclosure 1). The colour appearance of the matrix remains as light beige to cream throughout the 3 m thick deposit. However the composition and texture including the grainsize distribution, sorting, and bedding characteristics within Unit D varies with an increase in stratigraphic height up the column. Therefore the deposit has been separated into a lower phreatoplinian succession and an upper ignimbrite (Fig 4.5). The lower (2 m) succession is further subdivided into three facies (facies A, B and C). The upper ignimbrite (1 m) is subdivided into two separate facies (facies D and E). The abrupt or gradational change within the texture and composition between these individual facies will be described in detail.

The lower 25 cm (facies A) consists of a fine ash with the presence of accretionary lapilli which grades up and into facies B where the ash size is slightly coarser-grained and there is a pronounced increase in the abundance of crystals. There is no sign of accretionary lapilli in facies B and the deposit shows the first occurrence of diffuse layering. The grainsize abruptly declines marking the

transition back into the fine-grained and rich in accretionary lapilli characteristics of facies A. The grainsize again grades into the coarse ash of facies C where lapilli-sized lithic and pumice clasts are observed for the first time in the deposit. The upper boundary of facies C is sharp, marked by a considerable increase in grainsize and the abundance of lithics and crystals into facies D, however the pumice concentration slightly declines. Facies E directly overlies the sharp contact with facies D where the boundary marks a sudden drop in the average grainsize from the coarse ash and lapilli to coarse ash. The lithic and crystal abundance decreases notably whereas the pumice abundance remains fairly consistent through the stratigraphic height of the ignimbrite.

The measurements of the average maximum size for both lithic and pumice clasts up through the profile are displayed in Fig. 4.5. Facies A contains highly fragmented material, even clasts < 2 mm were not observed and hence measurements were not retrieved in the lower 25 cm and between 1 – 1.3 m of the profile. Despite this, there are notable trends in the average maximum size of both the pumice and lithic clasts with increasing stratigraphic height of the deposit. There is little variation within facies B although there is a slight decreasing trend for both within facies C. The variation between facies C and D is notable where the size significantly increases for both the pumice and lithic maximum clast size. The maximum pumice clast size continues to increase significantly from facies D into and up through the overlying facies E. However, the maximum lithic clast size decreases again and shows a slight increase from the base to the upper zone of facies E.

Plagioclase, quartz and iron oxides, in decreasing order of abundance are the three main crystals present within the Unit D fall deposit and overlying ignimbrite (Fig 4.5). Their individual abundances tend to follow a similar trend to the overall crystal abundance where there is an obvious increase in all three within facies B and D. Plagioclase however shows a marked increase in facies D, a much larger increase in comparison with quartz and iron oxides. Plagioclase therefore constitutes a much larger proportion of the overall crystal abundance in facies D than in any of the other facies.

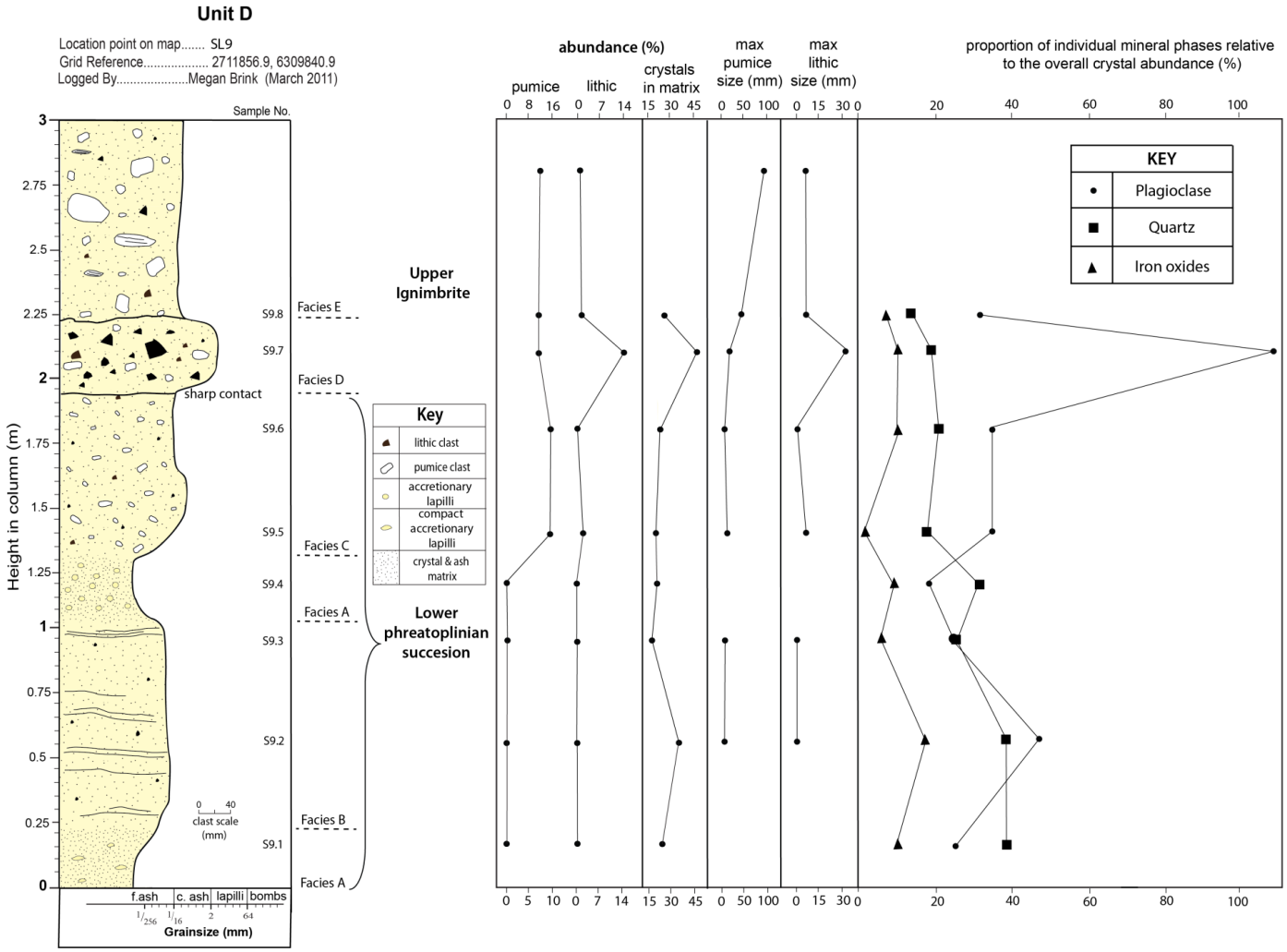

Figure 4.5: Stratigraphic log through the Unit D within the study area, highlighting the variation in the overall grainsize and appearance of the profile. The abundance of pumice lithics and crystals, the maximum clast size of the pumice and lithics and the individual proportions of the main mineral phases are plotted against the log. Note the pumice and lithic abundances and their maximum clast size are all bulk rock visual field estimates, and the crystal abundances have been determined in thin section by point counting. The sample numbers S9.1 – S9.8 refer to positions at which samples were collected for mineralogical and geochemical analysis.

4.3.2 Facies A

Facies A (Fig 4.5) is 25 – 30 cm thick and consists of a very fine-grained ash fall layer where there are no signs of bedding structures. It is poorly sorted as a result of containing a high abundance of accretionary lapilli. The abundance of accretionary lapilli and their distribution are not consistent throughout the deposit and tend to form small zones with high concentrations. At the base of the outcrop (lower 25 cm), facies A is compacted and this is further made evident by the slight flattening of the accretionary lapilli. They are elliptical in shape (Figs 4.6) with an average length of 10 mm and an average width of 3 mm.

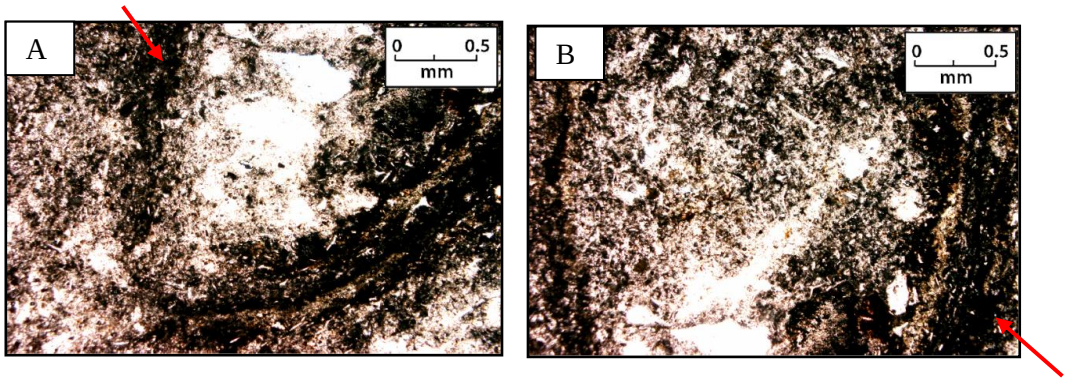

Figure 4.6: Microscopic view of an accretionary lapillus, (A) view of the curved end and (B) view of the centre; note their dark, compact and glassy outlines (red arrows).

Facies A between 1 – 1.3 m of the profile however contains more spherical (average diameter of 10 mm) accretionary lapilli (Fig 4.7, 4.8).

Figure 4.7: Concentration zone of accretionary lapilli in facies A of Unit D. Note the overall very fine grained nature of the matrix.

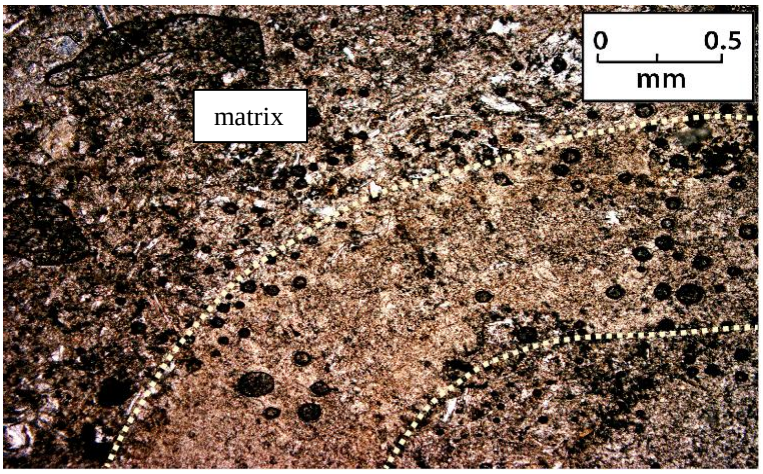

Figure 4.8: In thin section, the accretionary lapilli are poorly outlined. The outer boundary, as highlighted, is recognised by having a finer-grained and more compact composition than both the surrounding matrix and the inner component. This indicates there is concentric zoning of the accretionary lapilli.

No pumice or lithic clasts > 2 mm were observed in both thin section and in the outcrop. The matrix does however contain large glass shards and fragments of pumice (Fig 4.9). These were more commonly observed in facies A between 1-1.3 m rather than in the lower 25 cm of the profile.

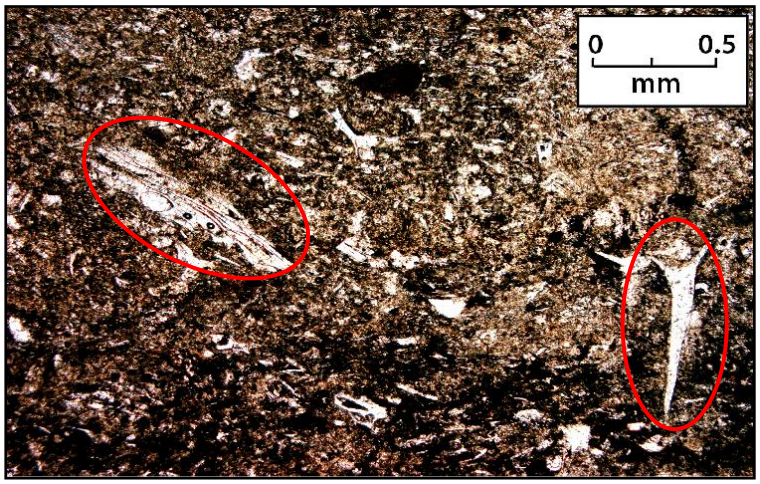

Figure 4.9: The matrix of facies A (sample S9.4, Fig 4.5) is mostly finely fragmented, but note the presence of large Y –shaped glass shards and pumiceous fragments.

The overall crystal abundance in the matrix is relatively low (19 - 24 %), compared with the remaining proportion which is comprised of glass shards and small (< 2mm) pumiceous fragments. Quartz crystals are the most abundant (Fig 4.5), and plagioclase and iron oxides are common. The crystals are small (< 0.2 mm) and angular and appear to be broken up fragments (Fig 4.10).

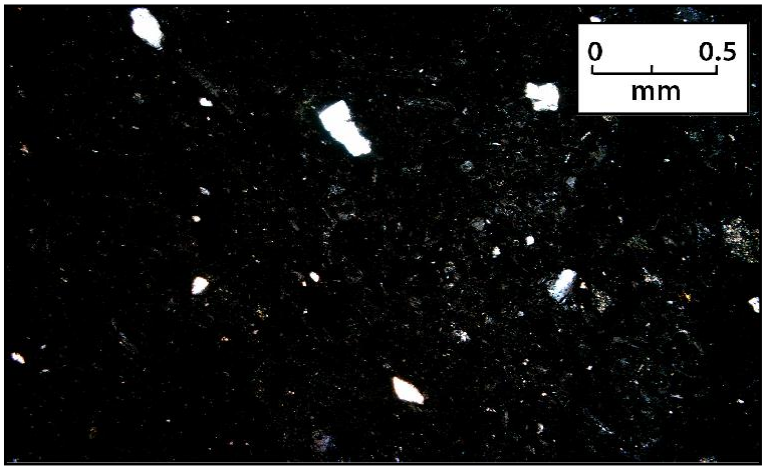

Figure 4.10: View in thin section under cross polarized light showing the low crystal abundance within the matrix of facies A (sample S9.1, Fig 3.5). Note the small size of the crystals and their broken nature and no crystals are bounded by smooth and straight edges.

4.3.3 Facies B

Facies B is 80 cm thick, poorly welded, moderately well sorted and diffusely laminated (Fig 4.5, 4.11).

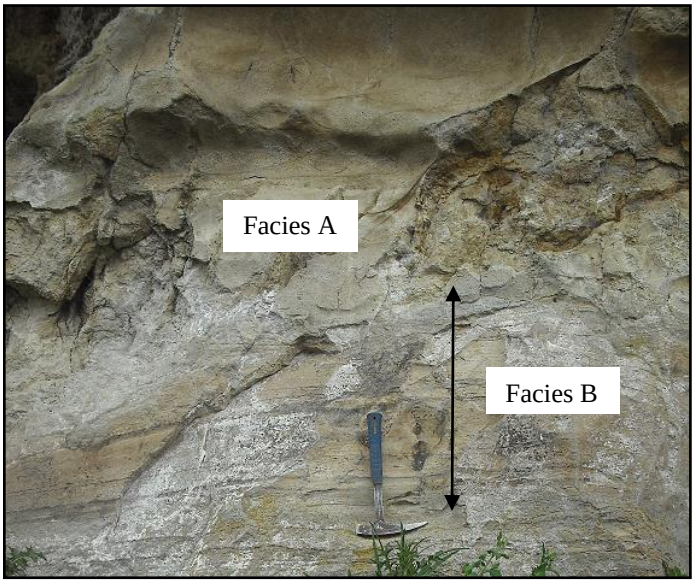

Figure 4.11: Outcrop photo at location SL9 (Enclosure 1). Note the boundary between Facies B and C where there is an abrupt change in appearance from the obvious bedded nature in Facies B which disappears abruptly at the base of facies A.

The average grainsize is categorised as fine ash, although it is coarser than the fine ash in facies A. Neither pumice clasts (coarser than 2 mm) nor accretionary lapilli were observed. Minimal (< 1 %) and small (2 mm) lithic clasts are present,

which consist of predominantly porphyritic (Fig 4.12) and glassy rhyolite lithic types with lesser amounts of welded ignimbrite clasts.

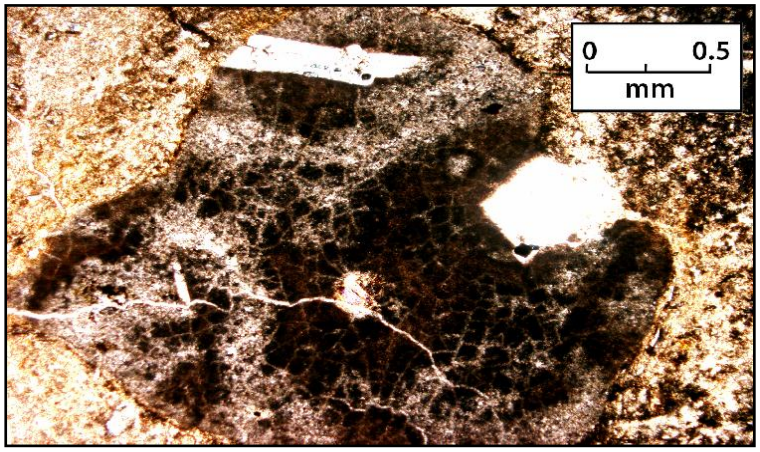

Figure 4.12: Small porphyritic rhyolite clasts are common within Facies C of Unit D.

The crystal abundance in the matrix of the lower zone of facies B is high (34%) but this gradually reduces with height to 16 % towards the upper zone of the facies. Glass shards and small (< 2 mm) pumice and lithic clasts make up the remaining proportion of the matrix. In the lower zone of facies B, the crystals are small, highly fragmented, angular and irregular in shape although their average size (0.3 mm) is slightly bigger in comparison to the crystal fragments in facies A (Fig 4.13).

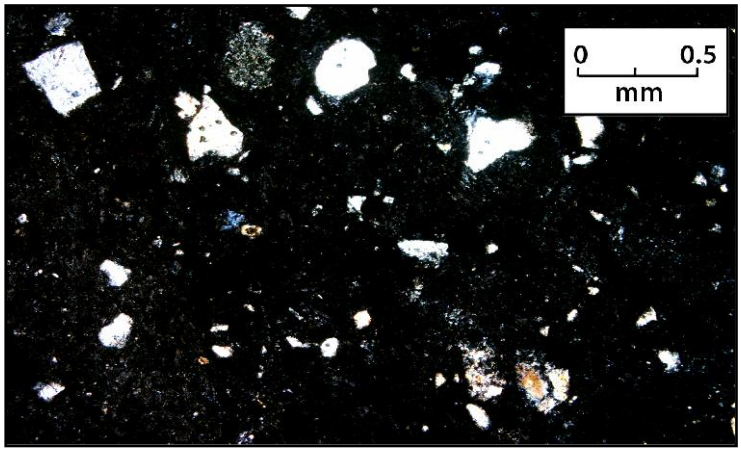

Figure 4.13: Photomicrograph of the matrix of facies B under cross polarized light. Note the significant increase in the abundance of crystals and the slight increase in their size in comparison to facies A (Fig 4.10).

The crystals become less fragmented and therefore are much bigger (Fig 4.14) in the upper zone of facies B. The most abundant crystals in this facies are plagioclase and quartz and iron oxides are common.

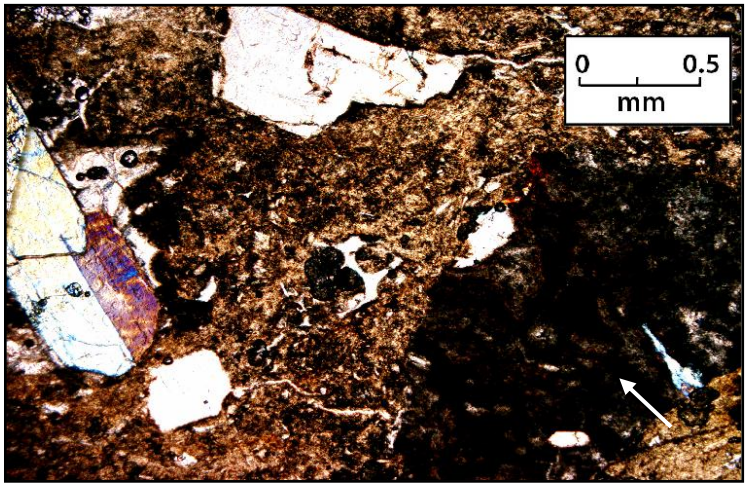

Figure 4.14: Photomicrograph under plane polarized light, note the presence of a porphyritic rhyolite clast in the right of the photo (white arrow). The crystals have increased in size relative to the lower zone of facies B and are less fragmented where the plagioclase crystals are tabular and subhedral in shape.

4.3.4 Facies C

Facies C is 70 cm thick, non-welded, massive and poorly sorted with no bedding structures present (Fig 4.5). The base of the facies consists of coarse ash, however this slightly decreases into the upper zone of the facies, where the maximum size of the pumice and lithic clasts also decline slightly.

The pumice clasts are small (< 5mm) but they are abundant (15 %) (Fig 4.15). The clasts are of irregular shapes and sizes and are evenly distributed with no evidence of concentration zones. Small (< 5mm) lithic clasts are common and these mostly consist of glassy rhyolites with few greywacke, argillite and welded ignimbrite types.

Figure 4.15: A close up view of facies C in outcrop. Note the massive nature of the deposit and the high abundance of small pumice (black outline) and lithic (red outline) clasts sporadically distributed throughout.

In thin section, the high abundance of pumice is observed (Fig 4.16). The clasts are predominantly highly vesicular with stretched and tubular vesicles, however there are a few poorly vesicular and dense clasts present.

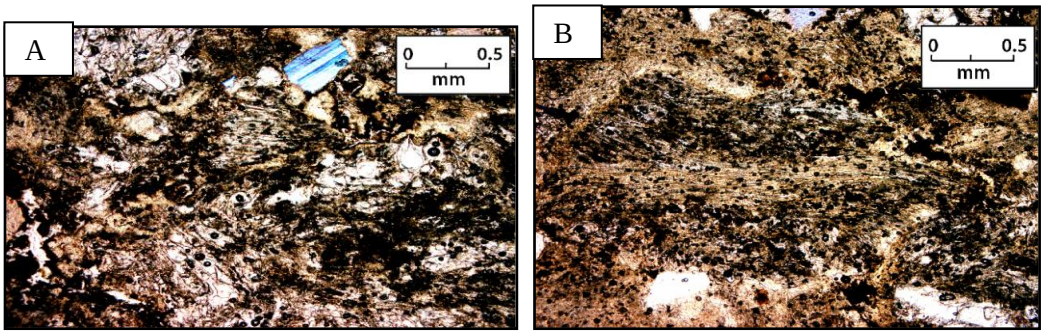

Figure 4.16: (A) Shows the high abundance of pumice in the matrix of facies C, these clasts are highly vesicular, the vesicles are large and tubular. (B) One of the few dense pumice clasts present, note how the vesicles are not as large or as abundant as they are in the clast shown in image A.

The overall abundance of crystals in the matrix increases from 18 % at the base to 22% at the top of the facies where plagioclase is the most common crystal present. Quartz and iron oxides are less abundant but still common (Fig 4.5). The crystals are fragmented, the sizes of the crystals are fairly small and irregular and their shapes are rough and jagged. However they are larger and much less fragmented than those in facies A. The remainder of the matrix consists of glass shards and small (< 2 mm) pumice and lithic clasts.

4.3.5 Facies D

Facies D is a thin (10-15 cm thick), poorly-welded and poorly-sorted coarse ash and lapilli breccia (Figs 4.5). It has a distinct appearance which makes it an effective marker that highlights and reinforces the wavy behaviour of the Unit D deposit (Fig 4.17).

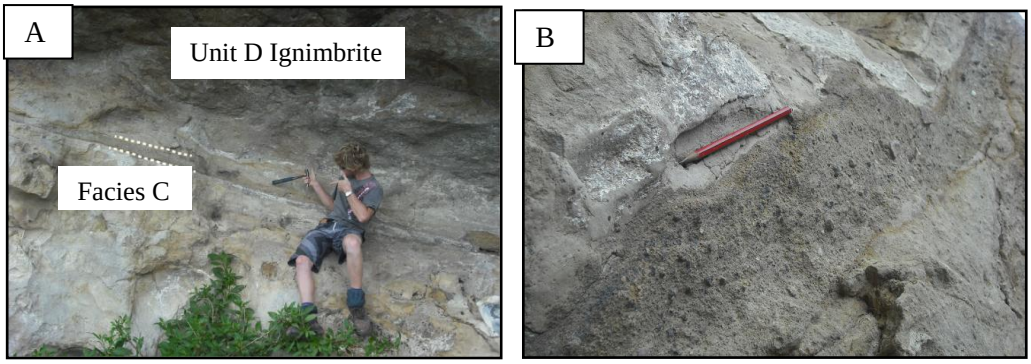

Figure 4.17: A view of the outcrop at SL9 (Enclosure 1) showing the thin nature of facies D. (A) The deposit is outlined by the white dashed lines and (B) is a close up view of it. Note the irregular distribution of Unit D as indicated by the high relief shown in both images A and B.

Pumice is common within facies D but the abundance is less than in facies C (Fig 4.5). The average maximum clast size measured is 14 mm. This is larger than the clasts observed in the previous 2 m of the deposit where the clasts were all less than 5 mm in diameter. The pumice clasts are highly vesicular with the vesicles ranging in size from elliptical to stretched and tubular shapes (Fig 4.18).

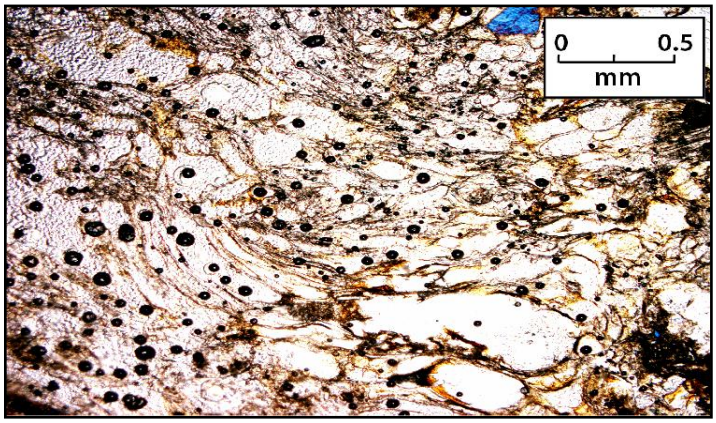

Figure 4.18: Photomicrograph of a large pumice clast within facies D of Unit D. Note the apparent range in size and shape of the vesicles.

Facies D contains a considerable amount of lithic clasts, where the abundance (14 %) and average maximum clast size (31 mm) is significantly different from the rest of the deposit (Figs 4.5, 4.19).There is a wide variety of different lithic clasts present, consisting in order of abundance, of glassy rhyolite, porphyritic rhyolite, welded ignimbrite and flow banded rhyolite.

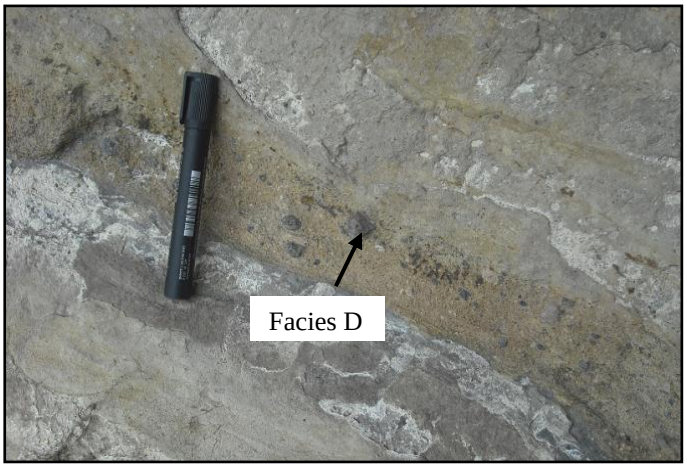

Figure 4.19: Facies D is very rich in lithics, the clasts range in size, shape and type.

The crystal content within the matrix of facies D is very high (46 %) (Fig 4.20), the other 54 % of the matrix comprises of glass shards and pumice and lithic clasts (< 2 mm). Facies D contains the highest concentration of crystals in comparison to the rest of the Unit D deposit and the crystals are not fragmented, but are large, tabular and subhedral.

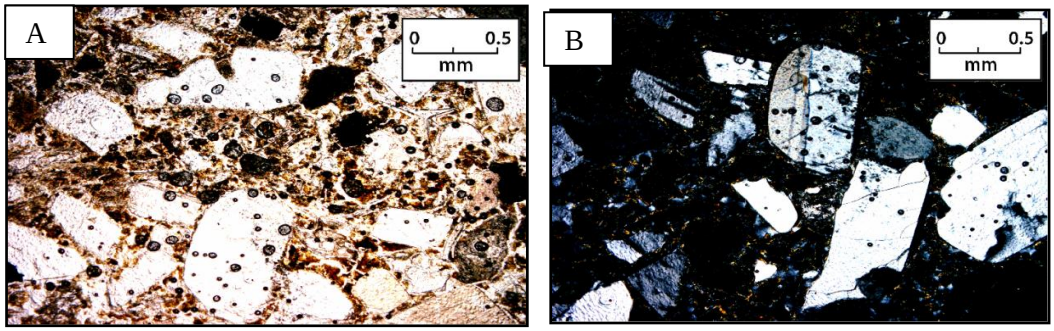

Figure 4.20: Crystal rich matrix of Facies D revealed under both plane polarized light (A) and cross polarized light (B).

Plagioclase constitutes 80 % of the total crystal abundance, and quartz and iron oxides are much less common (Fig 4.5). This is the largest proportion of plagioclase relative to the proportion of quartz and iron oxides present within Unit D.

4.3.6 Facies E

Facies E is a < 1 m thick, non-welded, massive ignimbrite which consists of a predominant coarse ash grainsize. It contains no obvious bedding, concentration zones or other depositional structures (Fig 4.5, 4.21).

Figure 4.21: Outcrop photo of the lower-mid zone of facies E at SL9 (Enclosure 1).

The overall pumice abundance represents 12 % and is fairly consistent throughout facies E. There are 2 pumice types present, with a dominant (85 %) white, fibrous and crystal-rich type and a less common (15 %) low aspect ratio, grey and streaky type. In thin section, the pumice clasts are mostly slightly wispy and poorly vesicular, but there are a few highly vesicular clasts similar to those in facies D (Fig 4.18).

The average maximum clast size within facies E is significantly larger than the pumice clasts observed within facies A - D of the Unit D deposit. They also tend to increase considerably between the lower and the upper zones of the facies where they increase from 49 mm to 96 mm (Fig 4.5).

The abundance of lithics (1 %) remains consistent throughout (Fig 4.5). The maximum sizes of the lithics are small (6 mm) in comparison to those in facies D, although they do increase with stratigraphic elevation to 12 mm in diameter

towards the top of the facies (Fig 4.5). The lithics identified consisted of porphyritic rhyolite and greywacke.

The crystal abundance within the matrix is low (17 %) (Fig 4.22) and consists mostly of plagioclase with quartz and iron oxides being common. The crystals are euhedral – subhedral in shape and have not been highly fragmented. Glass shards and pumice and lithic clasts smaller than 2 mm make up the remaining 83 % of the ash matrix.

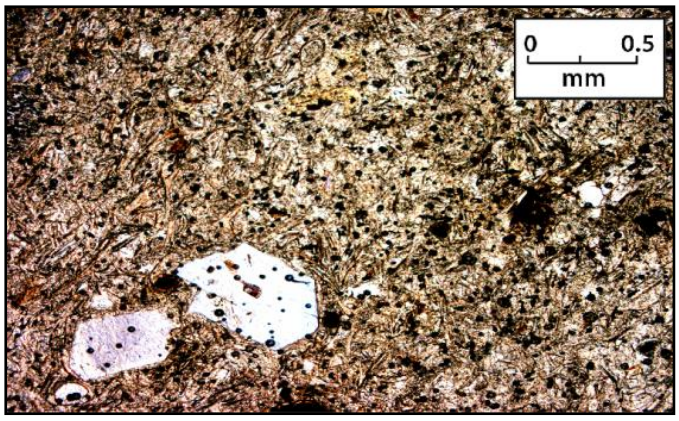

Figure 4.22: View of the matrix within facies E showing the low abundance and euhedral shapes of the crystals present.

The glass shard matrix shows a slight eutaxitic texture where the individual shards are fairly noticeable and consist of mainly platy with few cuspate types (Fig 4.23).

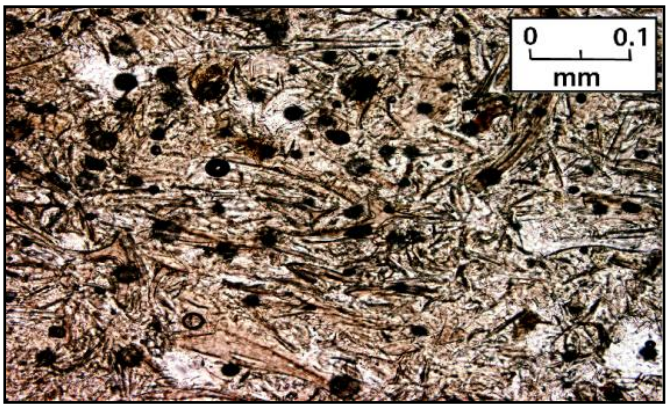

Figure 4.23: Platy shard textures on Facies E.

4.4 Geochemistry

4.4.1 Introduction

Single pumices were too small and therefore the seven samples (S9.1-S9.8) from Unit D are whole rock analyses. The samples collected are from different stratigraphic positions through Unit D (Fig 4.5) where they represent each of the facies (A-E) and the overlying ignimbrite. Major and trace element XRF analyses are given in Table 4.1 and the major element data from electron microprobe analyses are given in Table 4.2. Other trace element data from XRF and REE data from ICPMS analyses are given in Table 4.3 and 4.4 respectively.

4.4.2 Rock classification

Rock classification of Unit D is produced by using the subdivision of subalkalic rocks based on the K_2O vs silica wt % diagram of Rollinson (1993). The range in SiO_2 composition of Unit D (normalised to 100 %, volatile-free) is from 64 to 74 % where all seven of the whole rock compositions of the Unit D fall within the boundaries of the medium K calc-alkaline series and mostly fall within the dacite and extend through into the rhyolite fields (Fig 4.24). There is no obvious relationship between the silica content and stratigraphic height within the deposit (Table 4.1). However Unit D ignimbrite which forms the upper zone of the deposit has the highest silica content (74 %) and is categorised as a rhyolite.

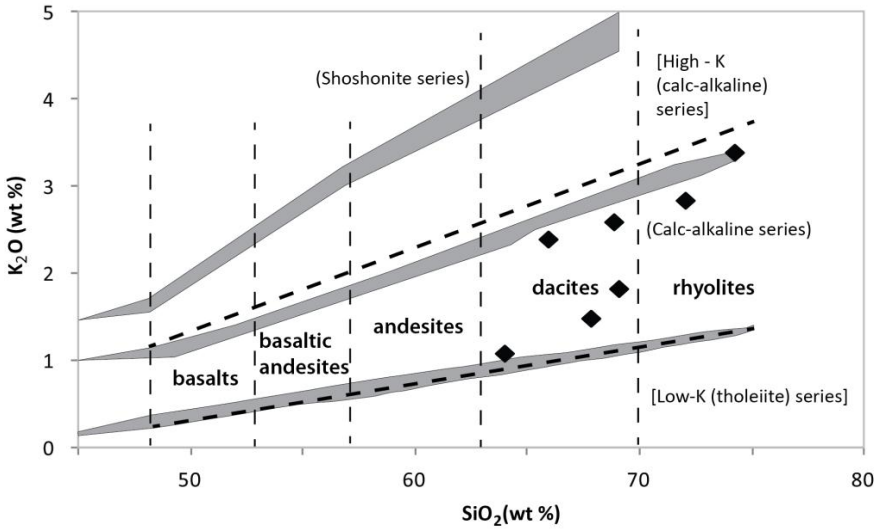

Figure 4.24: K_2O vs SiO_2 diagram (based on Fig 3.5 in Rollinson 1993) displaying and classifying the whole rock samples of the Unit D relative to the subdivision of subalkalic rocks.

Table 4.1: Major (normalised to 100 %, volatile-free) and trace element XRF analyses of seven whole rock samples from Unit D. Shaded analyses are those selected for presentation in Figs 3.25 and 3.26.

Unit D (Stratigraphic Log 9)							
UoW (petlab) no. 2011:	984	985	986	987	988	989	991
Sample no.	**S9.1**	**S9.2**	**S9.3**	**S9.4**	**S9.5**	**S9.6**	**S9.8**
Major elements (wt. %)							
SiO_2	68.96	66.02	67.93	72.15	69.18	64.07	74.35
TiO_2	0.43	0.52	0.33	0.25	0.34	0.62	0.28
$Al2O_3$	19.24	22.09	22.99	17.84	19.69	20.70	15.40
Fe_2O_3	5.10	5.12	4.00	3.57	4.50	7.77	2.85
MnO	0.05	0.04	0.03	0.04	0.03	0.03	0.09
MgO	0.32	0.28	0.30	0.35	0.31	0.40	0.10
CaO	1.01	1.13	0.84	0.84	1.35	2.03	1.41
Na_2O	2.24	2.37	1.79	2.08	2.72	3.21	2.02
K_2O	2.60	2.40	1.49	2.85	1.83	1.09	3.40
P_2O_5	0.04	0.03	0.30	0.05	0.06	0.10	0.10
LOI*	7.71	8.77	8.72	8.01	7.31	4.62	8.15
Total*	100.58	100.13	98.92	99.45	100.54	97.53	100.58
Trace elements (ppm)							
S	296	334	453	576	760	659	1323
Cl	943	1278	1172	2111	3064	12520	4788
V	–	10.6	8.5	8.5	8.3	10.6	–
Cr	8.9	15.4	6.1	7.9	8.5	6.1	5.6
Co	11.5	13.6	16.2	13.8	21	14.2	30
Ni	4.2	5	4	5.1	8.1	4.9	5
Cu	–	–	–	–	–	–	–
Zn	78	82	72	78	75	72	81
Ga	22	25	24	21	22	22	18.3
Ge	1.9	1.7	3.5	2.1	2.1	1.9	1.1
As	2.4	2.6	1.5	4.7	4	2.8	3.8
Se	0.4	0.3	0.4	0.3	0.4	0.4	0.8
Br	3.9	5	6.5	10.9	8.3	18.4	21.8
Rb	106	96	67	121	81	58	110
Sr	94	98	78	80	135	181	128
Y	29	33	15	32	25	19.4	44
Zr	396	403	343	282	332	310	307
Nb	12.5	14.2	14.8	13.2	12.9	12.6	11.1
Mo	1.2	1.1	0.9	0.9	0.7	1	1.7
Ba	681	474	347	527	347	207	756
La	31	48	21	25	27	8.9	39
Ce	59	81	39	45	45	15.1	67
Nd	29	43	19.1	21	30	12.8	35
Hf	11.5	11	10.5	9.9	10.2	9.8	10.1
Tl	1.3	1.5	1.1	1.2	1.2	0.6	2
Pb	23	26	26	21	19.2	16.9	18.7
Bi	0.7	1	0.6	0.7	0.7	–	0.5
Th	17.3	21	19.3	17	14.9	15	15.6
U	5.4	5.7	4.1	6.7	5.1	5.1	5.1

4.4.3 Major Element Chemistry

Specific major element oxides vs SiO_2 concentrations (wt %) for samples of Unit D are presented in Figure 4.25. The major element compositions of whole rock samples (S9.1 – S9.8) from XRF analysis (Table 4.1) are compared with the composition of glass determined by microprobe analysis (Table 4.2). This data includes the major element compositions of individual glass shards and the glass within the pumice of Unit D (S9.1, S9.4, S9.7, S9.8). The major element compositions of the whole rock samples are much more variable than the compositions of the glass shards and glass within the pumice. This is because the whole rock samples are a representation of the composition of glass plus phenocrysts rather than just the glass as it is with microprobe analyses. In comparison, glass compositions tend to clump and have high SiO_2 wt. % compositions.

The fractionating mineral assemblage of Unit D is reflected in Fig 4.25. Fractional crystallisation phases involved plagioclase (Al_2O_3, CaO) and iron oxides (Fe_2O_3). Hornblende was only found as a minor phase in facies B. This is made apparent by the strong negative correlations observed in Fig 4.25 where the quantities of Al_2O_3, Fe_2O_3, CaO decline with an increase in the SiO_2 wt %. The trends within the Na_2O and MgO plots are not pronounced and therefore are not as significant. K_2O shows a strong positive correlation with an increase in the SiO_2 content, indicating that it is behaving as an incompatible element and was not involved in crystal fractionation. The proportion of K_2O increased with the evolution of the fractional crystallisation phases of plagioclase and iron oxides and subsequent removal of Al_2O_3, Fe_2O_3 and CaO, plus hornblende in facies B (sample S9.2).

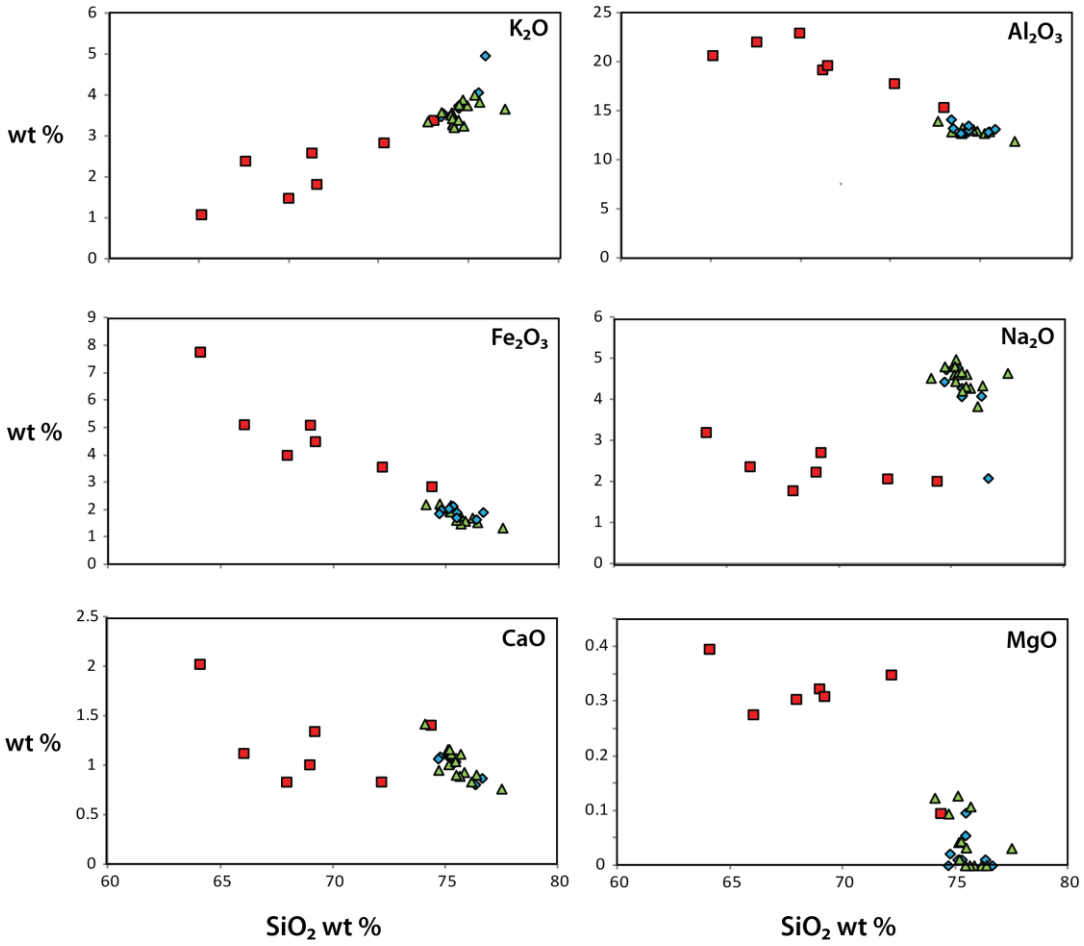

Figure 4.25: Major element Harker variation diagrams for whole rock samples (red square symbols), individual glass shards (green triangles) and the glass within pumice clasts (blue diamonds).

Table 4.2: Partial analyses of major elements (normalised to 100 %, volatile-free) from electron microprobe of seven whole rock, thirteen glass shard (from samples S9.1, S9.4, S9.7, S9.8) and eight pumice glass (from S9.4, S9.7, S9.8) analyses.

		Whole rock						
UoW (petlab) no (2011).	***Sample no.***	**SiO_2**	**$Al2O_3$**	**FeO**	**MgO**	**CaO**	**Na_2O**	**K_2O**
984	**S9.1**	68.96	19.24	5.10	0.32	1.01	2.24	2.60
985	**S9.2**	66.02	22.09	5.12	0.28	1.13	2.37	2.40
986	**S9.3**	67.93	22.99	4.00	0.30	0.84	1.79	1.49
987	**S9.4**	72.15	17.84	3.57	0.35	0.84	2.08	2.85
988	**S9.5**	69.18	19.69	4.50	0.31	1.35	2.72	1.83
989	**S9.6**	64.07	20.70	7.77	0.40	2.03	3.21	1.09
991	**S9.8**	74.35	15.40	2.85	0.10	1.41	2.02	3.40
		Glass Shards						
UoW (petlab) no (2011).	***Sample no.***	**SiO_2**	**$Al2O_3$**	**FeO**	**MgO**	**CaO**	**Na_2O**	**K_2O**
984	**S9.1**	74.09	13.99	2.20	0.12	1.42	4.53	3.36
984	**S9.1**	75.25	12.92	2.02	0.04	1.12	4.62	3.22
984	**S9.1**	75.18	13.31	1.93	0.01	1.16	4.45	3.44
984	**S9.1**	75.44	13.12	1.62	–	1.04	4.67	3.40
984	**S9.1**	75.48	13.05	1.91	0.03	0.91	4.21	3.77
987	**S9.4**	75.83	12.97	1.59	–	0.93	4.28	3.76
987	**S9.4**	76.16	12.75	1.71	–	0.84	3.84	4.01
987	**S9.4**	76.38	12.93	1.54	–	0.91	4.34	3.84
987	**S9.4**	75.64	13.09	1.49	–	0.89	4.32	3.90
990	**S9.7**	75.67	13.12	1.70	0.11	1.12	4.62	3.26
990	**S9.7**	75.19	13.10	1.97	0.01	1.13	4.68	3.31
990	**S9.7**	74.70	12.90	2.22	0.09	0.95	4.81	3.59
990	**S9.7**	75.19	12.89	2.17	0.04	1.03	4.98	3.28
991	**S9.8**	75.15	12.74	1.95	0.04	1.01	4.81	3.58
991	**S9.8**	77.50	11.94	1.34	0.03	0.77	4.65	3.67
991	**S9.8**	75.11	12.80	2.08	0.13	1.17	4.61	3.53
		Glass in pumice						
UoW (petlab) no (2011).	***Sample no.***	**SiO_2**	**$Al2O_3$**	**FeO**	**MgO**	**CaO**	**Na_2O**	**K_2O**
987	**S9.4**	75.45	13.52	1.72	0.05	1.04	4.08	3.75
987	**S9.4**	76.33	12.88	1.65	0.01	0.81	4.09	4.07
987	**S9.4**	76.63	13.17	1.91	–	0.87	2.09	4.97
990	**S9.7**	74.76	13.26	2.00	0.02	1.09	4.73	3.56
990	**S9.7**	75.29	12.90	2.14	0.01	1.06	4.78	3.34
990	**S9.7**	75.46	13.05	1.91	0.10	1.08	4.28	3.69
991	**S9.8**	74.68	14.16	1.86	–	1.07	4.44	3.48
991	**S9.8**	75.11	12.75	2.05	0.01	1.10	4.80	3.52

4.4.4 Trace Element Chemistry

Trace element compositions were determined by XRF analysis for all of the whole rock samples from Unit D. These are presented in the Harker variation diagrams (Fig 4.26) where their concentrations (ppm) are plotted against the SiO_2 wt %. Positive correlating trends for Ba, Rb, La, Ce and Y are observed with an increase in the SiO_2 content which represents that they were incompatible in the melt during crystal fractionation. Sr and Zr however show a slight negative correlation with an increase in the SiO_2 wt %, suggesting small amounts of fractional crystallisation of plagioclase (Sr) and zircon (Zr), respectively.

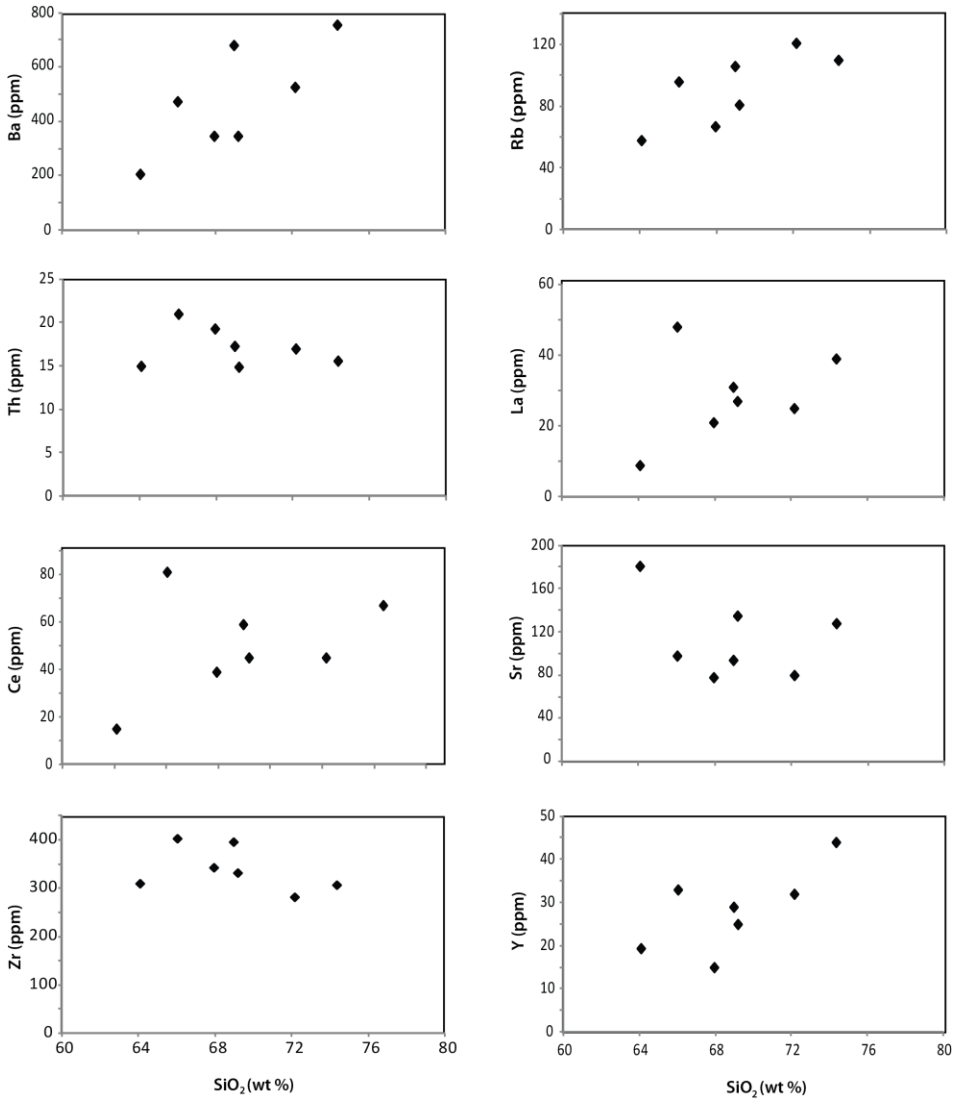

Figure 4.26: Harker variation diagrams for specific trace element compositions in the whole rock samples (S9.1-S9.8) of Unit D.

The trace element concentrations of selected whole rock samples of Unit D (S9.1, S9.4, S9.8) were further measured using ICP-MS analysis at Monash University, Melbourne. Their measurements have been normalized to the primitive mantle reference standards of Sun and Mc Donough (1989). The results are displayed as a multi-element diagram (Fig 4.27) and the data is shown in Table 4.3. All three samples follow the same pattern and show depletion in Sr, P and Ti and a slight depletion in Nb (compatible elements) and an obvious enrichment in Ba, Rb, Th, U, K and a slight enrichment in La (incompatible elements). This depletion of Sr, P, Ti and Nb could represent the fractional crystallisation of plagioclase (Sr), ilmenite and titanomagnetite (Ti), apatite (P) and titanomagnetite (Nb) (Bowyer 1997), or alternatively could be a source effect which is typical of TVZ rhyolites.

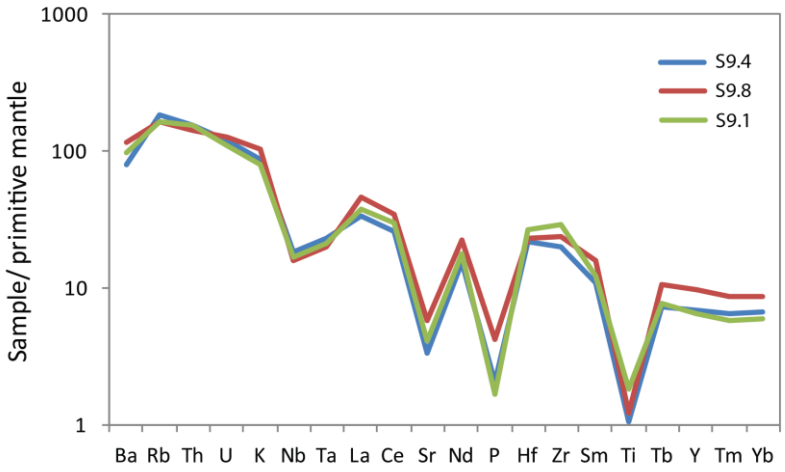

Figure 4.27: Multi-element abundance diagram (spider diagram) for the whole rock samples (S9.1, S9.4, S9.8) of Unit D normalized to the primitive mantle values of Sun and McDonough (1989).

Table 4.3: Trace element ICPMS analyses (normalised to the primitive mantle) of three selected whole rock samples in Unit D.

UoW (petlab) no. (2011)	984	987	991
Sample no.	**S9.1**	**S9.4**	**S9.8**
Rb	163.51	185.12	166.32
Sr	4.17	3.38	5.74
Y	6.44	6.96	9.76
Zr	29.26	20.04	24.14
Nb	16.71	18.54	15.71
Ba	96.94	80.02	116.15
La	37.91	34.09	45.94
Ce	29.73	25.75	34.65
Nd	17.95	15.58	22.21
Sm	12.17	11.09	15.80
Tb	7.82	7.27	10.73
Tm	5.88	6.49	8.62
Yb	5.92	6.77	8.64
Hf	26.80	21.70	23.15
Ta	21.28	23.47	20.20
Th	153.19	156.84	140.91
U	109.65	119.74	126.32

The rare earth element concentrations in the whole rock samples S9.1, S9.4, and S9.8 of the Unit D were also analysed using ICP-MS analysis. Their abundances have been normalised to a common chondritic reference standard of Sun and McDonough (1989) and are displayed in Fig 4.28 and Table 4.4. The concentration patterns of REE diagrams are significant because the REE are among the least soluble trace elements and can faithfully represent the original composition of the unaltered parent or source rock (Rollinson 1993).

The REE pattern is identical for all three of the whole rock samples. There is depletion in the heavy REE in comparison to the light REE. Felsic liquids that contain this sort of pattern could represent the fractional crystallisation of the accessory mineral zircon (Rollinson 1989). The pattern also reveals a negative Eu anomaly, controlled by fractional crystallisation of plagioclase.

However, recent studies on the evolution of TVZ rhyolites (e.g. Charlier et al 2005; Price et al 2005; Deering et al 2011) would favour the former hypothesis.

The negative Eu anomaly is consistent with the slight negative correlation trends of Sr shown in Fig 4.26.

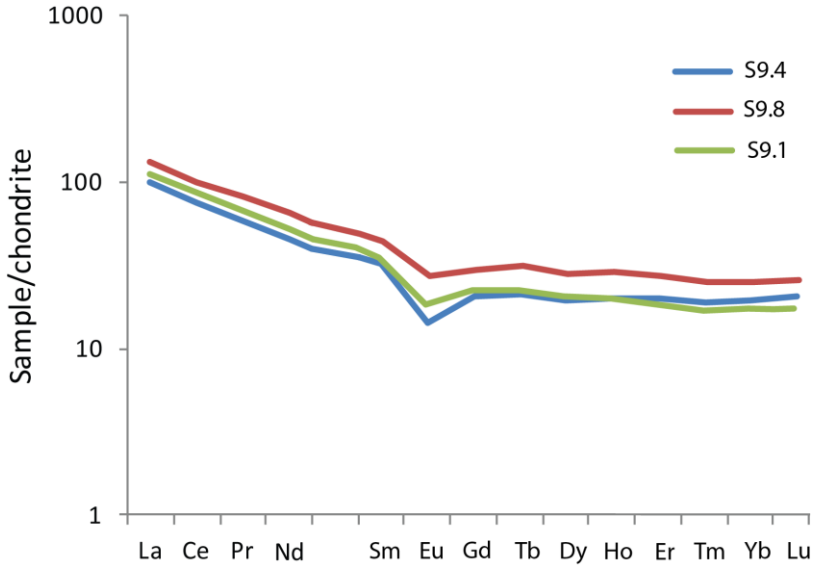

Figure 4.28: Rare earth element abundances in the Unit D whole rock samples (S9.1, S9.4, S9.8) normalized to chondritic values of Sun and McDonough (1989).

Table 4.4: Rare earth elements (normalised to a common chondritic reference) from ICPMS analysis of three selected whole rock samples in Unit D.

UoW (petlab) no. (2011)	984	987	991
Sample no.	**S9.1**	**S9.4**	**S9.8**
La	109.90	98.82	133.15
Ce	86.24	74.67	100.49
Pr	67.62	58.35	82.31
Nd	52.04	45.17	64.38
Sm	35.33	32.17	45.86
Eu	18.27	14.14	26.94
Gd	22.62	20.48	29.46
Tb	22.58	21.00	30.98
Dy	20.32	19.68	28.15
Ho	19.83	20.21	28.93
Er	18.53	19.78	27.60
Tm	17.07	18.82	25.02
Yb	17.17	19.65	25.05
Lu	17.32	20.60	25.94

Chapter 5

Taupo ignimbrite

5.1 Introduction

This chapter describes the Taupo Ignimbrite exposed in the study area. The main focus is on the discovery of fossilised tree trunks in the ignimbrite and the mechanism of forest destruction and preservation with reference to a few case studies from around the world. The lithology and petrography will be briefly described.

The Taupo Ignimbrite is complex in the fact that it has two contrasting morphological variants (Manville et al. 2009). Over 90% of the area but less than 50% of the volume of the deposit, the ignimbrite is landscape-mantling and is described as an ignimbrite veneer deposit (IVD). The rest is deposited as thick ponds within local topographic depressions (Walker et al. 1980, Manville et al. 2009).

There is a discontinuous coarse lithic breccia layer present near the source (within 5 km of the lake edge) underlying the ignimbrite where the boulders can reach up to one metre or more in diameter (Walker at al. 1981, Manville et al. 2009, Leonard et al. 2010).

The valley pond deposits of the Taupo Ignimbrite are inferred to be several hundred metres thick within the Taupo Caldera. It reaches up to 70 m thick within the primary depositional zone, and is typically a few tens of metres in the more distal areas (Walker at al. 1981, Manville et al. 2009, Leonard et al. 2010). Manville et al. (2009) mention that only a small proportion (between Taupo and Waitahanui) of this deposit forms welded cliffs, otherwise it is typically non-welded, and forms unconsolidated flat topped terraces upon valley floors. The basal facies is dominated by a pumice rich, ash-poor (fine material winnowed out of flow) and charcoal rich layer which ranges from a few centimetres to 8 m thick. This layer represents the material that was jetted forward from the front of the

flow as a consequence of the rapid expansion of ingested air and the interaction with abundant vegetation (Hudspith et al. 2010). A thick homogenous unit consisting of pale grey ash and white to pale pink pumice clasts, some of which are within coarse concentration zones (0.1-1m across) overlies this basal layer (Walker et al. 1980, Walker at al. 1981, Manville et al. 2009, Leonard et al. 2010). The IVD is inferred as the more turbulent component of the main pyroclastic flow and was derived from a combination of material elutriated out and fall out deposits. Proximal to the vent it reaches up to 10 m thick which gradually reduces to 15-30 cm within the more distal locations. It tends to mantle the slopes with an angle of up to 30° and has attained heights up to 1000 m above the lake level of Taupo. The IVD is non-welded and consists of the same material as the valley pond deposits but is not as coarse grained. The diagnostic feature of it, however, is the presence of bedding with varying grain size and lee-side lenses of lapilli concentration zones (Walker et al. 1980, Manville et al. 2009).

The Taupo Ignimbrite is renowned for its high content of charcoal fragments and carbonized logs (reaching up to 1 m in diameter close to the vent). These represent the remnants of the large-scale destruction that took place when the violent emplacement of the pyroclastic flow engulfed 1 km^3 of vegetation and charred and buried forestlands throughout the central North Island. (Hudspith et al. 2010, Hogg et al. 2011).

The 37 ha Pureora buried forest is the most well documented site of pre-eruptive preserved vegetation in the Taupo Ignimbrite which is currently protected within the Pureora Forest Park, 50 km northwest of the Taupo caldera (Hudspith et al. 2010). It contains both charred and uncharred wood fragments as well as 190 currently recovered uncharred tree cross sections with tree species recognized as *Dacrydium cupressinum* and *Phyllocladus trichomanoides* with lesser amounts of *Prumnopitys taxifolia*, *Dacrycarpus dacrydioides*, and *Prumnopitys ferruginea* (39). These tree logs have been preserved since the eruption in C.232 AD in the lower pumice rich, ash-sparse basal layer of the Taupo Ignimbrite, oriented radially in the direction of the flow with their bark intact and undamaged (Fig 5.1)

The larger logs are mostly found (diameter of at least 30 cm) protruding from the underlying forest floor into the base of the ignimbrite (Hudspith et al. 2010).

Figure 5.1: Large uncharred log in the basal layer of the Taupo Ignimbrite in Pureora Fossil Forest, image retrieved from Hudspith et al. (2010).

There has been another sighting of the remains of forests preserved in the Taupo Ignimbrite with tree stumps still in standing position of growth. Tree stumps were exposed protruding above the surface of the Rangitaiki River after the 1987 Edgecumbe earthquake when the river bed was down-faulted and then scoured back upstream (Fig 5.2) (Graham 2008).

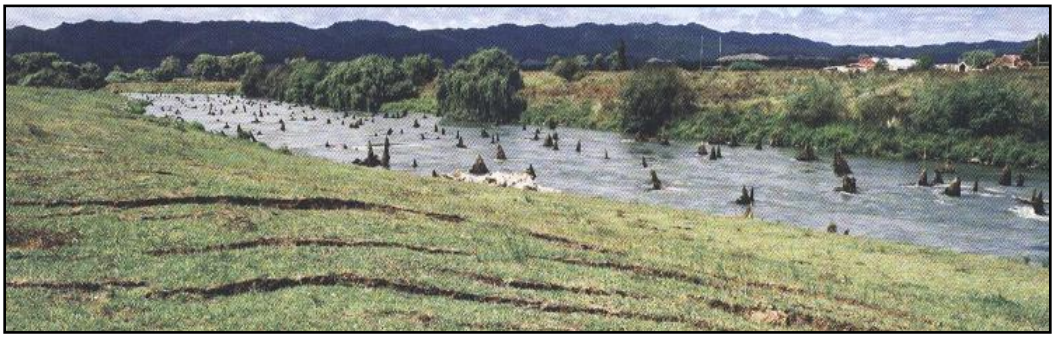

Figure 5.2: The image retrieved from Graham (2008) looking across into the Rangitaiki River, where numerous truncated fossil tree stumps were observed soon after the river bed subsided.

5.2 Description of the Taupo Ignimbrite in the study area

5.2.1 Outcrop appearance

The Taupo Ignimbrite is exposed as a thick (up to 20 m), non-welded terrace upon the Waipa Valley floor (Fig 5.3). The Waipa Valley floor which was essentially the substrate to the Taupo Ignimbrite consists of loosely packed cobbles, gravels and occasional boulders which have been transported and re-deposited by the Waipa River. These are predominantly greywacke and argillite with some welded ignimbrite.

Figure 5.3: The thickness of the Taupo Ignimbrite is variable within the Waipa Valley, Southeast of Te Kuiti. At this location it is approximately 12-15 m thick.

The ignimbrite terrace is not continuous throughout the valley and is only exposed clearly on the eastern bank of the Waipa River for approximately 150 m. It is difficult to determine how extensive the ignimbrite is in this area due to very limited outcrop exposure further up and downstream. The outcrop exists as a near vertical and unstable cliff (Fig 5.4) with a flat to very slightly undulating surface (Fig 5.5).

Figure 5.4: The Taupo Ignimbrite exposed as a very steep sided terrace upon the flat, low lying Waipa Valley floor.

Figure 5.5: The top of the Taupo Ignimbrite terrace is not completely horizontal or flat, instead it is exposed as a wavy and slightly undulating surface. Note how the ignimbrite has been deposited up and against the lower Waipa Valley wall and how it suddenly disappears at the northern end (left) of the photograph.

The outcrop has no signs of jointing or fractures with no variation in the overall structural appearance. It is non-welded and very poorly consolidated throughout, and as a result is very susceptible to erosion. The outcrop is always masked with a layer of material washed, fallen and blown down from higher above (Fig 5.6A). Or in some localised and badly affected areas, this occurs on a slightly larger scale where material has collapsed and slipped down to accumulate as a pile of talus at the bottom of the outcrop (Fig 5.6B).

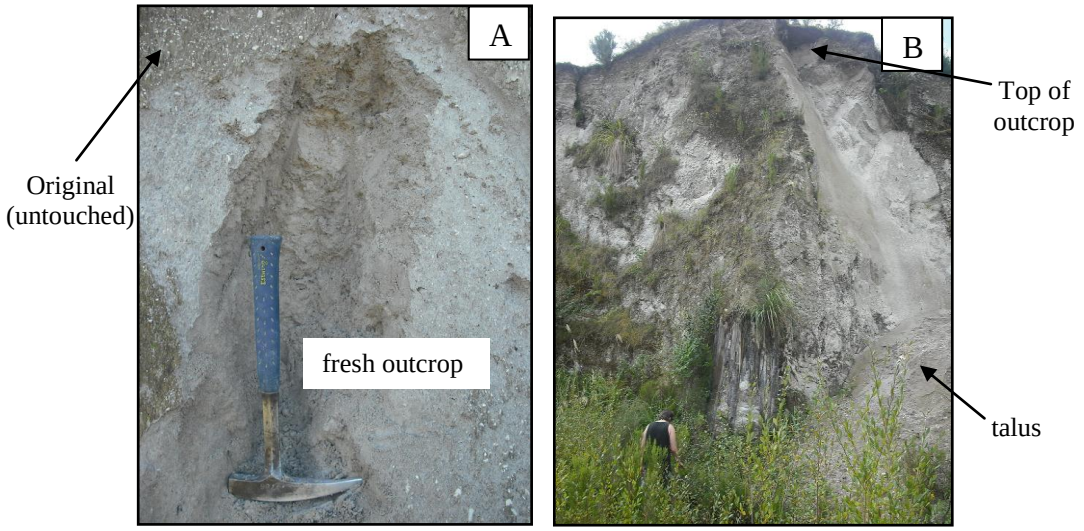

Figure 5.6: A- freshly exposed and original outcrop. The original appearance gives a false representation of the components within the ignimbrite, the coarse pumice clasts are left plastered as a mask over the fresh outcrop and the finer ash material has been completely washed away. B- an area where a small scale slip has occurred. Note the accumulation of talus at the base and the main source area at the top of the outcrop.

5.2.2 Lithology and petrographic description

A stratigraphic profile through the Taupo Ignimbrite was produced within the area of the preserved fossil forest (location SL11, Enclosure 1). This profile is a representation of the typical valley pond facies of the ignimbrite (Fig 5.7). The basal, pumice rich, ash-poor layer of the Taupo Ignimbrite however is not exposed along this section but it is present as a small (2 m high) outcrop 200 m further upstream (Fig 5.8).

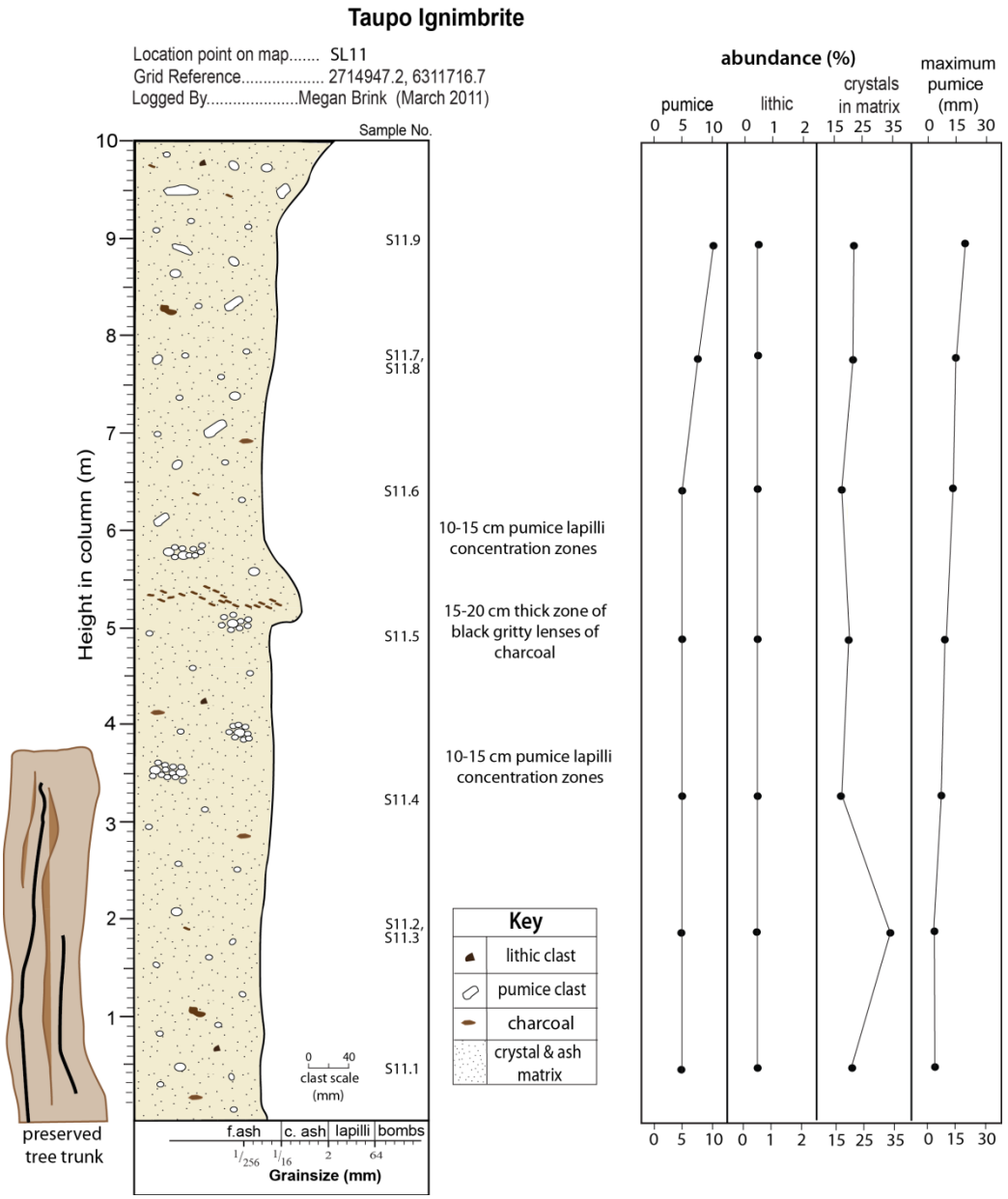

Figure 5.7: Stratigraphic log through the Taupo Ignimbrite within the study area, highlighting the variation in the overall grainsize and facies characteristics. The abundance of pumice, lithics, crystals and the maximum pumice size are plotted against the log. Note the pumice and lithic abundances are bulk rock visual field estimates, and crystal abundances have been determined in thin section by point counting.

Figure 5.8: The basal layer of the Taupo Ignimbrite is only observed in one specific location within the Waipa Valley. It is 1.5 – 2 m thick and consists pre-dominantly of pumice clasts (15 -20 mm in length), with minimal ash and rare lithics. Fragments of charcoal are commonly present (< 30 mm long). The unit is massive and homogenous throughout where there is no obvious sorting or specific orientation of the pumice clasts.

During construction of the stratigraphic profile, the sample collection, measurements and a detailed description were constrained to the lower – mid 10 metres of the profile. The description of the upper zone (5 m) was based only on observations made in the field due to the limited access available.

The lower 10 m of the Taupo Ignimbrite in this particular location is light grey, massive and homogeneous. It shows very little variation in appearance throughout and is mostly exposed as an ash-rich, moderately crystal-rich, pumice- and lithic-poor ignimbrite. It contains small pockets of discontinuous pumice lapilli concentration zones within the mid zone (3.5 – 6 m up the profile) (Fig 5.9).

Figure 5.9: Discontinuous pumice concentration zones (circled) are small (<100 mm long) and sporadically emplaced. The pumice abundance is very high (> 80%) within these zones where the clasts are typically rounded and < 15 mm across their long axis.

At approximately 5.5 m up the profile and in amongst the pumice concentration zones, there is a continuous horizon (15 cm thick) containing dark grey to black irregular-shaped lenses (Figure 5.10). The material within these lenses is much coarser than the surrounding ash matrix and is inferred to be highly fragmented charcoal.

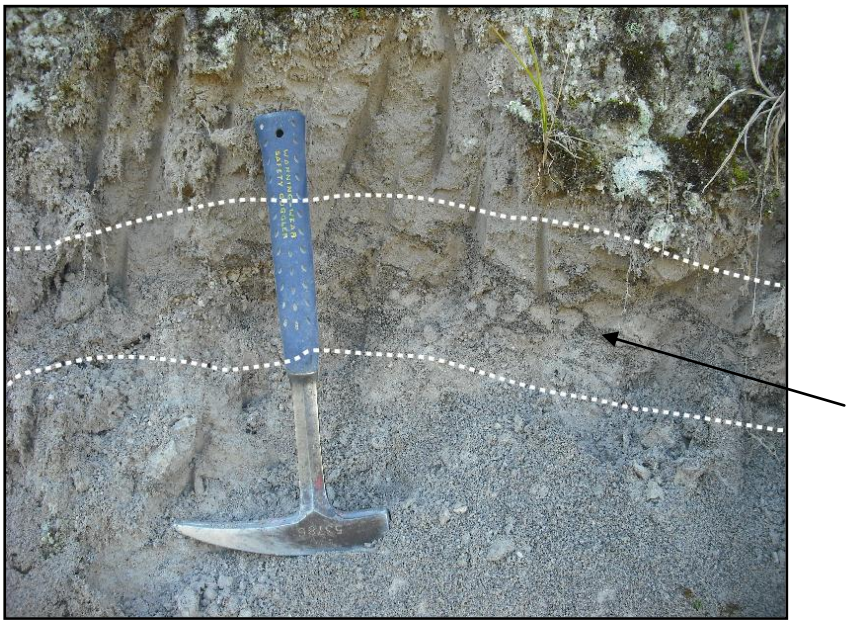

Figure 5.10: The lenses are thin (1-2 cm) and are restricted to a small but continuous zone in the ignimbrite.

The abundance of pumice clasts is fairly consistent throughout the outcrop where there is no variation from the base to approximately 7 m up the profile. At this

point there is a slight increase in pumice concentration from < 5 % to 7-10%. The maximum size of the pumice clasts tends to gradually increase with stratigraphic elevation where they are barely visible at the base of the outcrop and reach up to 40 mm at the maximum extent of the measured profile (Fig 5.7 and 5.11).

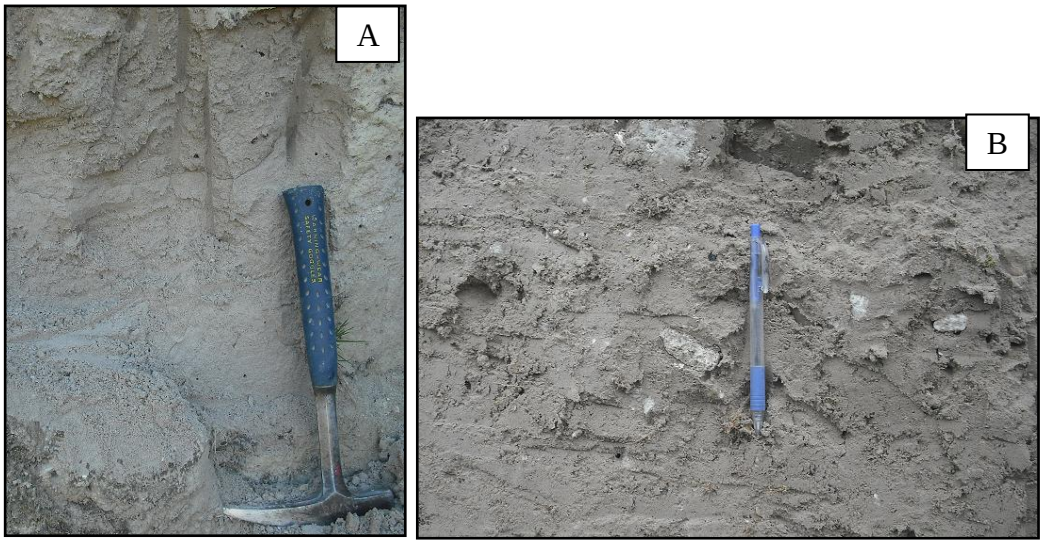

Fig 5.11: A- photo 2 m up the profile, showing small uncommon to rare pumice clasts. B- 7 m up the profile, note the increase in both the size of the pumice clasts and their abundance.

There is only a single type of pumice present throughout the Taupo Ignimbrite and these are mostly elongate, with lesser amounts of equant-shaped clasts. In hand specimen, the clasts are white, fibrous and vesicular. In thin section, the clasts are wispy or highly vesicular, glassy and non–devitrified. The crystal abundance within single pumice clasts is very poor (< 5%). The vesicles are mostly tubular and aligned although few (mostly within the more vesicular clasts) are spherical (Fig 5.12). The abundance of pumice as revealed in thin section is high (30-50%), but these are mostly ash-sized (< 2mm) (Fig 5.13). The clasts tend to become slightly more vesicular (with more spherical vesicles) towards the upper section of the measured outcrop.

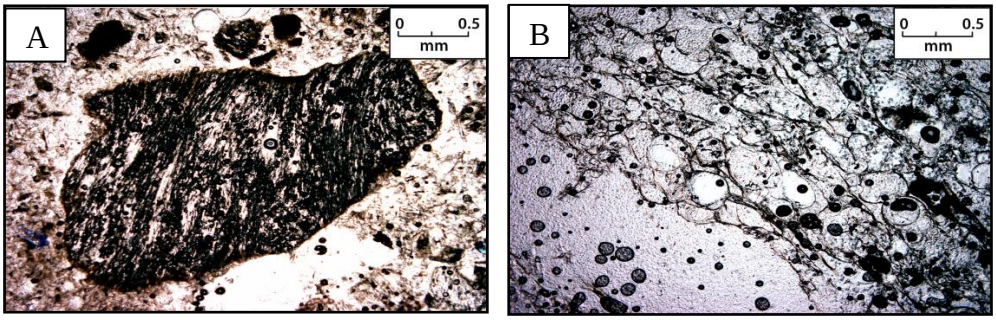

Figure 5.12: A- the pumice clasts are predominantly elliptical and tend to have a wispy appearance with tubular vesicles. B- upper zone of the outcrop, where the clasts become highly vesicular with large spherical shaped vesicles.

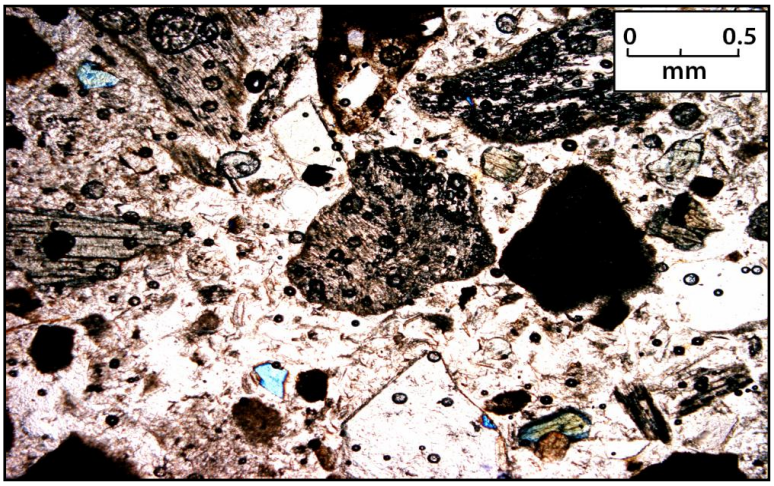

Figure 5.13: The ash matrix of the Taupo Ignimbrite has a high abundance of small (<1 mm) pumice fragments.

The abundance of the crystals within the matrix is fairly constant throughout the profile (15-20%). There is however quite a significant increase at approximately 2 m from the base and this is mainly due to a sudden increase in the size of the crystals. Plagioclase is the most dominant mineral present (50%), quartz is less common (25%), with traces of pyroxene (20%), and Fe –Ti oxides (5%). The crystals are small and mostly anhedral with ragged/rough edges and are of irregular shapes (Fig 5.14).

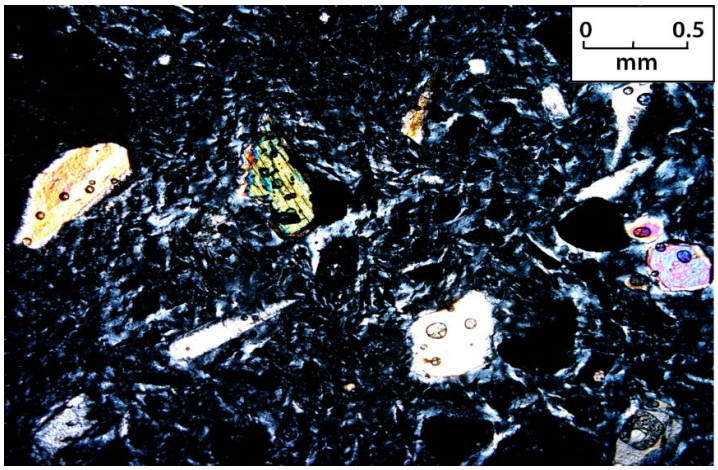

Figure 5.14: Looking under cross polarised light, the crystals within the Taupo Ignimbrite appear as small broken fragments where the edges are rough and the shapes of the fragments are highly irregular.

The abundance of lithic clasts is less than 1 % through the profile. Very few lithics were observed in the outcrop, but are visible in thin section. In thin section they are small and difficult to identify, and most appear to be grey and glassy rhyolite lava fragments with very few phenocrysts.

The overall matrix is predominantly composed of unbroken and small pumice fragments. The glass shard matrix shows no variation with stratigraphic elevation, it is poorly devitrified and vitriclastic with predominantly platy and lesser amounts of Y shaped shards.

5.2.3 Description of tree structures preserved within the outcrop

The unique aspect of this research on the Taupo Ignimbrite is the presence of the remnants of uncharred to partially charred fossil trees which have been effectively preserved in the Taupo Ignimbrite since the emplacement of the violent sequence of pyroclastic flows. The significance is not the fact that they are preserved, as this is a common feature in both the Taupo Ignimbrite and in ignimbrites in general, but it is how they have been preserved. There has been no previous scientific documentation or explanation on the mechanism of how this preservation took place. The identification of the trees is uncertain, but are likely to be totara, (pers. comm. B. Clarkson).

The local farmers (Jenni and Ian Templeton) mention that due to a sudden change in the course of the Waipa River less than 10 years ago, excavation of the Taupo Ignimbrite took place along the < 40 m segment of the eastern river bank. This caused the exposure of these peculiar fossilised trees in one specifically localised area (SL11, Enclosure 1).

There are approximately 15-20 fossil tree trunks, ranging in diameter from less than 30 cm to greater than 1.5 m preserved effectively in standing growth position. The remnants of the trunks appear to be all of a similar height (3-4 m) and concentrated within a 20 m^2 area (Figs 5.15 and 5.16). In addition to the upright trunks, 3 blown-over logs which are similar in appearance to the trunks in standing growth position are present within the zone. However it is difficult to determine if these are preserved remnants within the Taupo Ignimbrite or if they have been transported and deposited in this zone by the Waipa River. Interestingly, apart from the thick trunks, little else of the forest (smaller trees and shrubs) is preserved.

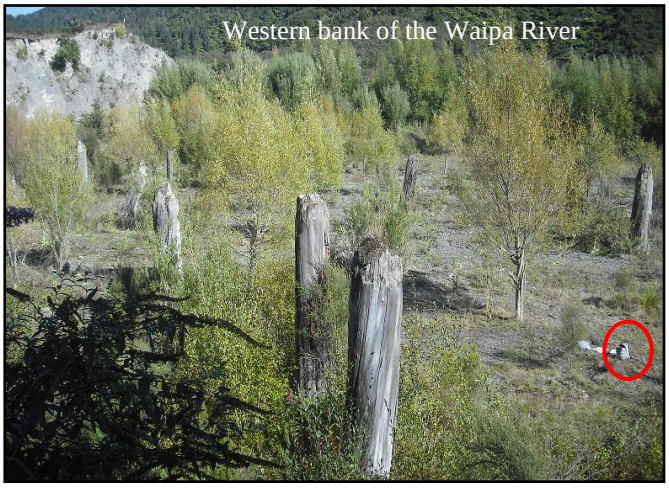

Figure 5.15: Looking towards the southwest with the western bank of the Waipa River in the distance. The remnants of a small, closely spaced forest are distributed in the foreground. Note how the tops of the tree trunks are all conical, sharp and jagged, and of the same height (refer to back pack, circled for scale). The tree trunks are all upright and vertical, and have not been bent over by the pyroclastic flow which flowed from left to right in this photo. The live vegetation (smaller willow trees and shrubs) is younger than the excavation event < 10 years ago.

Figure 5.16: Vertically standing tree trunks, Waipa Valley. Note the broken and tapered tops of the trunks.

The height of the trunks reduces quite substantially (< 2 m) on the outer boundary of this concentrated zone before the structures disappear (Fig 5.17). They tend to disappear towards the west in the direction of the current river path and to the north further downstream where they may have already been eroded. It is not possible to determine if they are present further to the south and east, and hence the extent of this buried forest is uncertain.

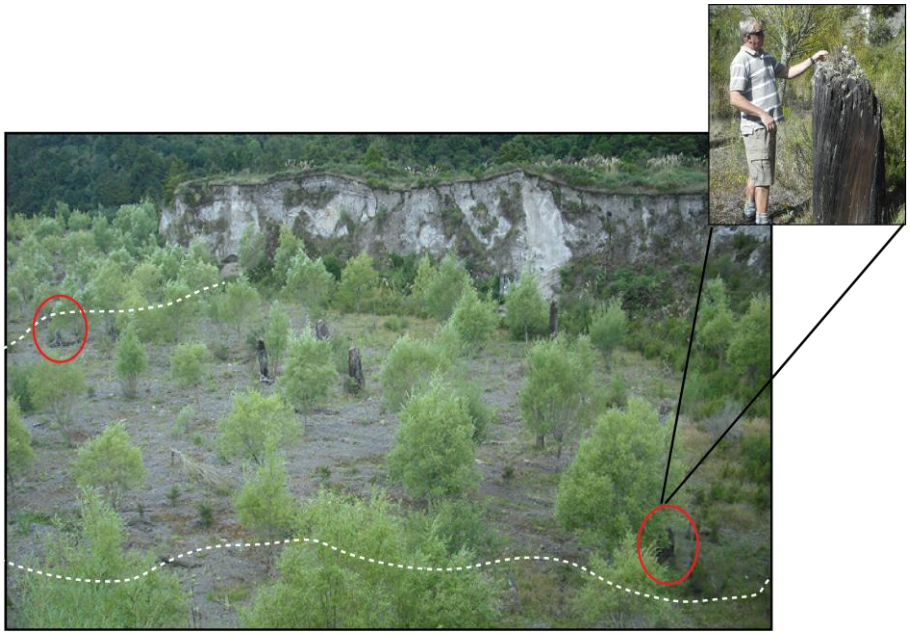

Figure 5.17: The fossil tree trunks are confined to a localised area within the Waipa Valley floor (outlined by the dashed line). The trunks circled in red are located on the boundary of this area and are much shorter than the trunks in the inner zone (refer to inset).

Pockets of the Taupo Ignimbrite are embedded inside the cracks and crevices of the trunks (Fig 5.18). On the tops of a few of the trunks, there are still remnants of the ignimbrite forming as small caps (Fig 5.19).This provides evidence that the trees existed before the Taupo eruption and were engulfed, completely buried and preserved by the deposition of the Taupo Ignimbrite.

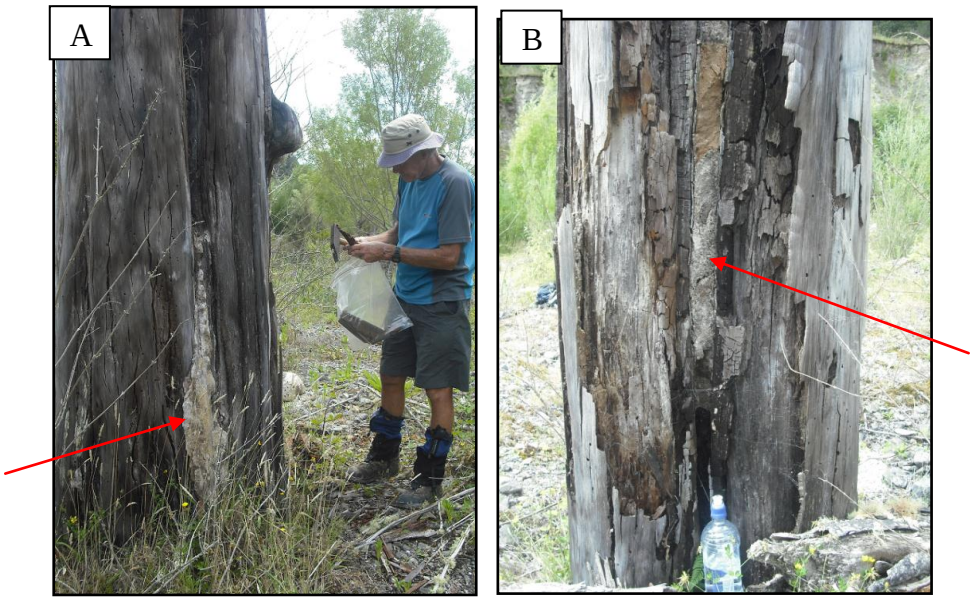

Figure 5.18: Pockets of Taupo Ignimbrite (red arrows) within the tree trunks. A- remains are plastered up against and partly infill the large cracks within the bark on the outside of the tree trunks. B- The deposit is also found embedded deeply within crevices in the inner core of the trunks.

Figure 5.19: The top of this tree trunk is capped with the Taupo Ignimbrite, which reinforces that it had to have been deposited at this level and the tree trunks must have been present prior to deposition.

One of the larger (>1.5 m in diameter) tree trunks is preserved in place within the ignimbrite outcrop (Fig 5.20). This provides key evidence for the engulfment of a living forest by the Taupo Ignimbrite and also suggests a more extensive forest is still buried beneath the remaining ignimbrite.

Figure 5.20: The base of a large tree trunk remains in standing growth position, preserved in the Taupo Ignimbrite outcrop. The observed side appears to have been uncharred, stripped and infilled with the ignimbrite. This infill material as shown in the inset is slightly more compact and consolidated than the material in the surrounding outcrop.

The tree trunks are truncated and abraded where some of the uppermost surfaces are pointed and jagged and fractured, suggesting that the upper parts of the trees have been torn off violently (Figs 5.15, 5.16, 5.17, 5.19). In a few instances, the tops seem to have broken and collapsed or caved inwards (Fig 5.21).

Most of the tree trunks are uncharred (Figs 5.18, 5.19, 5.20, 5.21) and the bark is either still intact (Fig 5.18A) or has been stripped from the trunks (Fig 5.18B). The degree of charring however varies between and even within a few specific individual trunks (Figs 5.22, 5.23).

Figure 5.21: Some of the tree tops have collapsed down into the base of one the trunks. The inset is a close up to show how the hollows have been infilled by the Taupo Ignimbrite.

Figure 5.22: Evidence of charring in one of the tree trunks. Although still intact, the outer bark has been completely transformed into charcoal.

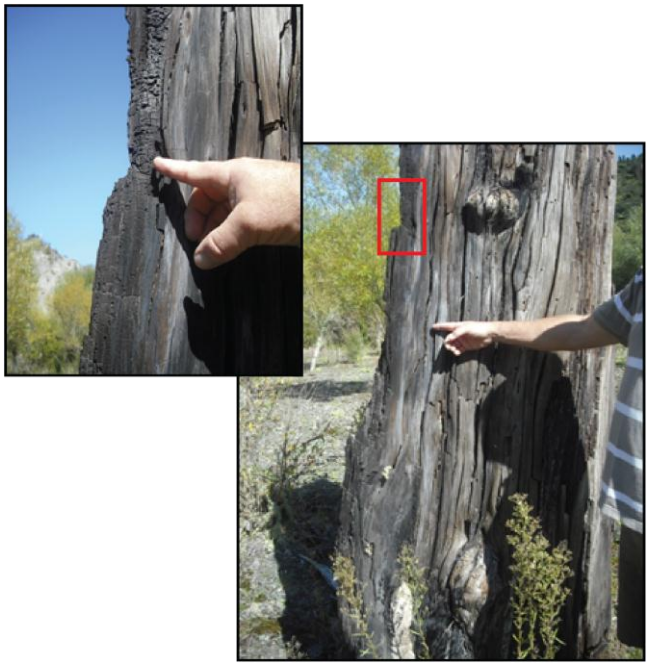

Figure 5.23: Charring occurring preferentially to a higher degree on the southeast facing side (the direction from which the pyroclastic flow was moving) as shown by the inset (closer view) in comparison to the northeast facing side. The bark along this segment of the trunk is a rich brown colour and shows little signs of charring.

Chapter 6
Discussion

6.1 Introduction

As Blank (1965), Wilson (1986a,b) and Briggs et al. (1993) state, the best exposures of the eruptives of the Mangakino volcanic centre is within the King Country, and many of the important eruptives are represented in the Ongatiti Valley. This chapter discusses possible scenarios for the volcanic evolution of the area and its geomorphic development, with specific focus on the Ongatiti, Unit D, and the Taupo Ignimbrite.

6.2 Geomorphic development of the Ongatiti Valley

6.2.1 Introduction

The geological evolution of the King Country is complex. The topography of the Ongatiti Valley prior to the deposition of the Quaternary Ignimbrites was highly irregular. As a result, it played a significant role in directing and controlling transport and emplacement processes of the earliest pyroclastic flows to travel through the area.

6.2.2 Geological history prior to Quaternary volcanism

1. Distribution of the Mesozoic basement (Manaia Hill Group)

The sporadic distribution and variable topographic heights of outcrops of Mesozoic basement within the King Country is suggested to have been the result of structurally and localised block faulting (Wilson et al. 1986b). The Hauhungaroa and Rangitoto Ranges reach up to 1100 metres above sea level and are strongly confined to the eastern boundary of the King country. The only other exposures are to the west of the Ranges as isolated block-faulted hills and ridge caps, otherwise the Mesozoic basement has been buried by Tertiary sediments and the thick ignimbrite plateaux (Blank 1965, Wilson et al. 1986b, Edbrooke 2005).

2. **Highly irregular thickness and lateral continuation of the Te Kuiti Group**

As Nelson (1978) and Edbrooke (2005) explain, localised tectonic subsidence during sedimentation of the Te Kuiti Group across the block-faulted surface of the Mesozoic basement produced an uneven and discontinuous extent to the different units within the Te Kuiti Group.

3. **The irregular relief of the Mahoenui Group**

During the inversion and erosion of the Te Kuiti depocentre, the soft nature of the Mahoenui Group typically weathered to produce a characteristically rounded and hummocky relief (Kamp et al. 2004).

4. **Varying degrees of erosion**

The magnitude of erosion over the King Country intensified (prior to the initiation of volcanism within the TVZ) during the long-wavelength up-doming of the central North Island in the Pliocene-Pleistocene (Kamp et al. 2004, Edbrooke 2005, Stern et al. 2006).There were variations in the intensity of erosion that took place overall on a regional scale (Kamp et al. 2004) that also applies on a smaller scale within the Ongatiti Valley. The amount of erosion would have varied between the different areas in relation to the river systems.

6.2.3 The eruption of the Ngaroma Ignimbrite

The earliest ignimbrite to have formed from the MVC is Ignimbrite C. This deposit is poorly exposed and is not found outcropping within the study area. It is therefore inferred that the first deposition of a pyroclastic flow within the Ongatiti Valley was the Ngaroma Ignimbrite 1.55 Ma. The Ngaroma Ignimbrite was deposited on a highly irregular topography and overlies Mesozoic basement and Te Kuiti Group, e.g. at Ngaroma, Rangitoto. Wilson (1986a) explains that the relatively widespread distribution and relatively thin nature (20-30 m thick) of the ignimbrite, indicates it was emplaced energetically. This is also suggested by the relatively high lithic abundance (3-4%) of the deposit in comparison to the other MVC derived ignimbrites, which implies it had a high erosive energy. The emplacement of the Ngaroma Ignimbrite is therefore suggested to have taken

place as a veneer deposit where it mantled the underlying and irregular topography, and is only sporadically preserved (Fig 6.1).

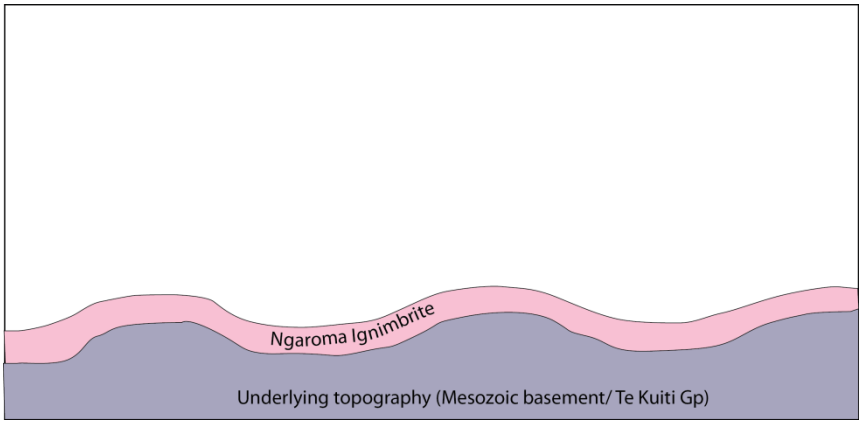

Figure 6.1: An illustration showing how the Ngaroma Ignimbrite was emplaced within the Ongatiti Valley.

6.2.4 The eruption of the unknown fall deposit

There is no sign of Ignimbrite B exposed overlying the Ngaroma Ignimbrite within the study area. However, there is a very fine grained phreatoplinian deposit exposed directly underlying the Ongatiti Ignimbrite, which is considered not to be related to the eruption due to it having a distinct composition. It is inferred that an explosive phreatoplinian eruption must have taken place at the MVC after the Ngaroma and very shortly before the Ongatiti eruptions (i.e. between 1.55 and 1.21 Ma) which has not previously been documented. The deposition of the fall deposit would have mantled the highly irregular and weathered surface of the underlying Ngaroma Ignimbrite as a thin (< 5 m thick) layer, and is unlikely to have been preserved unless it was erupted within a brief time before the Ongatiti eruption (Fig 6.2).

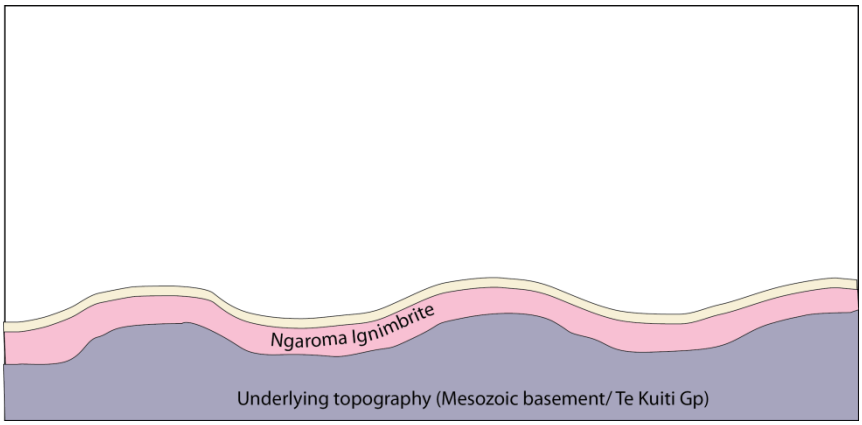

Figure 6.2: An illustration showing how the Unknown phreatomagmatic fall deposit was deposited into the Ongatiti Valley.

6.3 Ongatiti eruption

6.3.1 Introduction

Direct observation of pyroclastic flows is essentially deadly and unexposed due to the enveloping ash cloud (Druitt 1995, Pittari et al. 2005). The current perception and understanding of the transport and depositional dynamics of pyroclastic flows is based on the characteristics of the deposits left in the wake of the flows (Pittari et al. 2005). The nature, characteristics and composition of the Ongatiti Ignimbrite exposed within the study area has been described in chapter three. This discussion presents an interpretation of how the eruption, transport and emplacement processes of the pyroclastic flow sequence developed the vertical and lateral variations observed in the Ongatiti Valley.

6.3.2 Vertical and lateral variations in ignimbrite deposits

Lateral and vertical changes within the different facies of an ignimbrite are relative to the complex variation in the spatial and temporal behaviour of pyroclastic flows (Pittari et al. 2005, Pittari at al. 2006). The temporal changes reflect a variation in the eruption dynamics and conditions at the vent (Pittari et al. 2005, Pittari at al. 2006), which may include a change in source emissions, eruption durations and clast concentrations, sizes and densities (Branney and Kokelaar 2002).

As the pyroclastic flows move through an area, deposition will take place when the flow loses enough momentum to allow the material to drop out of suspension. This process is primarily controlled by the variation in the topography (Pittari et al.2006). Branney and Kokelaar (2002) state that whatever the concentration of the flow, deposition will take place as a sustained process which is controlled by the conditions and processes around the lower flow boundary. The underlying topography is a crucial parameter which influences the physics of the flows where a reduction in the momentum and/or turbulence can effectively initiate the deposition of the material from the flow (Sulpizio et al. 2008). However, other factors such as the distance from the vent and the densities of the clasts are also important.

6.3.3 Mechanism causing vertical and lateral variations within the study area

1. **Change in the eruption intensity over time**

The principal mechanism responsible for creating vertical variations within the Ongatiti Ignimbrite is the result of variations in particle density, internal flow processes, turbulence, topography and a change in the intensity of the eruption with time. As Wilson (1986a) and Briggs et al. (1993) explain, the commencing of the Ongatiti eruption was intense and violent, where a highly energetic, highly fragmented succession of hot pyroclastic flows generated the lower, pumice-poor unit of the Ongatiti Ignimbrite.

The nature and characteristics of the lower unit exposed within the study area confirms this theory. Sohn et al. (2009) state that overpressure can develop in rapidly ascending, highly viscous magma which can lead to full fragmentation of magma into ash through brittle rupture of individual bubble walls upon rapid decompression. It seems that this was the case during the initial, explosive stages of the eruption due to the minimal abundance of pumice and their relatively small clast size. The fact that both the abundance and the maximum clast size of the pumice increases with an increase in the stratigraphic elevation of the lower unit of the ignimbrite, implies that degassing, abrasion of the vent and magma ascent rate of the initial phase of the eruption and therefore the degree of fragmentation must have slightly and progressively reduced with time.

The lower unit of the Ongatiti Ignimbrite is distinctively crystal rich. The crystals constitute 45-65% of the matrix, and indicate strong crystal enrichment when compared with the abundance of phenocrysts within the pumice clasts. It seems that during the transportation and emplacement of the highly energetic flow, the fine material (glass shards) derived from the fragmentation of the pumice would have effectively been elutriated out from the bulk of the flow and into the associated ash cloud above, leaving the denser crystals to accumulate within the lower main body.

The initiation of possible caldera collapse and subsequent vent widening is assumed to have been associated with the eruption of these highly energetic flows (Wilson 1986a). The sudden widening of the vent would have reduced the intensity of the eruption and also the height of the column. The subsequent pyroclastic flows formed during the next phase of the eruption were less energetic and less violent and were responsible for generating the less fragmented and therefore coarser grained, lower crystal abundance, upper pumice-rich unit of the Ongatiti Ignimbrite (Wilson 1986a and Briggs et al. 1993).

Sohn et al. (2009), mention that several features within massive ignimbrites suggest emplacement as a progressive aggradation of several small flows rather than by en masse freezing. This is also considered to be the case for the emplacement processes of both the lower and upper units of the Ongatiti Ignimbrite. The abundance of the dense lithic clasts remains either fairly consistent or shows a slight increasing trend, and the abundance and maximum clast sizes of pumice increases with an increase in the stratigraphic height of the deposit. These stratigraphic relations imply that the Ongatiti Ignimbrite consisted of multiple flows which were erupted in a series of directional lobes (Briggs et al. 1993).

Despite the complex and two-part nature of the Ongatiti Ignimbrite, the whole eruption would have occurred within a short time period (Wilson 1986a). This is suggested by the lack of flow unit boundaries, and especially in between the lower and upper units of the Ongatiti Ignimbrite. The contact is gradational and is represented by a transitional unit.

There is no variation in the mineral assemblage between the lower and upper units. No clear distinction between the major element composition of the glass shards within the lower and the upper units can be made and there is no systematic relationship between the stratigraphic elevation and the geochemical composition of the Ignimbrite. So the differences in pumice and crystal abundance between the upper and lower units are the only distinguishing features.

2. **Relationship to underlying topography**

The evidence of high mobility and remarkable ability to surmount topographic obstacles indicates that the lower, pumice-poor unit was a low aspect ratio type ignimbrite which had a high flow velocity and high eruption rate (Walker 1983) and it represents a violently emplaced veneer deposit (Wilson 1986b). Areas inferred to have been at high elevations at the time of the Ongatiti eruption are capped with the densely to partially-welded, columnar jointed bluffs of the lower, pumice-poor unit (Wilson 1986a). Blank (1965) and Wilson (1986a,b) state that a succession of pyroclastic flows have spread across the Rangitoto and Hauhungaroa Ranges (which rise up to 1100 metres above sea level), where only the highly energetic flows could traverse these. The ignimbrite deposits preserved along the tops of the ranges are remnants of the Ongatiti Ignimbrite as presented on the 1:250 000 QMAP series (Geological map 4).

As previously discussed, the topography prior to the emplacement of the Ongatiti Ignimbrite would have been highly irregular as illustrated in Fig 6.3.

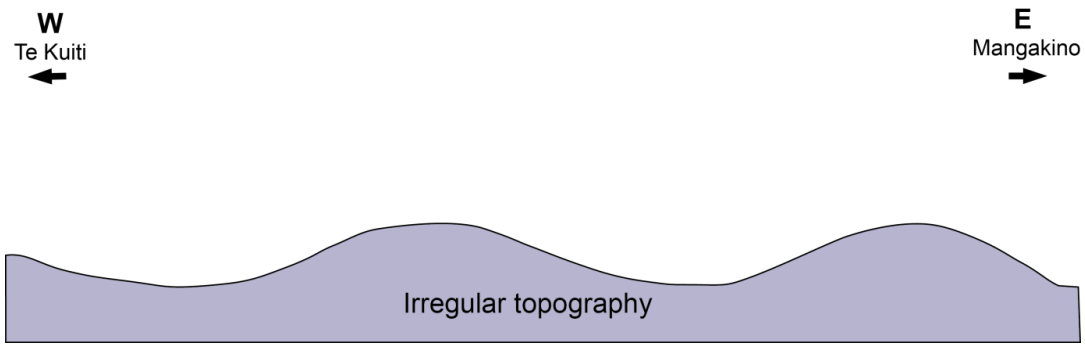

Figure 6.3: The highly irregular topography is represented by the Mesozoic basement, and/or the Te Kuiti Group rocks.

The energetic and high mobility nature of the pumice-poor unit however would have enabled deposition to take place as a topographic mantling veneer deposit across the study area where it would have had the ability to scale significant topographic highs (Fig 6.4).

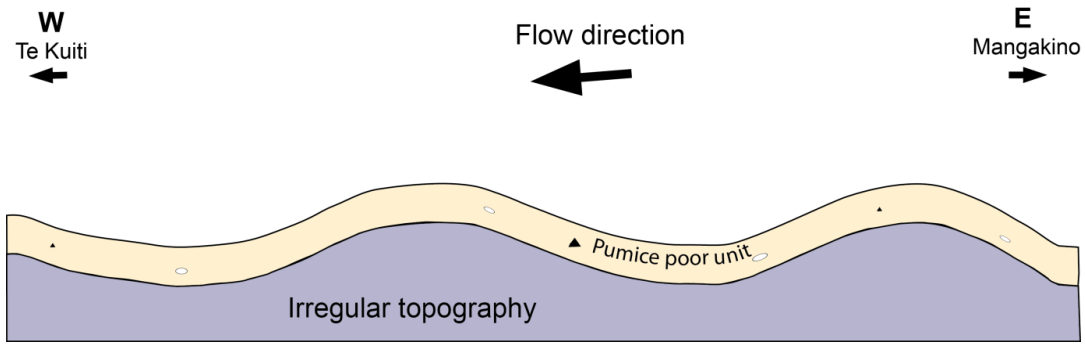

Figure 6.4: The initial deposition of the lower, pumice-poor unit would have mantled the topography as a relatively thin (< 20 m thick) veneer deposit.

The lower energy emplacement of the upper, pumice-rich unit was deposited as a valley ponded and plateau forming deposit (Fig 6.5).

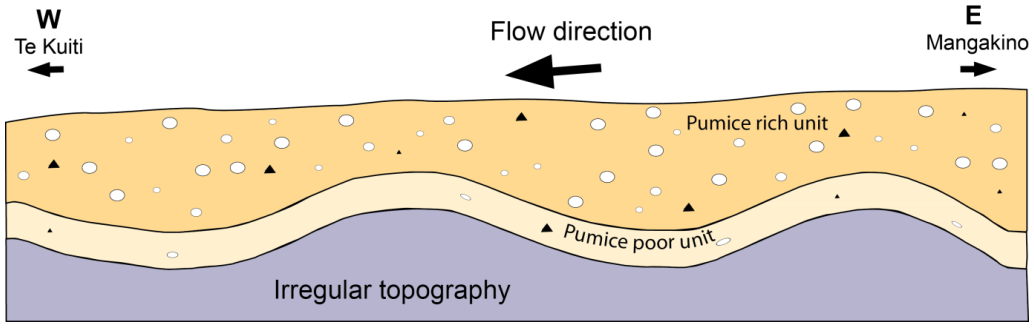

Figure 6.5: The deposition of the upper, pumice-rich unit would have infilled the irregularities and effectively transformed the study area into a relatively uniform and flat ignimbrite plateau.

The ongoing erosion of the Ongatiti Valley over the last 1.2 Ma has exposed the partially-welded zone of the Ongatiti Ignimbrite which outcrops as prominent bluffs. This zone exposes both the upper units (within the paleovalleys) and the lower units (along the paleoridges) and illustrates that along the slopes of the paleoridges, the transitional unit (transitions from the lower unit and up into the

upper unit) are exposed and explains the vertical variations observed (6.6). Specific sections of the lower and upper units of the Ongatiti Ignimbrite were deposited at the same topographic elevation due to a combined effect from both the different behaviour of their depositional systems and because of the influence from the highly irregular underlying topography.

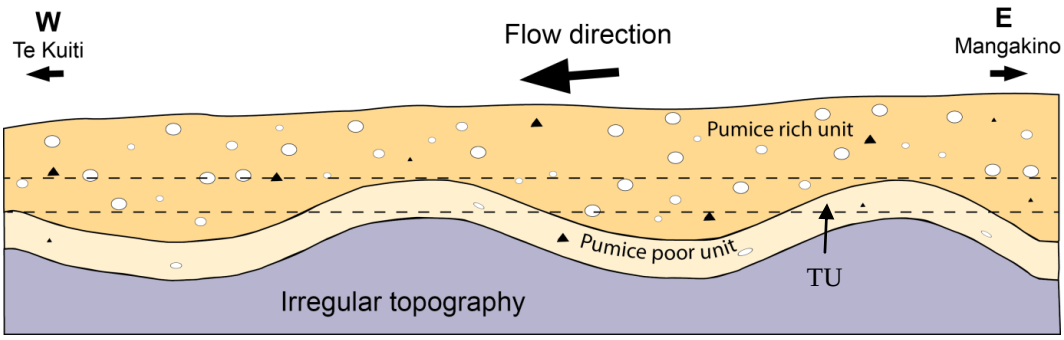

Figure 6.6: The current setting of the Ongatiti Ignimbrite within the Ongatiti Valley. The dashed lines represent the thin welded zone of the partially-densely welded zone of the ignimbrite which are exposed as the prominent and continuous bluffs through the area. Note how the lower, upper and transitional (TU) units are all exposed along this zone.

6.4 Unit D

6.4.1 Introduction

Unit D is representative of a short eruptive event triggered possibly by the interaction of magma with water within a lake that is likely to have formed following the collapse of the caldera during the eruption of the Ongatiti Ignimbrite (Moyle 1989). Wilson (1986a, b) and Moyle (1989) have classified the scale of the event as a phreatoplinian eruption.

Phreatoplinian volcanism is poorly understood, purely because of the lack of witnessed historic events. This eruption style is characterised by the interaction between magma and a significant volume of external water producing widespread and fine grained fall deposits (Houghton et al. 2003). However, as Carey et al. (2009) explains, large scale silicic eruptions have the common tendency to vary between eruption styles and intensities (mass discharge rate), and therefore between eruptive regimes.

As a result, it seems that examples of phreatoplinian deposits are typically produced during phreatomagmatic phases of much larger rhyolitic eruptions

which usually involve several different styles of activity (Cas and Wright 1987). The 1875 eruption of Askja Volcano, Iceland, is one of the very few eruptions recorded to include both phreatoplinian and plinian phases where there were three abrupt shifts between subplinian, phreatoplinian, pyroclastic surge and plinian activity (Carey et al. 2010). During the Taupo 232 AD eruption, the eruptive style shifted abruptly between 'wet' and 'dry' conditions three times (Houghton et al. 2003). Other examples include the widespread phreatoplinian ash layers in the Oruanui Formation, New Zealand; the Vesuvius AD 79 eruption also produced phreatoplinian layers (Cas and Wright 1987). The phreatoplinian eruption of the Kos Plateau tuff in the eastern Aegean Sea, Greece, consists of phreatoplinian and plinian dry explosive deposits as well as ignimbrites (Allen and Cas 1998), and the Neopolitan Yellow tuff, of the Campanian Volcanic area, Italy contained mostly a phreatoplinian eruptive phase that then turned into a phreatomagmatic and magmatic phase (Orsi et al. 1992). The triggers and relative roles of both the external (degree of interaction with water, vent position, vent and conduit geometries) and internal factors (conduit dynamics, conditions in the magma chamber) controlling these abrupt shifts in the eruption conditions and therefore deposit characteristics, are not fully understood for many eruptions (Carey et al. 2009).

The descriptions of Unit D reveal that the eruption appears to be a complex, eruptive event, similar to the examples discussed. The outcrop exposure of Unit D in the study area has been described in detail in chapter 4. It has been divided into a lower phreatoplinian succession which consists of three facies, and an upper ignimbrite with two separate facies (Fig 4.5). This section of the discussion compares and characterises the different facies within Unit D relative to the corresponding and varying eruption styles and intensities.

6.4.2 Process interpretations of Unit D facies

Facies A:

Facies A consists of the typical characteristics of a wet or phreatomagmatic style eruption, where the deposits are a very fine, poorly sorted ash composed of highly fragmented crystals, pumice and lithic clasts with abundant accretionary lapilli.

As Cas and Wright (1987) explain, phreatomagmatic eruptions characteristically form fine-grained deposits as a result of fragmentation. This is caused by the quenching of the magma and the explosive activity produced during the sudden transfer of heat from the magma into the water. Accretionary lapilli are also most frequently formed in the steam-rich columns of these eruptions (Cas and Wright 1987), and this is because, if water is available, strong particle bonds from short-range surface tension forces coalesce the particles to form aggregates (Textor et al. 2006a). (Textor et al.2006b) have determined that there is a weak influence of the atmospheric background conditions on ash aggregation for the strong eruptions, and that the aggregation of ash particles is more effective in the case of eruptions containing very large amounts of water or ice, such as phreatomagmatic events or within lower eruption columns where the temperatures are warmer and there are higher amounts of liquid water.

Facies B:

Facies B represents the waning phase from an explosive phreatoplinian eruption into a less explosive and possibly plinian episode. The fact that the deposit consists of a moderately well sorted fine ash with no coarse pumice (> 2 mm) indicates an explosive eruption style. However, with the presence of small (2 mm) lithic clasts, a slightly coarser grainsize and a higher abundance of less fragmented crystals than in facies A, facies B represents a less explosive phase of the eruption in comparison. The crystals increase in size and become less fragmented with an increase in stratigraphic elevation through facies B. This strongly represents waning in the explosive index of the eruption and due to the absence of accretionary lapilli, it possibly infers an alternation into a dry, magmatic eruptive stage.

Facies C:

Facies C is representative of a fine grained ignimbrite. This is made evident by the overall massive and poorly sorted nature of the deposit and the fact that the ash matrix is supporting the larger lapilli clasts (pumice and lithics). The pumice and lithic clasts are small (< 5mm) but they are abundant.

Facies D:

Facies D is a thin, poorly sorted, coarse ash and distinctive lithic-rich layer which is located with a sharp boundary at the base of the Unit D ignimbrite. These characteristics are typical of a layer 1 co-ignimbrite lithic breccia associated with the energetically emplaced, low aspect ratio type ignimbrites (Wilson and Walker 1982, Cas et al. 2011).

Facies E:

Facies E is the thin ignimbrite in the uppermost section of Unit D which has been described previously by Wilson (1986a,b) and Moyle (1989). It contains the typical features of an ignimbrite, as it is massive, non-welded and contains a moderate abundance of coarse pumice clasts (up to 96 mm in diameter) with minimal lithic clasts sporadically distributed within a finer ash matrix. As previously defined, the fact that the ignimbrite has the presence of a co-ignimbrite breccia at its base and also due to the thin (1 m thick) and massive nature of it (1 m thick), it is inferred to be the valley pond component of a low aspect ratio type ignimbrite deposit (Cas et al. 2011).

6.4.3 Interpretation of the eruption process

As Rosi (2011) explains, plinian eruptions can take place as either a single eruptive episode (lasting several hours), or evolve as a series of discrete pulses which can be separated by hours to month-long periods. Unit D is inferred to have occurred over a short period (Moyle 1989) and was therefore likely to have been a single eruptive type eruption. This is further made evident by the fact that when there is a significant change at the vent which effectively ceases the eruptive activity temporarily, individual deposits will be separated by a distinct and abrupt fall unit break, which effectively marks an abrupt change in the granulometric texture (Cas and Wright 1987). Contacts within Unit D are rarely observed as an abrupt fall unit break and the boundaries between the different facies are more gradational.

The interpretation of the eruption process of Unit D based on the characterisation of the different facies exposed within the study area may not represent the entire

sequence of the deposits produced during the eruption. This is because there is no contact revealed with the underlying Ongatiti Ignimbrite.

However, from what is revealed, there was an oscillation between wet, intense phreatoplinian phases with a less intense and perhaps dry, plinian episode. This is represented by the characteristics within the lower 1.25 m of the exposed deposit. The shift in eruption style and therefore intensity from wet (phreatomagmatic) to dry (magmatic) phases during an eruption is inferred by Zimanowski (2001), Houghton et al. (2003), and Carey et al. (2009) to not simply be the result of losing interaction with external water. Houghton et al. (2003) expresses that in some phreatoplinian eruptions, the principal role of external water was to flush and aggregate the fine particles from the plume rather than to drive or assist with the eruption itself. With reference to the Taupo eruption (232 AD), the vesiculation history of the melt and its ascent history played the dominant roles in the switches between wet and dry explosive volcanism where the availability of water was a second order determinant (Houghton et al. 2003). This is because slow ascent rates of the magma are necessary for large scale magma/water interaction (Houghton et al. 2003). Therefore, the gradation from facies A into Facies B and back into Facies A (Fig 4.5), most probably and primarily represents a fluctuation in the magma ascent rate which is effectively controlled by the conduit dynamics and the magma conditions (Fig 6.7). There was obviously a significant interaction with the external water within the Mangakino caldera when the magma ascent rate was reduced (Fig 6.7) and this is made evident by the flushing and deposition of the fine grains and accretionary lapilli of facies A.

In order to accurately confirm this inferred oscillation between the wet and dry eruption phases, it would be relevant to study the shard textures through the scanning electron microscope. This is because the morphologies of phreatomagmatic pyroclasts (Wohletz's five principal morphological types of phreatomagmatic ashes) are unique to these eruptions (Cas and Wright 1987). It would also be useful to investigate the vesicle textures of the pumice clasts as the textures can reveal the vesiculation process relative to the timescales of ascent and degassing (conduit dynamics) which can therefore determine whether the eruption was dry or wet (Carey et al. 2009).

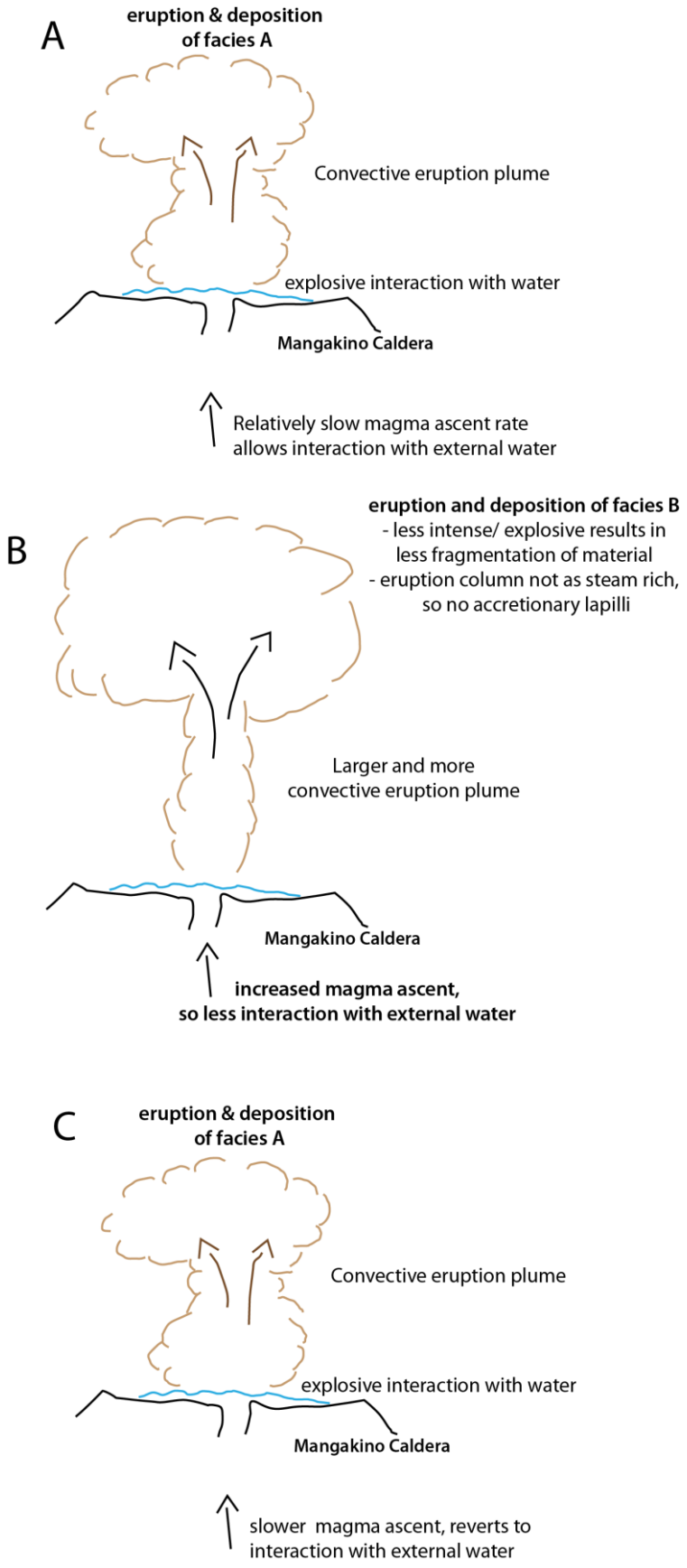

Figure 6.7: The step by step process of the initial phase of the Unit D eruption.

A common feature within large scale silicic eruption deposits is the occurrence of either a basal plinian fall deposit, often with an initial phreatomagmatic deposit overlain by pyroclastic flow deposits (Rosi 2001, Carey et al. 2009). A very similar pattern is observed within the exposed deposits of Unit D in the study area, where pyroclastic density currents overlie a lower succession of phreatoplinian and plinian fall deposits.

Although the column remains fully convective during a single eruptive type event, oscillations in plume height associated with the slightly fluctuating eruption conditions causes the column to become unstable. This can trigger short lived, partial column collapse of the margins during the eruption where both fall and flow regimes occur simultaneously (Cas and Wright 1987, Rosi 2001, Carey et al. 2009). Therefore, pyroclastic flow or surge deposits are often interbedded within pyroclastic ash fall deposits (Cas and Wright 1987, Rosi 2001). The transition observed from the phreatoplinian fall deposit (facies A) into the fine grained ignimbrite (facies C) at 1.25 m indicates a shift from a wet sustained buoyant plume into short lived instabilities of the margins of the phreatoplinian eruption column causing partial collapse and subsequent production of a PDC (Fig 6.8).

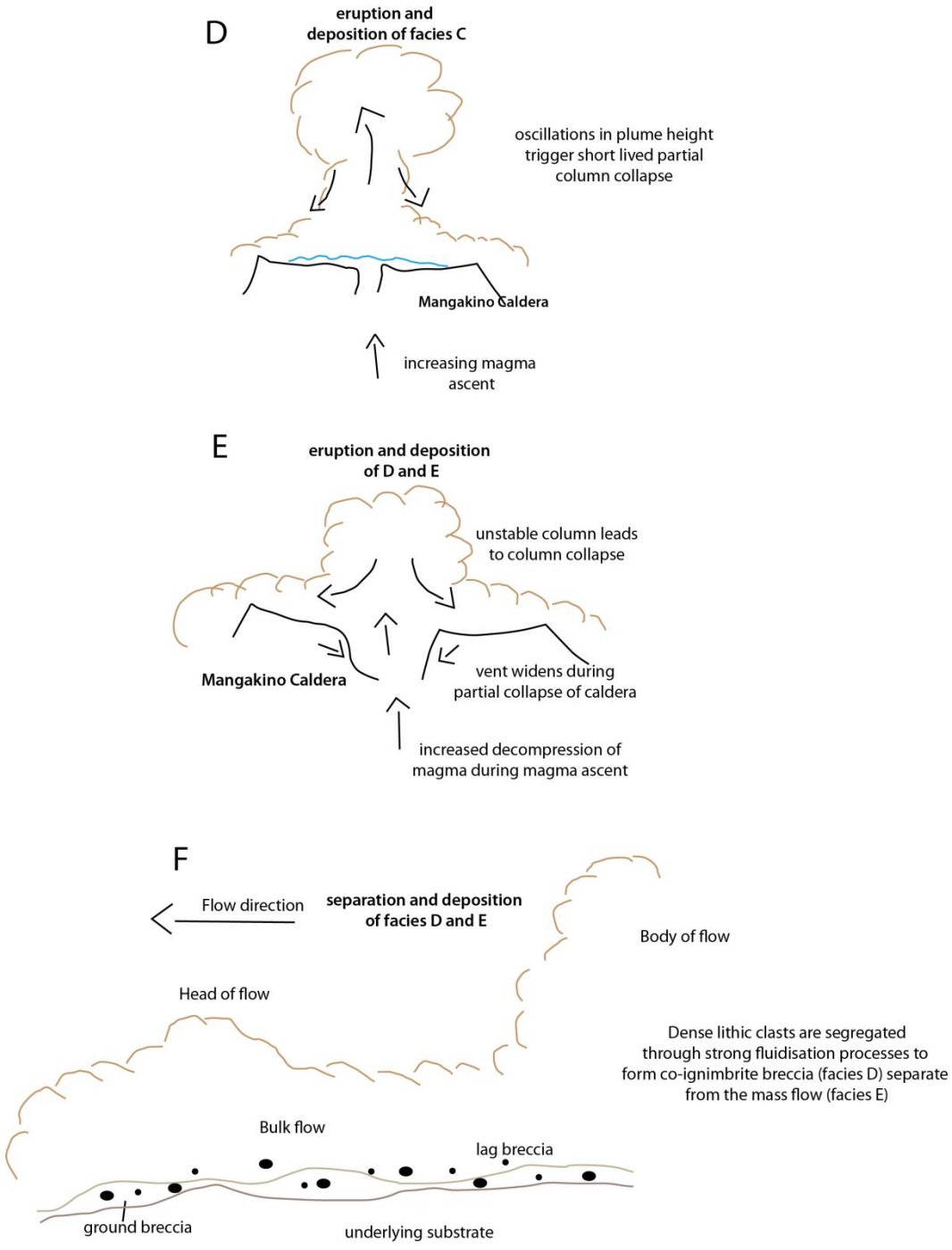

Figure 6.8: The step by step process of the closing phase of the Unit D eruption.

Carey et al. (2009) further explains that an increase in the decompression of the magma and an increase in the magma ascent rates can induce widening of the vent during an eruption. This suddenly affects the plume dynamics and results in significant column collapse or even caldera collapse (Fig 6.8). In association with initial caldera collapse, co-ignimbrite breccias are generated by the combination of both the eruption processes at the vent (erosion of the collapsing roof and walls

of the conduit), and within the emplacement of the pyroclastic flows. These deposits are commonly observed at the base or lower zone of the ignimbrites proximal to the vent and mark the transition from the fall to flow eruptive regime (Cas and Wright 1987). The sharp boundary between facies C (dilute ignimbrite) and facies D (co-ignimbrite breccia) (Fig 4.5) most likely represents an erosional contact produced during emplacement of facies D and E rather than a significant break in the eruption. This is because the low aspect ratio ignimbrite (facies D and E) produced by the collapse of the eruption column and possible partial collapse of the Mangakino Caldera, would have had a high velocity, and a high erosional capacity (Cas et al. 2011).

6.4.4 Interpretation of the depositional process

As previously discussed, the preceding voluminous eruption of the Ongatiti Ignimbrite effectively infilled topographic irregularities within the study area, and was the first eruption to significantly transform and smooth out the landscape into an ignimbrite plateau. The deposition of the Unit D phreatoplinian fall deposits and the subsequent energetic emplacement of the PDCs would have accumulated as a relatively thin layer which mantled the surface of the Ongatiti Ignimbrite (Fig 6.9). The deposition of Unit D took place approximately 100 000 years after the Ongatiti eruption.

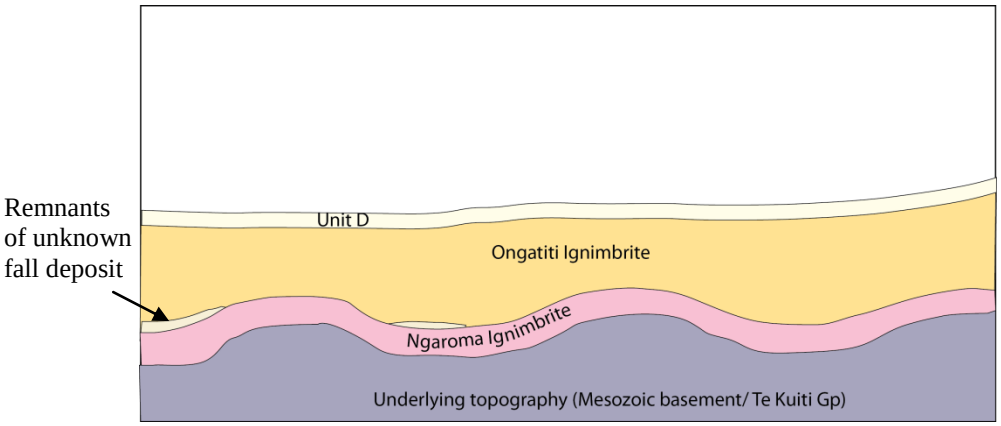

Figure 6.9: An illustration showing how the Unit D was deposited into the Ongatiti Valley.

6.5 Younger Mangakino eruptions and post-caldera erosion

6.5.1 The eruption of the Ahuroa Ignimbrite

Due to the non-welded nature of Unit D, it suffered severe erosion over the subsequent 200 000 years and as a result it is rarely exposed. The high relief of the contact observed between Unit D and the overlying Ahuroa Ignimbrite observed within the study area, suggests that the Ahuroa eruption was highly energetic. McGrath (2004) explains that the eruption rate was rapid and that it progressively increased over time, depositing the material as a topographic mantling veneer deposit (Fig 6.10). It appears that the bulk of the Ahuroa pyroclastic flow was constrained to the east of the study area. This is made evident by the significant decline in the thickness of the deposit within the west of the study area.

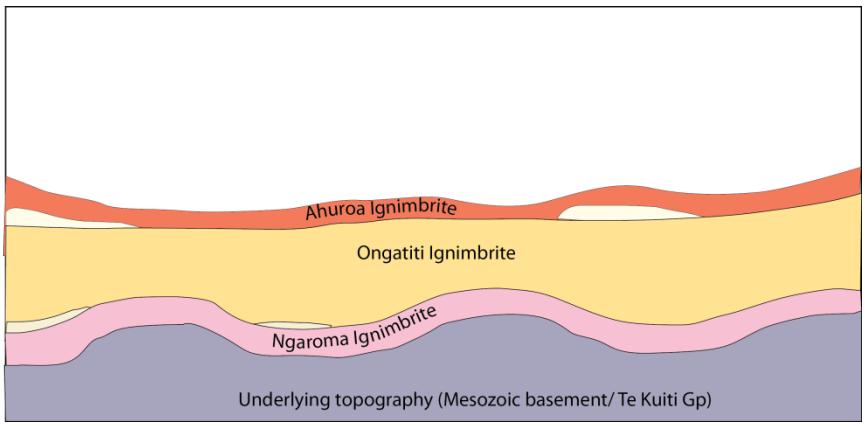

Figure 6.10: An illustration showing how the Ahuroa Ignimbrite was emplaced into the Ongatiti Valley.

6.5.2 The eruption of the Rocky Hill Ignimbrite

The emplacement of the Kidnappers deposit (Unit E) took place 1.01 Ma ago, but is not exposed in the study area. Hence it is not discussed further here.

The next significant development of the ignimbrite plateau within the study area occurred soon after the inferred emplacement of the Kidnappers deposit with the voluminous Rocky Hill eruption (1 Ma) which deposited up to 50 m of material onto the Ahuroa Ignimbrite. The inverse welding zonation of the ignimbrite

suggests the eruption rate must have increased with time. Deposition of the Rocky Hill initially occurred as a valley pond deposit where the topographic depressions were infilled, and as the rate of the eruption increased, the emplacement of the deposit transformed into an ignimbrite veneer deposit (Fig 6.11)

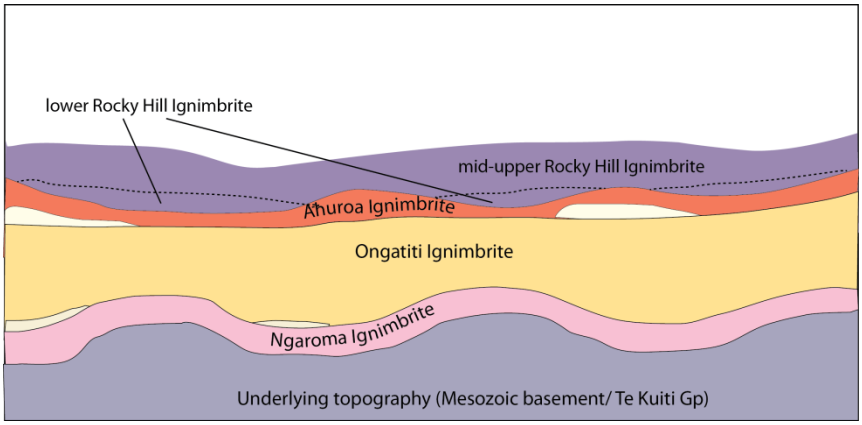

Figure 6.11: An illustration showing how the Rocky Hill Ignimbrite was emplaced within the Ongatiti Valley.

This explains why within the study area, the lower-mid section of the Rocky Hill Ignimbrite has been deposited at the same level as the uppermost sequence (Fig 6.12).

Figure 6.12: Variable distribution of the different sections of the Rocky Hill Ignimbrite.

Unit H and the Marshall Ignimbrites are not exposed in the study area, and it is not known whether they were not deposited or have been completely eroded.

6.5.3 Erosion after the cessation of activity from MVC

A significant amount of erosion has taken place over this period within the Waipa and Ongatiti Valleys. The Ongatiti Stream and Waipa River would have run a similar path as they do today. This is made evident by the > 300 m deep valleys formed, which have eroded large volumes from a once extensive plateau (Fig 6.13).

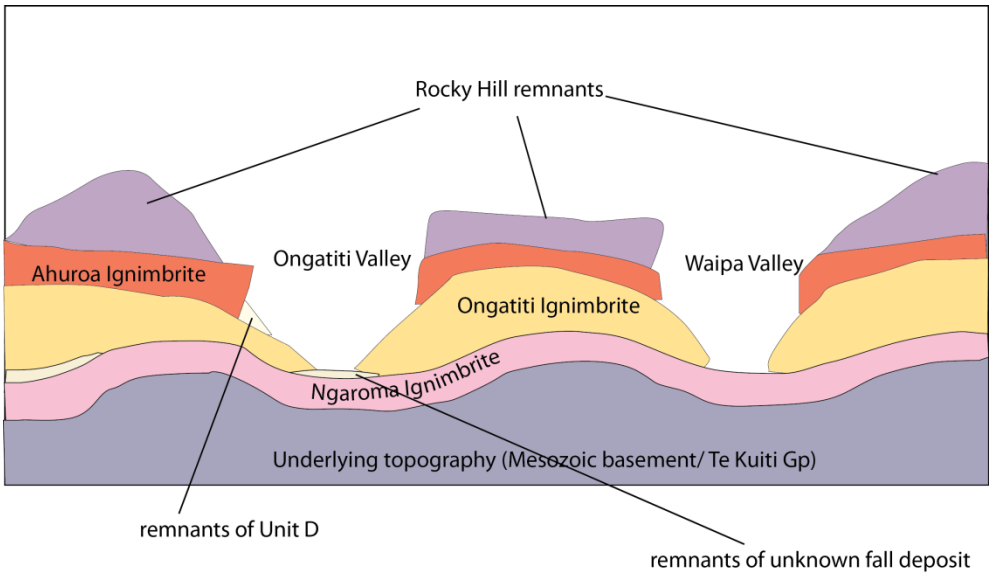

Figure 6.13: An illustration showing the geomorphologic changes made to the landscape of the Ongatiti Valley.

The rate of erosion along the steep slopes of the Ongatiti and Waipa valleys would have been amplified by small to large scale slumping, rock fall and landsliding of the ignimbrites. Ignimbrites are characteristically weak rocks under different kinds of stress, and their rock strengths vary (Moon 1993):

1. **Non-durable type (equivalent to soft, non-jointed and non-welded ignimbrite)**

This type of ignimbrite behaves as a very stiff soil which derives the bulk of its strength from frictional effects between the matrix and glass shards. The high cohesion and high angles of internal friction allows them to maintain a steep slope as they erode. However, they are susceptible to a sudden loss of strength and therefore respond in a dispersive behaviour which is caused by a structural change in the elevated pore water pressure within the material.

2. **Durable type (equivalent to densely-welded, jointed ignimbrites)**

The densely-welded type ignimbrites respond with a brittle failure under an applied load. The access of groundwater into the rock mass (through the jointing systems) develops high cleft water pressures and leads to rockfall and subsequent erosion of the jointed blocks.

3. **Intermediate type (equivalent to partially-welded ignimbrites)**

The partially-welded ignimbrites contain properties which are intermediate to the durable and non-durable types and the failure of these ignimbrites effectively takes place as a combination of the two types described.

The large amount of erosion of the Pakaumanu Group Ignimbrites that occurred after the deposition of the Rocky Hill Ignimbrite and prior to the deposition of the Taupo Ignimbrite in 232 AD has lead to topographic inversion of the study area.

6.6 Taupo eruption

6.6.1 Introduction

The deposition of the Taupo Ignimbrite is the most recent event and has ponded at a lower topographic elevation within the Waipa Valley than the Ongatiti Ignimbrite which was deposited approximately 1.2 Ma prior (Fig 6.14).

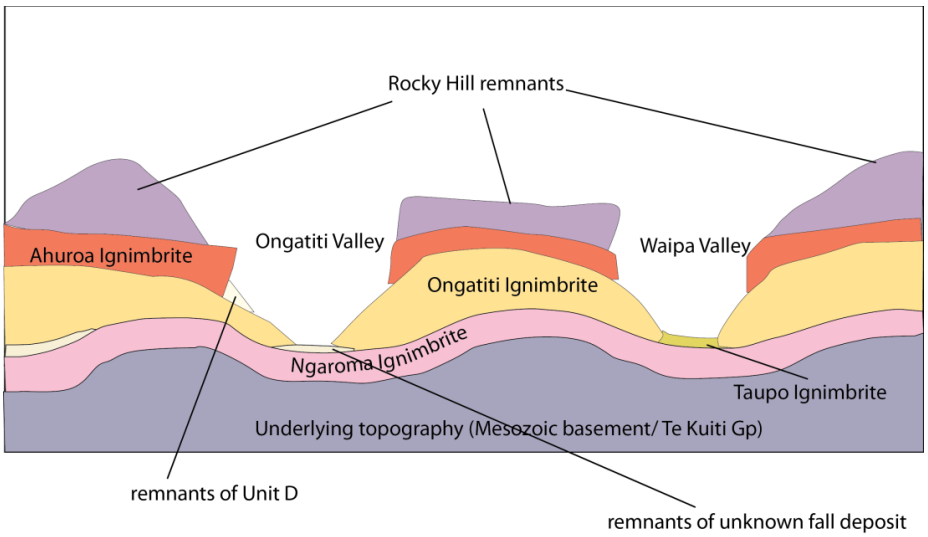

Figure 6.14: An illustration showing how the Taupo Ignimbrite was emplaced within the study area.

This section discusses the mechanism of forest destruction and the preservation of fossilised tree trunks within the Taupo Ignimbrite in the study area. The discovery of preserved tree trunks still in standing position of growth has been described in chapter 5 and is compared with several case studies from around the world.

Case study examples

1. **Merapi Volcano, Indonesia**

Kelfoun et al. (2000) describe that on the 22nd of November 1994, a dome-collapse eruption generated block and ash flows and ash-cloud surges, destroying the south-southwest flank of Merapi Volcano. The damage was constrained to a 9.5 km^2 area where all of the trees were stripped, singed and/or broken, with a high proportion blown down and uprooted. The block and ash flows were contained within the river channels. However, the surge deposits were distributed throughout the area and were responsible for the tree damage. Along the outer extremities of the damaged zone in a strip extending 200 m, trees were broken and singed but not blown down.

2. **Unzen Volcano, Japan**

A violent ash-cloud surge was generated during the 3 June 1991 eruption at the Unzen Volcano. Numerous telephone poles (10 m high, radius of 15 cm) were broken near their bases, and trees (12 m high, radius of 15 cm) were delimbed and uprooted from the effects of the ash-cloud surge approximately 3-3.5 km east – southeast of the dome (Clarke and Voight 2000).

3. **Mt St Helens, Washington**

One of the most well known examples of forest damage during a volcanic eruption was the 1980 directed blast surge from the north face of Mount St Helens Volcano, USA. Thousands of Douglas fir and Western hemlock trees were delimbed, ruptured and uprooted en masse from the force of the surge (Clarke and Voight 2000).

4. El Chichon Volcano, Mexico

The eruption that took place in early April 1982 on the El Chichon Volcano buried nine villages under pyroclastic fallout and density current deposits. This eruption is significant to this study because preserved in the PDC deposits, is a very similar feature to what is exposed in the Waipa Valley. The only object remaining in the village of Esquı´pula Guayabal, 3.5 km from the eruption crater is a steel basketball pole (made of AISI 1010 steel, 4 mm thick, yield strength of 380 MPa) (Fig 6.15) where the upper part has been torn off during the eruption (Scolamacchia and Schouwenaars 2009).

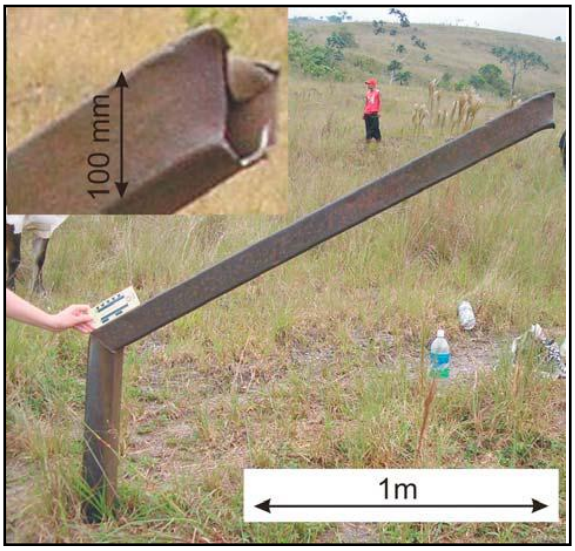

Figure 6.15: Image retrieved from Scolamacchia and Schouwenaars (2009), showing the remnants of the basketball pole extending 148 cm above the current ground surface. Note in the inset, the upper steel profile was completely torn off with the force of the eruption.

5. Manukau Harbour, Auckland

On the shore of the Manukau Harbour, the remains of a well-preserved fossil forest are located within phreatomagmatic volcanic deposits. Numerous, small trees with a diameter < 1m are preserved in standing position of growth (Fig 6.16) and are found protruding up into the overlying volcanic deposits. The tree trunk appears to have been snapped off during the initial eruptive phase as it is preserved leaning down current with a sharply truncated upper surface (Marra et al. 2006). This feature is almost identical to what is preserved within the Waipa Valley.

Figure 6.16: Large trees up to 1 m in diameter preserved in position of growth, Manukau Harbour (Marra et al. 2006).

6.6.2 Transport and emplacement mechanisms of Taupo pyroclastic flow

The ultra-plinian eruption of Taupo that took place in 232 AD produced an extremely high (> 50 km) eruption column. The collapse of this column from a great height and the high potential energy associated with it was responsible for the creation of the Taupo pyroclastic flow sequence which contained an extraordinary high velocity and mobility (Walker 1980, Wilson and Walker 1985). As McClelland et al. (2004) discusses, the ignimbrite was erupted and emplaced in one short-lived episode (400 s) where there is no evidence for any time breaks long enough to permit cooling between the different batches of material. The general model for the Taupo pyroclastic flow indicates that it was entirely erupted by the time its front had reached approximately 40 km from the vent and that the current represented a single large pulse of material from 40 km outwards (McClelland et al. 2004). The temperature of the flow was 380 – 500°C and 150 - 300°C at more than 40 km and within 30 – 40 km from the vent respectively (McClelland et al. 2004). As a result of the violent and energetic nature of the flow, it was able to flow over topographic highs with a large erosional force and this is reflected by the very coarse ground breccias, the high accessory and cognate lithic fragments and especially by the preserved blown down tree trunks within the Taupo Ignimbrite (Froggatt et al. 1981, Cas et al. 2011).

McClelland et al. (2004) mentions that the unusually and highly energetic nature of the Taupo pyroclastic flow tends to contradict the division of PDCs into supercritical or sub-critical types by Bursik and Woods (1996). This is because it contained characteristics from both. It was emplaced over a short period and at high speeds (200-300 m s^{-1}) which is typical of supercritical type flows. However, the distance travelled by the pyroclastic flow (radius of 80 km) far exceeds that of a supercritical and is more representative of a sub – critical type flow (McClelland et al. 2004, Hogg et al. 2011).

Despite the fact that the Taupo Ignimbrite can offer this prosperity of information, as Branney and Kokelaar (2002) state, ignimbrites offer only a limited insight into the transport and sedimentation processes of their parent pyroclastic flow. The main concern is trying to determine whether the pyroclastic flow was discrete, intergradational, instantaneous or progressive (Branney and Kokelaar 2002). As a result, the mechanism of forest destruction and preservation in the Taupo Ignimbrite with respect to the transport and emplacement processes of the Taupo Ignimbrite is a theoretical explanation.

6.6.3 Mechanism of destruction and preservation of fossilised trees in the Waipa Valley

Preserved vegetation in most pyroclastic density current (PDC) deposits exists as an incomplete combustion residue (charcoal). This is a typical feature within PDC deposits because of both the inert nature of the charcoal and the rapid burial by deposition from the PDCs, which creates conditions for high preservation potential (Hudspith et al. 2010). The preservation of uncharred and charred tree trunks, however, still in standing position of growth is a rare occurrence in both the Taupo Ignimbrite and in ignimbrites in general. Most examples from around the world discuss the preservation of logs in ignimbrites as being blown down or completely uprooted and broken. Graham (2008) and Marra et al. (2006) however document the preservation of tree trunks still in standing growth position within the Taupo Ignimbrite (Rangitaiki River) and within a phreatomagmatic deposit in the Manukau Harbour, New Zealand respectively. Despite these records,

neither offers an explanation on the mechanism of preservation of these unique structures.

The tops of the fossilised tree trunks preserved in the Waipa Valley within the Taupo Ignimbrite are of a similar height (3 – 4 m), regardless of the tree trunk size and they are all conical in shape, jagged and broken. This represents that the trees were exposed to an extreme force which as a result violently tore most of the tree trunk off and left only the lower 3-4 m base before the entire structures were buried and preserved in the ignimbrite.

The mechanism of how PDCs create so much destructive damage to objects and more specifically to trees is complex and is often evaluated in relation to nuclear explosions (Valentine 1998). The following theories on the destruction and preservation of these tree trunks in the Waipa Valley of the study area are proposed.

1. **Destruction by the initial air shock blast or shock driven surge**

It is speculated that in close proximity to the vent, structural damage during explosive eruptions is produced by the initial air shock when the expansion of the overpressurized and unsteady column penetrates the atmosphere (Fig 6.17A) (Valentine 1998). This is the mechanism inferred to have flattened the forested areas at Pureora and Bennydale which are both approximately 50 km northwest from the locality of the Taupo vent (Cas et al. 2011, Hogg et al. 2011). It is therefore a possible explanation for the damage observed in the fossilised trees within the Waipa Valley of the study area (80 km from the vent). The energy/force of the air shock blast may have reduced with an increase in distance from the vent. Therefore rather than the entire tree being flattened as they were in Pureora and Bennydale forests, only the weaker upper parts of the trees were torn off and the stronger base of the trunks were left in place before being buried by the pyroclastic flow which followed soon after.

As the initial air shock travels outward, the eruptive mixture expands, and some of that mixture may be pulled laterally by the shock to produce a shock driven surge

(Valentine 1998) (Fig 6.17B). Shock driven or ash cloud surges can also be transmitted during directed blasts and hydrovolcanic explosions which propagate ahead of the PDC, compressing ambient air to higher densities and temperatures (Scolamacchia and Schouwenaars 2009). This was the mechanism responsible for the destruction of thousands of trees during the 1980 eruption of Mount St Helens and during the 1991 eruption of the Unzen Volcano, where the more resistant telephone poles were snapped off at their bases and trees were completely uprooted. The force of the surge was not strong enough to completely uproot the more resistant vegetation (large tree trunks) and has instead snapped them 2-3 m from their bases. This explains why these large trunks are the only vegetation preserved and why the smaller trees and shrubs are not.

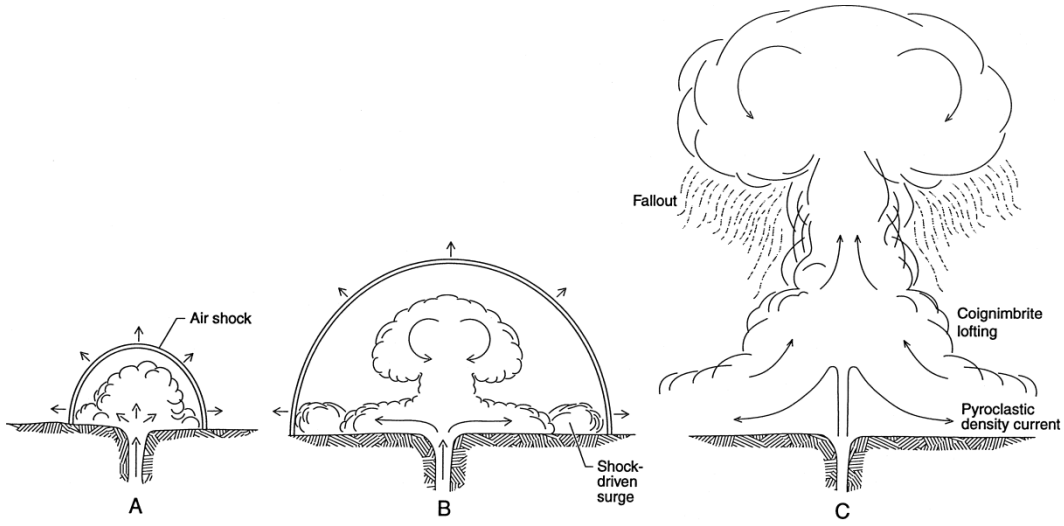

Figure 6.17: The sequence of events of explosive volcanic eruptions that produce PDCs (Valentine 1998). A and B represent the initial air shock and shock driven surges produced respectively before the buoyant portions of the mixture rise vertically as a plume to form a mushroom structure which may collapse to form PDCs (C).

Dynamic pressure (P_{dyn}) within pyroclastic flows is controlled by the bulk flow density (p) and the horizontal flow velocity (v) which determines the abrasive power of the particles in the currents (Valentine 1998, Pittari et al. 2006, Scolamacchia and Schouwenaars 2009).

$$P_{dyn} = pV^2$$

To emphasise the effective force of these PDCs, Kelfoun et al. (2000) explain that a surge with 10 times air density (volumetric concentration of particles approximately 0.5%) and a velocity of 50 m s^{-1} would apply the same drag as a wind of 570 km h^{-1}.

Referring to a more practical sense, 35 kPa is considered to be the minimum dynamic pressure value for creating total destruction during a nuclear explosion. A dynamic pressure of 38 kPa in the flow gusts of pyroclastic flows is equivalent to approximately 252 m s^{-1} in air flow and approximately 8.7 m s^{-1} in water flow. This is more powerful than any meteorological phenomena but can be compared to the current intensity at the crest of the Niagara Falls (Pittari et al. 2006). Total destruction of affected areas occurred during the eruptions at Montserrat in 1997 and Mt St Helens in 1980, where the dynamic pressure values were 25 and 40 kPa respectively (Scolamacchia and Schouwenaars 2009). Valentine (1998) describes that dynamic pressures in particle-laden PDCs can range from $1\text{-}10^4$ kPa where complete blow down of a forest (strongly dependent on tree shape and type) can occur during a PDC with a dynamic pressure as low as 2 kPa (dilute solid concentration of 10^{-3} travelling at 70 m/s).

2. **Reduced dynamic pressure at contact with substrate during en masse deposition**

Pittari et al (2006) explain that pyroclastic flows are complex and may contain vertical and horizontal gradients in bulk flow velocity and density where generally towards the flow-substrate boundary, there is a decrease in the flow velocity and an increase in the density. The combination of these disparities with the topographic irregularities may then cause variation in the degree of turbulence and the dynamic pressure within the flow.

It is significant to note that the occurrences of these fossilised tree trunks still standing up in growth position and preserved within the Taupo Ignimbrite are all valley ponds located within current river channels (Waipa River and Rangitaiki River). It seems apparent that as the pyroclastic flow moved through these areas, the interaction with the cool substrate of the river beds played a significant role in subsequently reducing the dynamic pressure of the flow. The 2- 3 m height of the tree breakdown could be the interface between the low velocity, high density flow and the high velocity, low density overriding ash cloud surge (Fig 6.18).This may be the reason why the base of the trunks although have been partly stripped, have not been blown over or completely charred. The fact that there is a sudden

increase in charcoal observed in the ignimbrite above the fossilised tree line infers that the dynamic pressure and therefore abrasive power must have been much more significant at this level in comparison to what it was at the base of the flow.

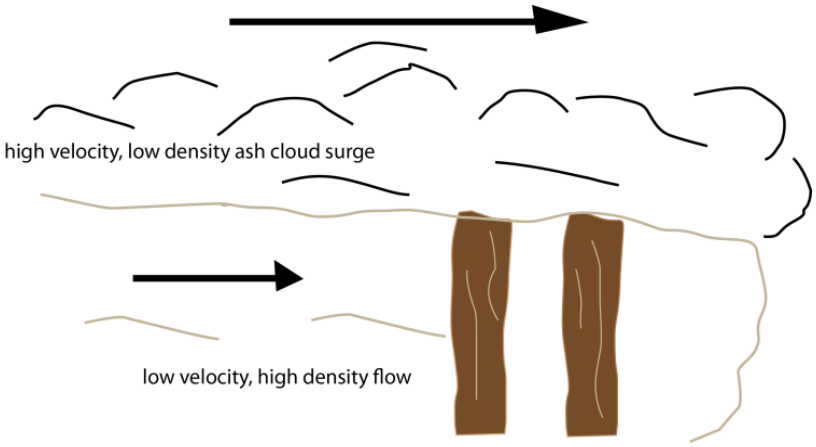

Figure 6.18: Possible 2-part flow mechanism within the Taupo pyroclastic flow.

3. An aggrading increase in the dynamic pressure of the pyroclastic flow

As Branney and Kokelaar (2002) states, homogeneous ignimbrites such as the main component of the Taupo Ignimbrite generally aggrade progressively (may vary from slow to extremely rapid) from the base upwards rather than being deposited en masse. Another potential scenario for the destruction and preservation of the fossilised trees in the Taupo Ignimbrite could be the product from an increase in the dynamic pressure of the pyroclastic flow during the emplacement of the aggrading deposit.

There are no obvious scour marks or signs of erosion along the contact between the valley floor and overlying Taupo Ignimbrite. It looks as if the base of the deposit was emplaced by an initial flow which had a low dynamic pressure and was emplaced with little erosional or abrasion force. This then allowed the ignimbrite to be deposited in and around the base of the tree trunks. The dynamic pressure of the next phase of the pyroclastic flow must have increased significantly where the exposed remnants of the trees were then violently torn off and completely destroyed. The base of the trunks which were buried and protected by the initial phase of deposition of the pyroclastic flow were therefore unaffected and left to be preserved.

This was the case for the structural damage in the township of Herculaneum during the 79 AD eruption of Vesuvius (Valentine 1998). The dynamic pressure of the first of the PDCs was in the order of 10-20 kPa where most walls remained standing. The next major PDC that followed was however significantly stronger with a dynamic pressure of 35-70 kPa and was therefore strong enough to complete the destruction of the town where the remaining walls were knocked down (Valentine 1998).

4. Standing shock waves within the pyroclastic flow

The multiphase mixtures of PDCs and the variations in topographic gradient can create an unsteady flow regime within a pyroclastic flow (Scolamacchia and Schouwenaars 2009). This can lead to the generation of shock waves (discrete and intense gusts or waves) during the transportation of the flow which are completely independent from the source conditions. These represent a change in the velocity, pressure and density (dynamic pressure) where there is a sudden transition from subsonic (tens of m/s) to supersonic (> 200 m/s) flow regimes even over a small distance (Scolamacchia and Schouwenaars 2009). This mechanism explains for such observations as ruptured trees adjacent to preserved trees within the same pathway of the pyroclastic flow (Clarke and Voight 2000). It has also been observed within wind tunnel tests of forests, where the wind striking the front of the edge of a forest rises sharply, becomes turbulent and strikes downwards some way into the forest, creating violent oscillating forces on the trees (Clarke and Voight 2000).

This explanation can be related to the evidence exposed in the study area where the fossilised tree trunks are constrained to a localised area and where their height significantly reduces along its northern and western boundaries. Perhaps oscillating shock waves were responsible for the complete (no fossilised trees present) and incomplete (fossilised trees still in standing position of growth) destruction within specific locations of the forest.

6.6.4 Preferred origin

Most of the preserved logs within the Taupo Ignimbrite and specifically within the Pureora buried forest (50 km northwest from vent) are blown down and located within the basal pumice rich, ash sparse layer which represents the material jetted forward from the front of the flow. The preserved tree trunks in the Waipa Valley (> 80 km northwest from the vent) of the study area however in comparison, are in standing position of growth and are located within the homogenous unit which overlies the basal layer. This evidence suggests that the mechanism of destruction and preservation of the tree trunks in the two areas must have been different and possibly independent of each other. The air shock produced during explosive eruptions is unlikely to be sufficiently strong enough to cause this destruction to the trees within the Waipa Valley at more than 80 km from the vent. Air shock creates structural damage only very close to the vent while the dynamic pressure loading should be quite high and for a long duration of the PDC (Valentine 1998). Therefore, theories 2 - 4 are more applicable in comparison.

Research within the Pureora Forest revealed that there was very little temperature difference within the Taupo Ignimbrite and between the basal pumice rich, ash sparse and the pumice and ash rich valley ponded layers (approximately 40 °C difference) (Hudspith et al. 2010). However, it would be inaccurate to assume that this was the same for the ignimbrite deposit in the Waipa Valley due to it being emplaced within a completely different setting. There is no variation observed in the texture of the deposit in the Waipa Valley below or above the fossilised tree line. This represents that there was no significant change in the transport and emplacement mechanism (no change in the flow velocity or density). Therefore in order to better determine whether theory two and/or three were the most justified mechanisms of destruction, it would be relevant to assess the emplacement temperature and the bulk density of the deposit above and below the fossilised tree line. This will help determine in more detail, if there was any change in the transport and emplacement process of the pyroclastic flow below and above the fossilised tree line.

The evidence revealed at this level of research shows a weak argument against theory two and there is little evidence that either contradicts or supports the mechanism of destruction explained in theory four. It is therefore likely that either,

or a combination of the three mechanisms were accountable for the destruction and preservation of the fossilised tree trunks.

6.7 Recent landscape modification and sedimentation

Since the eruption of the Taupo Ignimbrite in AD 232, the only significant changes made to the landscape of the study area is the result of ongoing erosion and the deposition of alluvium along the Ongatiti Stream and the Waipa River. The typical styles of slumping in the ignimbrites continued to take place where the scarps and the associated talus from the most recent events are commonly observed along the sides and at the base of the Ongatiti Valley. The persistent incision of the stream and river systems through the succession of ignimbrite deposits have deepened the main valleys and built up 2-5 m high terraces along their banks. Smaller and less defined valleys have established throughout the study area as a result of the drainage during rainfall.

6.8 Conclusions

The Ngaroma Ignimbrite (1.55 Ma), Ongatiti Ignimbrite (1.21 Ma), Unit D (1.2), Ahuroa Ignimbrite (1.18), Rocky Hill Ignimbrite (1.00) and the most recent Taupo Ignimbrite (232 AD) are all exposed within the Ongatiti Valley. The discovery of an unknown, fine-grained, pumice-poor fall deposit underlying the Ongatiti Ignimbrite suggests that a phreatomagmatic eruption occurred between 1.55 – 1.21 Ma.

The nature of the volcanic geology of the Ongatiti Valley exposes a detailed representation into its volcanic evolution and geomorphic development. The production and aggrading deposition of the 5 Mangakino Volcanic Centre eruptives built up and transformed the landscape of the Ongatiti Valley into thick ignimbrite plateaux.

Ignimbrites are characterised as weak rocks, they are therefore susceptible to high rates of erosion. The ignimbrite plateaux was dissected and heavily eroded after the cessation of the eruptive activity from the Mangakino Volcanic Centre. The

deep incision of the Waipa Valley allowed the subsequent valley ponded Taupo Ignimbrite to be deposited within the study area.

The eruption, transport and emplacement processes of the Ongatiti Ignimbrite were complex. The complexity of the eruption as a result, created vertical and lateral variations within the Ignimbrite which are clearly exposed in the Ongatiti Valley. Two separate and main units with contrasting pumice and crystal characteristics were produced during the eruption of the Ongatiti Ignimbrite and as a result of a significant change in the eruption conditions. A lower, pumice-poor and distinctly crystal-rich unit was produced during the initial intense phase of the eruption. An upper, pumice-rich unit was produced during the later and less intense phase of the eruption. The lower unit was emplaced as a topographic mantling deposit. The upper unit was emplaced as a valley ponded, plateau forming deposit. The Ongatiti ignimbrite was emplaced across a highly irregular topography and as a result, the lower and upper units were deposited at highly irregular topographic elevations.

The eruption of Unit D is poorly understood. The characterising of six different facies within the deposit indicates that the eruption was complex and that the eruption conditions varied over time. The magma ascent rate oscillated with time. Slower ascent rates allowed the interaction with the external water of the Mangakino caldera lake and consequently produced explosive style eruptions and phreatomagmatic style deposits (facies A). Increased magma ascent rates produced coarser and less fragmented fall deposits (facies B) and eventually lead to the partial and complete collapse of the eruption column where a series of ignimbrite deposits were formed (facies C, D and E).

There are four likely scenarios for the destruction and preservation of tree trunks in standing position of growth within the Taupo Ignimbrite:

Scenario 1: The trees were knocked down by a surge or air wave before the arrival and deposition of the pyroclastic flows; it assumes the tree trunks were weakest at 2-3 metres above their base.

Scenario 2: Assumes en masse deposition; and invokes vertical gradients in the dynamic pressure of the flow. It assumes the dynamic pressure was the highest at 2-3m above the base of the flow.

Scenario 3: Assumes deposition by progressive aggradation and also invokes vertical gradients in the dynamic pressure of the flow. Trees were snapped at a later stage during the flow deposition when the dynamic pressure increased.

Scenario 4: Assumes there were intense irregularities within the broader PDC system.

Either/or a combination of scenarios 2, 3 and 4 is the most likely theoretical explanation. However further research is required to better define and confirm the most plausible theory for explaining these fossilised tree trunks within the Taupo Ignimbrite.

References

Allan, A.S.R., Baker, J.A., Carter, L., Wysoczanksi, R.J. 2008 'Reconstructing the Quaternary evolution of the world's most active silicic volcanic system: insights from an w1.65 Ma deep ocean tephra record sourced from Taupo Volcanic Zone, New Zealand' *Quaternary Science Reviews*, vol.27, pp.2341-2360.

Allen, S.R. & Cas, R.A.F. 1998, 'Rhyolitic fallout and pyroclastic density current deposits from a phreatoplinian eruption in the eastern Aegean Sea, Greece', *Journal of Volcanology and Geothermal Research*, vol. 86, pp 219-251.

Blank, R. 1965, 'Ash-flow Deposits of the Central King Country, New Zealand' *New Zealand Journal of Geology and Geophysics*, vol. 8, no. 4' pp. 588-607.

Bowling,F.M. 1989, Volcanic Geology of Ignimbrites on the Western Margin of the Hauraki Depression and in the Mangatangi area, M. Sc. Thesis, University of Waikato.

Bowyer. D.A. 2001, Petrologic, Geochemical and Isotopic Evolution of Rhyolite Lavas from the Okataina, Rotorua and Kapenga Volcanic Centres, TVZ, M. Sc. Thesis, University of Waikato.

Branney, M.J. & Kokelaar, P. 2002, 'Pyroclastic Density Currents and the Sedimentation of Ignimbrites', *Geological Society Memoir* no.27.

Briggs, R.M., Gifford, M.G., Moyle, A.R., Taylor, S.R., Normaff, M.D., Houghton, B.F. & Wilson, C.J.N. 1993, 'Geochemical zoning and eruptive mixing in ignimbrites from Mangakino volcano, Taupo Volcanic Zone, New Zealand', *Journal of Iblcanology and Geothermal Research*, vol. 56, pp. 175-203.

Briggs R.M., Houghton, B.F., McWilliams, M. & Wilson, C.J.N. 2010 '40Ar/39Ar Ages of Silicic Volcanic Rocks in the Tauranga-Kaimai area, New Zealand: Dating the Transition between Volcanism in the Coromandel Arc and the Taupo Volcanic Zone', *New Zealand Journal of Geology & Geophysics*, vol.48, no.3, pp.459-469.

Carey, R.J., Houghton, B.F. & Thordaeson, T. 2009, 'Abrupt shifts between wet and dry phases of the 1875 eruption of Askja Volcano:Microscopic evidence for macroscopic dynamics', *Journal of Volcanology and Geothermal Research*, vol. 184, pp. 256-270.

Carey, R.J., Houghton, B.F. & Thordarson, T. 2010, 'Tephra dispersal and eruption dynamics of wet and dry phases of the 1875 eruption of Askja Volcano, Iceland', *Bulletin of Volcanology*, vol 72, pp.259-278.

Cartwright, S.J. 2003, Cenozoic Geological Evolution of the Central Eastern King Country Basin, North Island, M. Sc. Thesis, University of Waikato.

Cas, R.A.F. & Wright, J.V. 1987, *Volcanic successions, Modern and Ancient*, Allen and Unwin Ltd, London.

Cas, R.A.F., Wright, H.M.N., Folkes, C.B., Lesti, C., Porreca, M., Giordano, G. & Viramonte, J.G. 2011, 'The Flow Dynamics of an Extremely Large Volume Pyroclastic Flow, the 2.08-Ma Cerro Galán Ignimbrite, NW Argentina, and Comparison with other Flow Types', *Bulletin of Volcanology*, vol 73, pp.1583-1609.

Clarke, A.B. & Voight, B. 2000, 'Pyroclastic Current Dynamic Pressure from Aerodynamics of Tree or Pole Blow-down', *Journal of Volcanology and Geothermal Research*, vol. 100, pp. 395-412.

Davey, F.J. 2010, 'Crustal Seismic Reflection Measurements across the Northern Extension of the Taupo Volcanic Zone, North Island, New Zealand' *Journal of Volcanology and Geothermal Research*, vol. 190, pp. 75-81.

Druitt, T.H. 1995, 'Settling behaviour of concentrated dispersions and some volcanological applications', *Journal of Volcanology and Geothermal Research*, vol. 65, pp 27-39.

Edbrooke, S.W. (compiler) 2005, *Geology of the Waikato area. Institute of Geological and Nuclear Sciences 1:250000 geological map 4*, Institute of Geological and Nuclear Sciences, Lower Hutt, N.Z.

Ewarti, A., Brothers, R.N. & Mateen, A . 1977 'An Outline Of The Geology And Geochemistry, And The Possible Petrogenetic Evolution Of The Volcanic Rocks Of The Tonga-Kermadec-New Zealand Island Arc' *Journal of Volcanology and Geothermal Research*, vol. 2, pp.205-250.

Froggatt, P.C.1982, 'Review of Methods of Estimating Rhyolitic TephraVolumes; Applications to the Taupo Volcanic Zone, New Zealand', *Journal of Volcanology and Geothermal Research*, vol. 14, pp. 301-318.

Hastuti, E.W.D. 1992, Post – Depositional Alteration of Ignimbrite in the Western Taupo Volcanic Zone, N.Z. , M. Sc. Thesis, University of Waikato.

Hogg, A., Lowe, D.J., Palmer, J., Boswijk, G. & Ramsey, C.B. 2011, 'Revised Calendar Date for the Taupo Eruption Derived by 14 C Wiggle-matching using a New Zealand Kauri 14 C Calibration Data Set', *The Holocene*, vol. 1, pp.1-11.

Houghton, B.F., Wilson, C.J.N., McWilliams, M.O., Lanphere, M.A., Weaver, S.D., Briggs R.M. & Pringle, M. S. 1995, 'Chronology and dynamics of a large silicic magmatic system: Central Taupo Volcanic Zone, New Zealand', *Geology*, vol. 23, pp.13-16.

Houghton, B.F., Hobden, B.J., Cashman, K.V., Wilson, C.J.N. & Smith, R.T. 2003, 'Large-scale Interaction of Lake Water and Rhyolitic Magma during the 1.8ka Taupo Eruption, New Zealand', in White, J.D.L., Smellie, J.L. & Clague, D.A. (eds), *The Explosive Subaqueous Volcanism*, American Geophysical Union, Washingtom DC, pp. 97-109.

Hudspith, V.A., Scott, A.C., Wilson, C.J.N. & Collinson, M.E. 2010 'Charring of woods by volcanic processes: An example from the Taupo ignimbrite,New Zealand' *Palaeogeography, Palaeoclimatology, Palaeoecology*, vol.291, pp. 40–51.

Kamp, P.J.J., Vonk, A.J., Bland, K.J., Hansen, R.J., Hendy, A.J.W., McIntyre, A.P., Ngatai, M., Cartwright, S.J., Hayton, S., Nelson, C.S. 2004 'Neogene Stratigraphic Architecture and Tectonic Evolution of Wanganui, King Country, and Eastern Taranaki Basins, New Zealand' *New Zealand Journal of Geology & Geophysics*, vol.47, no.4, pp.625-644.

Kelfoun, K., Legros, F. & Gourgaud, A. 2000, 'A Statistical Study of Trees Damaged by the 22 November 1994 Eruption of Merapi Volcano (Java, Indonesia): Relationships between Ash-Cloud Surges and Block-and-Ash Flows', *Journal of Volcanology and Geothermal Research,* vol. 100, pp. 379-393.

Krippner, S.J.P. 2000, Volcanic geology, geochemistry and geochronology of the Kapowai Caldera Complex, Coromandel Volcanic Zone, New Zealand, M. Sc. Thesis, University of Waikato.

Krippner, S.J.P, Briggs, R.M, Wilson, C.J.N. & Cole, J.W. 2010, 'Petrography and geochemistry of lithic fragments in ignimbrites from the Mangakino Volcanic Centre: Implications for the composition of the subvolcanic crust in western Taupo Volcanic Zone, New Zealand', *New Zealand Journal of Geology and Geophysics,* vol.41, no.2, pp.187-199.

Leonard, G.S. , Begg, J.G. & Wilson, C.J.N. (compilers) 2010, *Geology of the Rotorua Area 1:250000 Geological Map 5*, Institute of Geological and Nuclear Sciences, Lower Hutt, N.Z.

Manville, V., Segschneider, B., Newton, E., White, J.D.L., Houghton, B.F. & Wilson, C.J.N. 2009 'Environmental impact of the 1.8ka Taupo Eruption, New Zealand: Landscape Responses to a Large-Scale Explosive Rhyolite Eruption' *Sedimentary Geology* vol.220, pp.318-336.

Marra, M.J., Alloway, B.V. & Newnham, R.M. 2006, 'Paleoenvironmental Reconstruction of a Well-preserved Stage 7 Forest Sequence Catastrophically Buried by Basaltic Eruptive Deposits, Northern New Zealand', *Quaternary Science Reviews,* vol. 25, pp. 2143–2161.

Martin, R.C. 1961, 'Stratigraphy and Structural Outline of the Taupo Volcanic Zone' *New Zealand Journal of Geology and Geophysics,* vol. 4, no. 4, pp. 449-477.

McClelland, E., Wilson, C.J.N. & Bardot, L. 2004, 'Palaeotemperature Determinations for the 1.8-ka Taupo Ignimbrite,New Zealand, and Implications for the Emplacement Historyof a high-velocity Pyroclastic flow', *Bulletin of Volcanology,* vol 66, pp.492-513.

McGrath, P.F. 2004, Volcanic Geology of the Ahuroa Ignimbrite at Wharepapa South, M. Sc. Thesis, University of Waikato.

Moon, V.G. 1993 'Geotechnical Characteristics of Ignibrite: A Soft Pyroclastic Rock Type' *Engineering Geology,* vol.35, pp.33-48.

Moyle, A.R. 1989, Volcanic Geology and Geochemistry of the Rocky Hill Ignimbrite, Upper Waipa Valley,. M. Sc. Thesis, University of Waikato.

Nelson, C.A. 1978, 'Stratigraphy and Paleontology of the Oligocene Te Kuiti Group, Waitomo Country, South Auckland, New Zealand', *New Zealand Journal of Geology and Geophysics*, vol. 21, no.5, pp. 553-594.

Orsi, G., D'Antonio, M., De Vita, Sandro. & Gallo, G. 1992, 'The Neapolitan Yellow Tuff, a large-magnitude trachytic phreatoplinian eruption: eruptive dynamics, magma withdrawl and caldera collapse', *Journal of Volcanology and Geothermal Research,* vol. 53, pp 275-287.

Pittari, A., Cas, R.A.F. & Marti, J. 2005, 'The occurrence and origin of prominent massive, pumice-rich ignimbrite lobes within the Late Pleistocene Abrigo Ignimbrite, Tenerife, Canary Islands', *Journal of Volcanology and Geothermal Research,* vol. 139, pp 271-293.

Pittari, A., Cas, R.A.F., Edgar, C.J., Nichols, H.J., Wolff, J. A. & Marti, J. 2006, 'The influence of paleotopography on facies architecture and pyroclastic flow processes of a lithic-rich ignimbrite in a high gradient setting: The Abrigo Ignimbrite, Tenerife, Canary Islands', *Journal of Volcanology and Geothermal Research,* vol. 152, pp 273-315.

Pittari, A., Cas. R.A.F., Monaghan, J.J. & Marti, J. 2007, 'Instantaneous Dynamic Pressure Effects on the Behaviour of Lithic Boulders in Pyroclastic Flows: The Abrigo Ignimbrite, Tenerife, Canary Islands', *Bulletin of Volcanology*, vol 69, pp.265-279.

Price, R.C., Gamble, J.A., Smith, I.E.M., Stewart, R.B., Eggins, S. & Wright, I.C. 2005, 'An Integrated Model for the Temporal Evolution of Andesites and Rhyolites and Crustal Development in New Zealand's North Island', *Journal of Volcanology and Geothermal Research,* vol.140, pp.1-24.

Rosi, M. 2001, 'Plinian Eruption Colums: Particle Transport and Fallout' in Freundt, A. & Rosi, M. (eds), *Developments in Volcanology 4, From Magma to Tephra, Modelling Physical Processes of Explosive Volcanic Eruptions*, Elsevier Science, Amsterdam pp. 139-172.

Rowland, J.V., Wilson, C.J.N. & Grayley, D.M. 2010, 'Spatial and Temporal Variations in Magma-assisted Rifting, Taupo Volcanic Zone, New Zealand', *Journal of Volcanology and Geothermal Research,* vol.190, pp.89–108.

Rollinson, H.R. 1993, *Using geochemical data: Evaluation, presentation, interpretation.* Longman Group, London.

Scolamacchia, T & Schouwenaars, R. 2009, 'High-speed Impacts by Ash Particles in the 1982 Eruption of El Chicho´n, Mexico', *Journal of Geophysical Research,* vol. 114, pp.1-14.

Smith, I.E.M. & Price, R.C. 2006, 'The Tonga–Kermadec Arc and Havre–Lau Back-Arc System: Their Role in the Development of Tectonic and Magmatic Models for the Western Pacific', *Journal of Volcanology and Geothermal Research,* vol.156, pp.315-331.

Sohn, Y.K., Son, M., Jeong, J.O. & Jeon, Y.M. 2009, 'Eruption and emplacement of a laterally extensive, crystal-rich, and pumice-free ignimbrite (the Cretaceous Kusandong Tuff, Korea)', *Sedimentary Geology,* vol. 220, pp 190-203.

Stern, T.A., Stratford, W.R. & Salmon, M.L. 2006, 'Subduction Evolution and Mantle Dynamics At A Continental Margin: Central North Island, New Zealand', *Reviews of Geophysics,* vol. 44, pp.1-36.

Stratford, W.R. & Stern, T.A. 2008, 'Geophysical Imaging of Buried Volcanic Structures within a Continental Back-arc Basin: The Central Volcanic Region, North Island, New Zealand', *Journal of Volcanology and Geothermal Research,* vol.174, pp.257-268.

Sulpizio, R., De Rosa, R. & Donato, P. 2008, 'The influence of variable topography on the depositional behaviour of pyroclastic density currents: The examples of the Upper Pollara eruption (Salina Island, southern Italy)', *Journal of Volcanology and Geothermal Research,* vol. 175, pp 367-385.

Sutton, A.N., Blake, S. & Wilson, C.J.N. 1995, 'An Outline Geochemistry Of Rhyolite Eruptives From Taupo Volcanic Centre, New Zealand', *Journal of Volcanology and Geothermal Research,* vol.68, pp.153-175.

Textor, C., Graf, H.F., Herzog, M., Oberhuber, J.M., Rose, W.I. & Ernst, G.G.J. 2006, 'Volcanic Particle Aggregation in Explosive Eruption Columns. Part I: Parameterization of the Microphysics of Hydrometeors and Ash', *Journal of Volcanology and Geothermal Research,* vol. 150, pp. 359-377.

Textor, C., Graf, H.F., Herzog, M., Oberhuber, J.M., Rose, W.I. & Ernst, G.G.J. 2006, 'Volcanic Particle Aggregation in Explosive Eruption Columns.Part II: Numerical Experiments', *Journal of Volcanology and Geothermal Research,* vol. 150, pp. 378-394.

Valentine, G.A. 1998, 'Damage to Structures by Pyroclastic Flows and Surges, Inferred from Nuclear Weapons Effects', *Journal of Volcanology and Geothermal Research,* vol.87, pp.117-140.

Walker, G.P.L. 1980, 'The Taupo Pumice: Product of the most powerful known (ultraplinian) eruption?' *Journal of Volcanology and Geothermal Research,* vol. 8, pp 69-94.

Walker, G.P.L., Wilson, C.J.N. & Froggatt, P.C. 1981, 'An Ignimbrite Veneer Deposit: The Trail-Marker of Apyroclastic Flow', *Journal of Volcanology and Geothermal Research* ,vol.9, pp. 409-421.

Walker, G.P.L., Self, S. & Froggatt, P.C. 1981, 'The Ground Layer of the Taupo Ignmibrite: A Striking Example of Sedimentation from a Pyroclastic Flow', *Journal of Volcanology and Geothermal Research,* vol.10, pp. 1-11 1.

Walker, G.P.L.1983, 'Ignimbrite types and ignimbrite problems', *Journal of Volcanology and Geothermal Research,* vol. 17, pp 65-88.

Walker, G.P.L. & Wilson, C.J.N. 1983, 'Lateral Variations in the Taupo Ignimbrite', *Journal of Volcanology and Geothermal Research,* vol. 18, pp. 117-133.

Wilson, C.J.N. & Walker, G.P.L. 1982, 'Ignimbrite depositional facies: the anatomy of a pyroclastic flow' *Journal of Geological Society, London,*vol. 139, pp 581-592

Wilson, C.J.N. 1986a, 'Reconnaissance Stratigraphy and Volcanology of Ignimbrites from Mangakino Volcano', in Smith, I.E.M. (ed), *Late Cenozoic Volcanism in New Zealand*. Royal Society of New Zealand Bulletin, vol.23, pp.179-193.

Wilson, C.J.N. 1986b, 'King Country Ignimbrites' in Houghton, B.F. & Weaver, S.D. (eds), *Taupo Volcanic Zone Tour Guides C1, C4, C5 & A2. New Zealand Gelogical Survey Rec.,* vol. 11, pp.115-144.

Wilson, C.J.N., Houghton, B.F., McWilliams, M.O., Lanphere, M.A., Weaver, S.D. & Briggs, R.M. 1995, 'Volcanic and Structural Evolution of Taupo Volcanic Zone, New Zealand: A Review', *Journal of Volcanology and Geothermal Research,* vol.68, pp.1-28.

Wilson, C.J.N. 2008, 'Supereruptions and Supervolcanoes: Processes and Products' *Elements,* vol.4, pp. 29-34.

Zimanowski, B. 2001, 'Phreatomagmatic Explosions' in Freundt, A. & Rosi, M. (eds), *Developments in Volcanology 4, From Magma to Tephra, Modelling Physical Processes of Explosive Volcanic Eruptions*, Elsevier Science, Amsterdam, pp. 25-53.

Appendix One
Field work data

Sample Catalogue: Samples collected from the Ongatiti Valley, (Note UoW no. represents the University of Waikato rock store numbers):

Sample no.	UoW no. (petlab numbers)	Sample description	GPS locality (x, y)	Location/ stratigraphic position
N.44	2011 0900	Ngaroma Ignimbrite	2714616.7, 6312036	poorly exposed outcrop
N.47	2011 0901	Ngaroma Ignimbrite	2714616.7, 6312036	poorly exposed outcrop
O.3	2011 0902	Ongatiti Ignimbrite (TU)	2712891.2, 6309470.8	mid section of transitional unit
O.4	2011 0903	Ongatiti Ignimbrite (LU)	2713455, 63091104	base of the lower unit
O.12	2011 0904	Ongatiti Ignimbrite (LU)	2713455, 63091104	base of the lower unit
O.16	2011 0905	Ongatiti Ignimbrite (LU)	2712188, 630900	base of the lower unit
O.17	2011 0906	Ongatiti Ignimbrite (LU)	2712145.8, 6309755	base of the lower unit
O.25	2011 0907	Ongatiti Ignimbrite (UU)	2712894.4, 6310510	top section of upper unit
O.27	2011 0908	Ongatiti Ignimbrite (UU)	2713226, 6310258	mid section of the upper unit
O.28	2011 0909	Ongatiti Ignimbrite (UU)	2713589.6, 6309993	base of the lower unit
O.29	2011 0910	Ongatiti Ignimbrite (UU)	2713725, 6310391.5	top section of upper unit
O.30	2011 0911	Ongatiti Ignimbrite (UU)	2713725, 6310391.5	top section of upper unit
O.31	2011 0912	Ongatiti Ignimbrite (UU)	2713730.1, 6310418.5	mid section of the upper unit
O.33	2011 0913	Ongatiti Ignimbrite (UU)	2713331.3, 6310509	mid section of the upper unit
O.45	2011 0914	Ongatiti Ignimbrite (LU)	2714476, 6312254.1	base of the lower unit
SL1.1	2011 0915	Ongatiti Ignimbrite (LU)	2712316.8, 6309818.4	Strat log 1 - 60cm
SL1.2	2011 0916	Ongatiti Ignimbrite (LU)	2712316.8, 6309818.4	Strat log 1 - 60cm
SL1.3	2011 0917	Ongatiti Ignimbrite (LU)	2712316.8, 6309818.4	Strat log 1 - 2m
SL1.4	2011 0918	Ongatiti Ignimbrite (LU)	2712316.8, 6309818.4	Strat log 1 - 2m (lithic clast)
SL1.5	2011 0919	Ongatiti Ignimbrite (LU)	2712316.8, 6309818.4	Strat log 1 - 3.4
SL1.6	2011 0920	Ongatiti Ignimbrite (LU)	2712316.8, 6309818.4	Strat log 1 - 6.5m
SL1.7	2011 0921	Ongatiti Ignimbrite (LU)	2712316.8, 6309818.4	Strat log 1 - 7.8m
SL1.8	2011 0922	Ongatiti Ignimbrite (LU)	2712316.8, 6309818.4	Strat log 1 - 9m

Sample no.	UoW no. (petlab numbers)	Sample description	GPS locality (x, y)	Location/ stratigraphic position
SL2.1	2011 0923	Unknown fall deposit	2712920.3, 6310396.5	fall deposit below Ongatiti (10 cm from base)
SL2.2	2011 0924	Ongatiti Ignimbrite (TU)	2712920.3, 6310396.5	Strat log 2- 1.4 m
SL2.3	2011 0925	Ongatiti Ignimbrite (TU)	2712920.3, 6310396.5	Strat log 2- 4 m
SL2.4	2011 0926	Ongatiti Ignimbrite (TU)	2712920.3, 6310396.5	Strat log 2- 5.2m
SL2.5	2011 0927	Ongatiti Ignimbrite (TU)	2712920.3, 6310396.5	Strat log 2- 6.5m
SL2.6	2011 0928	Ongatiti Ignimbrite (TU)	2712920.3, 6310396.5	Strat log 2 -8.2 m
SL2.7	2011 0929	Ongatiti Ignimbrite (TU)	2712920.3, 6310396.5	Strat log 2- 10 m
SL2.8	2011 0930	Ongatiti Ignimbrite (TU)	2712920.3, 6310396.5	Strat log 2- 13.2
SL2.9	2011 0931	Ongatiti Ignimbrite (TU)	2712920.3, 6310396.5	Strat log 2- 14.7
SL3.1	2011 0934	Ongatiti Ignimbrite (TU)	2711644, 6309880	strat log 3 - 20cm
SL3.2	2011 0935	Ongatiti Ignimbrite (TU)	2711644, 6309880	strat log 3 - 2m
SL3.3	2011 0936	Ongatiti Ignimbrite (TU)	2711644, 6309880	strat log 3 - 5.2m
SL3.4	2011 0937	Ongatiti Ignimbrite (TU)	2711644, 6309880	strat log 3 - 5.2m (pumice clast)
SL3.5	2011 0938	Ongatiti Ignimbrite (TU)	2711644, 6309880	strat log 3 - 7m
SL3.6	2011 0939	Ongatiti Ignimbrite (TU)	2711644, 6309880	strat log 3 - 10m
SL3.7	2011 0940	Ongatiti Ignimbrite (TU)	2711644, 6309880	strat log 3 - 11.5m
SL3.8	2011 0941	Ongatiti Ignimbrite (TU)	2711644, 6309880	strat log 3 - 15m
SL3.9	2011 0942	Ongatiti Ignimbrite (TU)	2711644, 6309880	strat log 3 - 16.5m
SL3.10	2011 0943	Ongatiti Ignimbrite (TU)	2711644, 6309880	strat log 3 - 16.5m
SL3.11	2011 0944	Ongatiti Ignimbrite (TU)	2711644, 6309880	strat log 3 - 17.8m
SL5.1	2011 0945	Ongatiti Ignimbrite (UU)	2711643, 6309950	strat log 5 - 10cm
SL5.2	2011 0946	Ongatiti Ignimbrite (UU)	2711643, 6309950	strat log 5 - 2.5m
SL5.3	2011 0947	Ongatiti Ignimbrite (UU)	2711643, 6309950	strat log 5 - 2.5m (pumice clast)

Sample no.	UoW no. (petlab numbers)	Sample description	GPS locality (x, y)	Location/ stratigraphic position
SL5.4	2011 0948	Ongatiti Ignimbrite (UU)	2711643, 6309950	strat log 5 - 7.8m
SL5.5	2011 0949	Ongatiti Ignimbrite (UU)	2711643, 6309950	strat log 5 - 16m
SL5.6	2011 0950	Ongatiti Ignimbrite (UU)	2711643, 6309950	strat log 5 - 16m (pumice clast)
SL5.7	2011 0951	Ongatiti Ignimbrite (UU)	2711643, 6309950	strat log 5 - 20 m
SL5L.1	2011 0952	Ongatiti Ignimbrite (UU)	2711643, 6309950	lithic clast from Strat log 5
SL5L.2	2011 0953	Ongatiti Ignimbrite (UU)	2711643, 6309950	lithic clast from Strat log 5
SL5L.3	2011 0954	Ongatiti Ignimbrite (UU)	2711643, 6309950	lithic clast from Strat log 5
SL5L.4	2011 0955	Ongatiti Ignimbrite (UU)	2711643, 6309950	lithic clast from Strat log 5
SL5L.5	2011 0956	Ongatiti Ignimbrite (UU)	2711643, 6309950	lithic clast from Strat log 5
SL5L.6	2011 0957	Ongatiti Ignimbrite (UU)	2711643, 6309950	lithic clast from Strat log 5
SL6.1	2011 0958	Ongatiti Ignimbrite (LU)	2710720, 6310470	Strat log 6 - 15cm
SL6.2	2011 0959	Ongatiti Ignimbrite (LU)	2710720, 6310470	Strat log 6 -6.3m
SL6.3	2011 0960	Ongatiti Ignimbrite (LU)	2710720, 6310470	Strat log 6 - 12.5m
SL6.4	2011 0961	Ongatiti Ignimbrite (LU)	2710720, 6310470	Strat log 6 - 19m
SL7.1	2011 0962	Ongatiti Ignimbrite (UU)	2712374, 6311521.6	Strat log 7 - 10cm
SL7.2	2011 0963	Ongatiti Ignimbrite (UU)	2712374, 6311521.6	Strat log 7 - 1.2m
SL7.3	2011 0964	Ongatiti Ignimbrite (UU)	2712374, 6311521.6	Strat log 7 - 1.2 m (pumice clast)
SL7.4	2011 0965	Ongatiti Ignimbrite (UU)	2712374, 6311521.6	Strat log 7 - 3m
SL7.5	2011 0966	Ongatiti Ignimbrite (UU)	2712374, 6311521.6	Strat log 7 - 3m
SL7.6	2011 0967	Ongatiti Ignimbrite (UU)	2712374, 6311521.6	Strat log 7 - 6m
SL7.7	2011 0968	Ongatiti Ignimbrite (UU)	2712374, 6311521.6	Strat log 7 - 11.3m
SL7.8	2011 0969	Ongatiti Ignimbrite (UU)	2712374, 6311521.6	Strat log 7 - 11.3m (lithic clast)
SL7.9	2011 0970	Ongatiti Ignimbrite (UU)	2712374, 6311521.6	Strat log 7 - 14.8m

Sample no.	UoW no. (petlab numbers)	Sample description	GPS locality (x, y)	Location/ stratigraphic position
SL7.10	2011 0971	Ongatiti Ignimbrite (UU)	2712374, 6311521.6	Strat log 7 - 14.8m
SL8.1	2011 0972	Ongatiti Ignimbrite (LU)	2712633, 6310104	Strat log 8 - 40cm
SL8.2	2011 0973	Ongatiti Ignimbrite (LU)	2712633, 6310104	Strat log 8 - 2.3m
SL8.3	2011 0974	Ongatiti Ignimbrite (LU)	2712633, 6310104	Strat log 8 - 4.7m
SL8.4	2011 0975	Ongatiti Ignimbrite (LU)	2712633, 6310104	Strat log 8 - 7m
SL8.5	2011 0976	Ongatiti Ignimbrite (LU)	2712633, 6310104	Strat log 8 - 8.6m
SL8.6	2011 0977	Ongatiti Ignimbrite (LU)	2712633, 6310104	Strat log 8 - 10.6m
SL8.7	2011 0978	Ongatiti Ignimbrite (LU)	2712633, 6310104	Strat log 8 - 12.2m
SL8.8	2011 0979	Ongatiti Ignimbrite (LU)	2712633, 6310104	Strat log 8 - 14.4m
OL.1	2011 0980	Ongatiti Ignimbrite (LU)	2712633, 6310104	lithic clast from Strat log 8
OL.2	2011 0981	Ongatiti Ignimbrite (LU)	2712633, 6310104	lithic clast from Strat log 8
OL.3	2011 0982	Ongatiti Ignimbrite (LU)	2712633, 6310104	lithic clast from Strat log 8
OL.4	2011 0983	Ongatiti Ignimbrite (LU)	2712633, 6310104	lithic clast from Strat log 8
SL9.1	2011 0984	Unit D	2713743, 6311762	Strat log 9 - 25cm
SL9.2	2011 0985	Unit D	2713743, 6311762	Strat log 9 - 65cm
SL9.3	2011 0986	Unit D	2713743, 6311762	Strat log 9 - 1m
SL9.4	2011 0987	Unit D	2713743, 6311762	Strat log 9 - 1.3m
SL9.5	2011 0988	Unit D	2713743, 6311762	Strat log 9 - 1.4m
SL9.6	2011 0989	Unit D	2713743, 6311762	Strat log 9 - 1.8m
SL9.7	2011 0990	Unit D	2713743, 6311762	Strat log 9 - 2.1m (contact)
SL9.8	2011 0991	Unit D	2713743, 6311762	Strat log 9 - 2.25m
A.7	2011 0992	Ahuroa Ignimbrite	2714121, 6310412	upper section
A.9	2011 0993	Ahuroa Ignimbrite	2714121, 6310412	mid-upper section
A.22	2011 0994	Ahuroa Ignimbrite	2711523, 6310312	upper section
SL10.1	2011 0995	Ahuroa Ignimbrite	2713314, 6311944	Strat log 10 - 40cm

Sample no.	UoW no. (petlab numbers)	Sample description	GPS locality (x, y)	Location/ stratigraphic position
SL10.2	2011 0996	Ahuroa Ignimbrite	2713314, 6311944	Strat log 10 - 1.2m
SL10.3	2011 0997	Ahuroa Ignimbrite	2713314, 6311944	Strat log 10 - 2m
SL10.4	2011 0998	Ahuroa Ignimbrite	2713314, 6311944	Strat log 10 - 2m
SL10.5	2011 0999	Ahuroa Ignimbrite	2713314, 6311944	Strat log 10 - 3m
SL10.6	2011 1000	Ahuroa Ignimbrite	2713314, 6311944	Strat log 10 - 4.4m
SL10.7	2011 1001	Ahuroa Ignimbrite	2713314, 6311944	Strat log 10 - 6m
SL10.8	2011 1002	Ahuroa Ignimbrite	2713314, 6311944	Strat log 10 - 7.3m
SL10.9	2011 1003	Ahuroa Ignimbrite	2713314, 6311944	Strat log 10 - 7.3m
SL10.10	2011 1004	Ahuroa Ignimbrite	2713314, 6311944	Strat log 10 - 8m
SL10.11	2011 1005	Ahuroa Ignimbrite	2713314, 6311944	Strat log 10 - 9.2m
SL10L.1	2011 1044	Ahuroa Ignimbrite	2713314, 6311944	lithic clast from Strat log 10
SL10L.2	2011 1045	Ahuroa Ignimbrite	2713314, 6311944	lithic clast from Strat log 10
SL10L.3	2011 1046	Ahuroa Ignimbrite	2713314, 6311944	lithic clast from Strat log 10
RH.1	2011 1006	Rocky Hill Ignimbrite	2711894, 6310988	Mid section from 'Rocky Hill' type locality
RH.8	2011 1007	Rocky Hill Ignimbrite	2713754, 6310593	upper section
RH.26	2011 1008	Rocky Hill Ignimbrite	2711894, 6310988	pumice clast from mid section
RH.36	2011 1009	Rocky Hill Ignimbrite	2714832.6, 6309512.5	mid-upper section
RH.38	2011 1010	Rocky Hill Ignimbrite	2713634.4, 6310713.5	upper section
RH.41	2011 1011	Rocky Hill Ignimbrite	2714857.5, 6309414.5	upper section
RH.55	2011 1012	Rocky Hill Ignimbrite	2713813.2, 6308876.9	lower-mid section
SL4.1	2011 1013	Rocky Hill Ignimbrite	2714059, 6308090.8	Strat log 4 - 15cm
SL4.2	2011 1014	Rocky Hill Ignimbrite	2714059, 6308090.8	Strat log 4 - 1.2m
SL4.3	2011 1015	Rocky Hill Ignimbrite	2714059, 6308090.8	Strat log 4 - 1.2m (pumice clast)
SL4.4	2011 1016	Rocky Hill Ignimbrite	2714059, 6308090.8	Strat log 4 - 3.4m
SL4.5	2011 1017	Rocky Hill Ignimbrite	2714059, 6308090.8	Strat log 4 - 5m

Sample no.	UoW (petlab)no.	Sample description	Thin section	Point counted	Crushed sample	XRF	EPMA	ICPMS
SL4.6	2011 1018	Rocky Hill Ignimbrite	X	X				
SL4.7	2011 1019	Rocky Hill Ignimbrite	X	X				
SL4.8	2011 1020	Rocky Hill Ignimbrite	X	X				
SL4.9	2011 1021	Rocky Hill Ignimbrite	X	X				
SL4.10	2011 1022	Rocky Hill Ignimbrite	X	X				
SL4.11	2011 1023	Rocky Hill Ignimbrite	X	X				
SL4.12	2011 1024	Rocky Hill Ignimbrite	X	X				
SL4.13	2011 1025	Rocky Hill Ignimbrite	X	X				
SL4.14	2011 1026	Rocky Hill Ignimbrite	X	X				
SL4.15	2011 1027	Rocky Hill Ignimbrite	X	X				
RHL.1	2011 1028	Rocky Hill Ignimbrite	X					
RHL.2	2011 1029	Rocky Hill Ignimbrite	X					
RHL.3	2011 1030	Rocky Hill Ignimbrite	X					
RHL.4	2011 1031	Rocky Hill Ignimbrite	X					
RHL.5	2011 1032	Rocky Hill Ignimbrite	X					
RHL.6	2011 1033	Rocky Hill Ignimbrite	X					
RHL.7	2011 1034	Rocky Hill Ignimbrite	X					
SL11.1	2011 1035	Taupo Ignimbrite	X	X				
SL11.2	2011 1036	Taupo Ignimbrite	X	X				
SL11.3	2011 1037	Taupo Ignimbrite	X	X				
SL11.4	2011 1038	Taupo Ignimbrite	X	X				
SL11.5	2011 1039	Taupo Ignimbrite	X	X				
SL11.6	2011 1040	Taupo Ignimbrite	X	X				
SL11.7	2011 1041	Taupo Ignimbrite	X	X				
SL11.8	2011 1042	Taupo Ignimbrite	X	X				
SL11.9	2011 1043	Taupo Ignimbrite	X	X				

Sample Catalogue: Listings of analytical procedures performed on each sample and the nature of the samples stored:

Sample no.	UoW (petlab)no.	Sample description	Thin section	Point counted	Crushed sample	XRF	EPMA	ICPMS
N.44	2011 0900	Ngaroma Ignimbrite	X	X				
N.47	2011 0901	Ngaroma Ignimbrite	X	X				
O.3	2011 0902	Ongatiti Ignimbrite (LU)	X					
O.4	2011 0903	Ongatiti Ignimbrite (LU)	X (2 thin sections)		X	X	X	X
O.12	2011 0904	Ongatiti Ignimbrite (LU)	X					
O.16	2011 0905	Ongatiti Ignimbrite (LU)						
O.17	2011 0906	Ongatiti Ignimbrite (LU)						
O.25	2011 0907	Ongatiti Ignimbrite (UU)	X					
O.27	2011 0908	Ongatiti Ignimbrite (UU)						
O.28	2011 0909	Ongatiti Ignimbrite (UU)	X		X	X	X	
O.29	2011 0910	Ongatiti Ignimbrite (UU)	X				X	
O.30	2011 0911	Ongatiti Ignimbrite (UU)	X	X	X	X		
O.31	2011 0912	Ongatiti Ignimbrite (UU)	X					
O.33	2011 0913	Ongatiti Ignimbrite (UU)	X					
O.45	2011 0914	Ongatiti Ignimbrite (LU)	X					
SL1.1	2011 0915	Ongatiti Ignimbrite (LU)	X					
SL1.2	2011 0916	Ongatiti Ignimbrite (LU)	X					
SL1.3	2011 0917	Ongatiti Ignimbrite (LU)	X					
SL1.4	2011 0918	Ongatiti Ignimbrite (LU)	X					
SL1.5	2011 0919	Ongatiti Ignimbrite (LU)	X					
SL1.6	2011 0920	Ongatiti Ignimbrite (LU)	X					
SL1.7	2011 0921	Ongatiti Ignimbrite (LU)	X					
SL1.8	2011 0922	Ongatiti Ignimbrite (LU)	X					

Sample no.	UoW (petlab)no.	Sample description	Thin section	Point counted	Crushed sample	XRF	EPMA	ICPMS
SL2.1	2011 0923	Ongatiti Ignimbrite (TU)	X					
SL2.2	2011 0924	Ongatiti Ignimbrite (TU)	X					
SL2.3	2011 0925	Ongatiti Ignimbrite (TU)	X					
SL2.4	2011 0926	Ongatiti Ignimbrite (TU)	X					
SL2.5	2011 0927	Ongatiti Ignimbrite (TU)	X					
SL2.6	2011 0928	Ongatiti Ignimbrite (TU)	X					
SL2.7	2011 0929	Ongatiti Ignimbrite (TU)	X					
SL2.8	2011 0930	Ongatiti Ignimbrite (TU)	X					
SL2.9	2011 0931	Ongatiti Ignimbrite (TU)	X					
SL3.1	2011 0934	Ongatiti Ignimbrite (TU)	X	X				
SL3.2	2011 0935	Ongatiti Ignimbrite (TU)	X	X				
SL3.3	2011 0936	Ongatiti Ignimbrite (TU)	X	X				
SL3.4	2011 0937	Ongatiti Ignimbrite (TU)	X	X				
SL3.5	2011 0938	Ongatiti Ignimbrite (TU)	X	X				
SL3.6	2011 0939	Ongatiti Ignimbrite (TU)	X	X				
SL3.7	2011 0940	Ongatiti Ignimbrite (TU)	X	X				
SL3.8	2011 0941	Ongatiti Ignimbrite (TU)	X	X				
SL3.9	2011 0942	Ongatiti Ignimbrite (TU)	X	X				
SL3.10	2011 0943	Ongatiti Ignimbrite (TU)	X	X				
SL3.11	2011 0944	Ongatiti Ignimbrite (TU)	X	X				
SL5.1	2011 0945	Ongatiti Ignimbrite (UU)	X	X	X	X	X	

Sample no.	UoW (petlab)no.	Sample description	Thin section	Point counted	Crushed sample	XRF	EPMA	ICPMS
SL5.2	2011 0946	Ongatiti Ignimbrite (UU)	X	X			X	
SL5.3	2011 0947	Ongatiti Ignimbrite (UU)	X	X	X	X		
SL5.4	2011 0948	Ongatiti Ignimbrite (UU)	X	X	X	X		
SL5.5	2011 0949	Ongatiti Ignimbrite (UU)	X		X	X		
SL5.6	2011 0950	Ongatiti Ignimbrite (UU)	X		X	X		
SL5.7	2011 0951	Ongatiti Ignimbrite (UU)	X					
SL5L.1	2011 0952	Ongatiti Ignimbrite (UU)					X	
SL5L.2	2011 0953	Ongatiti Ignimbrite (UU)						
SL5L.3	2011 0954	Ongatiti Ignimbrite (UU)						
SL5L.4	2011 0955	Ongatiti Ignimbrite (UU)						
SL5L.5	2011 0956	Ongatiti Ignimbrite (UU)						
SL5L.6	2011 0957	Ongatiti Ignimbrite (UU)						
SL6.1	2011 0958	Ongatiti Ignimbrite (LU)	X	X	X	X		
SL6.2	2011 0959	Ongatiti Ignimbrite (LU)	X	X	X	X		
SL6.3	2011 0960	Ongatiti Ignimbrite (LU)	X	X	X	X		
SL6.4	2011 0961	Ongatiti Ignimbrite (LU)	X	X	X	X		
SL7.1	2011 0962	Ongatiti Ignimbrite (UU)	X	X	X	X		
SL7.2	2011 0963	Ongatiti Ignimbrite (UU)	X	X	X	X		
SL7.3	2011 0964	Ongatiti Ignimbrite (UU)	X	X	X	X		
SL7.4	2011 0965	Ongatiti Ignimbrite (UU)	X	X	X	X		
SL7.5	2011 0966	Ongatiti Ignimbrite (UU)	X	X				
SL7.6	2011 0967	Ongatiti Ignimbrite (UU)	X	X	X	X		
SL7.7	2011 0968	Ongatiti Ignimbrite (UU)	X	X	X	X		
SL7.8	2011 0969	Ongatiti Ignimbrite (UU)	X					
SL7.9	2011 0970	Ongatiti Ignimbrite (UU)	X	X				

Sample no.	UoW (petlab)no.	Sample description	Thin section	Point counted	Crushed sample	XRF	EPMA	ICPMS
SL7.10	2011 0971	Ongatiti Ignimbrite (UU)	X	X	X	X		
SL8.1	2011 0972	Ongatiti Ignimbrite (LU)	X	X	X	X	X	X
SL8.2	2011 0973	Ongatiti Ignimbrite (LU)	X	X	X	X		X
SL8.3	2011 0974	Ongatiti Ignimbrite (LU)	X	X				
SL8.4	2011 0975	Ongatiti Ignimbrite (LU)	X	X	X	X		X
SL8.5	2011 0976	Ongatiti Ignimbrite (LU)	X	X	X	X		
SL8.6	2011 0977	Ongatiti Ignimbrite (LU)	X	X	X	X		X
SL8.7	2011 0978	Ongatiti Ignimbrite (LU)	X	X	X	X		
SL8.8	2011 0979	Ongatiti Ignimbrite (LU)	X	X	X	X		X
OL.1	2011 0980	Ongatiti Ignimbrite (LU)	X					
OL.2	2011 0981	Ongatiti Ignimbrite (LU)	X					
OL.3	2011 0982	Ongatiti Ignimbrite (LU)	X					
OL.4	2011 0983	Ongatiti Ignimbrite (LU)	X					
SL9.1	2011 0984	Unit D	X	X	X	X	X	X
SL9.2	2011 0985	Unit D	X	X	X	X		
SL9.3	2011 0986	Unit D	X	X	X	X		
SL9.4	2011 0987	Unit D	X	X	X	X	X	X
SL9.5	2011 0988	Unit D	X	X	X	X		
SL9.6	2011 0989	Unit D	X	X	X	X		
SL9.7	2011 0990	Unit D	X	X			X	
SL9.8	2011 0991	Unit D	X	X	X	X	X	X
A.7	2011 0992	Ahuroa Ignimbrite	X					
A.9	2011 0993	Ahuroa Ignimbrite	X					

Sample no.	UoW (petlab)no.	Sample description	Thin section	Point counted	Crushed sample	XRF	EPMA	ICPMS
A.22	2011 0994	Ahuroa Ignimbrite	X					
SL10.1	2011 0995	Ahuroa Ignimbrite	X	X				
SL10.2	2011 0996	Ahuroa Ignimbrite	X	X				
SL10.3	2011 0997	Ahuroa Ignimbrite	X	X				
SL10.4	2011 0998	Ahuroa Ignimbrite	X	X				
SL10.5	2011 0999	Ahuroa Ignimbrite	X	X				
SL10.6	2011 1000	Ahuroa Ignimbrite	X	X				
SL10.7	2011 1001	Ahuroa Ignimbrite	X	X				
SL10.8	2011 1002	Ahuroa Ignimbrite	X	X				
SL10.9	2011 1003	Ahuroa Ignimbrite	X	X				
SL10.10	2011 1004	Ahuroa Ignimbrite	X	X				
SL10.11	2011 1004	Ahuroa Ignimbrite	X	X				
SL10L.1	2011 1044	Ahuroa Ignimbrite	X					
SL10L.2	2011 1045	Ahuroa Ignimbrite	X					
SL10L.3	2011 1046	Ahuroa Ignimbrite	X					
RH.1	2011 1006	Rocky Hill Ignimbrite	X (2 thin sections)					
RH.8	2011 1007	Rocky Hill Ignimbrite	X (2 thin sections)					
RH.26	2011 1008	Rocky Hill Ignimbrite	X					
RH.36	2011 1009	Rocky Hill Ignimbrite	X (2 thin sections)					
RH.38	2011 1010	Rocky Hill Ignimbrite						
RH.41	2011 1011	Rocky Hill Ignimbrite	X (2 thin sections)					
RH.55	2011 1012	Rocky Hill Ignimbrite	X					
SL4.1	2011 1013	Rocky Hill Ignimbrite	X	X				
SL4.2	2011 1014	Rocky Hill Ignimbrite	X	X				
SL4.3	2011 1015	Rocky Hill Ignimbrite	X	X				
SL4.4	2011 1016	Rocky Hill Ignimbrite	X	X				
SL4.5	2011 1017	Rocky Hill Ignimbrite	X	X				

Sample no.	UoW (petlab)no.	Sample description	Thin section	Point counted	Crushed sample	XRF	EPMA	ICPMS
SL4.6	2011 1018	Rocky Hill Ignimbrite	X	X				
SL4.7	2011 1019	Rocky Hill Ignimbrite	X	X				
SL4.8	2011 1020	Rocky Hill Ignimbrite	X	X				
SL4.9	2011 1021	Rocky Hill Ignimbrite	X	X				
SL4.10	2011 1022	Rocky Hill Ignimbrite	X	X				
SL4.11	2011 1023	Rocky Hill Ignimbrite	X	X				
SL4.12	2011 1024	Rocky Hill Ignimbrite	X	X				
SL4.13	2011 1025	Rocky Hill Ignimbrite	X	X				
SL4.14	2011 1026	Rocky Hill Ignimbrite	X	X				
SL4.15	2011 1027	Rocky Hill Ignimbrite	X	X				
RHL.1	2011 1028	Rocky Hill Ignimbrite	X					
RHL.2	2011 1029	Rocky Hill Ignimbrite	X					
RHL.3	2011 1030	Rocky Hill Ignimbrite	X					
RHL.4	2011 1031	Rocky Hill Ignimbrite	X					
RHL.5	2011 1032	Rocky Hill Ignimbrite	X					
RHL.6	2011 1033	Rocky Hill Ignimbrite	X					
RHL.7	2011 1034	Rocky Hill Ignimbrite	X					
SL11.1	2011 1035	Taupo Ignimbrite	X	X				
SL11.2	2011 1036	Taupo Ignimbrite	X	X				
SL11.3	2011 1037	Taupo Ignimbrite	X	X				
SL11.4	2011 1038	Taupo Ignimbrite	X	X				
SL11.5	2011 1039	Taupo Ignimbrite	X	X				
SL11.6	2011 1040	Taupo Ignimbrite	X	X				
SL11.7	2011 1041	Taupo Ignimbrite	X	X				
SL11.8	2011 1042	Taupo Ignimbrite	X	X				
SL11.9	2011 1043	Taupo Ignimbrite	X	X				

Stratigraphic Logs: Component and clast measurements from every 1-3 m intervals:

Stratigraphic Log 1: Lower Unit, Ongatiti Ignimbrite						
Height of column (m)	**Pumice abundance (%)**	**Lithic abundance (%)**	**Crystal abundance (%)**	**Max P (mm)**	**Aspect ratio**	**Max L(mm)**
0.6	10	1	55	13.6	3.7	8.5
2	11	1	51	36.4	4.07	13.4
3.4	11	1	54	51.8	1.9	20.8
5	7	1	–	43.9	1.7	16.5
6.5	5	1	63	18.5	1.8	12.6
7.8	5	2	50	13.6	1.4	12
9	7	1	45	17.2	1.36	15.3

Stratigraphic Log 2: Transitional unit, Ongatiti Ignimbrite						
Height of column (m)	**Pumice abundance (%)**	**Lithic abundance (%)**	**Crystal abundance (%)**	**Max P (mm)**	**Aspect ratio**	**Max L(mm)**
1.4	6	1	49	22.4	3.58	18.4
3	7	1	–	10.6	2.63	15
4	9	1	48	48.4	3.56	28.8
5.2	11	1	47	96.4	2.3	19.2
6.5	16	1	48	109	2.42	27.8
8.2	18	1	40	88.8	2.2	32.6
10	16	1	40	106.8	2.1	33.2
11.6	17	1	–	65.6	1.58	16.8
13.2	17	1	38	69.2	1.6	19.4
14.7	19	1	36	60	1.8	47.6

Stratigraphic Log 5: Upper Unit, Ongatiti Ignimbrite						
Height of column (m)	**Pumice abundance (%)**	**Lithic abundance (%)**	**Crystal abundance (%)**	**Max P (mm)**	**Aspect ratio**	**Max L (mm)**
0.1	19	1	50	95.6	2.08	9
2.5	21	1	49	128.4	2.7	7.4
4.2	22	1	–	145.9	2.3	19.9
6	24	1	–	162		21
7.8	25	1	47	213	1.3	28.6
11.4	25	2	–	271	1.9	31.4
14	25	2	–	255		44
16	26	2	31	249	1.7	50.8
17.5	23	2	–	221	1.36	54.7
20	21	2	34	233.6	1.15	35.4

Stratigraphic Log 3: Transitional unit, Ongatiti Ignimbrite						
Height of column (m)	**Pumice abundance (%)**	**Lithic abundance (%)**	**Crystal abundance (%)**	**Max P (mm)**	**Aspect ratio**	**Max L (mm)**
0.2	15	2	50	22	2.58	19.2
2	17	1	54	71.3	1.9	24.8
3.5	15	1	–	74.2	2.3	21
5.2	18	3	58	100.8	1.98	27.6
7	22	3	63	127.8	1.82	36.6
8.6	20	2	–	129.6	1.6	25
10	19	1	55	69.2	1.68	31.2
11.5	20	1	46	126.2	1.88	21.2
13.3	18	1	–	98.2	1.54	24.4
15	20	1	51	88.2	1.45	18.4
16.5	17	2	51	79.8	1.86	33.4
17.8	14	1	55	110.4	2.44	32.2
19	12	1	–	97.4	1.89	26.4

Stratigraphic Log 6: Lower Unit, Ongatiti Ignimbrite						
Height of column (m)	**Pumice abundance (%)**	**Lithic abundance (%)**	**Crystal abundance (%)**	**Max P (mm)**	**Aspect ratio**	**Max L(mm)**
0.15	8	1	47	14.2	6.22	17.8
4.5	10	1	–	15.4	2.01	7
6.3	10	1	51	22	2	8.8
9	11	1	–	34	1.8	9.3
12.5	13	1	50	68.4	2.1	14.6
15.7	13	1	–	65.7	1.8	11.3
19	14	1	54	74.4	1.3	17.8

Stratigraphic Log 7: Upper Unit, Ongatiti Ignimbrite						
Height of column (m)	**Pumice abundance (%)**	**Lithic abundance (%)**	**Crystal abundance (%)**	**Max P (mm)**	**Aspect ratio**	**Max L (mm)**
0.1	18	1	31	99	1.5	50.6
1.2	30	1	38	72.6	1.3	29.2
3	30	3	32	117	1.6	23.6
4.5	29	3	–	105.4	1.7	22
6	25	1	40	92	1.7	23.6
8	23	1	–	151	1.7	24.6
9.7	24	1	–	107.8	1.62	19.2
11.3	20	1	30	83.6	1.3	8
13	19	1	–	93.2	1.5	13.8
14.8	18	1	36	86.2	1.3	8.8

Stratigraphic Log 8: Lower Unit, Ongatiti Ignimbrite						
Height of column (m)	**Pumice abundance (%)**	**Lithic abundance (%)**	**Crystal abundance (%)**	**Max P(mm)**	**Aspect ratio**	**Max L (mm)**
0.4	8	1	47	70.2	7.8	25
2.3	6	1	54	33	4.1	15
4.7	8	1	53	76.2	4.7	19
5.5	10	1	–	71.8	5.1	15.8
7	8	1	52	115.6	5	21
8.6	12	1	57	113.4	4.46	15.2
10.6	13	1	58	78	2.1	21.4
12.2	16	2	55	119	2.2	36.5
14.4	16	1	54	107.4	2.9	41.6

Stratigraphic Log 4: Rocky Hill Ignimbrite						
Height of column (m)	**Pumice abundance (%)**	**Lithic abundance (%)**	**Crystal abundance (%)**	**Max P (mm)**	**Aspect ratio**	**Max L (mm)**
0.15	8	1	21	35.6	1.4	3.8
1.2	12	1	25	19	1.3	4.6
3.4	10	1	34	61.2	1.9	14.4
5	15	1	40	46.7	1.18	5.2
7	14	2	34	65.4	1.3	10.4
8.2	15	2	–	70.6	1.3	12.2
16.5	20	2	38	59	1.7	12
18	23	2	47	59.8	2.4	23
19.4	28	1	38	42.2	2.36	15.6
21	22	2	48	28.4	5.03	11.8
22.8	20	3	39	107	3.6	34.6

Stratigraphic Log 9: Unit D						
Height of column (m)	**Pumice abundance (%)**	**Lithic abundance (%)**	**Crystal abundance (%)**	**Max P (mm)**	**Aspect ratio**	**Max L (mm)**
0.25	0	0	24	0	0	0
0.65	0	0.5	33	0	0	1.5
1	0	1	16	0	0	1
1.3	0	0	18	0	0	0
1.4	4	2	17	4.1	1.2	4.3
1.8	1	1	21	1	1.1	1
2.1	3	18	46	14	1.3	31
2.25	8	2	28	49.4	2.2	7.4
2.8	9	2	–	96.4	2.8	12.4

Stratigraphic Log 10: Ahuroa Ignimbrite						
Height of column (m)	**Pumice abundance (%)**	**Lithic abundance (%)**	**Crystal abundance (%)**	**Max P (mm)**	**Aspect ratio**	**Max L(mm)**
0.4	12	1	14	38.8	2.1	2
1.2	17	1	16	69.3	4.25	10.2
2	18	2	11	105.2	3.7	5
3	18	3	29	153.8	3.8	18.5
4.4	19	3	23	77.5	6.09	15.5
6	18	2	20	134.8	3.4	9.2
7.3	27	2	18	40.6	8.1	6.4
8	26	2	19	158.6	8.8	30
9.2	25	3	21	102.5	12.5	26.6

Stratigraphic Log 11: Taupo Ignimbrite				
Height of column (m)	**Pumice abundance (%)**	**Lithic abundance (%)**	**Crystal abundance (%)**	**Max P(mm)**
0.5	5	< 1	17	4
2	5	< 1	34	4
3.3	5	< 1	16	7
5	5	< 1	17	9
6.5	5	< 1	16	14
7.8	7	< 1	19	16
9	10	< 1	20	17

Appendix Two
Petrography data

Petrography: Based on 400 point counts per thin section, (300 for whole pumice thin sections). Note, the % of individual mineral assemblages are based on their proportions relative to the overall crystal abundance of the slide:

Stratigraphic Log 3: Transitional Unit, Ongatiti Ignimbrite											
%	**S3.1**	**S3.2**	**S3.3**	**S3.4(pumice)**	**S3.5**	**S3.6**	**S3.7**	**S3.8**	**S3.9**	**S3.10**	**S3.11**
Plag	25	26	28	26	26.25	27	27.7	24	26.5	24.7	27
Qz	17.2	14.2	18.7	13	23.75	12.2	10	12.7	14	11.7	14.5
Hyp	3.6	9	5	5.6	9.75	8.75	5	6	4	7	5
Hbl	1.5	1.2	1	2.6	1.25	0.7	0.5	2	1.5	1.7	1.5
titan	2	3.5	7.2	5.6	2.25	5.5	4.2	6	4.7	4.7	7.2
ilm				0.3			0.2				0.7
GM	36.7	30.5	34		36.25	32	40.2	32.5	38.5	33.2	36.5
lithic		0.7			0.5	0.5	5		4.7		1
Pumice	14	14.7	6	41.9		13.2	7	16.7	6	16.7	6.5
Vesicles				5							
% of individual mineral assemblages											
plag	50.76	48.15	46.67	48.75	41.50	49.77	58.12	47.29	52.22	49.50	48.21
quartz	35.03	26.39	31.25	24.38	37.55	22.58	20.94	25.12	27.59	23.50	25.89
hyp	7.11	16.67	8.33	10.63	15.42	16.13	10.47	11.82	7.88	14.00	8.93
hbl	3.05	2.31	1.67	5.00	1.98	1.38	1.05	3.94	2.96	3.50	2.68
iron oxides	4.06	6.48	12.08	11.25	3.56	10.14	9.42	11.82	9.36	9.50	14.29

Stratigraphic Log 5: Upper Unit, Ongatiti Ignimbrite							
%	**S5.1**	**S5.2**	**S5.3 (pumice)**	**S5.4**	**S5.5**	**S5.6(pumice)**	**S5.7**
Plag	28.7	28.7	18.6	21.2	16.5	16.6	16
Qz	13.5	13.5	8	9.7	9	9.6	12.5
Hyp	4	4	4.6	6	4	5	3.5
Hbl	1.5	1.5	1	2	1.2	0.3	1
titan	3.2	3.2	3	6.2	3.2	2	5
ilm					0.7		0.7
GM	21	21		29.2	35.7		27.5
lithic	2.5	2.5		3.5	5.7		4.5
Pumice	25.5	25.5	64.6	22	23.7	66.3	29.2
Vesicles							
% of individual mineral assemblages							
plag	56.37	49.23	52.83	46.96	47.48	49.50	41.29
quartz	26.47	24.10	22.64	21.55	25.90	28.71	32.26
hyp	7.84	10.77	13.21	13.26	11.51	14.85	9.03
hbl	2.94	5.64	2.83	4.42	3.60	0.99	2.58
iron oxides	6.37	10.26	8.49	13.81	11.51	5.94	14.84

Stratigraphic Log 8: Lower Unit, Ongatiti Ignimbrite								
%	**S8.1**	**S8.2**	**S8.3**	**S8.4**	**S8.5**	**S8.6**	**S8.7**	**S8.8**
Plag	28.7	25.5	29	34.7	29.5	27	30.2	28.5
Qz	8.2	16.7	15.7	12.2	12.2	17	16.5	14
Hyp	5.5	4.5	2.5	6.2	4.7	8	7.2	6.5
Hbl	3	2.7	2	2.2	2.5	0.7	1	1.2
titan	3.2	2.7	2.7	4.9	3	7	6.5	3.5
ilm	0.7	0.2	0.2		0.7	0.2		
GM	48.5	46.5	42.5	35	41.5	34	34.5	35
lithic	0.7	1	1.2	1.7	2		2.5	4.5
Pumice	1.2		4	2.7	3.7	5.5	1.5	6.7
Vesicles								
% of individual mineral assemblages								
plag	58.08	48.57	55.50	57.44	55.92	44.63	49.39	53.02
quartz	16.67	31.90	30.14	20.25	23.22	28.93	26.94	26.05
hyp	11.11	8.57	4.78	10.33	9.00	13.22	11.84	12.09
hbl	6.06	5.24	3.83	3.72	4.74	1.24	1.22	2.33
iron oxides	8.08	5.71	5.74	8.26	7.11	11.98	10.61	6.51

Stratigraphic Log 7: Upper Unit, Ongatiti Ignimbrite									
%	**S7.1**	**S7.2**	**S7.3 (pumice)**	**S7.4(pumice)**	**S7.5**	**S7.6**	**S7.7**	**S7.9(pumice)**	**S7.10**
Plag	14.5	17	5.3	5.6	13.7	22.2	15.5	13	25.2
Qz	10.5	10.7	3	1.6	7.2	10.2	10.5	2.3	6.2
Hyp	2.2	3.5	1	2.6	5.2	4.5	2.2	1	1.5
Hbl	0.7	2.2		1.6	0.7	1.5	1	1	1.2
titan	2.5	3.7	1	1.3	4.5	2.7	2.2	1.6	3
ilm	0.5	0.2	0.3				0.5		0.2
GM	49	40.2			32.2	47	50.2		40.7
lithic	0.2				2.5		2		1.2
Pumice	19.7	22.2	66	56.6	33.7	11.7	15.7	81	20.5
Vesicles			23.3	30.3					
% of individual mineral assemblages									
plag	46.77	45.33	50.00	43.59	43.65	53.94	48.44	68.42	67.33
quartz	33.87	28.67	28.13	12.82	23.02	24.85	32.81	12.28	16.67
hyp	7.26	9.33	9.38	20.51	16.67	10.91	7.03	5.26	4.00
hbl	6.41	19.85	0.00	11.47	6.87	11.12	8.26	4.38	7.43
iron oxides	9.68	10.67	12.50	10.26	14.29	6.67	8.59	8.77	8.67

Stratigraphic Log 6: Lower Unit, Ongatiti Ignimbrite				
%	**S6.1**	**S6.2**	**S6.3**	**S6.4**
Plag	21.5	30	27.5	30
Qz	17	13	15.7	16.2
Hyp	4.7	4.2	2.7	4
Hbl	1	1.5	0.7	
titan	4	4	3.5	3
ilm	0.2	0.2	0.7	0.2
GM	45.5	41.2	40.7	38.7
lithic	0.5		0.2	0.5
Pumice	5.5	5.7	8	7.2
Vesicles				
% of individual mineral assemblages				
plag	44.33	56.60	53.92	56.07
quartz	35.05	24.53	30.88	30.37
hyp	9.79	8.02	5.39	7.48
hbl	2.06	2.83	1.47	0.00
iron oxides	8.76	8.02	8.33	6.07

Appendix Three
XRF analysis data

Geochemistry: Major and trace element analyses for the Ongatiti Ignimbite, Ongatiti Valley:

Ongatiti Ignimbrite - lower unit		
UoW (petlab) no. 2011:	909	903
Sample no.	**0.28**	**0.4**
Major elements (wt. %)		
SiO_2	69.20	70.41
TiO_2	0.39	0.39
$Al2O_3$	16.26	16.26
Fe_2O_3	3.84	2.77
MnO	0.08	0.05
MgO	0.73	0.57
CaO	2.61	2.46
Na_2O	4.45	4.54
K_2O	2.35	2.46
P_2O_5	0.09	0.09
LOI*	2.03	1.22
Total*	99.32	129.20
Trace elements (ppm)		
S	96	88
Cl	578	213
V	23	15.7
Cr	5.8	9.3
Co	23	11.7
Ni	2.8	2.9
Cu	–	–
Zn	68	53
Ga	19.7	19.4
Ge	0.5	0.8
As	3.2	–
Se	0.8	0.5
Br	4	1.4
Rb	76	79
Sr	200	197
Y	25	26
Zr	217	215
Nb	9.4	9.7
Mo	2.3	1.4
Ba	622	700
La	28	37
Ce	46	60
Nd	25	35
Hf	6.9	6.9
Tl	1.1	1.4
Pb	14.2	14.1
Bi	0.4	0.5
Th	14.6	14.1
U	6.7	6.6

Ongatiti Ignimbrite - upper unit (Stratigraphic Log 5)					
UoW (petlab) no. 2011:	945	947	948	949	950
Sample no.	**SL5.1**	**SL5.3**	**SL5.4**	**SL5.5**	**SL5.6**
Major elements (wt. %)					
SiO_2	72.63	72.71	73.40	80.53	70.01
TiO_2	0.32	0.34	0.32	0.23	0.37
$Al2O_3$	14.55	14.66	13.92	10.45	16.06
Fe_2O_3	3.02	3.04	2.78	1.99	3.85
MnO	0.07	0.06	0.05	0.03	0.05
MgO	0.44	0.55	0.49	0.30	0.46
CaO	2.04	2.23	2.08	1.44	2.27
Na_2O	3.81	3.70	3.71	2.52	4.09
K_2O	3.09	2.63	3.13	2.45	2.79
P_2O_5	0.04	0.08	0.10	0.06	0.05
LOI*	2.59	4.15	2.18	3.05	2.88
Total*	100.85	100.34	100.05	100.07	98.70
Trace elements (ppm)					
S	216	7907	2807	306	131
Cl	850	973	907	179	343
V	17	10.8	10.5	7.7	25
Cr	2.7	4.6	3.9	4.8	5.7
Co	29	52	41	23	32
Ni	2.6	3.6	3.2	1.9	3.5
Cu	–	1	–	0.6	0.5
Zn	48	47	54	29	63
Ga	18.2	18.5	18.1	13.2	18.8
Ge	0.3	1.2	–	–	0.9
As	4	4.1	4	2.3	3
Se	0.9	1.4	1.5	1	1.3
Br	5.4	7.8	6.9	2.9	4.8
Rb	101	88	101	80	90
Sr	163	180	164	125	176
Y	27	25	27	21	34
Zr	211	216	218	155	224
Nb	9.2	9.1	9.4	7.1	9
Mo	1.8	1.9	2.1	1.3	2.2
Ba	669	832	754	967	637
La	24	31	35	36	37
Ce	45	51	57	56	52
Nd	24	33	33	32	33
Hf	7.1	6.1	6.6	5.4	6.8
Tl	1.5	2.4	2.1	1.6	2.2
Pb	11.8	10.9	10.7	6.2	13.9
Bi	1	2	1.5	1.1	1.5
Th	15.6	16.6	14.6	11.7	14.4
U	6.8	6.6	7.4	6.5	6.3

Ongatiti Ignimbrite - upper unit (Stratigraphic Log 7)							
UoW (petlab) no. 2011:	962	963	964	965	967	968	971
Sample no.	**SL7.1**	**SL7.2**	**SL7.3**	**SL7.4**	**SL7.6**	**SL7.7**	**SL7.10**
Major elements (wt. %)							
SiO_2	71.61	69.08	73.46	72.58	69.26	69.40	69.92
TiO_2	0.34	0.41	0.27	0.31	0.44	0.42	0.40
$Al2O_3$	15.19	15.99	13.31	14.52	16.12	17.08	16.32
Fe_2O_3	3.32	4.38	2.46	2.65	4.29	3.72	3.84
MnO	0.07	0.07	0.04	0.05	0.08	0.03	0.04
MgO	0.50	0.61	0.73	0.43	0.60	0.36	0.45
CaO	1.95	2.65	2.42	1.99	2.64	2.43	2.25
Na_2O	3.89	4.55	3.69	3.82	4.30	4.12	4.11
K_2O	3.11	2.22	3.24	3.57	2.23	2.31	2.64
P_2O_5	0.03	0.06	0.38	0.07	0.05	0.14	0.02
LOI*	2.30	1.85	2.83	1.99	1.36	2.10	3.37
Total*	99.58	98.86	100.02	99.64	100.64	100.45	100.60
Trace elements (ppm)							
S	143	189	2333	373	248	260	202
Cl	353	443	802	732	461	488	1772
V	11.4	22	12.8	12.9	27	17.7	27
Cr	7.6	8.3	7.9	8.2	3	7.7	6.6
Co	32	22	44	36	17.3	13.5	29
Ni	3.4	3.7	3.9	3.4	3.6	3.9	3.2
Cu	0.6	–	0.7	–	0.7	–	0.9
Zn	45	55	36	40	61	54	60
Ga	17.6	19.7	17.2	17.7	21	19.6	18.9
Ge	1.5	1.7	1.9	1.3	1.1	1	0.7
As	5.7	4.7	4.3	4.4	1.6	1.7	3.5
Se	0.8	0.9	1.9	1	0.7	0.7	0.7
Br	2.6	2.4	6.7	6.1	3.7	2.5	5.4
Rb	101	78	107	112	67	73	84
Sr	158	210	170	159	214	203	179
Y	27	23	27	27	22	23	24
Zr	231	225	191	206	234	234	241
Nb	9.9	9.2	8.2	9.1	9.3	9.3	9.5
Mo	1.7	2.1	2.1	1.9	1.2	0.7	1.7
Ba	680	609	631	676	667	648	632
La	26	25	25	28	22	43	43
Ce	48	42	47	51	38	64	66
Nd	25	24	21	28	21	43	45
Hf	7.4	8	7	7.2	7.3	8.4	7.6
Tl	2.2	2	2.7	2.3	1.8	1.9	1.8
Pb	10.2	10.1	9.6	12.2	19.1	11.3	14.6
Bi	0.7	0.7	2.1	1.3	0.8	1	1
Th	15.3	12.6	13.1	14.6	12.6	13.3	15.2
U	6.6	5.3	6.3	6.7	6	5.8	5.8

Ongatiti Ignimbrite - lower unit (Stratigraphic Log 6)				
UoW (petlab) no. 2011:	958	959	960	961
Sample no.	**SL6.1**	**SL6.2**	**SL6.3**	**SL6.4**
Major elements (wt. %)				
SiO_2	72.04	71.77	70.15	69.40
TiO_2	0.37	0.37	0.40	0.40
Al2O_3	15.55	15.77	16.99	16.49
Fe_2O_3	1.96	2.03	3.88	3.83
MnO	0.05	0.05	0.03	0.03
MgO	0.49	0.48	0.35	0.36
CaO	2.13	2.30	2.07	2.42
Na_2O	4.37	4.43	3.63	4.19
K_2O	2.95	2.71	2.46	2.30
P_2O_5	0.09	0.07	0.05	0.57
LOI*	0.75	0.68	2.36	1.80
Total*	98.63	100.11	100.21	100.07
Trace elements (ppm)				
S	119	127	243	179
Cl	407	219	217	114
V	19.2	11.5	24	23
Cr	8.2	9.5	6.6	10.1
Co	20	22	19.3	24
Ni	3.7	3	2.6	3.1
Cu	0.8	–	1.2	0.7
Zn	64	41	53	70
Ga	19.3	19.8	19.5	20
Ge	0.3	1.3	1.1	1
As	–	–	–	0.6
Se	0.8	0.8	0.5	0.8
Br	2.2	2	2.5	1.8
Rb	102	94	87	81
Sr	169	183	174	199
Y	33	25	16.9	23
Zr	223	230	223	217
Nb	9.9	9.6	9.4	9.2
Mo	1	1.3	1.3	1.6
Ba	743	711	640	651
La	39	45	19	36
Ce	64	66	30	45
Nd	33	42	16.4	32
Hf	7.6	7	6.3	7.1
Tl	1.9	1.5	1.3	1.2
Pb	13.6	13	9.8	12
Bi	1.2	1	0.7	1
Th	15.7	15.5	14.3	12.8
U	6.8	6.4	6.2	6

Ongatiti Ignimbrite - lower unit (Stratigraphic Log 8)							
UoW (petlab) no. 2011:	972	973	975	976	977	978	979
Sample no.	**SL8.1**	**SL8.2**	**SL8.4**	**SL8.5**	**SL8.6**	**SL8.7**	**SL8.8**
Major elements (wt. %)							
SiO_2	69.28	71.07	72.38	71.04	69.81	68.94	69.86
TiO_2	0.40	0.38	0.36	0.39	0.40	0.41	0.42
Al2O_3	16.42	15.31	14.58	15.26	15.92	17.72	15.99
Fe_2O_3	3.60	3.55	3.37	3.75	3.92	3.96	3.88
MnO	0.08	0.04	0.05	0.05	0.07	0.04	0.05
MgO	0.64	0.37	0.49	0.35	0.63	0.37	0.48
CaO	2.61	2.38	2.42	2.50	2.54	2.40	2.64
Na_2O	4.48	4.42	4.16	4.31	4.19	3.83	4.42
K_2O	2.43	2.42	2.10	2.27	2.41	2.19	2.23
P_2O_5	0.06	0.06	0.10	0.08	0.12	0.14	0.04
LOI*	2.16	0.54	1.19	1.25	0.91	2.29	0.86
Total*	99.81	98.99	100.16	97.66	100.02	100.37	99.24
Trace elements (ppm)							
S	53	262	266	161	138	199	169
Cl	953	658	208	373	293	334	176
V	23	24	17.1	27	23	26	27
Cr	6.7	9.6	10.5	9.4	6.6	10	9.6
Co	16.5	23	23	18.2	20	15.4	19.3
Ni	3.9	4.2	5.2	4.1	5	3	3.7
Cu	–	–	–	1.2	1.5	0.4	1.5
Zn	60	56	73	57	65	50	58
Ga	19.7	18.7	17.9	18.7	20	19.2	19.9
Ge	0.6	0.6	1.4	1.2	1.1	1	0.9
As	3.1	–	0.6	–	–	–	–
Se	1.2	0.7	0.7	0.6	0.7	0.6	0.6
Br	4.7	2.7	2.3	2.1	1.8	1.9	2
Rb	80	81	65	77	81	73	79
Sr	203	198	203	207	207	207	217
Y	24	25	23	24	27	21	21
Zr	224	227	211	209	224	236	233
Nb	9.8	9.1	8.1	8.5	9.2	8.7	9.1
Mo	1.9	1.3	1.3	1.7	1.4	1.3	1.6
Ba	643	647	1067	691	661	596	651
La	24	21	24	24	24	15.6	29
Ce	45	39	42	46	43	31	48
Nd	26	25	32	27	28	17.4	31
Hf	8.7	8.2	6.1	6.5	6.7	7	6.3
Tl	2.3	1.7	1.6	1.4	1.4	0.9	1.4
Pb	15	13.1	17.5	13.2	13.5	9.3	11.4
Bi	1.2	0.9	0.7	0.6	0.3	0.6	0.6
Th	12.9	13.2	11.8	12.5	13	12.6	11.3
U	5.3	5.6	5.1	5.2	5	5	4.8

Appendix Four

Electron Microprobe analysis (EPMA) data

Plagioclase crystals within the Ongatiti Ignimbrite, Ongatiti Valley:

UoW (petlab no.) 2011:	972	972	972	972	972	972
Sample no.	SL8.1	SL8.1	SL8.1	SL8.1	SL8.1	SL8.1
Crystal:	1	1	2	2	3	4
position on crystal:	core	rim	core	rim	mid	mid
(wt. %)						
SiO2	63.05	62.11	60.72	60.48	61.72	61.32
TiO2	0.16	-0.04	0.06	0.11	0.06	0.01
Al2O3	22.07	22.86	23.60	23.75	22.98	24.11
FeO	0.12	0.22	0.17	0.23	0.19	0.26
MnO	0.10	0.01	-0.03	-0.04	-0.04	-0.10
MgO	-0.01	-0.08	0.04	-0.09	-0.09	-0.06
CaO	4.14	4.99	5.62	5.73	4.89	5.71
Na2O	8.38	7.88	7.65	7.79	8.15	7.61
K2O	0.97	0.90	0.75	0.67	0.82	0.68
P2O5	-0.09	-0.02	-0.12	-0.10	-0.06	-0.19
SO3	-0.04	0.01	-0.01	0.00	0.06	0.02
Cl	-0.03	0.04	0.02	-0.01	0.08	-0.01
Cr2O3	-0.01	-0.15	0.00	-0.13	0.04	0.13
NiO	-0.03	0.06	-0.05	-0.14	-0.08	0.13
TOTAL	98.77	98.79	98.45	98.25	98.71	99.61

UoW (petlab no.) 2011:	945	945	945	945	945
Sample no.	SL5.1	SL5.1	SL5.1	SL5.1	SL5.1
Crystal:	5	5	6	6	6
position on crystal:	mid	mid	rim	mid	core
(wt. %)					
SiO2	60.96	60.96	59.91	61.51	62.22
TiO2	0.01	0.01	-0.04	0.02	0.15
Al2O3	23.28	23.28	23.79	23.31	23.22
FeO	0.13	0.13	0.29	0.21	0.27
MnO	-0.05	-0.05	-0.04	-0.06	0.10
MgO	-0.08	-0.08	-0.03	-0.06	-0.12
CaO	5.21	5.21	5.93	5.10	4.99
Na2O	8.15	8.15	7.51	8.04	8.31
K2O	0.76	0.76	0.62	0.72	0.83
P2O5	-0.17	-0.17	-0.12	0.10	-0.08
SO3	-0.03	-0.03	-0.09	-0.03	-0.06
Cl	-0.03	-0.03	0.03	0.05	-0.04
Cr2O3	0.09	0.09	-0.04	0.02	0.03
NiO	-0.03	-0.03	0.31	-0.06	0.09
TOTAL	98.20	98.20	98.03	98.86	99.89

UoW (petlab no.) 2011:	909	909	903	903	903
Sample no.	O.28	O.28	O.4	O.4	O.4
Crystal:	7	7	8	8	9
position on crystal:	rim	core	core	rim	core
(wt. %)					
SiO2	60.17	61.35	60.43	61.57	60.28
TiO2	0.00	0.06	0.09	0.03	0.07
Al2O3	24.12	23.51	24.54	23.79	24.49
FeO	0.21	0.32	0.28	0.25	0.24
MnO	0.12	0.11	-0.07	0.08	-0.02
MgO	-0.09	-0.05	0.01	0.00	-0.05
CaO	6.13	5.55	6.30	5.64	6.55
Na2O	7.77	7.97	7.37	7.85	7.56
K2O	0.69	0.76	0.52	0.76	0.55
P2O5	0.10	-0.07	-0.06	-0.04	-0.02
SO3	0.15	0.10	-0.08	-0.03	-0.10
Cl	0.00	-0.04	-0.01	0.02	-0.02
Cr2O3	-0.05	0.13	0.09	0.04	0.13
NiO	-0.24	0.09	-0.11	0.06	0.12
TOTAL	99.07	99.80	99.31	100.03	99.79

Hornblende crystals within the Ongatiti Ignimbrite, Ongatiti Valley:

UoW (petlab no.) 2011:	903	909	945	945	945	945	972	972
Sample no.	O.4	O.28	SL5.1	SL5.1	SL5.1	SL5.1	SL8.1	SL8.1
Crystal:	1	2	3	3	4	4	5	6
(wt. %)								
SiO2	43.24	45.41	43.99	45.05	45.05	44.73	45.60	44.85
TiO2	3.00	1.87	1.88	1.86	1.86	1.87	1.59	1.92
Al2O3	10.73	7.51	7.17	7.22	7.22	7.56	7.10	7.56
FeO	15.20	19.03	18.54	18.40	18.40	18.66	18.39	19.47
MnO	0.25	0.37	0.47	0.39	0.39	0.34	0.44	0.33
MgO	12.22	10.77	10.23	10.84	10.84	10.24	10.91	10.38
CaO	10.58	10.39	9.76	10.34	10.34	10.11	10.12	10.37
Na2O	2.50	1.77	1.73	1.78	1.78	1.79	1.51	1.78
K2O	0.41	0.65	0.66	0.65	0.65	0.74	0.60	0.76
P2O5	-0.03	0.06	-0.11	-0.04	-0.04	-0.13	-0.11	0.10
SO3	0.01	0.00	-0.03	-0.04	-0.04	0.04	-0.07	-0.05
Cl	0.03	0.34	0.33	0.33	0.33	0.31	0.30	0.37
Cr2O3	0.12	0.09	-0.03	-0.02	-0.02	0.08	0.02	0.11
NiO	0.09	0.06	-0.12	-0.01	-0.01	-0.14	-0.07	0.16
TOTAL	98.35	98.31	94.46	96.76	96.76	96.19	96.33	98.10

Orthopyroxene crystals within the Ongatiti Ignimbrite, Ongatiti Valley:

UoW (petlab no.) 2011:	903	903	909	945	945	972	972
Sample no.	O.4	O.4	O.28	SL5.1	SL5.1	SL8.1	SL8.1
Crystal:	1	2	3	4	4	5	6
(wt. %)							
SiO2	50.87	51.29	50.76	50.82	50.37	50.76	50.81
TiO2	0.27	0.17	0.09	0.11	0.14	0.28	0.21
Al2O3	0.12	0.20	0.19	0.15	0.20	0.20	0.23
FeO	31.38	31.82	31.51	30.26	30.46	30.71	31.36
MnO	1.70	1.67	1.47	1.31	1.37	1.41	1.50
MgO	13.93	14.68	14.55	14.93	14.87	14.97	14.44
CaO	1.23	1.28	1.17	1.10	1.09	1.13	1.16
Na2O	0.12	0.05	0.06	0.07	0.12	0.05	0.09
K2O	0.07	0.05	0.05	0.07	0.02	0.00	0.06
P2O5	0.04	-0.03	-0.02	-0.02	-0.13	0.04	-0.16
SO3	0.04	0.03	-0.03	0.05	0.04	0.10	-0.04
Cl	0.03	-0.03	0.05	-0.02	-0.06	0.00	-0.05
Cr2O3	0.07	0.05	-0.10	-0.06	0.03	-0.06	0.08
NiO	0.01	0.15	-0.19	0.07	0.10	-0.14	0.14
TOTAL	99.88	101.40	99.56	98.82	98.63	99.45	99.82

Pumice clasts within the Ongatiti Ignimbrite, Ongatiti Valley:

UoW (petlab no.) 2011:	972	972	972	972	910	910	910
Sample no.	SL8.1	SL8.1	SL8.1	SL8.1	O.29	O.29	O.29
pumice clast:	1	2	3	3	4	5	6
(wt. %)							
SiO2	75.22	74.88	73.64	72.76	73.49	74.28	73.40
TiO2	0.19	0.15	0.07	0.27	0.10	0.27	0.17
Al2O3	11.45	12.01	11.85	13.01	11.97	12.04	11.77
FeO	0.37	1.16	1.09	0.97	0.88	0.54	1.26
MnO	-0.01	0.11	0.13	0.08	0.11	0.09	0.06
MgO	0.03	0.11	0.09	-0.02	0.08	0.09	0.07
CaO	0.51	0.89	0.88	0.88	1.12	0.79	0.85
Na2O	4.77	2.43	2.56	3.58	3.57	3.30	3.46
K2O	2.89	3.86	3.81	4.09	4.11	4.33	4.17
P2O5	0.05	-0.10	0.01	-0.12	0.09	-0.15	-0.05
SO3	-0.05	-0.03	-0.11	-0.08	0.07	-0.09	-0.05
Cl	0.18	0.33	0.36	0.24	0.37	0.06	0.30
Cr2O3	0.04	-0.12	0.02	0.04	0.20	0.01	0.03
NiO	0.08	-0.01	-0.09	0.24	0.09	-0.17	-0.05
TOTAL	95.72	95.67	94.31	95.93	96.25	95.39	95.39

UoW (petlab no.) 2011:	910	945	945	945	909	909	946
Sample no.	O.29	SL5.1	SL5.1	SL5.1	O.28	O.28	SL5.2
pumice clast:	6	7	8	9	10	11	12
(wt. %)							
SiO2	74.59	74.24	73.53	73.79	73.36	73.57	73.26
TiO2	0.14	0.08	0.19	0.25	0.20	0.18	0.18
Al2O3	12.48	11.85	12.02	11.90	11.64	12.24	11.82
FeO	0.64	0.81	0.66	0.84	1.11	0.85	1.06
MnO	-0.08	0.09	0.04	0.13	0.03	0.02	-0.09
MgO	0.00	-0.05	-0.01	-0.03	0.07	0.06	0.17
CaO	0.80	0.82	0.89	0.80	0.91	0.92	0.85
Na2O	3.29	2.66	2.46	2.56	3.50	3.65	3.71
K2O	4.36	3.95	4.15	3.91	4.09	3.94	4.00
P2O5	-0.02	-0.08	0.04	-0.04	-0.11	-0.04	0.07
SO3	-0.07	0.02	0.00	0.00	0.00	-0.11	-0.07
Cl	0.10	0.17	0.12	0.15	0.30	0.12	0.33
Cr2O3	0.10	-0.07	0.06	-0.03	0.04	-0.02	0.01
NiO	-0.05	0.19	0.24	0.09	0.01	0.08	0.11
TOTAL	96.28	94.68	94.39	94.32	95.15	95.46	95.41

UoW (petlab no.) 2011:	946	946	946	946	946
Sample no.	SL5.2	SL5.2	SL5.2	SL5.2	SL5.2
pumice clast:	13	14	15	16	17
(wt. %)					
SiO2	64.04	73.24	71.75	72.23	72.54
TiO2	0.26	0.23	0.28	0.01	0.21
Al2O3	10.50	11.84	11.64	12.00	11.70
FeO	0.78	1.03	1.07	1.35	1.18
MnO	0.00	-0.01	0.12	-0.02	0.04
MgO	0.01	0.07	-0.06	0.12	0.12
CaO	0.79	0.86	0.88	0.82	0.91
Na2O	3.23	3.73	3.66	3.74	3.64
K2O	3.50	3.96	3.95	3.94	3.95
P2O5	-0.20	0.17	-0.17	-0.03	-0.07
SO3	0.02	-0.04	-0.07	0.00	-0.10
Cl	0.23	0.33	0.23	0.36	0.30
Cr2O3	-0.09	0.02	-0.08	-0.11	0.00
NiO	0.08	0.26	0.02	-0.01	-0.07
TOTAL	83.15	95.69	93.22	94.40	94.35

Glass shards within the Ongatiti Ignimbrite, Ongatiti Valley:

UoW (petlab no.) 2011:	972	909	909	909	903	903
Sample no.	S8.1	O.28	O.28	O.28	O.4	O.4
Glass shard:	1	2	3	3	4	5
(wt. %)						
SiO2	73.73	72.38	73.02	73.48	76.18	80.91
TiO2	0.16	0.25	0.15	0.15	0.20	0.05
Al2O3	11.73	11.89	11.69	12.15	12.87	9.95
FeO	1.22	1.00	1.23	1.20	0.27	0.35
MnO	-0.04	0.19	-0.01	0.04	-0.02	-0.09
MgO	0.17	0.21	0.02	0.03	0.11	0.02
CaO	0.82	0.76	0.94	0.96	0.91	0.51
Na2O	3.68	3.55	3.38	3.61	3.64	2.66
K2O	4.11	4.04	4.09	4.08	4.68	4.01
P2O5	0.06	-0.05	0.06	-0.01	0.05	0.24
SO3	-0.05	0.04	-0.10	-0.09	0.06	-0.02
Cl	0.39	0.32	0.33	0.40	0.22	0.12
Cr2O3	0.04	0.01	0.08	-0.11	-0.05	-0.07
NiO	-0.03	-0.06	0.11	0.17	0.09	-0.16
TOTAL	95.99	94.53	94.99	96.06	99.21	98.53

Appendix Five
ICPMS analysis data

Rare earth elements (normalised to a common chondritic reference) from ICPMS analysis of six selected whole rock samples in the Ongatiti Ignimbrite, Ongatiti Valley.

UoW (petlab) no. (2011):	903	972	973	975	977	979
Sample no.	**O.4**	**SL8.1**	**SL8.2**	**SL8.4**	**SL8.6**	**SL8.8**
(ppm)						
La	81.13	133.15	90.53	90.19	87.60	91.92
Ce	60.98	100.49	70.33	68.81	61.99	69.22
Pr	44.92	82.31	49.58	51.28	49.88	53.04
Nd	33.51	64.38	36.82	38.78	38.23	40.69
Sm	22.19	45.86	25.32	26.32	25.87	27.79
Eu	20.20	26.94	19.55	18.68	19.39	19.52
Gd	14.65	29.46	16.56	17.11	16.13	18.32
Tb	14.17	30.98	16.61	16.91	16.11	18.29
Dy	13.01	28.15	15.08	15.42	14.52	16.52
Ho	13.20	28.93	15.15	15.61	14.36	16.93
Er	13.02	27.60	14.85	15.28	13.61	16.21
Tm	12.05	25.02	13.80	14.22	12.53	15.21
Yb	12.47	25.05	13.94	14.42	12.74	15.36
Lu	12.70	25.94	14.73	15.09	13.00	15.96

Trace element ICPMS analyses (normalised to the primitive mantle) of six selected whole rock samples in the Ongatiti Ignimbrite, Ongatiti Valley.

UoW (petlab) no. (2011):	903	972	973	975	977	979
Sample no.	**O.4**	**SL8.1**	**SL8.2**	**SL8.4**	**SL8.6**	**SL8.8**
(ppm)						
Rb	76.9	77.7	77.0	62.5	80.5	71.2
Sr	188.4	195.9	188.8	191.4	200.4	204.5
Y	23.8	23.2	24.1	21.5	26.2	19.9
Zr	88.5	87.8	87.4	88.1	94.7	84.9
Nb	8.6	9.0	8.7	7.7	8.8	8.6
Ba	675.9	660.4	685.6	1086.6	672.9	649.3
La	22.1	21.5	21.4	20.8	21.8	19.1
Ce	43.8	43.0	42.1	37.9	42.4	36.8
Nd	19.2	17.2	18.1	17.9	19.0	15.6
Sm	4.3	3.9	4.0	4.0	4.3	3.4
Tb	0.6	0.6	0.6	0.6	0.7	0.5
Tm	0.3	0.4	0.4	0.3	0.4	0.3
Yb	2.4	2.4	2.5	2.2	2.6	2.1
Hf	2.7	2.9	2.9	2.7	3.0	2.6
Ta	0.7	0.7	0.7	0.6	0.7	0.6
Th	9.2	9.9	9.4	7.9	9.5	8.0
U	2.0	2.0	2.0	1.7	2.0	1.8